CORA Cork Open Research Archive
Cartlann Taighde Oscailte Chorcaí

Title	AI-based analysis of cerebral oxygenation in preterm and term infants
Authors	Ashoori, Minoo
Publication date	2024
Original Citation	Ashoori, M. 2024. AI-based analysis of cerebral oxygenation in preterm and term infants. PhD Thesis, University College Cork.
Type of publication	Doctoral thesis
Rights	© 2024, Minoo Ashoori. - https://creativecommons.org/licenses/by-nc-nd/4.0/
Download date	2026-09-16 18:51:05
Item downloaded from	https://hdl.handle.net/10468/17059

UCC
University College Cork, Ireland
Coláiste na hOllscoile Corcaigh

Ollscoil na hÉireann, Corcaigh

National University of Ireland, Cork

AI-based Analysis of Cerebral Oxygenation in Preterm and Term Infants

Thesis presented by

Minoo Ashoori, BSc, MSc

0000-0002-8000-9544

for the degree of

Doctor of Philosophy

University College Cork

Department of Physiology, School of Medicine, College of Medicine & Health

Head of Department: Prof Ken O'Halloran

Supervisors:

Dr. Fiona McDonald

Prof Ken O'Halloran

2024

Table of Contents

List of Figures 8

List of Tables 11

Declaration 13

Acknowledgement 14

Abbreviations 16

Publications and Presentations 19

Publications 19

Papers in Preparation 21

Oral Presentations 22

Poster Presentations 23

Awards 24

Chapter 1. Introduction 25

1.1. Newborn Brain Physiology 26

1.1.1. Extrauterine Transition 26

1.1.2. Common Complications in Neonatal Care 27

1.2. Brain Injuries in Infants 36

1.2.1. Intraventricular Haemorrhage (IVH) 36

1.2.2. Hypoxic Ischaemic Encephalopathy (HIE) 42

1.3. Physiological Monitoring and Brain Imaging in Early Life 46

1.3.1. The Role of MRI and Ultrasound in the Classification of Neonatal Brain Injuries 46

1.3.2. Introduction to Near-Infrared Spectroscopy (NIRS) and Its Application in Neonates. 50

1.3.3. Peripheral Oxygen Saturation (SpO_2) and EEG: Complementary Tools in Brain Injury Detection. 58
1.4. Components of NIRS ($rcSO_2$) Signal 67
1.4.1. Physiological Significance of Signal Components 67
1.4.2. Delving into Prolonged Relative Desaturations: What They Are and Why They Matter. 68
1.4.3. Methodological Approaches for Extracting and Analysing PRDs. 70
1.5. The Advent of Machine Learning in Neonatal Care 73
1.5.1. Introduction to Machine Learning and Its Transformative Role in Healthcare. 73
1.5.2. Focusing on Specific Machine Learning Tools: XGBoost and Deep Learning Methods 79
1.6. Thesis Objectives 82
1.7. References: 84
Chapter 2. Sparse-denoising Methods for Extracting Desaturation Transients in Cerebral Oxygenation Signals of Preterm Infants 128
2.1. Abstract 129
2.2. Introduction 130
2.3. Methods 131
2.3.1. Singular-spectrum Analysis for Extracting Transients 131
2.3.2. Total Variation Denoising Methods 133
2.3.3. Performance Comparison 135
2.4. Results 137
2.5. Discussion and Conclusion 141
2.6. References 143
Chapter 3. Management of Hypotension in Preterm Infants (HIP) 145
3.1. Abstract: 147

3.2. Introduction 150

3.3. Methods 152

3.3.1. Study Design and Participants 152
3.3.2. Data Collection 154
3.3.3. Signal Processing 156
3.3.4. Extracting Prolonged Relative Desaturations 157
3.3.5. Feature Extraction 157
3.3.6. Machine Learning Models 159
3.3.7. Combining Models 160
3.3.8. Statistical Analysis 162

3.4. Results 164

3.5. Discussion 170

3.6. References 175

3.7. Machine Learning Models Using NIRS and Clinical Data Predicts Two-year Neurodevelopmental Outcomes in Infants Born Extremely Preterm 183

3.7.1. Abstract: 184
3.7.2. Introduction 185
3.7.3. Methods 186
3.7.4. Results 188
3.7.5. Discussion 192
3.7.6. References 194

3.8. Blood Pressure and EEG 197

3.8.1. Abstract 198
3.8.2. Introduction 200
3.8.3. Methods 203
3.8.4. Results 209
3.8.5. Discussion 213
3.8.6. References 215

Chapter 4. Safeguarding the Brains of Our Smallest Children (SafeBoosC)-III 219

4.1. Abstract 220

4.2. Introduction 221

4.3. Methods 225

4.3.1. Ethical Approval 225
4.3.2. Study Design and Participants 227
4.3.3. Data Collection 227
4.3.4. Signal Processing 228
4.3.5. Machine Learning Model 230
4.3.5. Statistics 234

4.4. Results 235

4.4.1. Clinical Data 235
4.4.2. $rcSO_2$ 235
4.4.3. SpO_2 241
4.4.4. $rcSO_2$ & SpO_2 241

4.5. Discussion 245

4.6. References 251

Chapter 5. Multi-model Assessment of Newborns at Risk of Neonatal Hypoxic Ischaemic Encephalopathy – The MONItOr Study 259

5.1. Abstract: 260

5.2. Introduction: 263

5.2. Methods: 266

5.2.1. Ethical Approval 266
5.2.2. Data Collection 266
5.2.3. MRI 267
5.2.4. HIE Classification and Adverse Outcome 267
5.3.5. Signal Processing 267
5.3.6. Machine Learning 268

5.3.7. Deep Learning 269
5.3.8. CNN- XGBoost 270
5.3.9. Statistical Analysis 271
5.4. Results: 274

5.4.1. Machine Learning 275
5.4.2. Deep Learning 277
5.4.3. CNN-XGBoost 278
5.5. Discussion: 282

5.6. References 290

Chapter 6. AI Competition 299

6.1. Introduction 300

6.2. Methods 301

6.2.1. Study Design and Participants 301
6.2.2. EEG 301
6.2.3. Signal Processing 302
6.2.4. Feature Extraction 303
6.2.5. Machine Learning 303
6.2.6. Model Evaluation 304
6.3. Results: 306

6.4. Discussion: 308

6.5. References 311

Chapter 7. Thesis Discussion and Conclusion 315

7.1. Overview of Main Findings 316

7.2. Contribution to the Field 318

7.3. Strength and Limitations 319

7.4. Recommendations for Future Research 320

List of Figures

Chapter 1.

Figure1.1. Cerebral autoregulation in relation to vascular response..... 35

Figure1.2. Application of near-infrared spectroscopy probe for cerebral oxygen monitoring..... 52

Figure1. 3. Relationship between artificial intelligence (AI), machine learning (ML), deep learning, and convolutional neural networks (CNN)..... 74

Chapter 2.

Figure 2. 1. Grid search for the parameters of the LPF–TVD methods.....137

Figure 2. 2. Comparison between the LPF-TVD methods and between the SSA-DCT methods, and comparison between the best performing algorithm in each group when assessed on 100 synthetic NIRS-like signals.....140

Figure 2. 3. SSA-DCT2 and LPF-CSD1 decomposition methods on a NIRS-like synthetic signal 140

Chapter 3.

Figure 3. 1. Graphical abstract of HIP study..... 149

Figure 3. 2. HIP trial flow diagram..... 154

Figure 3. 3. Illustration of some of the quantitative features extracted from PRDs.159

Figure 3. 4. Summary of the steps taken to process the signal, extract the relative prolonged desaturations (PRDs) and features, and utilise the machine learning model 161

Figure 3. 5. Averaged curve of all $rcSO_2$ PRDs in the intraventricular haemorrhage group vs. no/mild intraventricular haemorrhage group. 163

Figure 3.6. Illustration of feature importance of the XGBoost model using rcSO2 prolonged relative desaturations (PRDs) in predicting intraventricular haemorrhage. 168

Figure 3.7. Summary of the workflow for EEG signal processing. 208

Figure 3. 8. Average of Mean arterial Blood Pressure (MABP) trend over time for all infants..... 210

Figure 3. 9. Mean ± SD MABP over time for four distinct groups: Normotensive <26weeks' GA, Normotensive <26 weeks' GA, for Hypotensive ≥26weeks' GA, Hypotensive ≥26 weeks' GA. 211

Chapter 4.

Figure 4. 1. SafeBoosC-III trial and follow-up study flow diagram (PREMI-NIRS). ... 226

Figure 4. 2. Illustration of some of the quantitative features extracted from PRDs. 230

Figure 4. 3. All possible scenarios between time synchronised PRDs in $rcSO_2$. 233

Figure 4. 4. Illustration of parameter optimisation in an XGBoost model using features extracted from PRDs. 238

Figure 4. 5. Illustration of feature importance of the XGBoost model using $rcSO_2$ prolonged relative desaturations (PRDs) in detecting IVH III-I..... 239

Figure 4. 6. The comparison of $rcSO_2$ PRD width, total power and slope-up between infants with brain injury and non-injury..... 240

Figure 4. 7. An example of $rcSO_2$ signal with corresponding time-synchronised SpO_2 and the resulting FTOE over a 10-hour duration 242

Figure 4. 8. The comparison of FTOE mean value and total power between infants with brain injury and non-injury..... 243

Chapter 5.

Figure 5. 1. Graphical abstract of MONItOr study. 262

Figure 5. 2. Illustration of NIRS signal processing 272

Figure 5. 3. Illustration of features extracted from $rcSO_2$ signals 273

Figure 5. 4. The AUC of the ROC along with the bootstrapping 95% confidence intervals for HIE grading 275

Figure 5. 5. The AUC of the ROC along with the bootstrapping 95% confidence intervals for the binary XGBoost models 277

Figure 5. 6. The AUC of the ROC along with the bootstrapping 95% confidence intervals for the multi-class XGBoost models 277

Figure 5. 7. The AUC of the ROC along with the bootstrapping 95% confidence intervals for the binary 1D-CNN model based on $rcSO_2$, and CNN-XGBoost model.279

List of Tables

Chapter 3.

Table 3. 1. Clinical data of the subset of infants from the HIP trial included in the current study. 166

Table 3. 2. Area under the curve (AUC) values for the signals used to predict brain injury in the first week of life. 167

Table 3. 3. Area under the curve (AUC) values for the individual features of rcSO2 PRDs used to predict brain injury in the first week of life..... 169

Table 3. 4. Area under the curve (AUC) values for the models based on $rcSO_2$ signal features used to predict long-term neurodevelopmental outcome at two years of age. 190

Table 3. 5. The features extracted from EEG signals 206

Table 3. 6. Number of infants in each group 209

Table 3. 7. Partial correlation between MABP and EEG quantitative features and corresponding p values 212

Chapter 4.

Table 4. 1. Clinical characteristics of the subset of infants from the SafeBoosC-III trial included in the current study. 235

Table 4. 2. Area under the curve (AUC) values for the rcSO2 and SpO2 signals used to detect brain injury in the first week of life. 244

Chapter 5.

Table 5. 1. Demographics of infants included in study.....280

Table 5. 2. Architecture Details of the Convolutional Neural Network Model. 281

Chapter 6.

Table 6. 1. The features extracted from EEG signals 305

Table 6. 2. Distribution of 4 grades of EEG.....306

Table 6. 3. Distribution of number of EEG epochs available per neonate 306

Table 6. 4. Model performance metrics for training and testing (unseen) dataset .307

Declaration

This is to certify that the work I am submitting is my own and has not been submitted for another degree, either at University College Cork or elsewhere. All external references and sources are clearly acknowledged and identified within the contents. I have read and understood the regulations of University College Cork concerning plagiarism and intellectual property.

Minoo Ashoori

01.10.2024

Acknowledgement

My PhD journey has been an incredible experience that has not only fostered my professional development but also shaped me on a personal level. It offered me a valuable opportunity to hone my problem-solving skills, step out of my comfort zone, and build resilience in the face of challenges. I could not have accomplished this without the unwavering support and encouragement of many wonderful people. I would like to take this moment to express my deepest gratitude to everyone who guided and supported me throughout this journey and contributed to my success.

First and foremost, I want to express my deepest thanks to **Dr Fiona McDonald** and **Prof. Ken O'Halloran**, my amazing supervisors. Fiona, you were always there for me, with your office door always open whenever I needed guidance. Your unwavering support, insightful feedback, and brilliant ideas shaped this PhD journey in ways I will never forget. Your dedication to securing the datasets and resources, along with your constant encouragement, pushed me to keep learning and growing. Beyond the academics, you taught me invaluable lessons in resilience and patience. Ken, I am deeply grateful for your constant support throughout this process. Your thoughtful insights and ongoing encouragement gave me the confidence to tackle challenges head-on, and you always created a welcoming and supportive environment. I cannot thank you both enough for everything you have done to help me along the way.

A special thank you goes to **Prof. Eugen Dempsey** and **Dr John O'Toole**. I cannot express how much I learned from you both. I genuinely enjoyed every single collaboration, and I am so glad I got to work with you on this exciting project.

To all the **families and hospital staff at Cork University Maternity Hospital**—you are the true heroes of this research. Thank you for trusting us with your data and for your willingness to participate. Your contributions will help improve neonatal care, and I am honoured to be part of that.

And now, it is time to thank the dearest people in my life—my beloved parents, **Manoochehr** and **Mottahareh**. Thank you for being my constant support, even with thousands of kilometres between us. You always believed in me and took more pride in my smallest successes than I ever could. I am deeply grateful that you encouraged me to be brave, independent, and unafraid to embrace new experiences and challenges. The distance between us was the most difficult part of this journey, but I hope this dissertation makes you proud, as it is, more than anything, a reflection of your patience and big hearts. **Milad** and **Zohreh**, thank you for all the positive energy and support you have shown me throughout this time. I love you!

و اما نوبت تشکر از عزیزای دلم؛ **مامان و بابای عزیزم**، مرسی که با وجود هزاران کیلومتر فاصله، برام پناه و حامی بودین و همیشه از هر موفقیت کوچیکی بیشتر از خودم خوشحال شدین و همیشه من رو باور داشتین. ممنون که منو تشویق کردین شجاع و مستقل باشم و از یاد گرفتن و تجربه کردن نترسم. دوری از شما سخت ترین قسمت این کار بود. امیدوارم این پایان‌نامه خوشحالتون کنه، چون بیشتر از هرچیزی، نتیجه زحمتای شماست. **میلاد و زهره عزیزم**، ازتون ممنونم بخاطر همه انرژی مثبت و همدلی که این مدت داشتین. دوستون دارم!

To my wonderful **friends** and my lovely boyfriend, **Cian**, thank you for being my anchors throughout this journey. Your constant support, laughter, and encouragement kept me focused and motivated, even during the toughest times. I am incredibly grateful for everything you've done to keep me going. I love you!

Abbreviations

aEEG	Amplitude-integrated Electroencephalogram
AI	Artificial Intelligence
AUC	Area Under the Curve
BG	Basal Ganglia
CA	Cerebral Autoregulation
CBF	Cerebral Blood Flow
CBFV	Cerebral Blood Flow Velocity
CFOE	Cerebral Fractional Oxygen Extraction
CNN	Convolutional Neural Network
CP	Cerebral Palsy
CPP	Cerebral Perfusion Pressure
CUS	Cranial Ultrasound
ECG	Electrocardiogram
EEG	Electroencephalogram
FC	Fully Connected
FIR	Finite-impulse Response
FTOE	Fractional Tissue Oxygen Extraction
GA	Gestational Age

GMH	Germinal Matrix Haemorrhage
Hb	Haemoglobin
HHb	Deoxygenated Haemoglobin
HIE	Hypoxic Ischaemic Encephalopathy
ICP	Intracranial pressure
IVH	Intraventricular Haemorrhage
LLA	Lower Limit of Autoregulation
LPF-CSD	Low-pass Filtering Compound Sparse Denoising
LPF-TVD	Low-pass Filtering Total Variation Denoising
MABP	Mean Arterial Blood Pressure
ML	Machine Learning
MRI	Magnetic Resonance Imaging
NEC	Necrotizing Enterocolitis
NICU	Neonatal Intensive Care Unit
NIRS	Near-infrared Spectroscopy
O_2Hb	Oxygenated Haemoglobin
PA	Postnatal Age
$PaCO_2$	Arterial Partial Pressure of Carbon Dioxide
PDA	Patent Ductus Arteriosus

PHH	Post-haemorrhagic Hydrocephalus
PIVH	Periventricular Haemorrhage
PRD	Prolonged Relative Desaturation
PVL	Periventricular Leukomalacia
$rcSO_2$	Regional Cerebral Oxygen Saturation
RDS	Respiratory Distress Syndrome
SaO_2	Arterial Oxygen Saturation
SGA	Small for Gestational Age
SpO_2	Peripheral Oxygen Saturation
SSA-DCT	Singular-spectrum Analysis Discrete Cosine Transform
TH	Therapeutic Hypothermia
THb	Total Haemoglobin
ULA	Upper Limit of Autoregulation
VLBW	Very Low Birth Weight
W	Watershed
XGBoost	eXtreme Gradient Boosting

Publications and Presentations

Publications

Publications

Ashoori, M., O'Toole, J.M., Garvey, A.A., O'Halloran, K.D., Walsh, B., Moore, M., Pavel, A.M., Boylan, G.B., Murray, D.M., Dempsey, E.M. & McDonald, F.B. (2024). Machine learning models of cerebral oxygenation (rcSO2) for brain injury detection in neonates with hypoxic-ischaemic encephalopathy. *The Journal of Physiology*, *602*(22), 6347-6360.

[I was responsible for conception and design of the work, and I performed the formal analysis. I was responsible for interpretation of the data and performed validation. I designed and performed the visualisation of methods and results. I wrote the original draft and reviewed and edited the manuscript critically for important intellectual content.]

Ashoori, M., O'Toole, J.M., O'Halloran, K.D., Naulaers, G., Thewissen, L., Miletin, J., Cheung, P.Y., El-Khuffash, A., Van Laere, D., Straňák, Z. & Dempsey, E.M. (2023). Machine learning detects intraventricular haemorrhage in extremely preterm infants. *Children*, *10*(6), 917.

[I was responsible for conception and design of the work, and I performed the formal analysis. I was responsible for interpretation of the data and performed validation. I designed and performed the visualisation of methods and results. I wrote the original draft and reviewed and edited the manuscript critically for important intellectual content.]

Ashoori, M., Dempsey, E. M., McDonald, F. B., & O'Toole, J. M. (2021, November). Sparse-Denoising Methods for Extracting Desaturation Transients in Cerebral Oxygenation Signals of Preterm Infants. In *2021 43rd Annual International Conference of the IEEE Engineering in Medicine & Biology Society (EMBC)* 1010-1013. IEEE.

[I was responsible for conception and design of the work, and I performed the formal analysis. I was responsible for interpretation of the data and performed validation. I designed and performed the visualisation of methods and results. I wrote the original draft and reviewed and edited the manuscript critically for important intellectual content.]

O'Connor, K. M., **Ashoori, M.**, Dias, M. L., Dempsey, E. M., O'Halloran, K. D., & McDonald, F. B. (2021). Influence of innate immune activation on endocrine and metabolic pathways in infancy. *American Journal of Physiology-Endocrinology and Metabolism*, *321*(1), E24-E46.

[I designed and performed the visualisation of the review paper.]

Papers in Preparation

Ashoori, M., O'Toole, J. M., O'Halloran, K. D., McDonald, F. B., Greisen, G., SafeBoosC-III Consortium, & Dempsey, E. M. Features of cerebral oxygen desaturation in preterm infants can detect IVH; data from SafeBoosC-III.

[I was responsible for conception and design of the work, and I performed the formal analysis. I was responsible for interpretation of the data and performed validation. I designed and performed the visualisation of methods and results. I wrote the original draft.]

Magarelli, F., Boylan, G. B., Montazeri, S., O'Sullivan, F., Lightbody, D., **Ashoori, M.**, Ceranic, T., & O'Toole, J. M. "Machine-Learning Competition to Grade EEG Background Activity in Newborns with Hypoxic-Ischaemic Encephalopathy"

[I was responsible for the formal analysis, interpretation of the data and validation.]

Oral Presentations

European Cooperation in Science and Technology (COST), Cork, Ireland, February-March 2024:

M Ashoori, JM O'Toole, KD O'Halloran, EM Dempsey, FB McDonald, MONItOr and HIP consortia. "AI-based analysis of cerebral oxygenation in preterm and term infants"

M Ashoori, "Machine-learning EEG challenge: competition and results"

Futures Life Sciences Conference, Cork, Ireland, December 2023:

M Ashoori, JM O'Toole, KD O'Halloran, EM Dempsey, FB McDonald, MONItOr consortium. "AI Models of Cerebral Oxygenation Detect Brain Injury in Term Neonates with Hypoxic-Ischaemic Encephalopathy"

8th International Neonatology Association Conference (INAC), Dublin, Ireland, September 2023:

M Ashoori, JM O'Toole, KD O'Halloran, EM Dempsey, FB McDonald, MONItOr and HIP consortia. "Artificial intelligence in analysis of cerebral near-infrared spectroscopy"

43rd Annual International Conference of the IEEE Engineering in Medicine and Biology Society (EMBC), Virtual event, November 2021:

M Ashoori, EM Dempsey, FB McDonald, JM O'Toole. "Sparse-Denoising Methods for Extracting Desaturation Transients in Cerebral Oxygenation Signals of Preterm Infants"

Poster Presentations

15th International Newborn Brain Conference (INBBC), Cork, Ireland, February-March 2024:

M Ashoori, JM O'Toole, KD O'Halloran, GB Boylan, EM Dempsey, FB McDonald, HIP consortium. "Exploring the relationships between mean arterial blood pressure and quantitative EEG features in extremely preterm Infants"

College of Medicine and Health (CoMH) Futures Research Conference, Cork, Ireland, September 2023:

M Ashoori, JM O'Toole, KD O'Halloran, EM Dempsey, FB McDonald, MONItOr and HIP consortia. "Feasibility of Utilising Deep Learning to Categorise Cerebral Near-infrared Spectroscopy in Neonates"

The Physiological Society Annual Conference, Harrogate, UK, July 2023:

M Ashoori, JM O'Toole, AA. Garvey, KD O'Halloran, FB McDonald, EM Dempsey, MONItOr consortium. "Machine-learning analysis of near-infrared spectroscopy to improve clinical decision making for hypoxic-ischaemic encephalopathy in term infants."

Paediatric Academic Society (PAS), Washington DC, USA, April 2023:

M Ashoori, JM O'Toole, AA. Garvey, KD O'Halloran, FB McDonald, EM Dempsey, MONItOr consortium. "Early prediction of brain injuries in term infants based on cerebral near-infrared spectroscopy"

Paediatric Academic Society (PAS), Denver, USA, April 2022:

M Ashoori, JM O'Toole, KD O'Halloran, EM Dempsey, FB McDonald. "Early cerebral desaturation events in extremely preterm infants are associated with intraventricular haemorrhage in the first week of life"

13th International Newborn Brain Conference (INBBC), Florida, USA, February 2022:

M Ashoori, JM O'Toole, KD O'Halloran, EM Dempsey, FB McDonald. "Early cerebral desaturation events in extremely preterm infants predict intraventricular haemorrhage in the first week of life"

Awards

College of Medicine and Health (COMH) Doctoral Bursary Awards, January 2024

Finalist in INFANT Research Centre Machine-learning EEG challenge, February 2024

Chapter 1. Introduction

1.1. Newborn Brain Physiology

1.1.1. Extrauterine Transition

In the human experience, the most rapid and intricate physiological adaptation takes place during the transition from a foetus to a newborn. The newborn's survival requires a swift transition before medicalisation of the delivery becomes necessary. To some degree, all organ systems are engaged, but the primary immediate adaptations are the cardiovascular adjustments to pressure and flow and the establishment of air-breathing (Hillman et al., 2012). Initiation of breathing is facilitated by clearance of foetal lung fluid in the airspaces within the lung during labour and after birth (Jain & Eaton, 2006). Surfactant is released by type II pneumocytes within the alveoli, starting late in gestation, reducing the surface tension at the air-liquid interface within the alveoli. This reduction in surface tension is vital for establishing functional residual capacity and preventing alveolar collapse, thereby ensuring efficient gas exchange (Faridy & Thliveris, 1987; Hallman, 2013). Significant changes take place in the cardiovascular system of a newborn following birth. Physiological cord clamping ends the infant’s dependence on the placenta, as the primary site for foetal gas exchange and nutrition. The cardiac output increases to facilitate the rise in basal metabolism and the work of breathing. The circulation pattern transitions from foetal (parallel) to adult-like (series) resulting in equivalent output of right and left ventricles to the pulmonary and systemic circulations, respectively (Hillman et al., 2012).

The newborn transition can be assessed using five signs evaluated at five minutes after birth in the Apgar score: heart rate, respiratory effort, reflex irritability/response,

muscle tone, and colour (Apgar, 1966; Drage et al., 1964). Each parameter is scored from 0 to 2, resulting in a total score ranging from 0 to 10, with a score of 10 indicating that the infant is "in the best possible condition". Apgar scores are typically categorised as low (0-3), intermediate (4-6), and normal (7-10) (Apgar, 2015). They are evaluated at 1 minute, 5 minutes, and then every 5 minutes until the score exceeds 7 (Thorngren-Jerneck & Herbst, 2001).

1.1.2. Common Complications in Neonatal Care

Prematurity

According to the World Health Organisation (WHO), preterm birth is defined as birth prior to 37 completed weeks of gestational age and can be subdivided into three categories: extremely preterm (< 28 weeks), very preterm (28-32 weeks) and moderate-to-late preterm (32-37 weeks) infants (World Health Organisation, 2023). Very Low Birth Weight (VLBW) is often associated with preterm birth, particularly with extremely and very preterm infants. VLBW is a term used to describe infants who are born weighing less than 1500 grams (Stoll & Hansen, 2003). It is understood that the risks of preterm birth increase with decreasing gestational age (GA) (Marlow, 2012). Immature cardiorespiratory physiology in preterm infants challenges the rapid and successful physiological transition to extrauterine conditions in terms of fluid dynamics in the lung, lack of surfactant, immature respiratory control network, poor cardiac output, limited pulmonary perfusion and the presence of anatomical shunts. Preterm infants are therefore at risk of hypoxia (hypoxic hypoxia and/or ischaemic hypoxia) and inflammation. Lung damage arising from resuscitation procedures and associated interventions including mechanical ventilation and supplemental oxygen

can also cause iatrogenic harm compounding infant morbidity (Hillman et al., 2012). Head circumference in preterm infants provides valuable insights into brain growth and development, typically being smaller than that of term infants, and is associated with brain injury (Ahn, 2011).

There are several potential causes of premature birth. Intrauterine infection in the mother, such as urinary tract infections or sexually transmitted infections, can increase the risk of preterm birth by triggering a cascade of inflammatory processes (Slattery & Morrison, 2002; Zhou et al., 2010). These infections introduce pathogens into the uterine environment, activating the maternal immune system to release proinflammatory cytokines like interleukin-6 (IL-6), interleukin-1β (IL-1β), and tumour necrosis factor-alpha (TNF-α). This inflammatory response weakens the foetal membranes, increases their susceptibility to rupture, and stimulates uterine contractions (Annells et al., 2004; Cappelletti et al., 2016). Furthermore, studies using animal models have shown that systemic inflammation can lead to significant cardiorespiratory disturbances in neonates, including severe apnoea's and bradycardias. This occurs as the inflammatory response affects brainstem centres responsible for respiratory and cardiovascular regulation, disrupting normal autonomic control (Nault et al., 2022; Kausch et al., 2024).

Maternal chronic health conditions, such as thyroid disease, asthma, diabetes, and hypertension, are linked to higher incidences of premature birth (Goldenberg et al., 2008). Incompetent cervix is another risk factor for premature birth. As labour approaches, the cervix undergoes changes such as shortening, softening, rotating forward, and opening. Research has found that a cervical length shorter than 25 mm

indicates a higher risk of preterm birth (Iams et al., 1996; Andrews et al., 2000). Furthermore, vaginal bleeding resulting from placental abruption or placenta previa can disrupt the flow of oxygen and nutrients to the foetus and is linked to a significantly elevated risk of premature delivery (Krupa et al., 2006). Each of the following factors—high levels of stress, smoking, drug use, and alcohol consumption during pregnancy—can significantly increase the risk of premature birth (Zuckerman et al., 1989; Orr et al., 2002; Tracy et al., 1997; Bermudez et al., 2002). Moreover, pregnancies involving multiple babies (e.g., twins or triplets) pose a significant risk for preterm birth, accounting for 15–20% of all preterm deliveries. It is believed that uterine overdistension plays a key role in triggering contractions and preterm premature rupture of the membranes, contributing to the increased rate of spontaneous preterm births (Romero et al., 2006).

Premature birth can have significant consequences for both the infant and the mother. Preterm neonates often suffer from respiratory distress syndrome (RDS), a condition that arises when their premature lungs are not fully developed and do not produce sufficient surfactant to keep the alveoli in the lungs patent (Jobe & Bancalari, 2001; Baraldi & Filippone, 2007). The systemic hypoxia and reduced oxygen delivery associated with RDS, or other complications of prematurity can contribute to necrotizing enterocolitis (NEC), an inflammatory condition that damages the intestines. NEC poses a serious threat to premature infants, potentially leading to intestinal perforation and sepsis (Neu & Walker, 2011). Additionally, the kidneys' limited ability to excrete acids and reabsorb bicarbonate in preterm infants disrupts the maintenance of pH and fluid homeostasis, impairing their capacity to regulate acid-base balance and manage blood volume effectively. As a result, these

deficiencies can worsen metabolic imbalances and complicate fluid management in this vulnerable group (Rubin et al., 1961; Edelmann et al., 1967). Moreover, preterm infants are at an increased risk of brain injuries, including white matter injury, intraventricular haemorrhage (IVH), and cerebellar haemorrhage. These forms of brain injury are associated with neurological disorders such as cerebral palsy, characterised by impaired movement and coordination, as well as delays in cognitive, language, social-emotional and adaptive development (Inder et al., 2023; Ballabh, 2010; Doyle & Anderson, 2010). Compared to full-term infants, preterm infants are more susceptible to cognitive deficits such as lower intelligence quotient scores and academic performance challenges; these deficits may persist into adolescence and adulthood (Bhutta et al., 2002; Drummond et al., 2019).

Hypotension

Exactly how one defines low blood pressure in premature infants, and how it is managed, especially in those born before 28 weeks, remain topics of debate. (Rabe & Rojas-Anaya, 2017; Cox & Groves, 2012). One method of defining abnormal blood pressure is based on normative values. Hypotension is often defined as persistent systolic and/or diastolic blood pressure more than two standard deviations below the normal mean values (Fanaroff & Fanaroff, 2006). However, blood pressure is correlated with both gestational age and birth weight and increases daily during the first week of life. Thus, for preterm infants, determining the normal blood pressure for their age is still a challenge.

Another definition of hypotension is based on the onset in the reduction of cerebral blood flow (CBF). The mean blood pressure at which CBF autoregulation is impaired,

known as the autoregulatory blood pressure threshold, is widely accepted as the definition of hypotension (Seri, 2001). Generally, at this level, cellular function and structural integrity are not impacted due to increased cerebral fractional oxygen extraction (CFOE), vascular vasodilation, and a leftward shift in the haemoglobin-oxygen dissociation curve (Munro et al., 2004; Kissack et al., 2005). The specific mean arterial blood pressure level at which cerebrovascular autoregulation fails in preterm infants is unknown. However, some studies report that this threshold might be around 28 to 30 mm Hg, even in infants with extremely low birth weights (Munro et al., 2004). When blood pressure drops further, a functional blood pressure threshold is reached where brain function is compromised. The exact mean arterial blood pressure at which this occurs in very preterm infants is not known, but it is thought to be around 24 mm Hg during the early days after birth (Victor et al., 2006; Kissack et al., 2005; Weindling & Subhedar, 2007). Finally, if blood pressure decreases further, it approaches an ischaemic blood pressure threshold, at which cell viability is jeopardised (McLean et al., 2012). While the ischaemic blood pressure threshold in VLBW neonates on their first day after birth remains uncertain, it is thought to possibly be lower than 20 mm Hg (Victor et al., 2006; Victor et al., 2006). However, it is important to highlight the fact that there is no prospectively gathered data on the mortality and morbidity associated with these varying blood pressure thresholds.

Currently, the most common criterion for diagnosis of hypotension in preterm infants is a mean blood pressure lower than a threshold, often determined as the mean blood pressure (in mm Hg), being less than the infant's gestational age, measured in completed weeks (Dempsey et al., 2021). In hypotensive preterm newborns, reduced cerebral blood flow (Børch et al., 2010; Munro et al., 2004) and impaired cerebral

autoregulation (CA) (Tsuji et al., 2000; Wong et al., 2008) are important pathophysiological mechanisms in the brain and are associated with increased rates of intraventricular haemorrhage (IVH), ischaemic cerebral lesions, and death (Miall-Allen et al., 1987). However, treatment for hypotension is also linked with poor neurodevelopmental outcome (Batton et al., 2009). Despite the lack of evidence to support such methods, many preterm newborns continue to receive interventions for low blood pressure (Dempsey & Barrington, 2007). A study on preterm piglets showed that saline infusion failed to increase blood volume or prevent cardiovascular decline (Eiby et al., 2023). The most popular course of treatment is dopamine infusion after a volume bolus (Stranak et al., 2014). Although dopamine often raises blood pressure, its short- and long-term consequences are unknown (Subhedar et al., 1996). There are concerns that inotrope therapy such as this may be linked to an increase in intraventricular haemorrhage (IVH) prevalence and unfavourable long-term outcomes (Faust et al., 2015; Batton et al., 2016). As such, a more restrictive approach, known as permissive hypotension, has been proposed (Dempsey et al., 2009). This treatment suggests that infants with blood pressure lower than their gestational age, yet displaying signs of good clinical perfusion, are carefully monitored instead of receiving immediate treatment (Dempsey et al., 2009).

The multicentre randomised trial, Management of Hypotension in Preterm Infants (HIP), investigated different approaches to treating hypotensive infants born before 28 weeks of gestational age. Participants were randomly assigned to receive a saline bolus followed by either a dopamine infusion (standard treatment) or a placebo infusion (restrictive approach). Unfortunately, the study was ultimately not powered sufficiently to identify any significant differences in clinical outcomes between the

two groups, likely due to strict inclusion criteria and low recruitment (Dempsey et al., 2021).

Cerebral Autoregulation

Cerebral autoregulation (CA) is a complex physiological mechanism that maintains relatively constant cerebral blood flow (CBF) despite variations in cerebral perfusion pressure (CPP). This autoregulatory process is crucial for ensuring that the brain receives a stable supply of oxygen and nutrients, which is essential for normal brain function and metabolism (Paulson et al., 1990). CA operates primarily through alterations in the diameter of cerebral blood vessels; when CPP increases, cerebral vessels constrict to reduce blood flow, and conversely, they dilate when CPP decreases (Silverman & Petersen, 2020). The prevailing hypothesis is that there are specific maximum and minimum thresholds in the regulation of vascular resistance and the maintenance of CA within these limits is generally illustrated as the autoregulatory plateau (Greisen, 2005). However, the upper and lower thresholds of cerebrovascular autoregulation are not yet known. This uncertainty is partly because these thresholds may vary among infants and even within the same infant, potentially influenced by various factors like the gestational (GA) and postnatal age (PA) as well as the partial pressure of carbon dioxide (Rhee et al., 2016; Hoffman et al., 2018). In other words, CA has a dynamic nature and can undergo changes due to evolving brain injury and/or because of ongoing medical supports (Rhee et al., 2018).

The typical mechanistic representation of CA is a sigmoid-shaped curve, showing stable cerebral blood flow (CBF) over a certain cerebral perfusion pressure (CPP) range, with pressure-passive CBF outside this range (as illustrated in Figure1.1.). The

functional autoregulation range, termed the autoregulatory plateau, is defined by the upper limit of autoregulation (ULA) and the lower limit of autoregulation (LLA). Cerebral vasoreactivity is operational only within this plateau range. When CPP is above the ULA or below the LLA, CBF becomes passive to blood pressure changes due to reduced vasoreactivity, placing the brain at risk of either hyperaemic or hypoperfusion injuries (Rhee et al., 2018). When CA is impaired, a decrease in mean arterial blood pressure can lead to a corresponding reduction in cerebral blood flow. This could result in inadequate oxygen and nutrient supply to the brain, potentially causing ischaemic hypoxia injury. Conversely, an increase in mean arterial blood pressure may lead to a proportional rise in cerebral blood flow, resulting in cerebral hyperperfusion which increases the risk of blood vessel rupture causing severe intraventricular haemorrhage and mortality (Toth et al., 2016). Infants who developed periventricular-intraventricular haemorrhage (PIVH – a haemorrhage that occurs when vessels of the germinal matrix in the periventricular area rupture, which can then extend into the ventricles as IVH) usually exhibit cerebral hyperperfusion and non-responsive cerebral blood flow under varying arterial blood pressure conditions before the development of severe PIVH. There is also correlation between regional cerebral oxygen saturation ($rcSO_2$) and arterial blood pressure that could indicate a lack of CA in neonates with PIVH (Tsuji et al., 2000; O'Leary et al., 2009; Alderliesten et al., 2013).

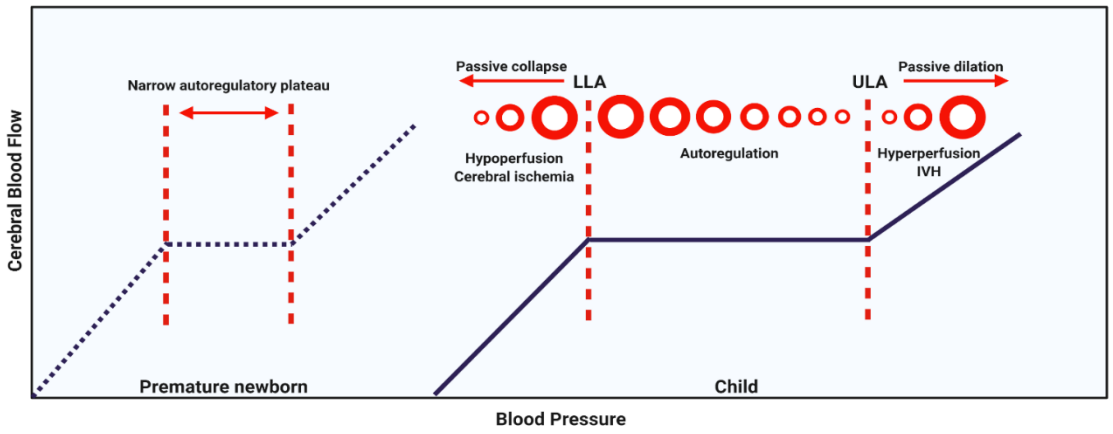

Figure1.1. Cerebral autoregulation in relation to vascular response

Whether preterm infants are born with intact cerebrovascular autoregulation, or if this capability develops gradually after birth remains a topic of research. CA is hypothesised to improve between 23 and 33 weeks of gestation (Rhee et al., 2014). Infants born during this time may exhibit immature vasoreactivity that is necessary to maintain CA (Rhee et al., 2018). It is also likely that premature infants face more physiological challenges which leads to changes in metabolism and fluctuations in perfusion pressure outside of the functional regulatory range which currently limit broad conclusions on the autoregulatory curve (Vesoulis & Mathur, 2017). Two studies revealed fully functional cerebrovascular autoregulation in all preterm infants they examined. These studies included preterm infants who were receiving high-frequency oscillatory ventilation and infants being treated for low blood pressure (Noone et al., 2003; Wardle et al., 2000). Conversely, Boylan et al. (2000) investigated dynamic autoregulation by measuring cerebral blood flow velocity (CBFV) and arterial blood pressure (ABP). They discovered a complete lack of autoregulation in both 'high-risk' preterm infants (characterised by cerebral issues like seizures or

intraventricular haemorrhage) and in their control group of preterm infants (Boylan et al., 2000). Similarly, Soul et al. (2007) observed impaired cerebrovascular autoregulation approximately 20% of the time using near-infrared spectroscopy (NIRS) in 87 out of 90 extremely preterm infants during their first five days after birth (Soul et al., 2007). It has been proposed that the autoregulatory plateau range and the position of lower and upper limits are narrower and lower in preterm infants compared to term infants (Wong et al., 2012) (Figure1.1).

1.2. Brain Injuries in Infants

1.2.1. Intraventricular Haemorrhage (IVH)

Intraventricular haemorrhage (IVH) is defined by bleeding within or near the ventricles of the brain where cerebrospinal fluid is located. IVH is common in infants born before 32 weeks of gestational age and particularly high in those born before 27 weeks of gestational age and is closely associated with neurodevelopmental disabilities (Yeo et al., 2020; Mukerji et al., 2015). Studies have consistently shown that male infants have a higher incidence of IVH compared to females, although the exact reasons for this sex difference are not fully understood. Factors such as hormonal influences and differences in brain development, however, may contribute to this disparity (Tioseco et al., 2006; Cuestas et al., 2009).

IVH primarily results from the vascular immaturity and the consequential injury can be dramatic as it often occurs near the germinal matrix, a highly vascularised region of the brain which contains stem cells amongst other cell types and from where cells migrate during brain development (Gilard et al., 2020).

The classification of IVH into four grades is based on the extent and location of the bleeding. Grade I involves limited germinal matrix haemorrhage, affecting less than 10% of the ventricle. Grade II is characterised by IVH spreading into the ventricle without enlarging it, occupying no more than 50% of the ventricular space. Grade III IVH involves blood filling and expanding the ventricular system, affecting more than 50% of the ventricular space. Grade IV, the most severe, involves periventricular venous infarction, indicating extensive IVH with involvement of surrounding brain tissue (McCrea & Ment, 2008; Hinson et al., 2010; Larroque et al. 2003). A study of 2,386 VLBW infants revealed the incidence rates for Grades I to IV IVH as 25.1%, 7.0%, 4.8%, and 5.5%, respectively (Ahn et al., 2015). There is a direct correlation between severity of IVH grade and increasingly adverse outcomes (Bolisetty et al., 2014).

Infants with IVH can clinically present in various ways; the condition may be silent, showing no symptoms at all, or have a saltatory presentation whereby symptoms such as altered consciousness, low muscle tone, respiratory distress, and changes in eye movements emerge within a few hours after birth. In more severe cases, known as catastrophic IVH, symptoms can develop rapidly, from minutes to hours after birth, and include seizures, stupor, coma, rigid posture, muscle weakness, and a swollen soft fontanelle (Robinson, 2012; Ballabh, 2010).

The presence of blood within the ventricles as a result of IVH, can lead to an increase in intracranial pressure (ICP), disrupting normal cerebral blood flow (CBF). This disruption can cause cerebral hypoxia, depriving the brain tissue of essential oxygen and nutrients (Volpe, 1998; Baburamani, et al., 2012; Vesoulis et al., 2019; Ballabh & de Vries, 2021). The haemorrhage also triggers inflammation and the release of

neurotoxic substances, exacerbating brain injury. The resulting blood clot can obstruct cerebrospinal fluid (CSF) pathways, leading to post-haemorrhagic hydrocephalus, which further elevates intracranial pressure and aggravates brain injury (Baburamani, et al., 2012; Leviton et al., 2013; Ballabh & de Vries, 2021; Chen et al., 2021). Furthermore, the blood loss and hypoxia associated with IVH can induce apoptosis of oligodendrocyte precursor cells (Oligodendrocytes are responsible for myelination in the developing brain). Oligodendrocyte precursor cells are highly vulnerable to hypoxic-ischemic injury, and their loss leads to a failure of normal myelination (Kuo & Huang, 2021; Ballabh & de Vries, 2021). The lack of myelination is crucial because myelin is essential for the speed of conduction of nerve impulses, and its deficiency disrupts neural communication, leading to both motor and cognitive deficits (Ballabh & de Vries, 2021). Preterm infants with IVH often face myriad developmental challenges: low scores in psychomotor and mental development, a high occurrence of cerebral palsy, and visual impairments. The severity of these developmental issues generally increases with the increasing severity of IVH (Bolisetty et al., 2014). In the short term, IVH can lead to significant complications like post-haemorrhagic hydrocephalus (PHH) and periventricular leukomalacia (PVL). In the long term, it can result in a range of cognitive, physical, and behavioural abnormalities (Klebermass-Schrehof et al., 2012; McCrea & Ment, 2008).

Cranial ultrasonography (CUS) is recommended for all preterm infants under 30 weeks, ideally conducted once between 7-14 days of age and again between 36- and 40-weeks' postmenstrual age. This screening is crucial for detecting conditions such as IVH, which can impact clinical care, as well as the progression of PVL, offering insights into long-term neurodevelopmental outcomes (McCrea & Ment, 2008; Ment

et al., 2002). Bedside assessment with CUS is a cost-effective, non-invasive method that causes minimal disturbance to infants. However, it is less sensitive in the detection of white matter abnormalities like PVL, compared to magnetic resonance imaging (MRI). Despite the increased sensitivity of MRI, data supporting its use in predicting adverse neurodevelopmental outcomes in premature infants remains limited (Ment et al., 2002, Rademaker et al., 2005; Leijser & Cowan, 2007; Panigrahy et al., 2012).

Near Infra-Red Spectroscopy (NIRS), another non-invasive, yet continuous bedside tool, complements these techniques by monitoring cerebral oxygenation and is often used as a surrogate measure of blood flow. It is especially useful in NICUs for real-time tracking of conditions that indicate IVH risk, aiding in early intervention and potentially improving outcomes. However, its routine clinical use has yet to be established (Noori et al., 2014; Verhagen et al., 2010; Alderliesten et al., 2013).

While there is no definitive treatment for IVH, the typical approach involves managing blood pressure, intracranial pressure, and respiratory stress in neonates. This includes preventing complications such as re-bleeding and addressing any coagulation disorders to blunt IVH progression. Additionally, IVH management focuses on screening and treating related sequelae like PHH and PVL (Shooman et al., 2009; McCrea & Ment, 2008; Hinson et al., 2010). Temporary surgical management of severe IVH can prevent PHH development prior to ventriculoperitoneal shunting, the ultimate treatment for PHH, effectively diverting cerebrospinal fluid in affected infants. However, PVL is associated with poor long-term outcomes, shunt infections,

and risk of shunt obstructions leading to shunt failure (Shooman et al., 2009; Robinson, 2012).

Alderliesten et al. (2013) suggested a correlation between cerebral hypoperfusion and PIVH. Research to date however has not determined if low cerebral oxygenation contributes to IVH, or if it should be considered a consequence of IVH. Vesoulis et al. (2019) found in a longitudinal multi-centre study that there was a connection between severe hypoxaemia during the first week of life and severe IVH. Sorensen et al. (2008) also observed that infants who experienced reduced cerebral oxygenation on the first day after birth were more likely to develop IVH later. Additionally, Pichler et al. (2019) suggested that neonates who developed IVH within the first week after birth had lower cerebral $rcSO_2$ values immediately following birth compared to those who did not develop IVH. Peng and colleagues (2015) suggested that there is a significant difference in cerebral oxygenation during the first 12 hours of life between infants with and without evidence of IVH on MRI examination.

More recently, Vesoulis et al. (2021) investigated the influence of different grades of IVH and white matter injury on brain oxygenation in preterm infants. They noted that IVH was associated with a decline in cerebral oxygen saturation, that could continue for 68 days in some cases. This result was more obvious in infants with severe IVH. It has been argued that this extended cerebral oxygen desaturation might increase the risk for further cerebral injuries. Similarly, Verhagen et al. (2010) postulated that preterm infants developing germinal matrix haemorrhage – intraventricular haemorrhage (GMH-IVH) had lower $rcSO_2$ and greater fractional tissue oxygen extraction (FTOE) during the following 2 weeks after birth compared to infants

without GMH-IVH. Increased FTOE represents either increased oxygen consumption or an increase in ability to extract oxygen in the presence of low blood flow. The decrease in $rcSO_2$ occurring after IVH, can cause a secondary injury (Vesoulis et al., 2021).

The reduction in cerebral oxygenation following IVH can be attributed to two factors: The presence of blood in the extravascular space in infants with IVH and impaired CA. The presence of extravascular blood in infants with IVH can absorb infrared light and may contribute to the "cerebral" saturation readings detected by the NIRS monitor although it remains in a deoxygenated state. Since a single-sensor NIRS device is unable to differentiate between intravascular and extravascular blood, this desaturated pool may theoretically lower the overall measured cerebral saturation by being averaged with the oxygenated blood still in circulation (Vesoulis et al., 2021). Furthermore, impaired CA contributes to the reduction in cerebral oxygenation. Evidence strongly indicates that the autoregulatory system is less robust and developmentally immature in preterm neonates, making it particularly vulnerable to the effects of IVH (Soul et al., 2008; Vesoulis et al., 2016; Wong et al., 2008).

Ng et al. (2019) suggested that infants with IVH spent a greater percentage of time in hypoxia than those without, in the first 24 hours of life. Alderliesten et al. (2013) proposed that a temporary increase in cerebral oxygenation may result in decreased oxygen utilisation and contribute to IVH. It has also been suggested that following IVH, there could be alterations in brain metabolism leading to increased extraction of cerebral tissue oxygen and subsequently significant desaturation of cerebral blood oxygen, which might play a crucial role in white matter injury. Ment et al. (1984)

indicated that reduced CBF could be due to the presence of the haemorrhage itself. While it remains uncertain if there is a direct link between hypoxemia and IVH, severe hypoxaemic burden during the first week of life likely contributes partially to brain injury in preterm infants (Vesoulis et al. 2019).

1.2.2. Hypoxic Ischaemic Encephalopathy (HIE)

Hypoxic-ischaemic encephalopathy (HIE) can occur in both term and preterm infants but is less well defined and more complex in preterm infants (Gopagondanahalli et al., 2016). In term infants, HIE is still a cause of significant neurological impairment despite the increasing application of therapeutic hypothermia (Kurinczuk et al., 2010).

Perinatal asphyxia stands as a primary cause of HIE. Intrauterine asphyxia is often caused by poor placental blood flows due to either umbilical cord occlusion, cord wrapped around the neck, cord prolapse, or poor gas exchange, arising from foetal issues like bradycardia, thrombosis, and haemorrhage or maternal complications such as preeclampsia, placental abruption, maternal hypotension, severe anaemia, asthma, and chronic vascular diseases. After birth, asphyxia is typically a result of neonatal respiratory failure caused by conditions like severe hyaline membrane disease, meconium aspiration syndrome, pneumonia, or congenital heart defects (Barkovich, 2005; Barkovich et al., 2001; Zarifi et al., 2002; Ferriero, 2004; Shalak & Perlman, 2004).

The degree and duration of the hypoxia determines the extent of brain injury, though this is not currently well defined in absolute terms. Mild-moderate reductions in cerebral blood flow can be compensated by redistributing blood flow from the anterior circulation to the posterior circulation, ensuring sufficient perfusion of critical

brain regions such as the brainstem, cerebellum, and basal ganglia (Macnab, 2020). Severe hypoxia can cause damage to vital brain regions such as the basal ganglia and Thalami (Harteman et al. 2013).

Though the aetiology of hypoxic-ischaemic encephalopathy is heterogenous, cerebral hypoxic ischaemic injury has common pathophysiological consequences that can be summarised as follows; the primary phase of injury or the acute phase is marked by reduced oxygen and glucose delivery to the brain, leading to anaerobic metabolism, decreased ATP production, and increased lactic acid levels, culminating with energy failure and acidosis leading to cell death (Wassink et al. 2014). Following the acute phase, a partial recovery may occur lasting from 1 to 6 hours, which is characterised by recovery of oxidative metabolism and inflammation. A secondary deterioration occurs within approximately 6 to 15 hours after the initial insult, in neonates with moderate to severe injury. This phase is associated with “secondary energy failure” which leads to cell death, clinical deterioration, and seizures (Bennet et al. 2006; Wassink et al. 2014).

Currently, there is no bedside tool for precisely diagnosing HIE in newborns. Instead, HIE is identified by observing neurological symptoms indicative of neonatal encephalopathy. Key signs of this condition include reduced consciousness often accompanied by respiratory issues, abnormalities in muscle tone and strength, disturbances of cranial nerve functions, and seizures (Volpe, 2012). Diagnosis also requires evidence of low Apgar scores and metabolic acidosis, observed in arterial cord blood gas. It is widely recognised that a low pH (<7.10) or a high base deficit (>12 mmol/L) are linked to poor outcomes (Yeh et al., 2012; Malin et al., 2010). pH and

base deficit are primarily utilised as screening tools for encephalopathy and are incorporated into the scoring systems used to determine the initiation of therapeutic hypothermia (TH) (Azzopardi et al., 2008).

Newborns suspected of having HIE are assessed using the Sarnat staging system (Sarnat & Sarnat, 1976). This system measures various factors including consciousness, muscle tone, tendon reflexes, complex reflexes, and autonomic function. Based on this, neonatal HIE is categorised into three levels: stage I (mild), stage II (moderate), and stage III (severe). To determine eligibility for hypothermia therapy, a modified version of the Sarnat staging system is used (Chalak et al., 2018). In newborns with HIE, monitoring, prognosis, and response to hypothermia therapy are evaluated using a blend of neurological examination, magnetic resonance imaging (MRI), and electroencephalography (EEG) (van Laerhoven et al., 2013). However, there are challenges to applying this additional monitoring. For example, severely ill neonates might not be stable enough to be transported for a brain MRI or to endure the duration of the MRI scan. Additionally, hypothermia therapy can reduce the effectiveness of amplitude-integrated EEG (aEEG) in early prognosis. It is also noted that improvements in aEEG readings might only become apparent after the rewarming process and when sedation has ceased (Thoresen et al., 2010). Furthermore, these existing technologies fail to provide all the essential physiological data required for continuous monitoring of changes in the newborn brain. Therefore, there is space for new or improved bedside tools to monitor these patients over time.

Therapeutic hypothermia (TH) is the accepted treatment for newborns with HIE. This approach involves maintaining a mild hypothermia of ~ 33.5°C to 35.0°C. Large

multicentre studies have provided evidence to support TH as a safe and effective intervention (Azzopardi et al., 2009; Gunn et al., 2008; Shankaran et al., 2005). A recent meta-analysis, which examined outcomes from seven hypothermia trials involving 1214 neonates randomised to either cooling or standard care, found that TH significantly lowers the risk of death or serious neurodevelopmental issues at 18 months for neonates with moderate to severe HIE (Tagin et al., 2012).

Currently, there are two primary methods of TH: whole-body cooling and selective head cooling. Both methods are equally effective, but whole-body cooling is more commonly used due to its lower cost and ease of application (Douglas-Escobar & Weiss, 2015). Meta-analysis also indicates that there is no significant difference in reducing long-term neurological problems between these two cooling methods (Tagin et al., 2012). It is recommended that TH is initiated within six hours following birth (Kattwinkel et al., 2010). However, given the undefined aetiology of HIE, the therapeutic window for therapy may extend up to 12 hours post-partum (Jia et al., 2018).

Infants diagnosed with HIE often exhibit significant long-term neurodevelopmental impairments, including behavioural and cognitive impairments (Van Handel et al., 2007), developmental delays (Belet et al., 2004), and motor deficits (van Schie et al., 2015). Previously, it was considered that infants with mild HIE would have normal developmental outcomes (Sarnat & Sarnat, 1976). However, recent insights reveal that these infants are at a higher risk for negative neurodevelopmental consequences, particularly in areas such as learning, emotional, and behavioural challenges (Conway et al., 2018).

1.3. Physiological Monitoring and Brain Imaging in Early Life

1.3.1. The Role of MRI and Ultrasound in the Classification of Neonatal Brain Injuries

Neuroimaging techniques like ultrasound (US), and magnetic resonance imaging (MRI) are helpful in identifying and characterising the precise location, scope, and severity of brain injuries in preterm and term infants (Bano et al., 2017). There are two imaging techniques that are used, T1 and T2. These techniques differ in the intervals between radio frequency pulses and capture of the echo signal. MRI is the most precise and sensitive diagnostic tool for assessing suspected Hypoxic-Ischaemic Encephalopathy in newborns (Bano et al., 2017). In MRI scans, injury to grey matter (including the cortex and deep grey matter) caused by hypoxic-ischaemic events is typically visually apparent as increased signal intensity on T1-weighted images and varied signal intensity on T2-weighted images. The appearance of injury on T2 images can change based on the duration since the initial injury relative to performing the MRI and the specific type of brain damage, like haemorrhage, encephalomalacia, or gliosis. Injuries to white matter are observed as decreased signal intensity on T1-weighted images and increased signal intensity on T2-weighted images, often due to oedema or cystic encephalomalacia resulting from ischaemia (Barkovich, 2005; Hüppi, 2002).

In full-term newborns, mild to moderate hypoxic-ischaemic (HI) injuries often lead to infarcts in the watershed areas located between the anterior/middle cerebral artery and the middle/posterior cerebral artery (Badve et al., 2012; Moghaddam et al, 2024). These infarcts affect both the cortex and the underlying subcortical white

matter. In cases of severe HI injury, the damage typically coincides with regions of high metabolic activity, such as the ventrolateral thalami, posterior putamen, hippocampi, brainstem, corticospinal tracts, and sensorimotor cortex. Damage to the basal ganglia (BG) is more frequent than the parasagittal pattern and is associated with a poorer prognosis (Barkovich, 2005; Barkovich, 2001; Heinz & Provenzale, 2009).

The Barkovich MRI scoring system evaluates brain injury in neonates with perinatal asphyxia, focusing on patterns of damage in deep grey matter and watershed zones. It includes several scores: the basal ganglia (BG) score (0-4), the watershed (W) score (0-5), the combined basal ganglia/watershed (BG/W) score (0-4), and the summation (S) score, which is the arithmetic sum of BG and W scores (0-4). Each score assesses different aspects of brain damage, with higher scores indicating more extensive injury. This system helps in evaluating the extent and severity of brain injury in affected neonates (Barkovich et al., 1998).

MRI is a valuable diagnostic tool for early detection of lesions in preterm infants, but it poses numerous challenges in the context of critically ill infants. Firstly, the procedure is costly due to the infrastructure around this advanced technology and the requirement for expertise both in performing the technique and evaluation of the arising images. Secondly, MRI scans are time-consuming and require patients to remain still for extended periods, which can be challenging and may necessitate a degree of sedation. Additionally, conducting an MRI on these newborns is difficult because they often need constant monitoring and life-support equipment that may not be compatible with the MRI environment (Plaisier et al., 2014; Plaisier et al., 2015).

Cranial ultrasonography (CUS) is an economical imaging method that allows for repeated scanning at the bedside with minimal disturbance to the infant. Historically, CUS has been primarily utilised for identifying germinal matrix haemorrhage and intraventricular haemorrhage (GMH-IVH), as well as PVL. However, its utility in detecting a broader range of lesions is growing, thanks to advances in technology such as high-resolution ultrasound (less than 200 micrometres), quantitative assessments, and the employment of additional acoustic windows like the mastoid and posterior fontanel (Leijser et al., 2006; Govaert & De Vries, 2010; van Wezel-Meijler et al., 2010).

While CUS is a useful imaging tool, it has several limitations that can impact its effectiveness and reliability. Firstly, it is observer dependent, so the accuracy and quality of CUS results can vary significantly depending on the skill and experience of the person conducting and interpreting the ultrasound. This means that consistently obtaining objective and reproducible measurements with CUS can be challenging. Secondly, the posterior fossa, a small space in the skull, which houses critical structures such as the cerebellum and brainstem, is difficult to image accurately with CUS. Due to its location and the bone structures surrounding it, obtaining clear and detailed images of this area can be challenging, which may lead to missed or inaccurate diagnoses of abnormalities in this region. Furthermore, CUS may also have limitations in effectively identifying changes in the cerebral cortex. Detecting subtle changes or early signs of pathology in the cerebral cortex is essential for accurate diagnosis and treatment planning, but CUS may not always provide the necessary resolution or contrast to detect such changes effectively (van Wezel-Meijler et al., 2010; Reynolds et al., 2001).

P/IVH (periventricular/intraventricular haemorrhage) is effectively detected using CUS (McCrea & Ment, 2008). Bleeding typically appears in the initial days following birth, often as a mild haemorrhage (grade I or II). However, in some cases it can progress over the following days and result in serious complications (van Wezel-Meijler et al., 2010). It is recommended that early and frequent CUS scans be conducted within the first weeks of birth for neonates born significantly prematurely, and in cases of P/IVH, that repeated CUS scans, including measurements of the lateral ventricles, be performed over the subsequent weeks. If, after several weeks, either no or just mild, non-worsening PHVD is observed, the frequency of the CUS scans can be reduced (Wezel-Meijler, 2007; van Wezel-Meijler et al., 2010).

In 2002, a practice guideline issued by the American Academy of Neurology and the Practice Committee of the Child Neurology Society advocated for standard screening using CUS in all infants born before 30 weeks of gestation. It is recommended that this screening be conducted at 7 and 14 days of age and then serially, ideally repeated between 36 and 40 weeks of postmenstrual age (Ment at al., 2002). Conducting CUS serially during the first two weeks after birth can identify over 80% of germinal matrix/intraventricular haemorrhage (GM/IVH). However, in a comprehensive study by Paneth et al. (1994), the authors compared ultrasound diagnoses of GM/IVH with postmortem brain examinations, where it was found that sonographic readers initially missed 50% of GM/IVH cases. However, the study also noted that when three consecutive scans were analysed and the lesion measured at least 1 cm in diameter, all instances of GM/IVH were successfully detected (Paneth et al., 1994).

1.3.2. Introduction to Near-Infrared Spectroscopy (NIRS) and Its Application in Neonates.

Inconsistent or insufficient blood flow and oxygen supply to the brain can lead to brain damage (Khwaja & Volpe, 2008). Conditions such as sustained or intermittent changes in the partial pressure of cerebral oxygen (hyperoxia or hypoxia) or variable partial pressure of cerebral carbon dioxide (hypercapnia or hypocapnia) can impair cerebral autoregulation and negatively impact upon the normal development of the brain (Alderliesten et al., 2013; Sola et al., 2014). Measurement of essential vital signs, including blood pressure, heart rate, respiratory rate, peripheral oxygen saturation (SpO_2) and arterial blood-gas analysis (arterial oxygen saturation (SaO_2), haematocrit, PaO_2 and $PaCO_2$ and pH), are necessary for evaluating the health status of a newborn. However, they do not provide a direct measurement of brain oxygenation (Lemmers et al., 2008; Lemmers et al., 2016; El-Dib & Soul, 2019). Near-Infrared Spectroscopy (NIRS) is used to measure regional cerebral oxygen saturation ($rcSO_2$) and provides a non-invasive approach that can be used to assess cerebral oxygen delivery. This technique allows for continuous monitoring at the bedside, over several days, without any adverse effects (Pavlek et al., 2021). Continuous monitoring is advantageous over imaging approaches such as CUS or MRI that capture single point measures. Moreover, NIRS can be employed rapidly in critically ill infants with minimal disturbance. NIRS devices are versatile, suitable for use in NICU settings, during surgeries, and in transit. Additionally, NIRS can be seamlessly integrated with cerebral electrical activity monitoring using amplitude-integrated electroencephalography (aEEG) (Kenosi et al., 2015; Dix et al., 2017).

The NIRS method utilises the relative transparency of biological tissues to near-infrared light. The thin layers of skin and skull in neonates allow for easy penetration of NIR light (ranging from 700 to 1,000 nm). This technique involves a light emitter projecting near-infrared light through the brain tissue, which travels through the cerebral tissue to a depth of 2-3 cm before being detected by optical sensors (Brown et al., 2002). Once near-infrared light reaches haemoglobin, it can be absorbed, reflected, scattered, or transmitted. Since the structure of monitored tissue remains consistent during the NIRS recording, reflected, scattered, and transmitted lights are considered stable. However, absorption is assumed to change based on the degree of oxygen saturation. Both oxygenated (O_2Hb) and deoxygenated (HHb) haemoglobin have distinct absorption rates for NIR light, which collectively determine the total haemoglobin (THb = O_2Hb + HHb). The sensor detects variations in the absorption of NIR light, enabling the calculation of O_2Hb and HHb concentrations based on the modified Lambert-Beer law (Suzuki et al., 1999). The proportion of O_2Hb to THb is represented as the regional cerebral oxygen saturation ($rcSO_2$) or, alternatively, as the tissue oxygenation index (TOI), with the specific terminology varying based on the manufacturer of the NIRS equipment (Thavasothy et al., 2002). Near-Infrared light is absorbed by both HHb and O_2Hb present in arterial and venous blood vessels, with a proportional distribution of approximately 25% arterial to 75% venous. Consequently, NIRS primarily indicates more closely the oxygen saturation levels in the cerebral venous system (Watzman et al., 2000). Non-absorbed photons are received by two detectors: the proximal arc detector detects signals from superficial tissues while the distal arc detector detects signals from both superficial and deep tissues. To calculate

the oxygen saturation in the deep tissue, the proximal value is subtracted from the distal value (Jöbsis, 1977; Edwards et al., 1988; McCormick et al., 1991).

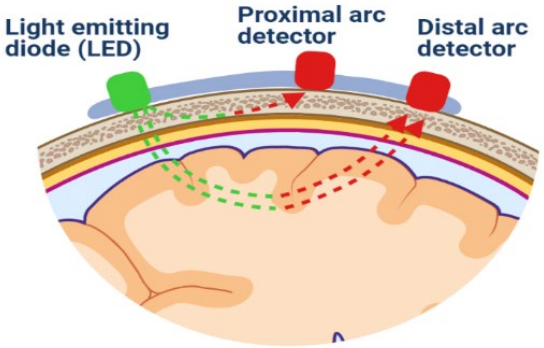

Figure1.2. Application of near-infrared spectroscopy probe for cerebral oxygen monitoring

Currently, the market offers a variety of NIRS devices and sensors, tailored for different needs. Comparative studies have generally found a satisfactory level of agreement between these devices, despite differences in their techniques and algorithms (Grubhofer et al., 1999; Cho et al., 2000; Yoshitani et al., 2002). The INVOS 5100 system (Covidien, Mansfield, MI, USA), equipped with the neonatal INVOS OxyAlert NIRSensor, is commonly used to measure $rcSO_2$ by monitoring the ratio of oxygenated haemoglobin to total haemoglobin in the tissue beneath the sensor, typically placed on the right frontotemporal region of the forehead. The Moberg CNS system (Moberg, PA, USA) is another device often employed for the synchronisation and storage of $rcSO_2$ and SpO_2 data. Additionally, the NIRO 200NX (Hamamatsu Photonics, USA,EU,Japan) is another widely utilised NIRS device, offering similar monitoring capabilities. Sensors specifically designed for neonatal use are smaller and more adaptable. It is noted, however, that these neonatal sensors tend to record measurements that are about 10% higher than those from adult sensors. This

discrepancy becomes evident when considering that most devices have an upper threshold set at 95%. As a result, when neonatal sensors measure high levels of cerebral oxygenation, the readings often appear as a continuous line, obscuring any fluctuations in the data (Dix et al., 2013; Alderliesten et al., 2016).

Multiple studies have examined the evolution of $rcSO_2$ over the course of postnatal development. Immediately following birth in term infants, regardless of the mode of delivery, $rcSO_2$ levels are typically in the range of 40 to 56% (Almaazmi et al., 2013; Urlesberger et al., 2011; Baik et al., 2015). This figure rises to as high as 78% during the initial two days after birth (Bailey et al., 2013). The increase in $rcSO_2$ during the first days after birth is primarily due to the transition from foetal to neonatal circulation, which enhances pulmonary oxygenation and systemic blood flow, along with the establishment of effective respiration, hemodynamic stability, and maturation of cerebral autoregulation mechanisms. These adaptations improve oxygen delivery and utilisation in the brain (Gao & Raj, 2010; Lara-Cantón et al., 2024; Dix et al., 2017; Garvey et al., 2018). Subsequently, over a period of 3 to 6 weeks post-birth, $rcSO_2$ gradually reaches a stable range, fluctuating between 55 and 85% (McNeill et al., 2011; Roche-Labarbe et al., 2010; Hyttel-Sorensen et al., 2015).

NIRS assessment of brain oxygen levels can be applicable in a variety of clinical scenarios, including monitoring the impact of haemodynamically significant patent ductus arteriosus (PDA) on cerebral oxygenation in neonates. PDA can lead to abnormal blood flow between the aorta and the pulmonary artery. When a PDA is present, it can significantly impact cerebral oxygenation (Lemmers et al., 2008; Dix et al., 2016). The diversion of blood through the duct away from the brain results in a

reduction of CBF. Despite normal arterial oxygen saturation (SaO_2) levels, the oxygen supply to the brain is reduced because less blood reaches the cerebral tissues. This explains why $rcSO_2$ levels, as measured by NIRS, can drop even when SaO_2 is normal. Due to the compromised cardiac output associated with PDA, the heart cannot efficiently pump blood to all parts of the body, including the brain. Once the PDA is closed, either surgically by physical ligation or clipping, or medically using nonsteroidal anti-inflammatory drugs to promote natural closure, the abnormal shunting of blood is eliminated (Gillam-Krakauer & Reese, 2018). As a result, the blood flow to the brain improves, restoring normal $rcSO_2$ levels (Lemmers et al., 2008; Dix et al., 2016). The functional size of the ductus arteriosus is proportional to brain oxygen saturation. A wider duct, indicating a more substantial left-to-right shunt, correlates with lower $rcSO_2$ (Dix et al., 2016). Furthermore, cerebral oxygenation can be altered by adequacy of respiratory support (Cambonie et al., 2003; Noone et al., 2003).

Ventilation primarily controls the arterial carbon dioxide pressure ($PaCO_2$), which has potent vasoactive effects on cerebral arteries. Elevated $PaCO_2$ leads to cerebral vasodilatation, while reduced $PaCO_2$ causes vasoconstriction (Hansen et al., 1984), though the relationship is altered depending on prevailing oxygen status and perfusion pressure (Brian, 1998). Consequently, $PaCO_2$ levels can impact both cerebral perfusion and tissue oxygenation, with both excessive (hypercapnia) and insufficient (hypocapnia) carbon dioxide levels associated with neurological pathologies (Fabres et al., 2007; McKee et al., 2009). A rise in $PaCO_2$ is associated with higher cerebral oxygen saturation measured by NIRS, coupled with a reduction in the amount of oxygen extracted (FTOE) (Vanderhaegen et al., 2009; Victor et al., 2005).

There is the potential that clinical use of continuous bedside NIRS would facilitate optimisation of ventilation, by monitoring trends in cerebral oxygenation and detection of $PaCO_2$-induced under or over-perfusion in the brain that may lead to brain damage.

The difference in oxygenated versus deoxygenated haemoglobin is often presented as an index of CBF. While the changes can correlate well, use of NIRS as an index of the blood flow assumes constant cerebral blood volume (CBV) and cerebral metabolism (Edwards et al., 1988; Wolf et al., 2007). Integrating monitoring of $rcSO_2$ with arterial blood pressure allows for the evaluation of cerebral autoregulation. When autoregulation is intact, fluctuations in arterial blood pressure do not significantly affect $rcSO_2$ levels, indicating stable cerebral perfusion. Conversely, if autoregulation is impaired, changes in blood pressure will correspond to changes in $rcSO_2$, signalling that cerebral blood flow is pressure-dependent and potentially compromised (da Costa et al., 2015). Assessing cerebral autoregulation at the bedside offers the opportunity to detect fluctuating cerebral blood flow. Once identified, suitable actions such as optimising CPP through vasoactive agents could be actioned to promote stable cerebral blood flow and oxygenation (Armstead, 2016). Various methods exist for calculating cerebral autoregulation, and currently, software solutions are being developed to enable this computation at the bedside (Caicedo et al., 2016).

Cerebral oxygenation assessment provides an insight into end organ perfusion in the context of evaluating the functional significance of hypotension and determining the need for positive inotropic therapy. There is growing recognition that traditional

definitions of hypotension in the preterm infant might not always signify actual cerebral hypoperfusion and tissue hypoxia, thereby facilitating a more tolerant approach towards lower blood pressures and therefore a more restrictive approach to administration of vasoactive drugs (Dempsey & Barrington, 2009; Noori & Seri, 2015; Alderliesten et al., 2014). Treatment for hypotension, which is not without risks and may negatively impact outcomes, should be cautiously considered (Alderliesten et al., 2013; Batton et al., 2015). Monitoring cerebral oxygenation serves as a key indicator of end-organ oxygenation and could aid in decision-making regarding treatment of hypotension preventing potential brain damage. This monitoring helps to detect early signs of serious conditions like IVH and PVL through imaging tests using CUS or MRIs. Additionally, it supports assessment of long-term neurodevelopmental outcomes, ensuring that interventions effectively protect and support brain health (Alderliesten et al., 2014; Binder-Heschl et al., 2016).

In some unfortunate cases severe asphyxia can occur peripartum. In the initial days following birth $rcSO_2$ tends to increase while cerebral FTOE decreases (Toet et al., 2006; Lemmers et al., 2013). These changes have been linked to poorer outcomes at two years of age, as measured by the Griffiths Mental Developmental Scales (Toet et al., 2006; Lemmers et al., 2013). The concurrent use of NIRS for monitoring cerebral oxygenation and amplitude-integrated electroencephalography (aEEG) to assess brain activity patterns is highly indicative of long-term neurodevelopmental outcomes. For example, in cases of severe asphyxiation treated with hypothermia at 12 hours of age, high $rcSO_2$ combined with abnormal aEEG patterns (indicating low brain activity) had a 91% positive predictive value for adverse outcomes; whereas the absence of these indicators carried a 100% negative predictive value (Lemmers et al.,

2013). These results emphasise the critical role of NIRS in early prognostication of neurodevelopmental outcomes. The tendency for cerebral hyperoxygenation in neonates with negative outcomes is often attributed to reduced energy metabolism following severe brain injury, leading to decreased oxygen use, increased cerebral blood flow, and impaired autoregulation in the brain's vascular system (Greisen, 2014; Howlett et al., 2013).

Despite the clinical applications mentioned earlier, there are some limitations of NIRS monitoring. These limitations include challenges posed by external factors such as the presence of hair, increased light absorption with more pigmented skin, and ambient light interference from devices like phototherapy units (Van Bel et al., 2008). Additionally, in smaller infants, issues such as subdural oedema or hematoma beneath the sensor may impinge on recording (Kahraman et al., 2006). Simultaneous placement of electrodes for aEEG monitoring can also be problematic. Both NIRS sensors and aEEG electrodes need to be placed on the infant's scalp, and their placement must be carefully managed to ensure accurate measurements from both devices. Therefore, the limited space on a small infant's scalp can make it challenging to position both types of sensors without interference. Additionally, the physical presence of multiple sensors can potentially affect the quality of data collected by each device. For example, the proximity of aEEG electrodes might interfere with NIRS measurements by obstructing or altering the light path used to assess cerebral oxygenation. Factors such as head circumference and skull curvature have been considered potential hindrances to NIRS monitoring (Wong, 2016). However, according to Alderliesten et al. (2016), there is no significant correlation between head circumference and $rcSO_2$, suggesting that head circumference is not a major

issue when recording NIRS measurements. It is important to recognise that NIRS is a surrogate of entire brain oxygenation in extremely preterm infants, not just the prefrontal cortex (Van Bel et al., 2008). However, skull curvature remains a critical consideration. The curvature of the skull can influence how light from the NIRS sensor interacts with brain tissues, potentially affecting the accuracy of measurements.

The specific type of NIRS device and sensor used also plays a crucial role in the interpretation of cerebral oxygenation values (Dix et al., 2013). Hyttel-Sorensen et al., (2011) evaluated three commercial NIRS instruments (INVOS 5100, NIRO 200 NX/300 and OxyPrem), on the forearm of adults and discovered that the absolute regional tissue oxygen saturation values varied between the devices, while their reproducibility and dynamic ranges were comparable. Furthermore, it is important to be aware of potential differences between sensors when comparing data across patients, institutions, or devices. For instance, an $rScO_2$ of 55% may be considered low using a neonatal sensor but acceptable with an adult sensor (Alderliesten et al., 2016). An $rScO_2$ of 55% with a neonatal sensor translates to approximately 40% with an adult sensor, which is near or below the reported thresholds (33–50%) associated with neuronal damage and adverse neurodevelopmental outcomes (Kurth et al., 2002; Hou et al., 2007; Alderliesten et al., 2014).

1.3.3. Peripheral Oxygen Saturation (SpO_2) and EEG: Complementary Tools in Brain Injury Detection.

Pulse Oximetry

Pulse oximetry is a method for continuously and non-invasively measuring oxygen saturation in the periphery (SpO_2) and is a close reflection of arterial oxygen

saturation (Hay Jr et al., 1989). Pulse oximetry operates by using red and infrared light to measure the absorption of oxygenated and deoxygenated haemoglobin. In the red spectrum, O_2Hb absorbs less visible light compared to HHb. However, this situation is the opposite when it comes to infrared light, where O_2Hb absorbs more (Moyle, 1996). In this method, a sensor is positioned on a hand or foot, and two light-emitting diodes transmit red and infrared light to a photodetector. Changes in absorption during the arterial pulsatile flow and non-pulsatile component of the signal are examined. SpO_2 levels are determined based on the light transmission through the pulsatile tissue bed. The surge of arterial blood volume with each heartbeat leads to increased light absorption, allowing for measurement of heart rate as peaks coincide with each heartbeat (Dawson et al., 2007).

Pulse oximetry has become widely adopted in neonatal wards over the last thirty years due to its simplicity and the minimal risk of heat-related issues, especially in extremely preterm infants. However, there are still significant differences in monitoring approaches for guiding oxygen therapy (Tin & Lal, 2015). In 2007, the American Academy of Paediatrics suggested ranges for oxygen therapy in preterm infants, with SpO_2 values between 85% and 95% and PaO_2 values between 50 and 80mmHg (Lemons & James, 2007). European guidelines in 2007 suggested maintaining an SpO_2 level of below 95% without specifying a lower limit (Sweet et al., 2007). However, revised guidelines as recently as 2010 advised for a range between 85% and 93%, with the upper limit set at 95% (Sweet et al., 2010). Even more recently, large clinical studies collated under the NeOProM study (Neonatal Oxygenation Prospective Meta-analysis) have narrowed the range of safe SpO_2. Pooled data from those clinical trials (including about 5000 infants) reported that extremely preterm

infants with SpO_2 values of 85-89% were at higher risk of mortality and necrotizing enterocolitis compared to ones with 91-95%. However, the risk of retinopathy of prematurity was higher in preterm infants with higher levels of SpO_2 (Askie et al., 2018). Sullivan et al., (2018) suggested that the combined features of SpO_2 (mean, SD, kurtosis and skewness) with clinical data in the first 12 hours and the first 7 days of life were associated with severe IVH (grade III and IV) and NEC. In terms of absolute values, Vesoulis et at., (2019) proposed that the time spent with SpO_2 of ≤ 70% was associated with severe grade III and IV IVH. A recent metanalysis, compared the morbidity and mortality in extremely preterm infants (approximately 5000 infants) who were exposed to restricted oxygen (SpO_2, 85% - 89%) vs liberal oxygen (SpO_2, 91% - 95) (Manja et al., 2015). They found that neonates receiving liberal oxygen experienced a decrease in mortality before hospital discharge compared to those with a restricted oxygen. Furthermore, the liberal oxygen group had fewer instances of necrotizing enterocolitis. However, there was no significant difference observed in terms of death or disability at 24 months, bronchopulmonary dysplasia, retinopathy of prematurity, neurodevelopmental outcomes, or hearing loss (Manja et al., 2015).

The primary physiological limitation of pulse oximetry is its inability to identify hyperoxaemia at SpO_2 levels above 90% due to the shape of the oxyhaemoglobin dissociation curve. As a result, a minor rise in SpO_2 may correspond to a significant increase in PaO_2 (Hay Jr, 1987; Wasunna & Whitelaw, 1987). There is particular risk of hyperoxia for preterm infants who are administered supplemental oxygen. Preterm infants are vulnerable to oxygen toxicity and localised oxidative stress can impair developing tissues as they have limited antioxidant reserves (Saugstad, 2003; Davis & Auten, 2010).

Anaemic hypoxia occurs when there is an inadequate supply of oxygen to tissues due to a reduction in the total amount of haemoglobin available to carry oxygen, despite normal SaO_2 levels. This type of hypoxia is not detected by standard SpO_2 monitoring because SpO_2 measures the percentage of haemoglobin saturated with oxygen, but it does not account for the total amount of haemoglobin in the blood. As a result, SpO_2 monitoring can provide a misleading sense of adequate oxygenation in the presence of anaemia (West, 2012; Sinex, 1999).

Most clinical oximeters have an averaging time of 10 to 20 seconds, which can lead to the omission of brief apnoea's and result in an underestimation of their frequency (Trivedi et al., 1977; Bohnhorst et al., 2000). This delay in detecting transient oxygen changes can also obscure early signs of physiological instability, such as the onset of infection. Alarm fatigue, a phenomenon whereby healthcare providers become desensitised to frequent alarms, can exacerbate this issue, leading to slower or inadequate responses to critical events (Johnson et al., 2017). The primary clinical response to SpO_2 alarms often involves increasing supplemental oxygen, based on the assumption that hypoxaemia is the primary issue. However, this approach may not address the underlying cause of the alarm and could potentially lead to hyperoxia (McClure et al., 2016; Buonocore et al., 2010). Therefore, while SpO_2 monitoring is a valuable tool, its limitations in detecting brief or subtle episodes of hypoxia highlight the need for a more nuanced approach. Furthermore, movement of the sensor probes and inadequate peripheral perfusion can result in motion artefacts, resulting in false alarms. Advanced pulse oximeters equipped with signal extraction technology are capable of accurately measuring SpO_2 even during patient motion and low perfusion by isolating the pulsatile arterial signal from other signals. In clinical

settings, it is important to verify the good quality of signal received by the sensor before accepting SpO_2 readings (Hay et al., 2002).

Electroencephalography

Electroencephalography (EEG) is a non-invasive continuous test for brain exploration which can be conveniently conducted at the bedside. It holds significant diagnostic and prognostic importance in newborns. This brain function assessment is an adjunct to clinical evaluations, which are often restricted in the intensive care unit, especially in sedated newborns or those at risk of seizures with minimal or no symptoms. It also complements morphological information gained using brain imaging techniques (Lamblin et al., 2015).

EEG captures the neural electrical activity of the brain, resulting from the action potentials of neurons using external surface electrodes. The EEG patterns depict a collective average of numerous action potentials, with some being excitatory and others inhibitory. Subcortical structures like the thalamus and brainstem play a significant role in this process, especially in premature newborns.

Once the signal has been recorded, it undergoes amplification and filtering to minimise artefacts before being electronically presented. The sequence in which the signals are presented determines the montage type. There are two kinds of montages: bipolar and unipolar (also known as referential montage). Bipolar montages assess the potential variance between two neighbouring electrodes. This setup is beneficial because it enhances the ability to localise the signal. However, a limitation of this setup is that signals with opposite signs might negate one another. Unipolar montages compare each electrode to a reference one or, in the case of

referential montage, to aggregated activity from all electrodes. This montage is beneficial because it offers a uniform reference point for all electrodes. EEG waves vary in their frequency, amplitude, and shape. The EEG records frequencies including Delta (< 4Hz), Theta (4-7Hz), Alpha (8-13Hz), Beta (13-30Hz), and Gamma (> 31Hz) (Alix et al., 2017). During EEG recordings, additional parameters such as the electrocardiogram (ECG), patterns of respiration, eye movements, activity of the submental muscle, and concurrent video recording can also be monitored. These parameters offer valuable insights, however, not all neonatal units are equipped to measure all of these (Alix et al., 2017).

Continuous, multi-channel EEG, also known as cEEG, has a high temporal resolution on the scale of milliseconds, allowing for real-time monitoring of electrical brain activity in a continuous way. However, trained personnel are required for both its application and interpretation (Murray et al., 2006). To overcome this limitation, many clinical units currently utilise amplitude EEG (aEEG), derived from cEEG. aEEG involves compressing, filtering, and processing the amplitude of raw EEG over time. It can be produced from single or double channels typically using central or frontocentral electrodes (Helstrõm-Westas et al., 1995; Toet et al., 1999). Assessment of aEEG is commonly conducted according to either background activity/amplitude or pattern recognition (al Naqeeb et al., 1999; Hellstrom-Westas et al., 2006). While aEEG is thought to be simpler to use and assess, the inconsistency between different observers is not ideal (Rakshasbhuvankar et al., 2020; Bourgoin et al., 2020). Thus, its interpretation depends on the user and is subjective.

EEG has long been essential in monitoring infants with encephalopathy (Murray et al., 2006; Murray et al., 2009; Selton & Andre, 1997; Van Lieshout et al., 1995). It has been integrated into the Sarnat clinical grading system and is listed as an inclusion criterion in the Total Body Hypothermia for Neonatal Encephalopathy (TOBY) trial (Sarnat & Sarnat, 1976; Azzopardi et al., 2009). It is utilised for grading and diagnosing encephalopathy, tracking its progression, and predicting outcomes in infants with HIE. Previous studies report that before TH commences, the earliest aEEG recordings of 3-6 hours after birth are highly predictive of outcomes (Shany et al., 2006; Osredkar et al., 2005; Ter Horst et al., 2004). This finding influenced the selection criteria for recruitment of infants into the TOBY trial (Azzopardi et al., 2009). However, since the introduction of TH, the early predictive capability of aEEG for outcomes has decreased (Csekő et al., 2013; Hamelin et al., 2011; Thoresen et al., 2010; Niezen et al., 2018). Furthermore, a meta-analysis (incorporating 9 studies, 520 patients) conducted more recently indicates that abnormal aEEG readings before 6 hours of age do not always signify an adverse outcome (Chandrasekaran et al., 2017). Furthermore, EEG when combined with CBF measurements, can provide deeper insights into neurovascular coupling (NVC). NVC plays a crucial role in maintaining brain health by linking neuronal activity with local blood flow changes (Phillips et al., 2016). When neurons become active, NVC ensures that CBF increases to meet the heightened metabolic demands of the active brain regions. This precise adjustment of blood flow is essential for sustaining normal brain function and preventing neuronal damage (Kozberg & Hillman, 2016).

aEEG can also be valuable in identifying seizures (Osredkar et al., 2005); however, it may overlook brief seizures (< 30 seconds), low-intensity seizures, or focal seizures

originating from brain areas not monitored (Rennie et al., 2004; Shellhaas et al., 2007; Shah et al., 2008; Toet et al., 2002). Thus, cEEG continues to be the preferred method for identifying and categorising seizures (Shellhaas et al., 2011; Pressler et al., 2021). Because interpretation by experts is necessary, automated seizure detection algorithms have been created to assist physicians in identifying seizures at the bedside (Pavel et al., 2020; Navakatikyan et al., 2006). Recently, an android-based app, called Neurobell, was used to monitor long term continuous EEG, and detect seizures. This app was implemented on low-cost electronics, works with minimal power consumption and can be used as a valid alternative for non-experts in assessing seizure activity (O'Sullivan et al., 2018). Like Neurobell, CergenX aims to fill the gap in timely detection and intervention for brain injuries in newborns, particularly in critical care environments where access to expert neurologists may be limited (CergenX).

Quantitative analysis of EEG data has the potential to offer an objective and repeatable description of the EEG without relying on expert interpretation. It also possesses the capability to identify subtle characteristics that may not be readily apparent through visual assessment alone (O'Toole & Boylan, 2017). Quantitative EEG analysis offers a mathematical summary of EEG signals. It utilises multiple attributes related to amplitude, frequency, and inter-hemispheric connectivity for characterising neonatal EEG (O'Toole & Boylan, 2017). Establishing a standardised definition for these quantitative EEG characteristics is important, as it ensures replicability and enables consistent comparisons across different studies. O'Toole and Boylan (2017) have previously introduced an open-source computational framework, termed NEURAL (Neonatal Eeg featURe set in mAtLab; https://github.com/otoolej/qEEG_feature_set), which extracts the specific sets of

quantitative features. These features are categorised into three primary domains: time-domain features, frequency-domain features, and features that define the connectivity across cerebral hemispheres.

Among time-domain features, the power or amplitude of the EEG signal is a primary feature. Range-EEG, which is like aEEG, emerges as a standardised alternative. This standardisation is imperative given the diversity in algorithms used by different EEG/aEEG machines to generate the aEEG signal, which range-EEG seeks to uniformly address (O'Toole & Boylan, 2017).

Frequency-domain features are characterised by aspects of spectral power and shape. The EEG signals are decomposed into four frequency bandwidths as part of this analysis. Spectral power quantifies the amplitude across various frequency bandwidths. Relative spectral power, however, assesses the power within each band in relation to one another. The spectral edge frequency represents a threshold frequency, below which 95% of the power frequencies are contained. To describe spectral shape, features such as spectral flatness, indicative of spectral entropy, and spectral difference, reflecting the variation in spectral shape over time, are utilised (O'Toole & Boylan, 2017).

To characterise inter-hemispheric connectivity, features such as correlation and coherence between the cerebral hemispheres are extracted. Furthermore, inter-burst intervals are analysed separately for each channel, and the median value across all channels is then used to summarise the results.

1.4. Components of NIRS ($rcSO_2$) Signal

1.4.1. Physiological Significance of Signal Components

A considerable amount of literature has been published about determining an absolute value of cerebral oxygen saturation that can predict brain damage in humans and animals. The animal model of choice for these studies is the newborn piglet since the anatomical and physiological features of newborn piglets are similar to preterm infants (Sun et al., 2023). Furthermore, there are similarities in brain maturation, cerebral haemodynamics, and thickness of the skull between piglets and human neonatal infants (Chapados & Cheung, 2008; Armstead, 2000). Hou et al. (2007) grouped piglets according to varying degrees of hypoxia that the piglets had been exposed to for 30 minutes. They found that the piglets who spent 30 minutes with cerebral oxygen saturation between 30% and 40%, experienced hypoxic brain injury, and that brain function was even more abnormal for the group that spent 30 minutes with $rcSO_2$ <30%. Similarly, Kurth et al. (2002) found that $rcSO_2$ = 40% was the threshold for cerebral hypoxic ischaemia in piglets.

In a recent study of preterm infants (<32 weeks), Alderliesten et al. (2019) proposed an association between unfavourable cognitive outcomes at 24 months of age and a threshold of $rcSO_2$ <55%, using adult near-infrared sensors. They suggested a threshold of 65% of $rcSO_2$ when a neonatal/paediatric sensor is used. In a recent study in very preterm infants with a birth weight of <1250 g, Chock et al. (2020) set $rcSO_2$ <50% for at least 1% of the monitoring period as cut-point for identifying adverse outcomes. These findings differ from those of Kenosi et al. (2018) who argued that absolute values of $rcSO_2$ are not indicative of brain injury. They recorded cerebral

regional oxygenation in 120 infants of GA < 32 weeks for the first 48 hours of life using a neonatal sensor. The outcome included no IVH/PVL and survival at one month, grade 1 or 2 IVH, and IVH ≥ 3 or PVL or death before one month age. No difference in absolute values of $rcSO_2$ was observed between three different outcome groups.

To overcome the inconsistency in $rcSO_2$ absolute values in predicting brain injury in preterm infants during the first days of life, O'Toole et al. (2016), used signal processing methods, and proposed features from the frequency domain to detect brain injury in a small cohort of very preterm infants. Further testing in larger sample populations however is required.

When analysing NIRS, substantial increases or decreases from baseline values typically serve as more critical clinical indicators of an infant's underlying condition than the absolute value of $rcSO_2$. Neonatal $rcSO_2$ values exhibit considerable variability, with normal ranges reported between 55% and 85%. This range can be 10% higher when utilising a neonatal probe (El-Dib & Soul, 2019). Furthermore, male newborns generally display higher $rcSO_2$ values compared to female newborns (Cohen et al., 2015). Additionally, small for gestational age (SGA) neonates exhibit higher $rcSO_2$ values than neonates with appropriate weight during the initial three days after birth (Cohen et al., 2015).

1.4.2. Delving into Prolonged Relative Desaturations: What They Are and Why They Matter.

Recorded NIRS signals include repetitive desaturations, which are reported to be more common in extremely preterm infants compared to very late preterm infant cohorts (Hansen et al. 2019). In the study by O'Toole et al. (2018), it was

demonstrated that these transient components of NIRS signals, which appear as prolonged decreases in the signal relative to the baseline, were not predictive of brain injury and extracting them led to a better prediction of outcome. However, there has been no detailed investigation of suitable methods for de-noising short duration desaturations. Effective decomposition of these desaturations would provide an excellent opportunity to test their clinical utility. Further work needs to be done to establish whether such transients are predictive of brain injury in preterm infants or not. If they are not predictive, these components of the NIRS signal could be removed at the pre-processing stage to facilitate optimal decomposition of the remaining signal.

Reduced $rcSO_2$ from baseline may be linked to decreased cerebral oxygen delivery/perfusion or an increase in oxygen utilisation. It is advisable to assess a neonate exhibiting a notable decline in $rcSO_2$ from baseline values or an absolute $rcSO_2$ below 60% for potential causes such as hypoxic hypoxia, decreased cardiac output, hypotension, chest hyperinflation, and hypocarbia, and to administer appropriate treatment. On the other hand, an elevated $rcSO_2$ may indicate enhanced cerebral oxygen delivery/perfusion or reduced oxygen consumption. In cases where a neonate exhibits a substantial rise in $rcSO_2$ from baseline levels or an absolute $rcSO_2$ exceeding 90%, investigation of potential causes including hyperoxia, hypercarbia, oversedation, or severe brain injury, should be conducted, and suitable interventions made (El-Dib & Soul, 2019).

It is important to acknowledge that $rcSO_2$ readings can be affected by artefacts, such as movement or poor sensor placement, as well as physiological factors like changes

in blood pressure, CBF and oxygenation, and pathological conditions such as IVH. Such artefacts can make it difficult to accurately interpret $rcSO_2$ values or to determine what constitutes an abnormal $rcSO_2$ reading or a significant change in $rcSO_2$. Consequently, defining a clear threshold for abnormality or sudden changes in $rcSO_2$ can be challenging.

1.4.3. Methodological Approaches for Extracting and Analysing PRDs.

NIRS signals often exhibit a sparse nature, accompanied by instrumental noise, motion artefacts, and sudden decreases from the baseline in the low-frequency background. Depending on the experimental setup, either the low-frequency component or the sparse signal may represent the biological signal of interest. There are two separate methods for isolating and extracting these relative desaturations within NIRS signals: simultaneous low-pass filtering and total variation denoising (LPF-TVD) methods, and singular-spectrum analysis and the discrete cosine transform (SSA-DCT) methods (Selesnick et al., 2014a; O'Toole et al., 2018).

Let us assume that the NIRS signal can be modelled as

$$y(n) = f(n) + x(n) + w(n),\ n = 0, \ldots, N-1$$

where f is low-pass signal, x is sparse and/or sparse-derivative signal and w is stationary white Gaussian noise. Conventional low-pass filtering and sparsity-based denoising are not appropriate for handling noisy data like this. If the low-pass signal f were observed solely in noise, then low-pass filtering (LPF) would provide a reliable estimate of f; $f \approx \text{LPF}(f + w)$. Conversely, if x was a sparse-derivative signal observed only in noise, then total variation denoising (TVD) would offer an accurate estimate of x; $x \approx \text{TVD}(x + w)$. In the case of noisy data represented as $y = f + x + w$, a

simultaneous use of LPF and TVD for estimating f and x separately can be applied (Selesnick et al., 2014a). Total variation denoising (TVD), is characterised by minimising a non-quadratic cost function. Consequently, the output of the TVD filter is determined by a nonlinear function of the data, necessitating the use of numerical algorithms to obtain it (Selesnick et al., 2012; Rudin et al., 1992). Considering the selection of the suitable λ, we solve this problem:

Arg min $\{½ ||H (y – x)||_2^2 + \lambda||Dx||_1\}$,

where H represents high-pass filter matrix, D is defined as the matrix of the first-order difference of signal x (Selesnick et al., 2014a).

The signal x can be considered as being sparse itself and having a sparse derivative. In this case, low-pass filtering compound sparse denoising (LPF-CSD) can be employed. In this method, we are solving the following problem,

Arg min $\{½ ||H (y – x)||_2^2 + \lambda_0||x||_1 + \lambda_1||Dx||_1\}$, where there are two parameters λ_0 and λ_1 to be optimised (Selesnick et al., 2014).

LPF-CSD method can be improved by replacing l_1 norm with non-convex penalty functions Φ_0 and Φ_1 (Selesnick et al., 2014). Employing these penalty functions enables a more accurate estimation of transient components because they are less biased towards zero. In this method, the problem that is solved is,

Arg min $\{½ ||H (y – x)||_2^2 + \lambda_0 \Sigma \Phi_0(x[n]) + \lambda_1 \Sigma \Phi_1(x[n+1] – x[n])\}$.

singular-spectrum analysis and the discrete cosine transform (SSA-DCT) methods rely on the concept that an impulse in the time domain is represented as a sinusoidal signal in the frequency domain when analysed through the cosine transform. These

methods utilise the data-driven filter-bank operation provided by singular-spectrum analysis (SSA) to separate and extract the transient components. This method involves forming lagged vectors from the input signal and combining them to create a trajectory matrix. The correlation matrix of this trajectory matrix is decomposed into orthogonal basis vectors, termed eigenvectors, and associated weights, termed eigenvalues. Each component of the signal is then generated using a finite-impulse response (FIR) filter with the eigenvector as the impulse response. Rejecting noise-associated components can improve the signal-to-noise ratio. Additionally, the method involves extracting transient components by transforming the signal using the discrete cosine transform (DCT), which rotates impulses or impulse-like transients to sinusoidal-type components in the time-frequency plane. The SSA applied to the real-valued DCT signal enables the extraction of oscillating components, representing transient components when transformed back to the time domain through an inverse DCT (O'Toole et al., 2018). This method was developed on a set of synthetic $rcSO_2$ signals and subsequently, tested on 10 extremely preterm infants. The results demonstrated that employing the decomposition technique to eliminate transient components enhanced the detection accuracy of brain injury, elevating the area-under-the-receiver-operator characteristic from 0.91 to 1.00 (O'Toole et al., 2018).

1.5. The Advent of Machine Learning in Neonatal Care

1.5.1. Introduction to Machine Learning and Its Transformative Role in Healthcare.

Machine Learning

Artificial intelligence (AI) is defined as the scientific and engineering effort to enable computers to exhibit behaviours that are typically associated with human intelligence. In other words, it involves creating computers that can mimic human thinking or behaviour. Artificial intelligence is a rapidly growing area of study within the medical sector (Moore, 2017). Machine learning (ML), as a subset of AI, covers a broad array of methods. Deep learning, a specialised area of ML, focuses on neural networks with multiple layers that learn hierarchical representations of data. A Common example of deep learning is the convolutional neural network (CNN), which is effective for processing images and signals (Nozari & Sadeghi, 2021; Ekman, 2021). The relationship between AI, ML, deep learning and CNN is represented in Figure1. 3.The fundamental machine learning process involves building and improving a predictive model using a training dataset, followed by evaluating its performance/predictive capacity using an unseen test dataset. Once validated, the model can be used to predict outcomes based on real-world data (Liu et al., 2019). In contrast to conventional logistic/linear regression methods, ML approaches can uncover non-linear or binary interactions and provide highly reliable forecasts for extensive datasets where identifying correlations can be difficult (Panesar et al., 2019).

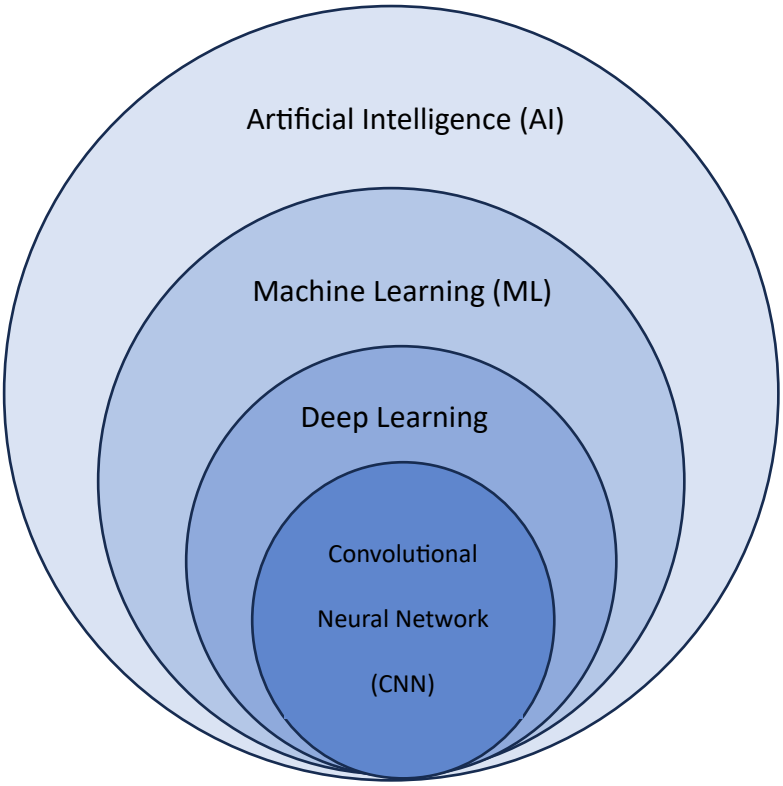

Figure1. 3. Relationship between artificial intelligence (AI), machine learning (ML), deep learning, and convolutional neural networks (CNN). The sizes of the circles are not proportional to the relative sizes of the fields they represent.

Prediction models developed using AI often rely on a variety of metrics for assessment. One commonly used test to evaluate the predictive performance of these models is the area under the receiver operating characteristic curve. This graphical representation takes into account sensitivity (true positive/true positive + false negative) and specificity (true negative/true negative + false positive) (Mangold et al., 2021).

Machine learning employs diverse learning approaches to predict outcomes. These approaches include supervised, unsupervised, and reinforcement learning, each employing distinct methodologies for model development. In supervised learning, a model is trained using a dataset where the outcomes, such as IVH or adverse MRI, are

predefined by clinicians. This labelled dataset is utilised to construct a model that is capable of predicting outcomes in new, unlabelled cases (Shirwaikar et al., 2016). Unsupervised learning, on the other hand, involves identifying patterns or groups within data, such as NICU data, without predefined outcomes. For instance, this approach can be used to discover clusters of sepsis cases in neonates based on common clinical or physiological characteristics observed in NICU care. The model autonomously identifies these clusters without prior labelling (Afrin et al., 2019). Reinforcement learning operates on the principle of defining reward and punishment mechanisms for each possible action in a sequential manner. In this approach, the system is rewarded for correct actions and penalised for incorrect ones. The objective is to determine a series of steps that maximises rewards, ultimately leading to the accurate diagnosis of conditions like sepsis (Nemati et al., 2019; Raghu et al., 2017).

Mangold et al., (2021) reviewing 11 papers systematically, suggested that ML models can accurately predict neonatal death, defined as death within the first 28 days of life. The primary four features were birth weight, gestational age, Apgar scores, and instances of multiple births. Similarly, Sheikhtaheri et al., (2021) also developed machine learning models to predict neonatal death in NICUs. They first identified key risk factors for neonatal death and then used several machine learning models to predict neonatal death in NICU. Then, the predicted outcomes of the neonates were compared to their actual outcomes.

EEG for Seizure Prediction as Case Study

AI also has been used in screening and alert models to continuous electroencephalogram (EEG) monitoring in the context of seizure detection in recent

studies. Specifically, a randomised trial was conducted involving neonates at risk of seizures (Pavel et al., 2020). This trial utilised continuous conventional EEG monitoring, enhanced by a software designed to recognise seizures and trigger alarms upon their detection (Pavel et al., 2020). Although the implementation of this software did not increase the rate of seizure diagnosis in neonates, it did demonstrate a superior ability for quantifying seizure burden. This superiority was evidenced by the more precise assessment of the total time and duration of seizures, particularly notable during weekends. The trial, carried out in centres adept at monitoring, diagnosing, and treating neonatal seizures, highlighted the potential of machine learning-based clinical support tools for enhancing seizure management, especially in less experienced centres and during off-peak hours. Furthermore, using clinical and EEG parameters in the first 12 hours of birth in infants with HIE, they predicted infants at higher risk of seizures, prior to a seizure event (Pavel et al., 2023).

Detecting seizures in preterm infants is particularly challenging due to the multitude of jerky movements they exhibit, many of which are a normal part of typical sensorimotor development (Khazipov et al., 2004; Milh et al., 2007). These movements can closely resemble seizures, leading to the potential for unnecessary administration of anti-epileptic drugs in affected infants. Continuous EEG monitoring is the most effective means for identifying seizures in preterm infants, but its interpretation demands specialised expertise, restricting its application to specialised centres. Furthermore, obtaining multichannel EEG recordings in preterm infants poses challenges due to their clinical condition and physical constraints, such as small head circumference. Acquiring high-quality datasets containing both seizure and non-seizure instances for training, testing, and validating automated analysis algorithms is

challenging. Furthermore, preterm infants have distinct EEG morphology compared to full-term infants (Patrizi et al., 2003). O'Shea et al. (2021) explored various deep learning architectures to detect seizure in preterm infants, including training on data from full-term infants, preterm infants, age-specific preterm data, and transfer learning. They achieved an AUC of 93.3% for the term-trained algorithm and 95.0% through transfer learning from the term model using available preterm data.

Use of EEG is not limited to seizure detection and machine learning has been applied to predict other clinically significant outcomes. For example, Bakheet et al. (2021) employed machine learning techniques to analyse EEG signals from infants with HIE to predict the development of cerebral palsy (CP) at an early stage. Furthermore, Sánchez Fernández et al., (2018) used machine learning models of EEG to predict mortality in critically ill children.

Use of Routine Clinical Data in Prediction of Adverse Outcome

The potential for ML models to aid in diagnosing long-term outcomes has been evidenced in recent research. Investigations have demonstrated the effectiveness of using routine, non-invasive physiological data collected in neonatal intensive care units. Such data can be instrumental in developing scoring systems that forecast long-term outcomes in premature infants (Crilly et al., 2021). Additionally, predictive models have been formulated for assessing six-month outcomes in cases of traumatic brain injury, utilising readily available clinical data such as lactate, pH, and glucose on admission (Kayhanian et al., 2019). These studies underscore the growing relevance of ML models for enhancing prognostic capabilities in clinical settings.

While ML represents significant potential for revolutionising healthcare, its widespread application faces notable challenges. A key issue is the lack of linear correlations in some ML algorithms, which means that they may not always provide a clear explanation for their outputs when compared to traditional clinical decision-making processes often illustrated with the use of flow-diagrams. Additionally, the quality of the model is heavily dependent on the accuracy and consistency of the data used, which includes the reliability of diagnoses and the use of standardised criteria (Clarke et al., 2021). Data storage also poses a significant issue, particularly in terms of maintaining secure, scalable systems that can handle large datasets. Furthermore, the computational power needed for rapid processing and model training is critical for timely decision-making in clinical settings. Validation of these models can be complicated by the need for anonymised data to comply with privacy regulations such as General Data Protection Regulation, which can limit the ability to fully assess the model's accuracy in real-world scenarios. Furthermore, the debate between fixed models and open ML approaches is crucial; while fixed models rely on static data and may become outdated as new treatments emerge, open ML models continuously improve by integrating new data, allowing them to adapt to changing clinical landscapes. These considerations highlight the complexity of developing and implementing effective ML models in neonatal care and underscore the need for collaborative efforts across academia, healthcare, and industry to address these challenges (Clarke et al., 2021).

1.5.2. Focusing on Specific Machine Learning Tools: XGBoost and Deep Learning Methods

eXtreme Gradient Boosting or XGBoost, has emerged as a prominent machine learning framework renowned for its exceptional performance in predictive modelling tasks and represents a significant advancement in tree boosting algorithms. Gradient boosting is a form of supervised learning whereby the algorithm aims to predict a target variable by aggregating the predictions of several simpler models (usually decision trees). There are several key components and features in XGBoost that distinguish it from traditional boosting algorithms. These include customisable loss functions, which enable users to tailor the learning process to specific tasks, and regularisation techniques that prevent overfitting and improve generalisation (Chen & Guestrin, 2016). XGBoost also incorporates efficient handling of missing values and advanced tree pruning methods, enhancing its ability to learn complex patterns from data while minimising computational resources (Chen & Guestrin, 2016).

One of the most significant advantages of XGBoost is its scalability and efficiency, allowing it to handle large datasets and complex models with ease. By leveraging distributed computing frameworks and parallel processing techniques, XGBoost can effectively utilise multicore processors and distributed computing clusters to accelerate training times and improve performance. This scalability makes XGBoost particularly well-suited for big data analytics and real-time applications where speed and efficiency are paramount (Chen & Guestrin, 2016).

XGBoost operates by constructing a series of decision trees iteratively, with each subsequent tree aiming to correct the errors made by the previous ones. The key

principle behind XGBoost is to minimise a predefined loss function by adding new trees to the ensemble in a way that optimally reduces the overall error. XGBoost uses a gradient boosting framework, optimising an objective function. The objective function is a measure of how well the model is fitting the training data. The objective function of XGBoost is a combination of a loss function (e.g., mean squared error for regression, log loss for classification) and a regularisation term, which helps prevent overfitting by penalising overly complex models. Gradient boosting involves fitting new models to the residual errors made by the previous models. In XGBoost, instead of fitting the new model to the raw residuals, it fits the model to the gradients (first-order derivatives) of the loss function with respect to the predictions of the previous model. This approach allows for more fine-tuned adjustments and can lead to better performance (Chen & Guestrin, 2016).

CNN consists of neurons that adjust themselves through learning. Each neuron receives input and performs an operation, such as a scalar product followed by a non-linear function. The last layer typically contains loss functions associated with classes. CNNs includes three types of layers: convolutional layers, pooling layers and fully connected layers. The convolutional layer consists of kernels (filters) which are rather small in the spatial dimension but move along the input data and convolve the input data to produce the activation layer. Convolutional layers decrease the complexity of the input, using three hyperparameters, the depth, the stride and padding. The depth sets the number of kernels (filters) in each layer. The total number of the neurons in the network as well as pattern recognition abilities of the model are decreased as this hyperparameter reduces. Stride defines the number of pixels by which the filters move across the input. If the stride is set to 1, there is an overlap between receptive

fields. However, increasing stride to larger numbers, decreases the overlapping and results in an output with lower spatial dimensions. Padding in CNN refers to the addition of extra pixels around the borders of the input to make sure every pixel gets considered. Pooling layers help to decrease the dimension of the representation and computational complexity of the model, while preserving important information, and overcoming the challenge of overfitting. The last few layers of the CNN architecture are usually Fully Connected (FC) layers. These layers consist of the weights and biases along with the neurons and are used to connect the neurons between two different layers and are followed by the output layer (O'Shea & Nash, 2015).

1.6. Thesis Objectives

The objectives of this thesis were to deepen our understanding of NIRS signals, explore their clinical utility, and to identify the most effective methods for interpreting these signals. We have employed advanced machine learning techniques to maximise the utility of these signals, enabling the discovery of complex, non-linear relationships between variables that might otherwise be overlooked.

In Chapter 2, I focus on investigating various methods for extracting prolonged relative desaturations (PRDs) from NIRS signals. I compare these methods using synthesised NIRS data and identify the optimal approach, which performed best with my dataset.

In chapter 3, I use the method described in chapter 2 to extract PRDs, followed by feature extraction from $rcSO_2$ signals with and without PRDs, as well as from the PRDs themselves. Machine learning models are then developed and utilised to predict adverse outcomes in extremely preterm infants. This chapter also describes the development of a model that used specific signals features to predict long-term adverse outcomes.

In Chapter 4, I apply similar methodology to that described in chapter 3 to a larger dataset in order to assess the replicability of my results. I examine whether the models developed from a multicentre international study, with a larger sample size than that used in chapter 3, could accurately detect adverse outcomes in a different cohort. Additionally, I explore the relationship between $rcSO_2$ and SpO_2, analysing whether this relationship could be a predictor of adverse outcomes.

Chapter 5 investigates the role of NIRS in detecting brain injuries that had been confirmed by MRI in term infants with different grades of hypoxic-ischaemic

encephalopathy (HIE). I also employ deep learning techniques to analyse NIRS signals, automating feature extraction and pattern recognition using convolutional neural networks (CNNs).

In Chapter 6, I expand the scope of our investigation by focusing on the analysis of electroencephalogram (EEG) signals to assess their utility in grading hypoxic-ischaemic encephalopathy (HIE) in term neonates.

Finally, Chapter 7 synthesises all of my findings, discussing the strengths and limitations of applying AI in healthcare, and highlights the benefits and potential of this transformative technology.

1.7. References:

Afrin, R., Haddad, H., & Shahriar, H. (2019, July). Supervised and unsupervised-based analytics of intensive care unit data. In *2019 IEEE 43rd Annual Computer Software and Applications Conference (COMPSAC)* (Vol. 2, 417-422). IEEE.

Ahn, Y.M. (2011). Relationship Between Brain Injury and Head Circumference Growth in Extremely Premature Infants. *Journal of Korean Academy of Child Health Nursing*, *17*(4), 281-287.

Ahn, S. Y., Shim, S. Y., & Sung, I. K. (2015). Intraventricular haemorrhage and post haemorrhagic hydrocephalus among very-low-birth-weight infants in Korea. *Journal of Korean Medical Science*, *30*(Suppl 1), S52-S58.

Alderliesten, T., Dix, L., Baerts, W., Caicedo, A., Van Huffel, S., Naulaers, G., Groenendaal, F., Van Bel, F., & Lemmers, P. (2016). Reference values of regional cerebral oxygen saturation during the first 3 days of life in preterm neonates. *Pediatric Research*, *79*(1), 55-64.

Alderliesten, T., Lemmers, P. M., Smarius, J. J., van de Vosse, R. E., Baerts, W., & van Bel, F. (2013). Cerebral oxygenation, extraction, and autoregulation in very preterm infants who develop peri-intraventricular haemorrhage. *The Journal of Pediatrics*, *162*(4), 698-704.

Alderliesten, T., Lemmers, P.M., van Haastert, I.C., de Vries, L.S., Bonestroo, H.J., Baerts, W., & van Bel, F. (2014). Hypotension in preterm neonates: low blood pressure alone does not affect neurodevelopmental outcome. *The Journal of Pediatrics*, *164*(5), 986-991.

Almaazmi, M., Schmid, M.B., Havers, S., Reister, F., Lindner, W., Mayer, B., Hummler, H.D., & Fuchs, H. (2013). Cerebral near-infrared spectroscopy during transition of healthy term newborns. *Neonatology*, *103*(4), 246-251.

Alderliesten, T., van Bel, F., van der Aa, N.E., Steendijk, P., van Haastert, I.C., de Vries, L.S., Groenendaal, F., & Lemmers, P. (2019). Low cerebral oxygenation in preterm infants is associated with adverse neurodevelopmental outcome. *The Journal of Pediatrics*, *207*, 109-116.

Alix, J. J., Ponnusamy, A., Pilling, E., & Hart, A. R. (2017). An introduction to neonatal EEG. *Paediatrics and Child Health*, *27*(3), 135-142.

al Naqeeb, N., Edwards, A. D., Cowan, F. M., & Azzopardi, D. (1999). Assessment of neonatal encephalopathy by amplitude-integrated electroencephalography. *Pediatrics*, *103*(6), 1263-1271.

Andrews, W. W., Copper, R., Hauth, J. C., Goldenberg, R. L., Neely, C., & DuBard, M. (2000). Second-trimester cervical ultrasound: associations with increased risk for recurrent early spontaneous delivery. *Obstetrics & Gynecology*, *95*(2), 222-226.

Annells, M. F., Hart, P. H., Mullighan, C. G., Heatley, S. L., Robinson, J. S., Bardy, P., & McDonald, H. M. (2004). Interleukins-1,-4,-6,-10, tumor necrosis factor, transforming growth factor-β, FAS, and mannose-binding protein C gene polymorphisms in Australian women: risk of preterm birth. *American Journal of Obstetrics and Gynecology*, *191*(6), 2056-2067.

Apgar, V. (1966). The newborn (Apgar) scoring system: reflections and advice. *Pediatric Clinics of North America*, *13*(3), 645-650.

Apgar, V. (2015). A proposal for a new method of evaluation of the newborn infant. *Anesthesia & Analgesia*, *120*(5), 1056-1059.

Armstead, W. M. (2000). Age-dependent cerebral hemodynamic effects of traumatic brain injury in newborn and juvenile pigs. *Microcirculation*, *7*(4), 225-235.

Armstead, W. M. (2016). Cerebral blood flow autoregulation and dysautoregulation. *Anesthesiology Clinics*, *34*(3), 465-477.

Askie, L.M., Darlow, B.A., Finer, N., Schmidt, B., Stenson, B., Tarnow-Mordi, W., Davis, P.G., Carlo, W.A., Brocklehurst, P., Davies, L.C., & Das, A. (2018). Association between oxygen saturation targeting and death or disability in extremely preterm infants in the neonatal oxygenation prospective meta-analysis collaboration. *The Journal of the American Medical Association*, *319*(21), 2190-2201.

Azzopardi, D., Brocklehurst, P., Edwards, D., Halliday, H., Levene, M., Thoresen, M., Whitelaw, A., & TOBY Study Group (2008). The TOBY Study. Whole body hypothermia for the treatment of perinatal asphyxial encephalopathy: a randomised controlled trial. *BMC Pediatrics*, *8*, pp.1-12.

Azzopardi, D.V., Strohm, B., Edwards, A.D., Dyet, L., Halliday, H.L., Juszczak, E., Kapellou, O., Levene, M., Marlow, N., Porter, E., & Thoresen, M. (2009). Moderate hypothermia to treat perinatal asphyxial encephalopathy. *New England Journal of Medicine*, *361*(14), 1349-1358.

Baburamani, A.A., Ek, C.J., Walker, D.W., & Castillo-Melendez, M. (2012). Vulnerability of the developing brain to hypoxic-ischemic damage: contribution of the cerebral vasculature to injury and repair?. *Frontiers in Physiology*, *3*, 424.

Badve, C. A., Khanna, P. C., & Ishak, G. E. (2012). Neonatal ischemic brain injury: what every radiologist needs to know. *Pediatric Radiology*, *42*, 606-619.

Baik, N., Urlesberger, B., Schwaberger, B., Schmölzer, G. M., Mileder, L., Avian, A., & Pichler, G. (2015). Reference ranges for cerebral tissue oxygen saturation index in term neonates during immediate neonatal transition after birth. *Neonatology*, *108*(4), 283-286.

Bailey, S. M., Hendricks-Munoz, K. D., & Mally, P. (2013). Cerebral, renal, and splanchnic tissue oxygen saturation values in healthy term newborns. *American Journal of Perinatology*, 339-344.

Bakheet, D., Alotaibi, N., Konn, D., Vollmer, B., & Maharatna, K. (2021). Prediction of cerebral palsy in newborns with hypoxic-ischaemic encephalopathy using multivariate EEG analysis and machine learning. *IEEE Access*, *9*, 137833-137846.

Ballabh, P. (2010). Intraventricular haemorrhage in premature infants: mechanism of disease. *Pediatric Research*, *67*(1), 1-8.

Ballabh, P., & de Vries, L.S. (2021). White matter injury in infants with intraventricular haemorrhage: mechanisms and therapies. *Nature Reviews Neurology*, *17*(4), 199-214.

Bano, S., Chaudhary, V., & Garga, U. C. (2017). Neonatal hypoxic-ischaemic encephalopathy: a radiological review. *Journal of Pediatric Neurosciences*, *12*(1), 1.

Baraldi, E., & Filippone, M. (2007). Chronic lung disease after premature birth. *New England Journal of Medicine*, *357*(19), 1946-1955.

Barkovich, A. J. (2001). Pediatric neuroimaging, 3rd edn. *European Radiology*, *11*(11), 2347-2347.

Barkovich, A. J. (2005). *Pediatric neuroimaging*. Lippincott Williams & Wilkins.

Barkovich, A. J., Hajnal, B. L., Vigneron, D., Sola, A., Partridge, J. C., Allen, F., & Ferriero, D. M. (1998). Prediction of neuromotor outcome in perinatal asphyxia: evaluation of MR scoring systems. *American Journal of Neuroradiology*, *19*(1), 143-149.

Barkovich, A. J., Westmark, K. D., Bedi, H. S., Partridge, J. C., Ferriero, D. M., & Vigneron, D. B. (2001). Proton spectroscopy and diffusion imaging on the first day of life after perinatal asphyxia: preliminary report. *American Journal of Neuroradiology*, *22*(9), 1786-1794.

Batton, B., Li, L., Newman, N.S., Das, A., Watterberg, K.L., Yoder, B.A., Faix, R.G., Laughon, M.M., Stoll, B.J., Higgins, R.D., & Walsh, M.C. (2016). Early blood pressure, antihypotensive therapy and outcomes at 18–22 months' corrected age in extremely preterm infants. *Archives of Disease in Childhood-Fetal and Neonatal Edition*, *101*(3), F201-F206.

Batton, B., Zhu, X., Fanaroff, J., Kirchner, H. L., Berlin, S., Wilson-Costello, D., & Walsh, M. (2009). Blood pressure, anti-hypotensive therapy, and neurodevelopment in extremely preterm infants. *The Journal of pediatrics*, *154*(3), 351-357.

Belet, N., Belet, U., ütfi İncesu, L., Uysal, S., Özinal, S., ülay Keskin, T., Sunter, A.T., & ükrü Küçüködük, S. (2004). Hypoxic-ischemic encephalopathy: correlation of serial MRI and outcome. *Pediatric Neurology*, *31*(4), 267-274.

Bennet, L., Roelfsema, V., Pathipati, P., Quaedackers, J. S., & Gunn, A. J. (2006). Relationship between evolving epileptiform activity and delayed loss of mitochondrial activity after asphyxia measured by near-infrared spectroscopy in preterm fetal sheep. *The Journal of Physiology*, *572*(1), 141-154.

Bermudez, E. A., Rifai, N., Buring, J. E., Manson, J. E., & Ridker, P. M. (2002). Relation between markers of systemic vascular inflammation and smoking in women. *American Journal of Cardiology*, *89*(9), 1117-1119.

Bhutta, A. T., Cleves, M. A., Casey, P. H., Cradock, M. M., & Anand, K. J. (2002). Cognitive and behavioral outcomes of school-aged children who were born preterm: a meta-analysis. *The Journal of the American Medical Association*, *288*(6), 728-737.

Binder-Heschl, C., Urlesberger, B., Schwaberger, B., Koestenberger, M., & Pichler, G. (2016). Borderline hypotension: how does it influence cerebral regional tissue oxygenation in preterm infants?. *The Journal of Maternal-Fetal & Neonatal Medicine*, *29*(14), 2341-2346.

Bohnhorst, B., Peter, C.S., & Poets, C.F. (2000). Pulse oximeters' reliability in detecting hypoxemia and bradycardia: comparison between a conventional and two new generation oximeters. *Critical Care Medicine*, *28*(5), 1565-1568.

Bolisetty, S., Dhawan, A., Abdel-Latif, M., Bajuk, B., Stack, J., Oei, J.L., Lui, K., & New South Wales and Australian Capital Territory Neonatal Intensive Care Units' Data Collection (2014). Intraventricular hemorrhage and neurodevelopmental outcomes in extreme preterm infants. *Pediatrics*, *133*(1), 55-62.

Børch, K., Lou, H. C., & Greisen, G. (2010). Cerebral white matter blood flow and arterial blood pressure in preterm infants. *Acta Paediatrica*, *99*(10), 1489-1492.

Bourgoin, P., Barrault, V., Loron, G., Roger, A., Bataille, E., Leclair-Visonneau, L., Joram, N., & Chenouard, A. (2020). Interrater agreement between critical care providers for background classification and seizure detection after implementation of amplitude-integrated electroencephalography in neonates, infants, and children. *Journal of Clinical Neurophysiology*, *37*(3), 259-262.

Boylan, G. B., Young, K., Panerai, R. B., Rennie, J. M., & Evans, D. H. (2000). Dynamic cerebral autoregulation in sick newborn infants. *Pediatric Research*, *48*(1), 12-17.

Brian, J.E. (1998). Carbon dioxide and the cerebral circulation. *The Journal of the American Society of Anesthesiologists*, *88*(5), 1365-1386.

Brown, D. W., Picot, P. A., Gharavi Naeini, J., Springett, R., Delpy, D. T., & Lee, T. Y. (2002). Quantitative near infrared spectroscopy measurement of cerebral hemodynamics in newborn piglets. *Pediatric Research*, *51*(5), 564-570.

Buonocore, G., Perrone, S., & Tataranno, M.L. (2010), August. Oxygen toxicity: chemistry and biology of reactive oxygen species. In *Seminars in Fetal and Neonatal Medicine* (Vol. 15, No. 4, 186-190). WB Saunders.

Caicedo, A., Alderliesten, T., Naulaers, G., Lemmers, P., Van Bel, F., & Van Huffel, S. (2016). A new framework for the assessment of cerebral hemodynamics regulation in neonates using NIRS. In *Oxygen Transport to Tissue XXXVII* (501-509). Springer New York.

Cambonie, G., Guillaumont, S., Luc, F., Vergnes, C., Milesi, C., & Voisin, M. (2003). Haemodynamic features during high-frequency oscillatory ventilation in preterms. *Acta Paediatrica*, *92*(9), 1068-1073.

Cappelletti, M., Della Bella, S., Ferrazzi, E., Mavilio, D., & Divanovic, S. (2016). Inflammation and preterm birth. *Journal of Leucocyte Biology*, *99*(1), 67-78.

CergenX. (n.d.). Home. CergenX. https://www.cergenx.com/

Chalak, L.F., Nguyen, K.A., Prempunpong, C., Heyne, R., Thayyil, S., Shankaran, S., Laptook, A.R., Rollins, N., Pappas, A., Koclas, L., & Shah, B. (2018). Prospective research in infants with mild encephalopathy identified in the first six hours of life: neurodevelopmental outcomes at 18–22 months. *Pediatric Research*, *84*(6), 861-868.

Chandrasekaran, M., Chaban, B., Montaldo, P., & Thayyil, S. (2017). Predictive value of amplitude-integrated EEG (aEEG) after rescue hypothermic neuroprotection for hypoxic ischaemic encephalopathy: a meta-analysis. *Journal of Perinatology*, *37*(6), 684-689.

Chapados, I., & Cheung, P. Y. (2008). Not all models are created equal: animal models to study hypoxic-ischaemic encephalopathy of the newborn. *Neonatology*, *94*(4), 300.

Chen, T., Tan, X., Xia, F., Hua, Y., Keep, R.F., & Xi, G. (2021). Hydrocephalus induced by intraventricular peroxiredoxin-2: the role of macrophages in the choroid plexus. *Biomolecules*, *11*(5), 654.

Chen, T., & Guestrin, C. (2016, August). Xgboost: A scalable tree boosting system. In *Proceedings of the 22nd acm sigkdd international conference on knowledge discovery and data mining*,785-794.

Cho, H., Nemoto, E. M., Sanders, M., Fernandez, K., & Yonas, H. (2000). Comparison of two commercially available near-infrared spectroscopy instruments for cerebral oximetry. *Journal of Neurosurgery*, *93*(2), 351-354.

Chock, V.Y., Kwon, S.H., Ambalavanan, N., Batton, B., Nelin, L.D., Chalak, L.F., Tian, L., & Van Meurs, K.P. (2020). Cerebral oxygenation and autoregulation in preterm infants (early NIRS study). *The Journal of Pediatrics*, *227*, 94-100.

Clarke, S. L., Parmesar, K., Saleem, M. A., & Ramanan, A. V. (2021). Future of machine learning in paediatrics. *Archives of Disease in Childhood*.

Cohen, E., Baerts, W., Alderliesten, T., Derks, J., Lemmers, P., & van Bel, F. (2015). Growth restriction and gender influence cerebral oxygenation in preterm neonates. *Archives of Disease in Childhood-Fetal and Neonatal Edition*.

Conway, J. M., Walsh, B. H., Boylan, G. B., & Murray, D. M. (2018). Mild hypoxic ischaemic encephalopathy and long term neurodevelopmental outcome-A systematic review. *Early Human Development*, *120*, 80-87.

Cox, D. J., & Groves, A. M. (2012). Inotropes in preterm infants–evidence for and against. *Acta Paediatrica*, *101*, 17-23.

Crilly, C. J., Haneuse, S., & Litt, J. S. (2021). Predicting the outcomes of preterm neonates beyond the neonatal intensive care unit: what are we missing?. *Pediatric Research*, *89*(3), 426-445.

Csekő, A. J., Bangó, M., Lakatos, P., Kárdási, J., Pusztai, L., & Szabó, M. (2013). Accuracy of amplitude-integrated electroencephalography in the prediction of neurodevelopmental outcome in asphyxiated infants receiving hypothermia treatment. *Acta Paediatrica*, *102*(7), 707-711.

Cuestas, E., Bas, J., & Pautasso, J. (2009). Sex differences in intraventricular hemorrhage rates among very low birth weight newborns. *Gender Medicine*, *6*(2), 376-382.

da Costa, C. S., Greisen, G., & Austin, T. (2015). Is near-infrared spectroscopy clinically useful in the preterm infant?. *Archives of Disease in Childhood-Fetal and Neonatal Edition*, *100*(6), F558-F561.

Davis, J.M., & Auten, R.L. (2010), August. Maturation of the antioxidant system and the effects on preterm birth. In *Seminars in Fetal and Neonatal Medicine* (Vol. 15, No. 4, 191-195). WB Saunders.

Dawson, J. A., Davis, P. G., O'Donnell, C. P. F., Kamlin, C. O. F., & Morley, C. J. (2007). Pulse oximetry for monitoring infants in the delivery room: a review. *Archives of Disease in Childhood-Fetal and Neonatal Edition*, *92*(1), F4-F7.

Dempsey, E. M., Al Hazzani, F., & Barrington, K. J. (2009). Permissive hypotension in the extremely low birthweight infant with signs of good perfusion. *Archives of Disease in Childhood-Fetal and Neonatal Edition*, *94*(4), F241-F244.

Dempsey, E. M., & Barrington, K. J. (2007). Treating hypotension in the preterm infant: when and with what: a critical and systematic review. *Journal of Perinatology*, *27*(8), 469-478.

Dempsey, E. M., & Barrington, K. J. (2009). Evaluation and treatment of hypotension in the preterm infant. *Clinics in Perinatology*, *36*(1), 75-85.

Dempsey, E.M., Barrington, K.J., Marlow, N., O'Donnell, C.P.F., Miletin, J., Naulaers, G., Cheung, P.Y., Corcoran, J.D., El-Khuffash, A.F., Boylan, G.B., & Livingstone, V. (2021). Hypotension in Preterm Infants (HIP) randomised trial. *Archives of Disease in Childhood-Fetal and Neonatal Edition*, *106*(4), 398-403.

Dix, L., Molenschot, M., Breur, J., de Vries, W., Vijlbrief, D., Groenendaal, F., Van Bel, F., & Lemmers, P. (2016). Cerebral oxygenation and echocardiographic parameters in preterm neonates with a patent ductus arteriosus: an observational study. *Archives of Disease in Childhood-Fetal and Neonatal Edition*, *101*(6), F520-F526.

Dix, L. M., van Bel, F., Baerts, W., & Lemmers, P. (2013). Comparing near-infrared spectroscopy devices and their sensors for monitoring regional cerebral oxygen saturation in the neonate. *Pediatric Research*, *74*(5), 557-563.

Dix, L. M. L., Van Bel, F., & Lemmers, P. M. A. (2017). Monitoring cerebral oxygenation in neonates: an update. *Frontiers in Pediatrics*, *5*, 46.

Douglas-Escobar, M., & Weiss, M. D. (2015). Hypoxic-ischaemic encephalopathy: a review for the clinician. *JAMA Pediatrics*, *169*(4), 397-403.

Doyle, L. W., & Anderson, P. J. (2010). Adult outcome of extremely preterm infants. *Pediatrics*, *126*(2), 342-351.

Drage, J.S., Kennedy, C., & Schwarz, B.K. (1964). The Apgar score as an index of neonatal mortality: a report from the Collaborative Study of Cerebral Palsy. *Obstetrics & Gynecology*, *24*(2), 222-230.

Drummond, D., Hadchouel, A., Torchin, H., Rozé, J.C., Arnaud, C., Bellino, A., Couderc, L., Marret, S., Mittaine, M., Pinquier, D., & Vestraete, M. (2019). Educational and health outcomes associated with bronchopulmonary dysplasia in 15-year-olds born preterm. *PLoS One*, *14*(9), e0222286.

Edelmann, C.M., Soriano, J.R., Boichis, H., Gruskin, A.B., & Acosta, M.I. (1967). Renal bicarbonate reabsorption and hydrogen ion excretion in normal infants. *The Journal of Clinical Investigation*, *46*(8), 1309-1317.

Edwards, A.D., Richardson, C., Cope, M., Wyatt, J.S., Delpy, D.T., & Reynolds, E.O.R. (1988). Cotside measurement of cerebral blood flow in ill newborn infants by near infrared spectroscopy. *The Lancet*, *332*(8614), 770-771.

Eiby, Y.A., Wright, I.M., Stark, M.J., & Lingwood, B.E. (2023). Red cell infusion but not saline is effective for volume expansion in preterm piglets. *Pediatric Research*, *94*(1), 112-118.

Ekman, M. (2021). *Learning deep learning: Theory and practice of neural networks, computer vision, natural language processing, and transformers using TensorFlow*. Addison-Wesley Professional.

El-Dib, M., & Soul, J. S. (2019). Monitoring and management of brain hemodynamics and oxygenation. *Handbook of clinical neurology*, *162*, 295-314.

Fabres, J., Carlo, W. A., Phillips, V., Howard, G., & Ambalavanan, N. (2007). Both extremes of arterial carbon dioxide pressure and the magnitude of fluctuations in arterial carbon dioxide pressure are associated with severe intraventricular haemorrhage in preterm infants. *Pediatrics*, *119*(2), 299-305.

Fanaroff, J. M., & Fanaroff, A. A. (2006, June). Blood pressure disorders in the neonate: hypotension and hypertension. In *Seminars in Fetal and Neonatal Medicine* (Vol. 11, No. 3, 174-181). WB Saunders.

Faridy, E. E., & Thliveris, J. A. (1987). Rate of secretion of lung surfactant before and after birth. *Respiration physiology*, 68(3), 269-277.

Faust, K., Härtel, C., Preuß, M., Rabe, H., Roll, C., Emeis, M., Wieg, C., Szabo, M., Herting, E., & Göpel, W. (2015). Short-term outcome of very-low-birthweight infants with arterial hypotension in the first 24 h of life. *Archives of Disease in Childhood-Fetal and Neonatal Edition*, *100*(5), F388-F392.

Ferriero, D. M. (2004). Neonatal brain injury. *New England Journal of Medicine*, *351*(19), 1985-1995.

Gao, Y., & Raj, J. U. (2010). Regulation of the pulmonary circulation in the fetus and newborn. *Physiological Reviews*, *90*(4), 1291-1335.

Garvey, A. A., Kooi, E. M., Smith, A., & Dempsey, E. M. (2018). Interpretation of cerebral oxygenation changes in the preterm infant. *Children*, *5*(7), 94.

Gilard, V., Tebani, A., Bekri, S., & Marret, S. (2020). Intraventricular haemorrhage in very preterm infants: a comprehensive review. *Journal of Clinical Medicine*, *9*(8), 2447.

Gillam-Krakauer, M., & Reese, J. (2018). Diagnosis and management of patent ductus arteriosus. *Neoreviews*, *19*(7), e394-e402.

Goldenberg, R. L., Culhane, J. F., Iams, J. D., & Romero, R. (2008). Epidemiology and causes of preterm birth. *The lancet*, *371*(9606), 75-84.

Gopagondanahalli, K. R., Li, J., Fahey, M. C., Hunt, R. W., Jenkin, G., Miller, S. L., & Malhotra, A. (2016). Preterm hypoxic–ischaemic encephalopathy. *Frontiers in Pediatrics*, *4*, 114.

Govaert, P., & De Vries, L. S. (2010). *An atlas of neonatal brain sonography* (Vol. 182). John Wiley & Sons.

Greisen, G. (2005). Autoregulation of cerebral blood flow in newborn babies. *Early Human Development*, *81*(5), 423-428.

Greisen, G. (2014). Cerebral blood flow and oxygenation in infants after birth asphyxia. Clinically useful information?. *Early Human Development*, *90*(10), 703-705.

Grubhofer, G., Tonninger, W., Keznickl, P., Skyllouriotis, P., Ehrlich, M., Hiesmayr, M., & Lassnigg, A. (1999). A comparison of the monitors INVOS 3100 and NIRO 500 in detecting changes in cerebral oxygenation. *Acta Anaesthesiologica Scandinavica*, *43*(4), 470-475.

Gunn, A.J., Wyatt, J.S., Whitelaw, A., Barks, J., Azzopardi, D., Ballard, R., Edwards, A.D., Ferriero, D.M., Gluckman, P.D., Polin, R.A., & Robertson, C.M. (2008). Therapeutic hypothermia changes the prognostic value of clinical evaluation of neonatal encephalopathy. *The Journal of Pediatrics*, *152*(1), 55-58.

Hallman, M. (2013). The surfactant system protects both fetus and newborn. *Neonatology*, 103(4), 320-326.

Hamelin, S., Delnard, N., Cneude, F., Debillon, T., & Vercueil, L. (2011). Influence of hypothermia on the prognostic value of early EEG in full-term neonates with hypoxic

ischaemic encephalopathy. *Neurophysiologie Clinique/Clinical Neurophysiology*, *41*(1), 19-27.

Hansen, N. B., Brubakk, A. M., Bratlid, D. A. G., Oh, W., & Stonestreet, B. S. (1984). The effects of variations in PaCO2 on brain blood flow and cardiac output in the newborn piglet. *Pediatric Research*, *18*(11), 1132-1136.

Hansen, M.L., Pellicer, A., Gluud, C., Dempsey, E., Mintzer, J., Hyttel-Sørensen, S., Heuchan, A.M., Hagmann, C., Ergenekon, E., Dimitriou, G., & Pichler, G. (2019). Cerebral near-infrared spectroscopy monitoring versus treatment as usual for extremely preterm infants: a protocol for the SafeBoosC randomised clinical phase III trial. *Trials*, *20*, 1-11.

Harteman, J. C., Nikkels, P. G., Benders, M. J., Kwee, A., Groenendaal, F., & de Vries, L. S. (2013). Placental pathology in full-term infants with hypoxic-ischaemic neonatal encephalopathy and association with magnetic resonance imaging pattern of brain injury. *The Journal of Pediatrics*, *163*(4), 968-975.

Hay Jr, W. W. (1987). The uses, benefits, and limitations of pulse oximetry in neonatal medicine: consensus on key issues. *Journal of Perinatology: Official Journal of the California Perinatal Association*, *7*(4), 347-349.

Hay Jr, W. W., Brockway, J. M., & Eyzaguirre, M. (1989). Neonatal pulse oximetry: accuracy and reliability. *Pediatrics*, *83*(5), 717-722.

Hay, W. W., Rodden, D. J., Collins, S. M., Melara, D. L., Hale, K. A., & Fashaw, L. M. (2002). Reliability of conventional and new pulse oximetry in neonatal patients. *Journal of Perinatology*, *22*(5), 360-366.

Heinz, E. R., & Provenzale, J. M. (2009). Imaging findings in neonatal hypoxia: a practical review. *American Journal of Roentgenology*, *192*(1), 41-47.

Hellstrom-Westas, L., Rosén, I., De Vries, L. S., & Greisen, G. (2006). Amplitude-integrated EEG classification and interpretation in preterm and term infants. *NeoReviews*, *7*(2), e76-e87.

Hellström-Westas, L., Rosen, I., & Svenningsen, N. W. (1995). Predictive value of early continuous amplitude integrated EEG recordings on outcome after severe birth asphyxia in full term infants. *Archives of Disease in Childhood-Fetal and Neonatal Edition*, *72*(1), F34-F38.

Hillman, N. H., Kallapur, S. G., & Jobe, A. H. (2012). Physiology of transition from intrauterine to extrauterine life. *Clinics in Perinatology*, 39(4), 769-783.

Hinson, H. E., Hanley, D. F., & Ziai, W. C. (2010). Management of intraventricular haemorrhage. *Current Neurology and Neuroscience Reports*, *10*, 73-82.

Hoffman, S. B., Cheng, Y. J., Magder, L. S., Shet, N., & Viscardi, R. M. (2019). Cerebral autoregulation in premature infants during the first 96 hours of life and relationship to adverse outcomes. *Archives of Disease in Childhood-Fetal and Neonatal Edition*, *104*(5), F473-F479.

Hou, X., Ding, H., Teng, Y., Zhou, C., Tang, X., Li, S., & Ding, H. (2007). Research on the relationship between brain anoxia at different regional oxygen saturations and brain damage using near-infrared spectroscopy. *Physiological Measurement*, *28*(10), 1251.

Howlett, J.A., Northington, F.J., Gilmore, M.M., Tekes, A., Huisman, T.A., Parkinson, C., Chung, S.E., Jennings, J.M., Jamrogowicz, J.J., Larson, A.C., & Lehmann, C.U. (2013).

Cerebrovascular autoregulation and neurologic injury in neonatal hypoxic–ischemic encephalopathy. *Pediatric Research*, *74*(5), 525-535.

Hüppi, P. S. (2002). Advances in postnatal neuroimaging: relevance to pathogenesis and treatment of brain injury. *Clinics in Perinatology*, *29*(4), 827-856.

Hyttel-Sorensen, S., Pellicer, A., Alderliesten, T., Austin, T., Van Bel, F., Benders, M., Claris, O., Dempsey, E., Franz, A.R., Fumagalli, M., & Gluud, C. (2015). Cerebral near infrared spectroscopy oximetry in extremely preterm infants: phase II randomised clinical trial. *Bmj*, *350*.

Hyttel-Sorensen, S., Sorensen, L.C., Riera, J., & Greisen, G. (2011). Tissue oximetry: a comparison of mean values of regional tissue saturation, reproducibility and dynamic range of four NIRS-instruments on the human forearm. *Biomedical Optics Express*, *2*(11), 3047-3057.

Iams, J.D., Goldenberg, R.L., Meis, P.J., Mercer, B.M., Moawad, A., Das, A., Thom, E., McNellis, D., Copper, R.L., Johnson, F., & Roberts, J.M. (1996). The length of the cervix and the risk of spontaneous premature delivery. *New England Journal of Medicine*, *334*(9), 567-573.

Inder, T. E., Volpe, J. J., & Anderson, P. J. (2023). Defining the neurologic consequences of preterm birth. *New England Journal of Medicine*, *389*(5), 441-453.

Jain, L., & Eaton, D. C. (2006, February). Physiology of fetal lung fluid clearance and the effect of labor. In *Seminars in Perinatology* (Vol. 30, No. 1, 34-43). WB Saunders.

Jia, W., Lei, X., Dong, W., & Li, Q. (2018). Benefits of starting hypothermia treatment within 6 h vs. 6–12 h in newborns with moderate neonatal hypoxic-ischaemic encephalopathy. *BMC Pediatrics*, *18*, 1-8.

Jobe, A. H., & Bancalari, E. (2001). Bronchopulmonary dysplasia. *American Journal of Respiratory and Critical Care Medicine*, *163*(7), 1723-1729.

Jöbsis, F. F. (1977). Noninvasive, infrared monitoring of cerebral and myocardial oxygen sufficiency and circulatory parameters. *Science*, *198*(4323), 1264-1267.

Johnson, K.R., Hagadorn, J.I., & Sink, D.W. (2017). Alarm safety and alarm fatigue. *Clinics in Perinatology*, *44*(3), 713-728.

Kahraman, S., Kayali, H., Atabey, C., Acar, F., & Gocmen, S. (2006). The accuracy of near-infrared spectroscopy in detection of subdural and epidural hematomas. *Journal of Trauma and Acute Care Surgery*, *61*(6), 1480-1483.

Kattwinkel, J., Perlman, J.M., Aziz, K., Colby, C., Fairchild, K., Gallagher, J., Hazinski, M.F., Halamek, L.P., Kumar, P., Little, G., & McGowan, J.E. (2010). Part 15: neonatal resuscitation: 2010 American Heart Association guidelines for cardiopulmonary resuscitation and emergency cardiovascular care. *Circulation*, *122*(18_suppl_3), S909-S919.

Kausch, S.L., Slevin, C.C., Duncan, A., Fairchild, K.D., Lake, D.E., Keim-Malpass, J., Vesoulis, Z.A., & Sullivan, B.A (2024). Clinical correlates of a high cardiorespiratory risk score for very low birth weight infants. *Pediatric Research*, 1-5.

Kayhanian, S., Young, A.M., Mangla, C., Jalloh, I., Fernandes, H.M., Garnett, M.R., Hutchinson, P.J., & Agrawal, S. (2019). Modelling outcomes after paediatric brain

injury with admission laboratory values: a machine-learning approach. *Pediatric Research*, *86*(5), 641-645.

Kenosi, M., Naulaers, G., Ryan, C. A., & Dempsey, E. M. (2015). Current research suggests that the future looks brighter for cerebral oxygenation monitoring in preterm infants. *Acta Paediatrica*, *104*(3), 225-231.

Kenosi, M., O'Toole, J.M., Hawkes, G.A., Hutch, W., Low, E., Wall, M., Boylan, G.B., Ryan, C.A., & Dempsey, E.M. (2018). Monitoring cerebral oxygenation of preterm infants using a neonatal specific sensor. *Journal of Perinatology*, *38*(3), 264-270.

Khazipov, R., Sirota, A., Leinekugel, X., Holmes, G. L., Ben-Ari, Y., & Buzsáki, G. (2004). Early motor activity drives spindle bursts in the developing somatosensory cortex. *Nature*, *432*(7018), 758-761.

Khwaja, O., & Volpe, J. J. (2008). Pathogenesis of cerebral white matter injury of prematurity. *Archives of Disease in Childhood. Fetal and Neonatal Edition*, *93*(2), F153.

Kissack, C. M., Garr, R., Wardle, S. P., & Weindling, A. M. (2005). Cerebral fractional oxygen extraction is inversely correlated with oxygen delivery in the sick, newborn, preterm infant. *Journal of Cerebral Blood Flow & Metabolism*, *25*(5), 545-553.

Klebermass-Schrehof, K., Czaba, C., Olischar, M., Fuiko, R., Waldhoer, T., Rona, Z., Pollak, A., & Weninger, M. (2012). Impact of low-grade intraventricular hemorrhage on long-term neurodevelopmental outcome in preterm infants. *Child's Nervous System*, *28*, 2085-2092.

Kuo, L.T., & Huang, A.P.H (2021). The pathogenesis of hydrocephalus following aneurysmal subarachnoid hemorrhage. *International Journal of Molecular Sciences*, *22*(9), 5050.

Kozberg, M., & Hillman, E. (2016). Neurovascular coupling and energy metabolism in the developing brain. *Progress in Brain Research*, *225*, 213-242.

Krupa, F. G., Faltin, D., Cecatti, J. G., Surita, F. G. C., & Souza, J. P. (2006). Predictors of preterm birth. *International Journal of Gynecology & Obstetrics*, *94*(1), 5-11.

Kurinczuk, J. J., White-Koning, M., & Badawi, N. (2010). Epidemiology of neonatal encephalopathy and hypoxic–ischaemic encephalopathy. *Early Human Development*, *86*(6), 329-338.

Kurth, C. D., Levy, W. J., & McCann, J. (2002). Near-infrared spectroscopy cerebral oxygen saturation thresholds for hypoxia–ischaemia in piglets. *Journal of Cerebral Blood Flow & Metabolism*, *22*(3), 335-341.

Lamblin, M. D., & de Villepin-Touzery, A. (2015). EEG in the neonatal unit. *Neurophysiologie Clinique/Clinical Neurophysiology*, *45*(1), 87-95.

Lara-Cantón, I., Badurdeen, S., Dekker, J., Davis, P., Roberts, C., Te Pas, A., & Vento, M. (2024). Oxygen saturation and heart rate in healthy term and late preterm infants with delayed cord clamping. *Pediatric Research*, *96*(3), 604-609.

Larroque, B., Marret, S., Ancel, P.Y., Arnaud, C., Marpeau, L., Supernant, K., Pierrat, V., Rozé, J.C., Matis, J., Cambonie, G., & Burguet, A. (2003). White matter damage and intraventricular hemorrhage in very preterm infants: the EPIPAGE study. *The Journal of Pediatrics*, *143*(4), 477-483.

Leijser, L. M., & Cowan, F. M. (2007). 'State-of-the-Art' neonatal cranial ultrasound. *Ultrasound*, *15*(1), 6-17.

Lemmers, P., Benders, M.J., D'Ascenzo, R., Zethof, J., Alderliesten, T., Kersbergen, K.J., Isgum, I., de Vries, L.S., Groenendaal, F., & van Bel, F. (2016). Patent ductus arteriosus and brain volume. *Pediatrics*, *137*(4).

Lemmers, P. M., Toet, M. C., & van Bel, F. (2008). Impact of patent ductus arteriosus and subsequent therapy with indomethacin on cerebral oxygenation in preterm infants. *Pediatrics*, *121*(1), 142-147.

Lemmers, P., Zwanenburg, R. J., Benders, M. J., de Vries, L. S., Groenendaal, F., van Bel, F., & Toet, M. C. (2013). Cerebral oxygenation and brain activity after perinatal asphyxia: does hypothermia change their prognostic value?. *Pediatric Research*, *74*(2), 180-185.

Lemons, A., & James, M. D. (2007). *Guidelines for perinatal care*. American Academy of Pediatrics.

Leijser, L. M., de Vries, L. S., & Cowan, F. M. (2006). Using cerebral ultrasound effectively in the newborn infant. *Early Human Development*, *82*(12), 827-835.

Leviton, A., Allred, E.N., Dammann, O., Engelke, S., Fichorova, R.N., Hirtz, D., Kuban, K.C., Ment, L.R., O'shea, T.M., Paneth, N., & Shah, B. (2013). Systemic inflammation, intraventricular hemorrhage, and white matter injury. *Journal of Child Neurology*, *28*(12), 1637-1645.

Liu, Y., Chen, P. H. C., Krause, J., & Peng, L. (2019). How to read articles that use machine learning: users' guides to the medical literature. *The Journal of the American Medical Association*, *322*(18), 1806-1816.

Macnab, A. (2020). *Pathogenesis and Prevention of Fetal and Neonatal Brain Injury* (Vol. 4). Rijeka, Croatia: IntechOpen.Malin, G.L., Morris, R.K., & Khan, K.S. (2010). Strength of association between umbilical cord pH and perinatal and long term outcomes: systematic review and meta-analysis. *Bmj*, *340*.

Mangold, C., Zoretic, S., Thallapureddy, K., Moreira, A., Chorath, K., & Moreira, A. (2021). Machine learning models for predicting neonatal mortality: a systematic review. *Neonatology*, *118*(4), 394-405.

Manja, V., Lakshminrusimha, S., & Cook, D. J. (2015). Oxygen saturation target range for extremely preterm infants: a systematic review and meta-analysis. *JAMA pediatrics*, *169*(4), 332-340.

Marlow, N. (2012). Full term; an artificial concept. *Archives of Disease in Childhood-Fetal and Neonatal Edition*, 97(3), F158-F159.

McClure, C., Jang, S.Y., & Fairchild, K. (2016). Alarms, oxygen saturations, and SpO2 averaging time in the NICU. *Journal of Neonatal-Perinatal Medicine*, *9*(4), 357-362.

McCormick, P. W., Stewart, M. E. L. V. I. L. L. E., Goetting, M. G., Dujovny, M. A. N. U. E. L., Lewis, G., & Ausman, J. I. (1991). Noninvasive cerebral optical spectroscopy for monitoring cerebral oxygen delivery and hemodynamics. *Critical Care Medicine*, *19*(1), 89-97.

McCrea, H. J., & Ment, L. R. (2008). The diagnosis, management, and postnatal prevention of intraventricular haemorrhage in the preterm neonate. *Clinics in Perinatology*, *35*(4), 777-792.

McKee, L. A., Fabres, J., Howard, G., Peralta-Carcelen, M., Carlo, W. A., & Ambalavanan, N. (2009). PaCO2 and neurodevelopment in extremely low birth weight infants. *The Journal of Pediatrics*, *155*(2), 217-221.

McLean, C. W., Noori, S., Cayabyab, R. G., & Seri, I. (2012). Cerebral circulation and hypotension in the premature infant: diagnosis and treatment. *Neurology: Neonatology Questions and Controversies: Expert Consult-Online and Print*, 2.

McNeill, S., Gatenby, J. C., McElroy, S., & Engelhardt, B. (2011). Normal cerebral, renal and abdominal regional oxygen saturations using near-infrared spectroscopy in preterm infants. *Journal of Perinatology*, *31*(1), 51-57.

Ment, L.R., Bada, H.S., Barnes, P., Grant, P.E., Hirtz, D., Papile, L.A., Pinto-Martin, J., & Slovis, T.L. (2002). Practice parameter: Neuroimaging of the neonate: Report of the QSS of the AAN and the Practice Committee of the CNS: Reply from the Authors. *Neurology-Minneapolis*, *59*(11), 1663-1663.

Ment, L.R., Duncan, C.C., Ehrenkranz, R.A., Lange, R.C., Taylor, K.J., Kleinman, C.S., Scott, D.T., Sivo, J., & Gettner, P. (1984). Intraventricular hemorrhage in the preterm neonate: timing and cerebral blood flow changes. *The Journal of Pediatrics*, *104*(3), 419-425.

Miall-Allen, V. M., De Vries, L. S., & Whitelaw, A. G. (1987). Mean arterial blood pressure and neonatal cerebral lesions. *Archives of disease in childhood*, *62*(10), 1068-1069.

Milh, M., Kaminska, A., Huon, C., Lapillonne, A., Ben-Ari, Y., & Khazipov, R. (2007). Rapid cortical oscillations and early motor activity in premature human neonate. *Cerebral Cortex*, *17*(7), 1582-1594.

Moghaddam, P. S., Aghaali, M., Modarresy, S. Z., Shahhamzei, S., & Aljaboori, M. (2024). Hypoxic Ischemic Encephalopathy Indicators of Sarnat and Sarnat Scoring in Neonatal Subjects with Perinatal Asphyxia. *Iranian Journal of Child Neurology*, *18*(1), 81.

Moore, A. (2017). Carnegie Mellon Dean of Computer Science on the future of AI. *Forbes*.

Moyle, J. T. (1996). Uses and abuses of pulse oximetry. *Archives of Disease in Childhood*, *74*(1), 77.

Mukerji, A., Shah, V., & Shah, P. S. (2015). Periventricular/intraventricular hemorrhage and neurodevelopmental outcomes: a meta-analysis. *Pediatrics*, *136*(6), 1132-1143.

Munro, M. J., Walker, A. M., & Barfield, C. P. (2004). Hypotensive extremely low birth weight infants have reduced cerebral blood flow. *Pediatrics*, *114*(6), 1591-1596.

Murray, D. M., Boylan, G. B., Ryan, C. A., & Connolly, S. (2009). Early EEG findings in hypoxic-ischaemic encephalopathy predict outcomes at 2 years. *Pediatrics*, *124*(3), e459-e467.

Murray, D. M., Ryan, C. A., Boylan, G. B., Fitzgerald, A. P., & Connolly, S. (2006). Prediction of seizures in asphyxiated neonates: correlation with continuous video-electroencephalographic monitoring. *Pediatrics*, *118*(1), 41-46.

Nault, S., Tremblay, S., Imane, R., Al-Omar, S., Nadeau, C., Samson, N., Creuze, V., Carrault, G., Pladys, P., & Praud, J.P. (2022). Cardiorespiratory alterations in a newborn ovine model of systemic viral inflammation. *Pediatric Research*, *92*(5), 1288-1298.

Navakatikyan, M. A., Colditz, P. B., Burke, C. J., Inder, T. E., Richmond, J., & Williams, C. E. (2006). Seizure detection algorithm for neonates based on wave-sequence analysis. *Clinical Neurophysiology*, *117*(6), 1190-1203.

Nemati, S., Ghassemi, M. M., & Clifford, G. D. (2016, August). Optimal medication dosing from suboptimal clinical examples: A deep reinforcement learning approach. In *2016 38th Annual International Conference of the IEEE Engineering in Medicine and Biology Society (EMBC)* (pp. 2978-2981). IEEE.

Neu, J., & Walker, W. A. (2011). Necrotizing enterocolitis. *New England Journal of Medicine*, *364*(3), 255-264.

Ng, I.H.X., Da Costa, C.S., Zeiler, F.A., Wong, F.Y., Smielewski, P., Czosnyka, M., & Austin, T. (2020). Burden of hypoxia and intraventricular haemorrhage in extremely preterm infants. *Archives of Disease in Childhood-Fetal and Neonatal Edition*, *105*(3), 242-247.

Niezen, C. K., Bos, A. F., Sival, D. A., Meiners, L. C., & Ter Horst, H. J. (2018). Amplitude-integrated EEG and cerebral near-infrared spectroscopy in cooled, asphyxiated infants. *American Journal of Perinatology*, *35*(9), 904-910.

Noone, M. A., Sellwood, M., Meek, J. H., & Wyatt, J. S. (2003). Postnatal adaptation of cerebral blood flow using near infrared spectroscopy in extremely preterm infants undergoing high-frequency oscillatory ventilation. *Acta Paediatrica*, *92*(9), 1079-1084.

Noori, S., McCoy, M., Anderson, M. P., Ramji, F., & Seri, I. (2014). Changes in cardiac function and cerebral blood flow in relation to peri/intraventricular haemorrhage in extremely preterm infants. *The Journal of Pediatrics*, *164*(2), 264-270.

Noori, S., & Seri, I. (2015, August). Evidence-based versus pathophysiology-based approach to diagnosis and treatment of neonatal cardiovascular compromise. In *Seminars in Fetal and Neonatal Medicine* (Vol. 20, No. 4, 238-245). WB Saunders.

Nozari, H., & Sadeghi, M. E. (2021). Artificial intelligence and Machine Learning for Real-world problems (A survey). *International Journal of Innovation in Engineering*, *1*(3), 38-47.

O'Leary, H., Gregas, M.C., Limperopoulos, C., Zaretskaya, I., Bassan, H., Soul, J.S., Di Salvo, D.N., & du Plessis, A.J. (2009). Elevated cerebral pressure passivity is associated with prematurity-related intracranial hemorrhage. *Pediatrics*, *124*(1), 302-309.

Orr, S. T., James, S. A., & Blackmore Prince, C. (2002). Maternal prenatal depressive symptoms and spontaneous preterm births among African American women in Baltimore, Maryland. *American Journal of Epidemiology*, *156*(9), 797-802.

O'Shea, A., Ahmed, R., Lightbody, G., Pavlidis, E., Lloyd, R., Pisani, F., Marnane, W., Mathieson, S., Boylan, G., & Temko, A. (2021). Deep learning for EEG seizure detection in preterm infants. *International Journal of Neural Systems*, *31*(08), p.2150008.

O'Shea, K., & Nash, R. (2015). An introduction to convolutional neural networks. *arXiv preprint arXiv:1511.08458*.

Osredkar, D., Toet, M. C., van Rooij, L. G., van Huffelen, A. C., Groenendaal, F., & de Vries, L. S. (2005). Sleep-wake cycling on amplitude-integrated electroencephalography in term newborns with hypoxic-ischaemic encephalopathy. *Pediatrics*, *115*(2), 327-332.

O'Sullivan, M., Gomez, S., O'Shea, A., Salgado, E., Huillca, K., Mathieson, S., Boylan, G., Popovici, E., & Temko, A. (2018, July). Neonatal EEG interpretation and decision support framework for mobile platforms. In *2018 40th Annual International Conference of the IEEE Engineering in Medicine and Biology Society (EMBC)* 4881-4884. IEEE.

O'Toole, J. M., & Boylan, G. B. (2017). NEURAL: quantitative features for newborn EEG using Matlab. *arXiv preprint arXiv:1704.05694*.

O'Toole, J. M., Dempsey, E. M., & Boylan, G. B. (2018, July). Extracting transients from cerebral oxygenation signals of preterm infants: a new singular-spectrum analysis method. In *2018 40th Annual International Conference of the IEEE Engineering in Medicine and Biology Society (EMBC)* 5882-5885. IEEE.

O'Toole, J. M., Kenosi, M., Finn, D., Boylan, G. B., & Dempsey, E. M. (2016, August). Features of cerebral oxygenation detects brain injury in premature infants. In *2016 38th Annual International Conference of the IEEE Engineering in Medicine and Biology Society (EMBC)* 3614-3617. IEEE.

Panesar, S. S., D'Souza, R. N., Yeh, F. C., & Fernandez-Miranda, J. C. (2019). Machine learning versus logistic regression methods for 2-year mortality prognostication in a small, heterogeneous glioma database. *World Neurosurgery: X*, *2*, 100012.

Paneth, N., Rudelli, R., Kazam, E., & Monte, W. (1994). *Brain damage in the preterm infant* (No. 131). Cambridge University Press.

Panigrahy, A., Wisnowski, J. L., Furtado, A., Lepore, N., Paquette, L., & Bluml, S. (2012). Neuroimaging biomarkers of preterm brain injury: toward developing the preterm connectome. *Pediatric Radiology*, *42*, 33-61.

Patrizi, S., Holmes, G. L., Orzalesi, M., & Allemand, F. (2003). Neonatal seizures: characteristics of EEG ictal activity in preterm and fullterm infants. *Brain and Development*, *25*(6), 427-437.

Paulson, O. B., Strandgaard, S., & Edvinsson, L. (1990). Cerebral autoregulation. *Cerebrovascular and Brain Metabolism Reviews*, *2*(2), 161-192.

Pavel, A.M., O'Toole, J.M., Proietti, J., Livingstone, V., Mitra, S., Marnane, W.P., Finder, M., Dempsey, E.M., Murray, D.M., Boylan, G.B., & ANSeR Consortium (2023). Machine learning for the early prediction of infants with electrographic seizures in neonatal hypoxic-ischemic encephalopathy. *Epilepsia*, *64*(2), 456-468.

Pavel, A.M., Rennie, J.M., de Vries, L.S., Blennow, M., Foran, A., Shah, D.K., Pressler, R.M., Kapellou, O., Dempsey, E.M., Mathieson, S.R., & Pavlidis, E. (2020). A machine-learning algorithm for neonatal seizure recognition: a multicentre, randomised, controlled trial. *The Lancet Child & Adolescent Health*, *4*(10), 740-749.

Pavlek, L. R., Mueller, C., Jebbia, M. R., Kielt, M. J., & Fathi, O. (2021). Near-infrared spectroscopy in extremely preterm infants. *Frontiers in Pediatrics*, *8*, 624113.

Peng, S., Boudes, E., Tan, X., Saint-Martin, C., Shevell, M., & Wintermark, P. (2015). Does near-infrared spectroscopy identify asphyxiated newborns at risk of developing brain injury during hypothermia treatment?. *American Journal of Perinatology*, 555-564.

Pichler, G., Baumgartner, S., Biermayr, M., Dempsey, E., Fuchs, H., Goos, T.G., Lista, G., Lorenz, L., Karpinski, L., Mitra, S., & Kornhauser-Cerar, L. (2019). Cerebral regional tissue Oxygen Saturation to Guide Oxygen Delivery in preterm neonates during immediate transition after birth (COSGOD III): an investigator-initiated, randomized, multi-center, multi-national, clinical trial on additional cerebral tissue oxygen saturation monitoring combined with defined treatment guidelines versus standard monitoring and treatment as usual in premature infants during immediate transition: study protocol for a randomized controlled trial. *Trials*, *20*, 1-10.

Phillips, A.A., Chan, F.H., Zheng, M.M.Z., Krassioukov, A.V., & Ainslie, P.N. (2016). Neurovascular coupling in humans: physiology, methodological advances and clinical implications. *Journal of Cerebral Blood Flow & Metabolism*, *36*(4), 647-664.

Plaisier, A., Govaert, P., Lequin, M. H., & Dudink, J. (2014). Optimal timing of cerebral MRI in preterm infants to predict long-term neurodevelopmental outcome: a systematic review. *American Journal of Neuroradiology*, *35*(5), 841-847.

Plaisier, A., Raets, M.M., Ecury-Goossen, G.M., Govaert, P., Feijen-Roon, M., Reiss, I.K., Smit, L.S., Lequin, M.H., & Dudink, J. (2015). Serial cranial ultrasonography or early

MRI for detecting preterm brain injury?. *Archives of Disease in Childhood-Fetal and Neonatal Edition*, *100*(4), F293-F300.

Pressler, R.M., Cilio, M.R., Mizrahi, E.M., Moshé, S.L., Nunes, M.L., Plouin, P., Vanhatalo, S., Yozawitz, E., de Vries, L.S., Puthenveettil Vinayan, K., & Triki, C.C. (2021). The ILAE classification of seizures and the epilepsies: Modification for seizures in the neonate. Position paper by the ILAE Task Force on Neonatal Seizures. *Epilepsia*, *62*(3), 615-628.

Rabe, H., & Rojas-Anaya, H. (2017). Inotropes for preterm babies during the transition period after birth: friend or foe?. *Archives of Disease in Childhood-Fetal and Neonatal Edition*, *102*(6), F547-F550.

Rademaker, K.J., Uiterwaal, C.S., Beek, F.J., van Haastert, I.C., Lieftink, A.F., Groenendaal, F., Grobbee, D.E., & de Vries, L.S. (2005). Neonatal cranial ultrasound versus MRI and neurodevelopmental outcome at school age in children born preterm. *Archives of Disease in Childhood-Fetal and Neonatal Edition*, *90*(6), F489-F493.

Raghu, A., Komorowski, M., Celi, L. A., Szolovits, P., & Ghassemi, M. (2017, November). Continuous state-space models for optimal sepsis treatment: a deep reinforcement learning approach. In *Machine Learning for Healthcare Conference*, 147-163. PMLR.

Rakshasbhuvankar, A.A., Wagh, D., Athikarisamy, S.E., Davis, J., Nathan, E.A., Palumbo, L., Ghosh, S., Nagarajan, L., & Rao, S.C. (2020). Inter-rater reliability of amplitude-integrated EEG for the detection of neonatal seizures. *Early Human Development*, *143*, p.105011.

Rennie, J., Chorley, G., Boylan, G., Pressler, R., Nguyen, Y., & Hooper, R. (2004). Non-expert use of the cerebral function monitor for neonatal seizure detection. *Archives of Disease in Childhood Fetal and Neonatal Edition*, *89*(1), F37.

Reynolds, P., Dale, R., & Cowan, F. (2001). Neonatal cranial ultrasound interpretation: a clinical audit. *Archives of Disease in Childhood. Fetal and Neonatal Edition*, *84*(2), F92.

Rhee, C. J., da Costa, C. S., Austin, T., Brady, K. M., Czosnyka, M., & Lee, J. K. (2018). Neonatal cerebrovascular autoregulation. *Pediatric Research*, *84*(5), 602-610.

Rhee, C.J., Fraser III, C.D., Kibler, K., Easley, R.B., Andropoulos, D.B., Czosnyka, M., Varsos, G.V., Smielewski, P., Rusin, C.G., Brady, K.M., & Kaiser, J.R. (2014). The ontogeny of cerebrovascular pressure autoregulation in premature infants. *Journal of Perinatology*, *34*(12), 926-931.

Rhee, C.J., Fraser, C.D., Kibler, K., Easley, R.B., Andropoulos, D.B., Czosnyka, M., Varsos, G.V., Smielewski, P., Rusin, C.G., Brady, K.M., & Kaiser, J.R. (2016). The ontogeny of cerebrovascular pressure autoregulation in premature infants. *Intracranial Pressure and Brain Monitoring XV*, 151-155.

Robinson, S. (2012). Neonatal posthaemorrhagic hydrocephalus from prematurity: pathophysiology and current treatment concepts: a review. *Journal of Neurosurgery: Pediatrics*, *9*(3), 242-258.

Roche-Labarbe, N., Carp, S. A., Surova, A., Patel, M., Boas, D. A., Grant, P. E., & Franceschini, M. A. (2010). Noninvasive optical measures of CBV, StO2, CBF index, and

rCMRO2 in human premature neonates' brains in the first six weeks of life. *Human Brain Mapping*, *31*(3), 341-352.

Romero, R., Espinoza, J., Kusanovic, J.P., Gotsch, F., Hassan, S., Erez, O., Chaiworapongsa, T., & Mazor, M. (2006). The preterm parturition syndrome. *BJOG: An International Journal of Obstetrics & Gynaecology*, *113*, 17-42.

Rubin, M.I., Calcagno, P.L., &Ruben, B.L. (1961). Renal excretion of hydrogen ions: a defense against acidosis in premature infants. *The Journal of Pediatrics*, *59*(6), 848-860.

Rudin, L. I., Osher, S., & Fatemi, E. (1992). Nonlinear total variation based noise removal algorithms. *Physica D: Nonlinear Phenomena*, *60*(1-4), 259-268.

Sánchez Fernández, I., Sansevere, A. J., Gaínza-Lein, M., Kapur, K., & Loddenkemper, T. (2018). Machine learning for outcome prediction in electroencephalograph (EEG)-monitored children in the intensive care unit. *Journal of Child Neurology*, *33*(8), 546-553.

Sarnat, H. B., & Sarnat, M. S. (1976). Neonatal encephalopathy following fetal distress: a clinical and electroencephalographic study. *Archives of Neurology*, *33*(10), 696-705.

Saugstad, O. D. (2003, February). Bronchopulmonary dysplasia—oxidative stress and antioxidants. In *Seminars in Neonatology* (Vol. 8, No. 1, 39-49). WB Saunders.

Selesnick, I. W., Arnold, S., & Dantham, V. R. (2012). Polynomial smoothing of time series with additive step discontinuities. *IEEE Transactions on Signal Processing*, *60*(12), 6305-6318.

Selesnick, I. W., Graber, H. L., Ding, Y., Zhang, T., & Barbour, R. L. (2014). Transient artifact reduction algorithm (TARA) based on sparse optimisation. *IEEE Transactions on Signal Processing*, *62*(24), 6596-6611.

Selesnick, I. W., Graber, H. L., Pfeil, D. S., & Barbour, R. L. (2014a). Simultaneous low-pass filtering and total variation denoising. *IEEE Transactions on Signal Processing*, *62*(5), 1109-1124.

Selton, D., & Andre, M. (1997). Prognosis of hypoxic-ischaemic encephalopathy in full-term newborns-value of neonatal electroencephalography. *Neuropediatrics*, *28*(05), 276-280.

Seri, I. (2001, February). Circulatory support of the sick preterm infant. In *Seminars in Neonatology* (Vol. 6, No. 1, 85-95). WB Saunders.

Shah, D.K., Mackay, M.T., Lavery, S., Watson, S., Harvey, A.S., Zempel, J., Mathur, A., & Inder, T.E. (2008). Accuracy of bedside electroencephalographic monitoring in comparison with simultaneous continuous conventional electroencephalography for seizure detection in term infants. *Pediatrics*, *121*(6), 1146-1154.

Shalak, L., & Perlman, J. M. (2004). Hypoxic–ischaemic brain injury in the term infant-current concepts. *Early Human Development*, *80*(2), 125-141.

Shankaran, S., Laptook, A.R., Ehrenkranz, R.A., Tyson, J.E., McDonald, S.A., Donovan, E.F., Fanaroff, A.A., Poole, W.K., Wright, L.L., Higgins, R.D., & Finer, N.N. (2005). Whole-body hypothermia for neonates with hypoxic–ischemic encephalopathy. *New England Journal of Medicine*, *353*(15), 1574-1584.

Shany, E., Goldstein, E., Khvatskin, S., Friger, M.D., Heiman, N., Goldstein, M., Karplus, M., & Galil, A. (2006). Predictive value of amplitude-integrated electroencephalography pattern and voltage in asphyxiated term infants. *Pediatric Neurology*, *35*(5), 335-342.

Sheikhtaheri, A., Zarkesh, M. R., Moradi, R., & Kermani, F. (2021). Prediction of neonatal deaths in NICUs: development and validation of machine learning models. *BMC Medical Informatics and Decision Making*, *21*(1), 1-14.

Shellhaas, R.A., Chang, T., Tsuchida, T., Scher, M.S., Riviello, J.J., Abend, N.S., Nguyen, S., Wusthoff, C.J., & Clancy, R.R. (2011). The American Clinical Neurophysiology Society's guideline on continuous electroencephalography monitoring in neonates. *Journal of Clinical Neurophysiology*, *28*(6), 611-617.

Shellhaas, R. A., Soaita, A. I., & Clancy, R. R. (2007). Sensitivity of amplitude-integrated electroencephalography for neonatal seizure detection. *Pediatrics*, *120*(4), 770-777.

Shirwaikar, R. D., Mago, N., Acharya, D., & Makkithaya, K. (2016, July). Supervised learning techniques for analysis of neonatal data. In *2016 2nd International Conference on Applied and Theoretical Computing and Communication Technology (iCATccT)*,25-31. IEEE.

Shooman, D., Portess, H., & Sparrow, O. (2009). A review of the current treatment methods for posthaemorrhagic hydrocephalus of infants. *Cerebrospinal Fluid Research*, *6*(1), 1-15.

Silverman, A., & Petersen, N. H. (2020). Physiology, cerebral autoregulation.

Sinex, J.E. (1999). Pulse oximetry: principles and limitations. *The American Journal of Emergency Medicine*, *17*(1), 59-66.

Slattery, M. M., & Morrison, J. J. (2002). Preterm delivery. *The Lancet*, *360*(9344), 1489-1497.

Sola, A., Golombek, S.G., Montes Bueno, M.T., Lemus-Varela, L., Zuluaga, C., Domínguez, F., Baquero, H., Young Sarmiento, A.E., Natta, D., Rodriguez Perez, J.M., & Deulofeut, R. (2014). Safe oxygen saturation targeting and monitoring in preterm infants: can we avoid hypoxia and hyperoxia?. *Acta Paediatrica*, *103*(10), 1009-1018.

Sorensen, L. C., Maroun, L. L., Borch, K., Lou, H. C., & Greisen, G. (2008). Neonatal cerebral oxygenation is not linked to foetal vasculitis and predicts intraventricular haemorrhage in preterm infants. *Acta Paediatrica*, *97*(11), 1529-1534.

Soul, J.S., Hammer, P.E., Tsuji, M., Saul, J.P., Bassan, H., Limperopoulos, C., Disalvo, D.N., Moore, M., Akins, P., Ringer, S., & Volpe, J.J. (2007). Fluctuating pressure-passivity is common in the cerebral circulation of sick premature infants. *Pediatric Research*, *61*(4), 467-473.

Stoll, B. J., & Hansen, N. (2003, August). Infections in VLBW infants: studies from the NICHD Neonatal Research Network. In *Seminars in Perinatology* (Vol. 27, No. 4, 293-301). WB Saunders.

Stranak, Z., Semberova, J., Barrington, K., O'Donnell, C., Marlow, N., Naulaers, G., Dempsey, E., & HIP consortium (2014). International survey on diagnosis and management of hypotension in extremely preterm babies. *European Journal of Pediatrics*, *173*, 793-798.

Subhedar, N. V., Shaw, N. J., & Cochrane Neonatal Group. (1996). Dopamine versus dobutamine for hypotensive preterm infants. *Cochrane Database of Systematic Reviews*, *2010*(1).

Sullivan, B. A., Wallman-Stokes, A., Isler, J., Sahni, R., Moorman, J. R., Fairchild, K. D., & Lake, D. E. (2018). Early pulse oximetry data improves prediction of death and adverse outcomes in a two-center cohort of very low birth weight infants. *American Journal of Perinatology*, *35*(13), 1331-1338.

Sun, J., Chong, J., Zhang, J., & Ge, L. (2023). Preterm pigs for preterm birth research: reasonably feasible. *Frontiers in Physiology*, *14*, 1189422.

Suzuki, S., Takasaki, S., Ozaki, T., & Kobayashi, Y. (1999, July). Tissue oxygenation monitor using NIR spatially resolved spectroscopy. In *Optical Tomography and Spectroscopy of Tissue III* (Vol. 3597, 582-592). SPIE.

Sweet, D., Bevilacqua, G., Carnielli, V., Greisen, G., Plavka, R., Didrik Saugstad, O., Simeoni, U., Speer, C.P., Valls-i-Soler, A., & Halliday, H. (2007). European consensus guidelines on the management of neonatal respiratory distress syndrome.

Sweet, D.G., Carnielli, V., Greisen, G., Hallman, M., Ozek, E., Plavka, R., Saugstad, O.D., Simeoni, U., Speer, C.P., & Halliday, H.L. (2010). European consensus guidelines on the management of neonatal respiratory distress syndrome in preterm infants–2010 update. *Neonatology*, *97*(4), 402-417.

Tagin, M. A., Woolcott, C. G., Vincer, M. J., Whyte, R. K., & Stinson, D. A. (2012). Hypothermia for neonatal hypoxic ischaemic encephalopathy: an updated systematic

review and meta-analysis. *Archives of Pediatrics & Adolescent Medicine*, *166*(6), 558-566.

Ter Horst, H. J., Sommer, C., Bergman, K. A., Fock, J. M., Van Weerden, T. W., & Bos, A. F. (2004). Prognostic significance of amplitude-integrated EEG during the first 72 hours after birth in severely asphyxiated neonates. *Pediatric Research*, *55*(6), 1026-1033.

Thavasothy, M., Broadhead, M., Elwell, C., Peters, M., & Smith, M. (2002). A comparison of cerebral oxygenation as measured by the NIRO 300 and the INVOS 5100 near-infrared spectrophotometers. *Anaesthesia*, *57*(10), 999-1006.

Thoresen, M., Hellström-Westas, L., Liu, X., & de Vries, L. S. (2010). Effect of hypothermia on amplitude-integrated electroencephalogram in infants with asphyxia. *Pediatrics*, *126*(1), e131-e139.

Thorngren-Jerneck, K., & Herbst, A. (2001). Low 5-minute Apgar score: a population-based register study of 1 million term births. *Obstetrics & Gynecology*, *98*(1), 65-70.

Tin, W., & Lal, M. (2015, June). Principles of pulse oximetry and its clinical application in neonatal medicine. In *Seminars in Fetal and Neonatal Medicine* (Vol. 20, No. 3, 192-197). WB Saunders.

Tioseco, J.A., Aly, H., Essers, J., Patel, K., & El-Mohandes, A.A. (2006). Male sex and intraventricular hemorrhage. *Pediatric Critical Care Medicine*, *7*(1), 40-44.

Toet, M., Hellstrom-Westas, L., Groenendaal, F., Eken, P., & De Vries, L. S. (1999). Amplitude integrated EEG 3 and 6 hours after birth in full term neonates with hypoxic-

ischaemic encephalopathy. *Archives of Disease in Childhood. Fetal and Neonatal Edition*, *81*(1), F19.

Toet, M. C., Lemmers, P. M., van Schelven, L. J., & van Bel, F. (2006). Cerebral oxygenation and electrical activity after birth asphyxia: their relation to outcome. *Pediatrics*, *117*(2), 333-339.

Toet, M. C., van der Meij, W., de Vries, L. S., Uiterwaal, C. S., & van Huffelen, K. C. (2002). Comparison between simultaneously recorded amplitude integrated electroencephalogram (cerebral function monitor) and standard electroencephalogram in neonates. *Pediatrics*, *109*(5), 772-779.

Tracy, R. P., Psaty, B. M., Macy, E., Bovill, E. G., Cushman, M., Cornell, E. S., & Kuller, L. H. (1997). Lifetime smoking exposure affects the association of C-reactive protein with cardiovascular disease risk factors and subclinical disease in healthy elderly subjects. *Arteriosclerosis, Thrombosis, and Vascular Biology*, *17*(10), 2167-2176.

Trivedi, N.S., Ghouri, A.F., Shah, N.K., Lai, E., & Barker, S.J. (1997). Pulse oximeter performance during desaturation and resaturation: a comparison of seven models. *Journal of Clinical Anesthesia*, *9*(3), 184-188.

Toth, P., Szarka, N., Farkas, E., Ezer, E., Czeiter, E., Amrein, K., Ungvari, Z., Hartings, J.A., Buki, A., & Koller, A. (2016). Traumatic brain injury-induced autoregulatory dysfunction and spreading depression-related neurovascular uncoupling: Pathomechanisms, perspectives, and therapeutic implications. *American Journal of Physiology-Heart and Circulatory Physiology*, *311*(5), H1118-H1131.

Tsuji, M., Saul, J. P., du Plessis, A., Eichenwald, E., Sobh, J., Crocker, R., & Volpe, J. J. (2000). Cerebral intravascular oxygenation correlates with mean arterial pressure in critically ill premature infants. *Pediatrics*, *106*(4), 625-632.

Urlesberger, B., Kratky, E., Rehak, T., Pocivalnik, M., Avian, A., Czihak, J., Müller, W., & Pichler, G. (2011). Regional oxygen saturation of the brain during birth transition of term infants: comparison between elective cesarean and vaginal deliveries. *The Journal of Pediatrics*, *159*(3), 404-408.

Van Bel, F., Lemmers, P., & Naulaers, G. (2008). Monitoring neonatal regional cerebral oxygen saturation in clinical practice: value and pitfalls. *Neonatology*, *94*(4), 237-244.

Vanderhaegen, J., Naulaers, G., Vanhole, C., De Smet, D., Van Huffel, S., Vanhaesebrouck, S., & Devlieger, H. (2009). The effect of changes in tPCO2 on the fractional tissue oxygen extraction–as measured by near-infrared spectroscopy–in neonates during the first days of life. *European Journal of Paediatric Neurology*, *13*(2), 128-134.

Van Handel, M., Swaab, H., De Vries, L. S., & Jongmans, M. J. (2007). Long-term cognitive and behavioral consequences of neonatal encephalopathy following perinatal asphyxia: a review. *European Journal of Pediatrics*, *166*, 645-654.

van Laerhoven, H., de Haan, T. R., Offringa, M., Post, B., & van der Lee, J. H. (2013). Prognostic tests in term neonates with hypoxic-ischaemic encephalopathy: a systematic review. *Pediatrics*, *131*(1), 88-98.

Van Lieshout, H. B. M., Jacobs, J. W. F. M., Rotteveel, J. J., Geven, W., & Hof, M. V. T. (1995). The prognostic value of the EEG in asphyxiated newborns. *Acta Neurologica Scandinavica*, *91*(3), 203-207.

van Schie, P. E., Schijns, J., Becher, J. G., Barkhof, F., van Weissenbruch, M. M., & Vermeulen, R. J. (2015). Long-term motor and behavioral outcome after perinatal hypoxic-ischaemic encephalopathy. *European Journal of Paediatric Neurology*, *19*(3), 354-359.

van Wezel-Meijler, G., Steggerda, S. J., & Leijser, L. M. (2010, February). Cranial ultrasonography in neonates: role and limitations. In *Seminars in Perinatology* (Vol. 34, No. 1, 28-38). WB Saunders.

Verhagen, E. A., Ter Horst, H. J., Keating, P., Martijn, A., Van Braeckel, K. N., & Bos, A. F. (2010). Cerebral oxygenation in preterm infants with germinal matrix–intraventricular haemorrhages. *Stroke*, *41*(12), 2901-2907.

Vesoulis, Z.A., Bank, R.L., Lake, D., Wallman-Stokes, A., Sahni, R., Moorman, J.R., Isler, J.R., Fairchild, K.D., & Mathur, A.M. (2019). Early hypoxemia burden is strongly associated with severe intracranial hemorrhage in preterm infants. *Journal of Perinatology*, *39*(1), 48-53.

Vesoulis, Z.A., Liao, S.M., Trivedi, S.B., Ters, N.E., & Mathur, A.M. (2016). A novel method for assessing cerebral autoregulation in preterm infants using transfer function analysis. *Pediatric Research*, *79*(3), 453-459.

Vesoulis, Z. A., & Mathur, A. M. (2017). Cerebral autoregulation, brain injury, and the transitioning premature infant. *Frontiers in Pediatrics*, *5*, 64.

Vesoulis, Z.A., Whitehead, H.V., Liao, S.M., & Mathur, A.M. (2021). The hidden consequence of intraventricular hemorrhage: persistent cerebral desaturation after IVH in preterm infants. *Pediatric Research*, *89*(4), 869-877.

Victor, S., Appleton, R. E., Beirne, M., Marson, A. G., & Weindling, A. M. (2005). Effect of carbon dioxide on background cerebral electrical activity and fractional oxygen extraction in very low birth weight infants just after birth. *Pediatric Research*, *58*(3), 579-585.

Victor, S., Appleton, R. E., Beirne, M., Marson, A. G., & Weindling, A. M. (2006). The relationship between cardiac output, cerebral electrical activity, cerebral fractional oxygen extraction and peripheral blood flow in premature newborn infants. *Pediatric Research*, *60*(4), 456-460.

Victor, S., Marson, A. G., Appleton, R. E., Beirne, M., & Weindling, A. M. (2006). Relationship between blood pressure, cerebral electrical activity, cerebral fractional oxygen extraction, and peripheral blood flow in very low birth weight newborn infants. *Pediatric Research*, *59*(2), 314-319.

Volpe, J.J. (1998), September. Brain injury in the premature infant: overview of clinical aspects, neuropathology, and pathogenesis. In *Seminars in Pediatric Neurology* (Vol. 5, No. 3, 135-151). WB Saunders.

Volpe, J. J. (2012). Neonatal encephalopathy: an inadequate term for hypoxic–ischaemic encephalopathy. *Annals of Neurology*, *72*(2), 156-166.

Wardle, S. P., Yoxall, C. W., & Weindling, A. M. (2000). Determinants of cerebral fractional oxygen extraction using near infrared spectroscopy in preterm neonates. *Journal of Cerebral Blood Flow & Metabolism*, *20*(2), 272-279.

Wassink, G., Gunn, E. R., Drury, P. P., Bennet, L., & Gunn, A. J. (2014). The mechanisms and treatment of asphyxial encephalopathy. *Frontiers in Neuroscience*, *8*, 40.

Wasunna, A., & Whitelaw, A. G. (1987). Pulse oximetry in preterm infants. *Archives of Disease in Childhood*, *62*(9), 957.

Watzman, H. M., Kurth, C. D., Montenegro, L. M., Rome, J., Steven, J. M., & Nicolson, S. C. (2000). Arterial and venous contributions to near-infrared cerebral oximetry. *The Journal of the American Society of Anesthesiologists*, *93*(4), 947-953.

Weindling, A. M., & Subhedar, N. V. (2007). The definition of hypotension in very low-birthweight infants during the immediate neonatal period. *NeoReviews*, *8*(1), e32-e43.

West, J.B. (2012). *Respiratory physiology: the essentials*. Lippincott Williams & Wilkins.

Wezel-Meijler, G. (2007). *Neonatal cranial ultrasonography* (pp. 30-2). Berlin, Germany: Springer-Verlag.

Wolf, M., Ferrari, M., & Quaresima, V. (2007). Progress of near-infrared spectroscopy and topography for brain and muscle clinical applications. *Journal of Biomedical Optics*, *12*(6), 062104-062104.

Wong, F. (2016). Cerebral blood flow measurements in the neonatal brain. *Prenatal and Postnatal Determinants of Development*, 69-87.

Wong, F. Y., Leung, T. S., Austin, T., Wilkinson, M., Meek, J. H., Wyatt, J. S., & Walker, A. M. (2008). Impaired autoregulation in preterm infants identified by using spatially resolved spectroscopy. *Pediatrics*, *121*(3), e604-e611.

Wong, F. Y., Silas, R., Hew, S., Samarasinghe, T., & Walker, A. M. (2012). Cerebral oxygenation is highly sensitive to blood pressure variability in sick preterm infants.

World Health Organisation. (2023). Preterm birth. Retrieved from https://www.who.int/news-room/fact-sheets/detail/preterm-birth

Yeh, P., Emary, K., & Impey, L. (2012). The relationship between umbilical cord arterial pH and serious adverse neonatal outcome: analysis of 51 519 consecutive validated samples. *BJOG: An International Journal of Obstetrics & Gynaecology*, *119*(7), 824-831.

Yeo, K. T., Thomas, R., Chow, S. S., Bolisetty, S., Haslam, R., Tarnow-Mordi, W., & Lui, K. (2020). Improving incidence trends of severe intraventricular haemorrhages in preterm infants< 32 weeks gestation: a cohort study. *Archives of Disease in Childhood-Fetal and Neonatal Edition*, *105*(2), 145-150.

Yoshitani, K., Kawaguchi, M., Tatsumi, K., Kitaguchi, K., & Furuya, H. (2002). A comparison of the INVOS 4100 and the NIRO 300 near-infrared spectrophotometers. *Anaesthesia & Analgesia*, *94*(3), 586-590.

Zarifi, M. K., Astrakas, L. G., Poussaint, T. Y., Plessis, A. D., Zurakowski, D., & Tzika, A. A. (2002). Prediction of adverse outcome with cerebral lactate level and apparent diffusion coefficient in infants with perinatal asphyxia. *Radiology*, *225*(3), 859-870.

Zhou, X., Brotman, R.M., Gajer, P., Abdo, Z., Schüette, U., Ma, S., Ravel, J., & Forney, L.J. (2010). Recent advances in understanding the microbiology of the female reproductive tract and the causes of premature birth. *Infectious Diseases in Obstetrics and Gynecology*, *2010*(1), p.737425.

Zuckerman, B., Amaro, H., Bauchner, H., & Cabral, H. (1989). Depressive symptoms during pregnancy: relationship to poor health behaviors. *American Journal of Obstetrics and Gynecology*, *160*(5), 1107-1111.

Chapter 2. Sparse-denoising Methods for Extracting Desaturation Transients in Cerebral Oxygenation Signals of Preterm Infants

Title: Sparse-denoising methods for extracting desaturation transients in cerebral oxygenation signals of preterm infants

Minoo Ashoori [1,2], Eugene M. Dempsey [1,3], Fiona B. McDonald [1,2], John M. O'Toole[1,3]

1. INFANT Research Centre, University College Cork, Ireland

2. Department of Physiology, School of Medicine, College of Medicine and Health, University College Cork, Ireland

3. Department of Paediatrics and Child Health, School of Medicine, College of Medicine and Health, University College Cork, Ireland

2.1. Abstract

Preterm infants are at high risk of developing brain injury in the first days of life as a consequence of poor cerebral oxygen delivery. Near-infrared spectroscopy (NIRS) is an established technology developed to monitor regional tissue oxygenation. Detailed waveform analysis of the cerebral NIRS signal could improve the clinical utility of this method for accurately predicting brain injury. Frequent transient cerebral oxygen desaturations are commonly observed in extremely preterm infants, yet their clinical significance remains unclear. The aim of this study was to examine and compare the performance of two distinct approaches for isolating and extracting transient deflections within NIRS signals. We optimised three different simultaneous low-pass filtering and total variation denoising (LPF–TVD) methods and compared their performance with a recently proposed method that uses singular-spectrum analysis, and the discrete cosine transform (SSA–DCT). Parameters for the LPF–TVD methods were optimised over a grid search using synthetic NIRS-like signals. The SSA–DCT method was modified with a post-processing procedure to increase sparsity in the extracted components. Our analysis, using a synthetic NIRS-like dataset, showed that an LPF–TVD method outperformed the modified SSA–DCT method: median mean-squared error of 0.97 (95% CI: 0.86 to 1.07) was lower for the LPF–TVD method compared to the modified SSA–DCT method of 1.48 (95% CI: 1.33 to 1.63), $P < 0.001$. The dual low-pass filter and total variation denoising methods are considerably more computational efficient, by 3 to 4 orders of magnitude, than the SSA–DCT method. More research is needed to examine the efficacy of these methods in extracting oxygen desaturation in real NIRS signals.

2.2. Introduction

Near-infrared spectroscopy (NIRS) is a non-invasive optical technology used for continuous monitoring of cerebral regional oxygen saturation (Rolfe et al., 1992). Despite the widespread use of NIRS in the neonatal intensive care unit, ranges remain poorly described for extremely preterm infants. In an ongoing clinical trial (Hansen et al., 2019) to evaluate the use of NIRS-guided treatment of extremely preterm infants, short duration desaturations are commonly observed in the NIRS signal. Isolating these transient deflections within the signals without removing other components of the signal is an important aspect of processing these signals for post-hoc analysis (Vesoulis et al., 2021).

A recent study developed a novel method to isolate transient waveforms in NIRS signals and showed that these transient components of the signal are not predictive of brain injury (O'Toole et al., 2018). However there has been no detailed investigation of the most suitable method for extracting these short duration desaturations. Effective and efficient decomposition of these short duration desaturations would provide an excellent opportunity to test their clinical utility. The aim of this study was therefore to identify the best method to isolate and extract transient deflections within synthetic NIRS signals.

We optimised two distinct methods independently; singular spectrum analysis and the discrete cosine transform (SSA–DCT) method (SSA–DCT1 and SSA–DCT2) (O'Toole et al., 2018) and lowpass filtering total variation denoising (LPF–TVD) method (LPF–TVD1, LPF–CS1, LPF–CSD2) (Selesnick et al., 2014,2014a). We then compared their performance in isolating and extracting transient deflections within NIRS-like signals.

2.3. Methods

We present a simple post-processing method to increase sparsity of the SSA–DCT decomposition method (O'Toole et al., 2018) and compared this modified algorithm with multiple algorithms of LPF–TVD. To validate and compare these methods, we used a set of synthetic $rcSO_2$ (regional cerebral oxygenation) signals with various numbers of transients (O'Toole et al., 2018).

2.3.1. Singular-spectrum Analysis for Extracting Transients

Singular-spectrum Analysis:

The SSA method is presented as a data-driven filter-bank operation. For signal x = x[n] for n = 0, 1, …, N-1 we form the k-th lagged vector with embedding dimension M as $x_k = \{ x [k + M - 1 - m] \}^T$ for m = 1, 2, …, M. Combining these lagged vectors, for k = 1, …, K with K = N - M + 1, we form the trajectory M × K matrix as $X = (x_1, x_2, \ldots, x_K)$ (Figueiredo et al., 2010). The correlation matrix of the trajectory matrix is decomposed into an orthogonal basis using eigenvalue decomposition:

$$R = XX^T = U\lambda U$$

Matrix $U = (u_1, \ldots, u_M)^T$ contains the basis vectors u_m, known as eigenvectors; matrix $\lambda = \mathrm{diag}(\lambda_1, \ldots, \lambda_M)$ contains the weights λ_m, known as eigenvalues. Each component x_m is generated through a finite-impulse response (FIR) filter with the eigenvector um as the impulse response as

$$x_m = F^{-1} \{F\{x\} | F\{u_m\}|^2\}.$$

Here, F represents the discrete-time Fourier transform, and F^{-1} indicates the inverse transform of F. Thus, the SSA method decomposes signal x into M components x_m,

where x = $\sum_{m=1}^{M} x_m$.

Rejecting components x_m associated with noise can increase the signal-to-noise ratio of $\hat{x}$ (Figueiredo et al., 2010; Vautard et al., 1992), where $\hat{x} = \sum_{m \in D} x_m$ and D is a subset of {1, 2, …, M}. There are different methods to select this subset D, usually based on the values of the associated eigenvalues. Here, we used a method proposed by Vautard et al. (1992) based on a previous comparison of different methods for the same class of signals (O'Toole et al., 2018). The method compares the possible noise components $\sum_{m \notin D} x_m$ in the autocorrelation domain to upper limits of a white Gaussian noise process. These upper-limits are estimated from a 95% confidence interval generated from 100 iterations of white Gaussian noise.

Extracting Transients:

The signal x is transformed using the discrete cosine transform (DCT). This equates to a 90° rotation in the time–frequency plane. Therefore impulses, or impulse-like transients, are transformed to sinusoidal-type components. Thus, applying the SSA to the real-valued DCT signal enables the algorithm to extract oscillating components, which when transformed back to the time-domain through an inverse DCT, represents transient components. This decomposition was refined through an iterative procedure. Full details can be found in (O'Toole et al., 2018).

Post-processing:

Although initial results were promising for the SSA–DCT method (O'Toole et al., 2018), we found that the method did not perform well when applied to long duration cerebral oxygenation signals. In particular, we found that the extracted transient components included a wandering baseline that distorted the $rcSO_2$ signal. To rectify

this, we applied a simple post-processing procedure that generates a mask, bounded within [0,1], to limit the wandering baseline by multiplying the mask with the extract transient component. We refer to this modified method as SSA–DCT2 and the original method as SSA–DCT1. The mask was generated as follows. First, a threshold is applied to the extracted transient component x_t, so that the mask m[n] = 1 when x_t [n] < -T; otherwise, m[n] = 0. This ensures that transient components must be at >T (% $rcSO_2$) in amplitude and always negative. Second, the sharp edges of the binary mask were expanded using one-half of a 10-minute Blackman-Harris window to enable a smooth transition from 0 to 1. Lastly, the mask was bounded to [0;1], as overlapping transitions may have increased m[n]>1. From initial testing, T was set to 8 (% $rcSO_2$), although this could be changed in future iterations based on physiological definitions of cerebral desaturations. MATLAB code for both SSA—DCT methods are freely available at https://github.com/otoolej/transient_decomp_ssa (version 0.2.0).

2.3.2. Total Variation Denoising Methods

Total variation denoising (TVD) is a sparsity-based denoising method that estimates a signal component with a sparse derivative. TVD methods can be extended to enforce sparsity on the signal itself, in addition to the derivative. Here we examine methods that combine low-pass filtering with TVD (LPF-TVD) to allow for the decomposition of the signal into a low-pass component in addition to a sparse component. This process differs to low pass filtering the signal first, which can dampen transients (Selesnick et al., 2014a). Given signal y, we find x by minimising the following cost function

$$\arg\min_{x} \{\frac{1}{2}||H(y-x)||_2^2 + \lambda_0||x||_1 + \lambda_1||Dx||_1\} \quad (1)$$

where $||x||_p = (\sum_n |x[n]|^p)^{1/p}$ represents the l_p norm for x and D represents the finite-difference matrix, such that $||Dx||_1 = \sum_n |x[n+1] - x[n]|$. Matrix H is a high-pass filter. Regularisation parameters λ_0 and λ_1 are application dependent.

For the first method, which we refer to as LPF–TVD1, λ_0 =0. Thus, the signal $\hat{x}$ from (1) may not be sparse but will have a sparse derivative. This minimisation problem in (1) is solved using a majorization–minimisation convex optimisation algorithm. The second method, known as the low pass filtering compound sparse denoising (LPF–CSD1) method, estimates $\hat{x}$ from (1) using another convex optimisation algorithm, the alternating direction method of multipliers. Further details on both algorithms can be found in (Selesnick et al., 2014a).

The third method is an improved version of the LPF-CSD1 method (Selesnick et al., 2014a). This method, which we call LPF–CSD2, uses the optimisation problem in (1) but replaces the l_1 norm with non-convex penalty functions Φ_0 and Φ_1

$$\arg\min_x \{\frac{1}{2}||H(y-x)||_2^2 + \lambda_0 \sum_{n=0}^{N-1} \Phi_0(x[n]) + \lambda_1 \sum_{n=0}^{N-1} \Phi_1(x[n+1] - x[n])\} \quad (2)$$

The use of these penalty functions allows for a better estimate of transient components as they are less biased towards zero (Selesnick et al., 2014). We used the following function, with parameter r, for Φ_0 and Φ_1

$$\Phi(u;r) = \frac{2}{r\sqrt{3}} \left[\tan^{-1}\left(\frac{1+2r\sqrt{u^2+\varepsilon}}{\sqrt{3}}\right) - \frac{\pi}{6}\right] \quad (3)$$

With ε set to 10^{-10} to avoid singularities at u = 0 in the derivative of Φ.

2.3.3. Performance Comparison

To compare methods, we used 100 synthetic $rcSO_2$-like signals of length 43,200 sample points, corresponding to 72 hours with sampling frequency of 1/6 Hz, typical of our NIRS recordings over the first days of life. The synthetic signals were a linear combination of transient components and nonstationary coloured noise; full details can be found in (O'Toole et al., 2018). The number and amplitude of the transient components were adjusted such that they were representative of NIRS signals of extremely pre-term infants (< 28 weeks gestational age).

For the three LPF–TVD methods, we optimised the parameters for each method using a grid search. Each method has a different set of parameters: LPF-TVD1 has λ_1; LPF-CSD1 has λ_0 and λ_1; LPF-CSD2 has λ_0, λ_1, r_0 and r_1, as parameters of the penalty functions Φ_0 and Φ_1 in (2) and (3). Parameters λ_0 and λ_1 in LPF-CSD2 were estimated using the procedure proposed in (Selesnick et al., 2014). The correlation coefficient between the estimated and pre-defined transient component was used as the optimisation metric. A different set of 50 synthetic $rcSO_2$ of length 12-hours were used in the grid search. Based on initial testing on a subset of the data, we used a 1st order high-pass filter, H in (1) and (2), with a normalised cut-off frequency f c = 0.01. The 5 methods were compared with each other using Kruskal-Wallis test utilising the selected parameters from the grid search on the data set of 100 $rcSO_2$-like signals. Dunn's post-hoc test was performed to compare the three LPF-TVD methods with each other, SSA-DCT1 versus SSA-DCT2 as well as the best performing SSA-DCT method versus the best performing LPF-TVD method.

Methods were compared using two metrics - the mean squared error and correlation coefficient between the predefined and estimated transient components- to test the performance at estimating the transient components of the synthetic signals. Statistical significance was determined as $P < 0.05$.

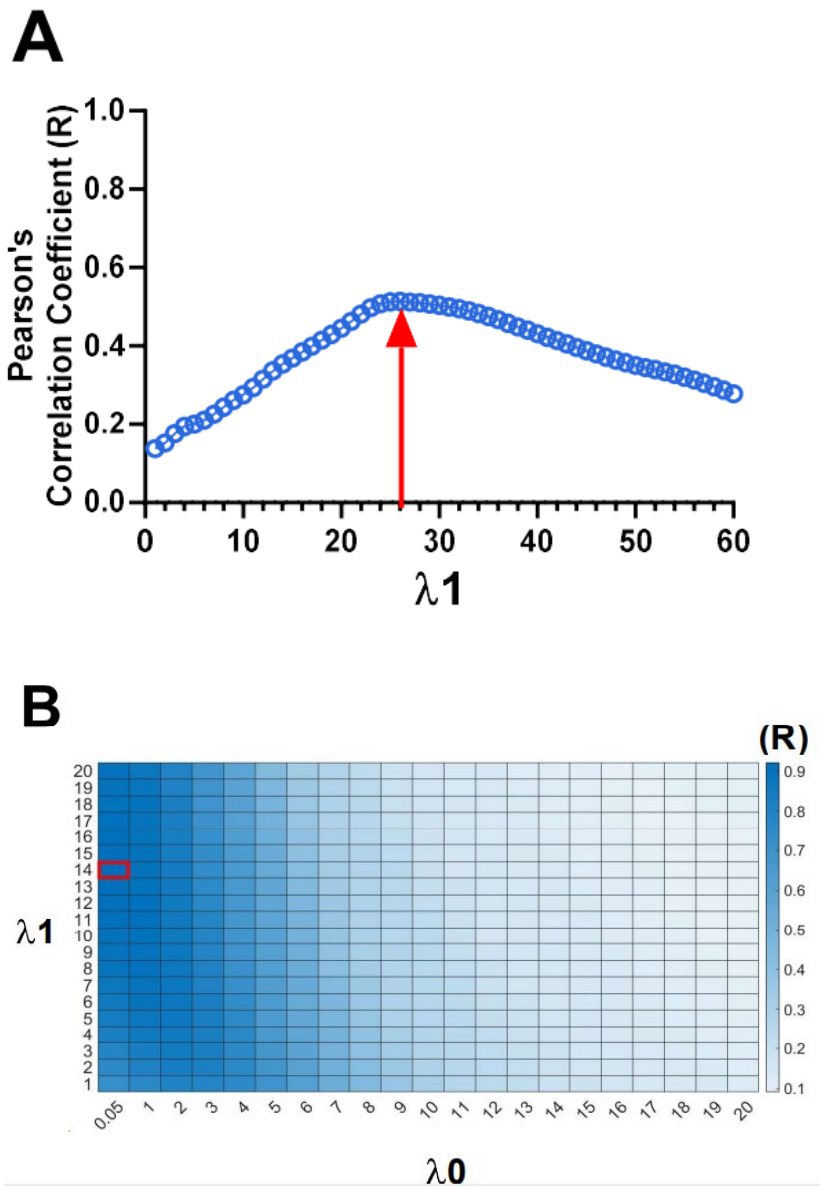

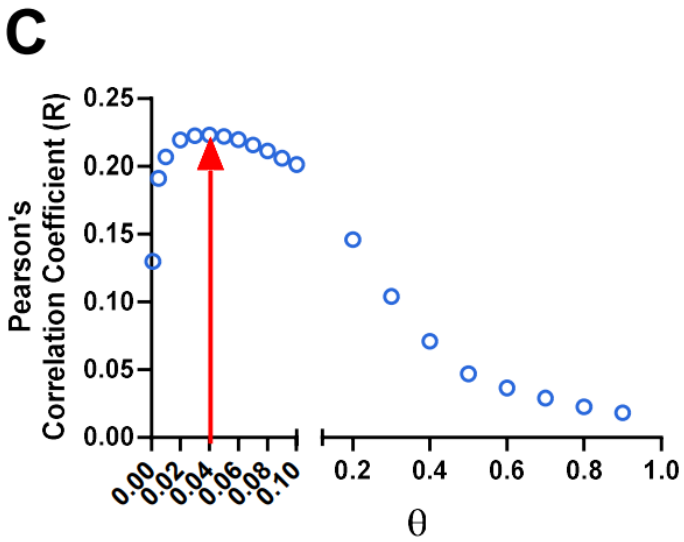

Figure 2. 1. Grid search for the parameters of the LPF–TVD methods; A. Correlation coefficient (R) for values of λ1 in LPF-TVD1; B. Correlation coefficient for values of λ0 and λ1 in LPF-CSD1; C. Correlation coefficient for values of ϑ in LPF-CSD2; Arrow denotes maximum value of R; LPF-TVD1 - low-pass filtering total variation denoising; LPF-CSD1 - low-pass filtering compound sparse denoising; LPF-CSD2 - the improved version of LPF-CSD1

2.4. Results

Grid search for the LPF-TVD parameters found the following. For the LPF-TVD1 method $\lambda_1 = 26$ (Figure 2. 1. A); for the LPF-CSD1 method, the best combination of λ_0 and λ_1 was $\lambda_0 = 0.5$ and $\lambda_1 = 14$ (Figure 2. 1. B); for the LPF-CSD2 method, we used a standard deviation (SD) estimate of the noise component as 4.69 and an optimised θ value of 0.04, which results in $\lambda_0 = 0.54$, $\lambda_1 = 21.32$, $r_0 = 0.001$ and $r_1 = 0.17$ (Figure 2. 1. C) (3).

A comparison between the three LPF-TVD methods showed that the LPF-CSD1 method outperformed the other two methods (Figure 2. 2). LPF-CSD1 had a statistically significantly higher correlation coefficient compared to LPF-CSD2; median correlation for LPF-CSD1 was 0.94 (95% CI: 0.93 to 0.94), compared to median correlation of 0.92 (95% CI: 0.91 to 0.93) for LPF-CSD2, $P < 0.01$. Moreover, LPF-TVD1

method had the lowest performance compared to the LPF-CSD1 and LPF-CSD2 methods with median correlation of 0.28 (95% CI: 0.26 to 0.30) (Figure 2. 2). Mean square error of LPF-CSD1 and LPF-CSD2 did not differ significantly; median error for LPF-CSD1 and LPF-CSD2 were 07 (95% CI: 0.86 to 1.07) and 0.84 (95% CI: 0.75 to 0.93) respectively, $P > 0.1$ (Figure 2. 2). The post-processing component improved the performance of the SSA-DCT method such that SSA-DCT2 outperformed SSA-DCT1. The SSA-DCT2 method had a significantly higher correlation coefficient compared to SSA-DCT1 method; median correlation 0.86 (95% CI: 0.83 to 0.88) in SSA-DCT2 compared to median correlation 0.6 (95% CI: 0.57 to 0.63) in SSA-DCT1 method, $P < 0.001$. In addition, the SSA–DCT1 method had significantly higher median error compared to SSA–DCT2, 5.8 (CI of 5.55 to 6.06) vs 1.48 (CI of 1.33 to 1.63), $P < 0.001$ respectively (Figure 2. 2). The comparison of SSA-DCT2 and LPF-CSD1 revealed that LPF-CSD1 outperformed SSA-DCT2 with a higher correlation coefficient and lower mean-squared error ($P<0.001$). An example of these two methods for a synthetic signal is shown in Figure 2. 3. Both methods appear to remove all transients (Figure 2. 3. A); however, on closer inspection (Figure 2. 3. B & Figure 2. 3. C), we find that neither method is perfect. LPF-CSD1 tends towards a very sparse solution, and undershoots the transients; in contrast, SSA-DCT2 does a better job in estimating the amplitude of the transients but also tends to overshoot around the edge of the transients, possibly due to the filtering operation of the SSA-DCT2.

Low pass filter total Singular-spectrum analysis

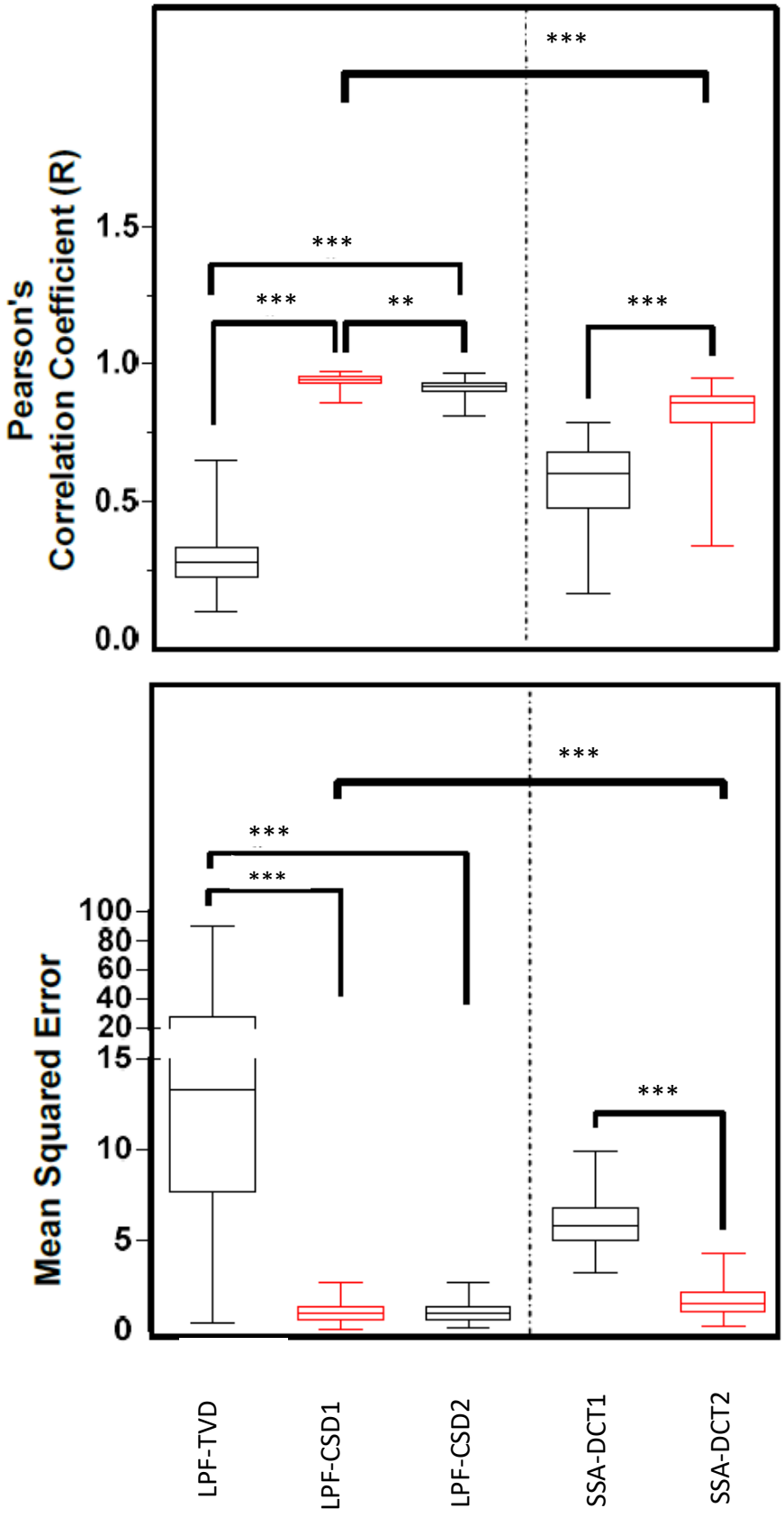

*Figure 2. 2. Comparison between the LPF-TVD methods and between the SSA-DCT methods, and comparison between the best performing algorithm in each group when assessed on 100 synthetic NIRS-like signals; * indicates p < 0.05, ** indicates p < 0.01, and *** indicates p < 0.001; LPF-TVD1 - low-pass filtering total variation denoising; LPF-CSD1 - low-pass filtering compound sparse denoising; LPF-CSD2 - the improved version of LPF-CSD1; SSA-DCT1 – singular spectrum analysis and the discrete cosine transform; SSA-DCT2 – SSA-DCT1 with post-processing.*

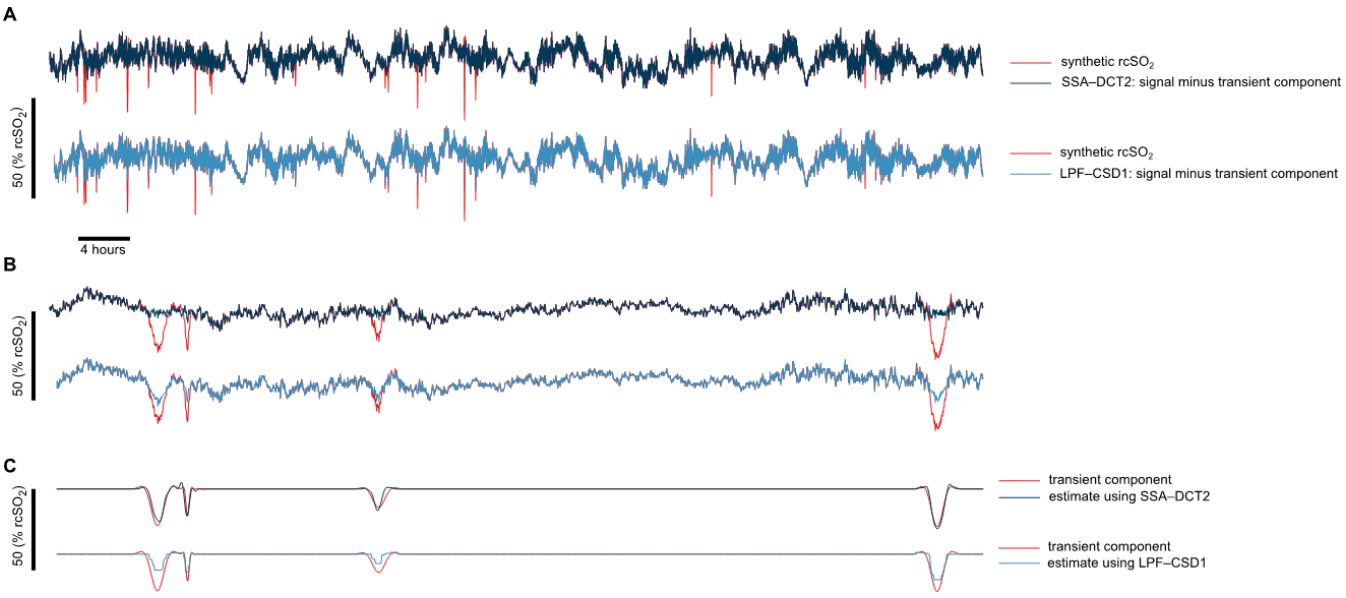

Figure 2. 3. A. SSA-DCT2 and LPF-CSD1 decomposition methods on a NIRS-like synthetic signal; B. Magnified area from A, indicated by the '4 hours' line; c. Zoomed-in predefined transients and extracted ones; rcSO2 – regional cerebral oxygen saturation; SSA-DCT2 - singular-spectrum analysis and the discrete cosine transform with post-processing; LPF-CSD1 - low-pass filtering compound sparse denoising

2.5. Discussion and Conclusion

This study sought to identify the best method to isolate and extract transient deflections within synthetic NIRS signals. We report that LPF-CSD1 was an effective and efficient method to isolate predefined transients in synthetic NIRS signals. Not only does the LPF-CSD1 perform better than LPF-CSD2 on synthetic NIRS signals, it also is computationally efficient in comparison to the SSA-DCT method, as it is approximately 3 to 4 orders of magnitude faster than the SSA-DCT methods. We found that the LPF-CSD1 method outperforms other methods for decomposing the transient components in synthetic preterm NIRS-like signals. Although the post-processing component of the SSA-DCT considerably improved performance of this method (correlation of 0.86 compared to 0.6), it did not outperform the best LPF-TVD method. Performance of LPF-CSD1 appears robust to a range of lambda values (see Figure 2. 2.), nevertheless the optimisation of these parameters may have provided this method with an advantage over SSA-DCT2. Future studies could consider optimising parameters of the SSA-DCT method, although the computational overhead for this method may hinder a brute-force grid search. LPF-CSD2 had been proposed as an improved version of LPF-CSD1, particularly with regard to estimating transient components, but we did not find this to be the case. Although we used a procedure to estimate these 4 parameters through a SD estimate of the noise as previously reported (Selesnick et al., 2014) and optimised one parameter, this method may not be optimal for synthetic NIRS signals that have a level of convexity. Furthermore, the non-convex penalty functions used in LPF-CSD2 can have local minima which makes it challenging to find the global minimum (Selesnick et al., 2014). However, one limitation of the LPF-CSD1, relative to the SSD-DCT2 method is that preliminary

analysis suggests that SSA-DCT2 identifies transient amplitude more effectively than the LPF-CSD1 method. The amplitude of the NIRS signal is an important component of NIRS-guided therapy in this on-going clinical trial (Hansen et al., 2019). Therefore, extracting the full amplitude of transient oxygen desaturations is extremely important. Future studies will explore the suitability of LPF-CSD1 and SSA-DCT2 methods on larger datasets of real NIRS signals and investigate the role of cerebral oxygenation desaturations in preterm brain injury.

2.6. References

Figueiredo, N., Georgieva, P., Lang, E. W., Santos, I. M., Teixeira, A. R., & Tomé, A. M. (2010). SSA of biomedical signals: A linear invariant systems approach. *Statistics and its Interface*, *3*(3), 345-355.

Hansen, M.L., Pellicer, A., Gluud, C., Dempsey, E., Mintzer, J., Hyttel-Sørensen, S., Heuchan, A.M., Hagmann, C., Ergenekon, E., Dimitriou, G., & Pichler, G. (2019). Cerebral near-infrared spectroscopy monitoring versus treatment as usual for extremely preterm infants: a protocol for the SafeBoosC randomised clinical phase III trial. *Trials*, *20*, 1-11.

O'Toole, J. M., Dempsey, E. M., & Boylan, G. B. (2018, July). Extracting transients from cerebral oxygenation signals of preterm infants: a new singular-spectrum analysis method. In *2018 40th Annual International Conference of the IEEE Engineering in Medicine and Biology Society (EMBC)* 5882-5885. IEEE.

Rolfe, P., Wickramasinghe, Y.A.B.D., Thorniley, M.S., Faris, F., Houston, R., Kai, Z., Yamakoshi, K., O'Brien, S., Doyle, M., Palmer, K., & Spencer, S. (1992). Fetal and neonatal cerebral oxygen monitoring with NIRS: theory and practice. *Early Human Development*, *29*(1-3), 269-273.

Selesnick, I. W., Graber, H. L., Ding, Y., Zhang, T., & Barbour, R. L. (2014). Transient artifact reduction algorithm (TARA) based on sparse optimization. *IEEE Transactions on Signal Processing*, *62*(24), 6596-6611.

Selesnick, I. W., Graber, H. L., Pfeil, D. S., & Barbour, R. L. (2014a). Simultaneous low-pass filtering and total variation denoising. *IEEE Transactions on Signal Processing*, *62*(5), 1109-1124.

Vautard, R., Yiou, P., & Ghil, M. (1992). Singular-spectrum analysis: A toolkit for short, noisy chaotic signals. *Physica D: Nonlinear Phenomena*, *58*(1-4), 95-126.

Vesoulis, Z. A., Mintzer, J. P., & Chock, V. Y. (2021). Neonatal NIRS monitoring: recommendations for data capture and review of analytics. *Journal of Perinatology*, *41*(4), 675-688.

Chapter 3. Management of Hypotension in Preterm Infants (HIP)

Title: Machine Learning Detects Intraventricular Haemorrhage in Extremely Preterm Infants

Minoo Ashoori *[1,2], John M. O'Toole [1,3], Ken D. O'Halloran [1,2], Gunnar Naulaers [4,5], Liesbeth Thewissen [5], Jan Miletin [6], Po-Yin Cheung [7], Afif Faisal EL-Khuffash [8], David Van Laere [9], Zbyněk Straňák [10], Eugene M. Dempsey [1,3] and Fiona B. McDonald [1,2]

1. INFANT Research Centre, University College Cork, Ireland

2. Department of Physiology, School of Medicine, College of Medicine and Health, University College Cork, Ireland

3. Department of Paediatrics and Child Health, School of Medicine, College of Medicine and Health, University College Cork, Ireland

4. Department of Development and Regeneration, KU Leuven, Belgium

5. Neonatal Intensive Care, Katholieke Universiteit Hospital Leuven, Belgium

6. Paediatric and Newborn Medicine, Coombe Women's Hospital, Dublin, Ireland

7. Department of Paediatrics, University of Alberta, Edmonton, Alberta, Canada

8. Faculty of Medicine and Health Sciences, Royal College of Surgeons in Ireland, Dublin, Ireland

9. NICU, UZ Antwerp, Edegem, Antwerp, Belgium

10. Institute for the Care of Mother and Child, Third Faculty of Medicine, Charles University, Prague, Czech Republic

Corresponding author: Fiona McDonald, Fiona.mcdonald@ucc.ie; Department of Physiology, School of Medicine, College of Medicine and Health, University College Cork, Ireland.

3.1. Abstract:

Objective: To test the potential utility of applying machine learning methods to regional cerebral ($rcSO_2$) and peripheral oxygen saturation (SpO_2) signals to detect brain injury in extremely preterm infants. Study design: A subset of infants enrolled in the Management of Hypotension in Preterm infants (HIP) trial were analysed (n=46). All eligible infants were <28 weeks gestational age and had continuous $rcSO_2$ measurements performed over the first 72 hours and cranial ultrasounds performed during the first week after birth. SpO_2 data were available for 32 infants. The $rcSO_2$ and SpO_2 signals were pre-processed, and prolonged relative desaturations (PRDs; data-driven desaturation lying in the 2-to-15-minute range) were extracted. Numerous quantitative features were extracted from the bio-signals before and after exclusion of the PRDs within the signals. PRDs were also evaluated as a stand-alone feature. A machine learning model was used to detect brain injury (Intraventricular haemorrhage-IVH grade II-IV) using a leave-one-out cross validation approach. Results: The area under the receiver operating characteristic curve (AUC) for the PRD $rcSO_2$ was 0.846 (95% CI: 0.720 - 0.948), outperforming the $rcSO_2$ threshold approach (0.691, 95% CI: 0.494 - 0.861). Neither the clinical model nor any of the SpO_2 models were significantly associated with brain injury. Conclusion: There was a significant association between data-driven definition of PRDs in $rcSO_2$ and brain injury. Automated analysis of PRDs of the cerebral NIRS signal in extremely preterm infants may aid better prediction of IVH compared to a threshold-based approach. Further investigation of the definition of the extracted PRDs and an understanding of the physiology underlying these events is required.

Keywords: Near-infrared spectroscopy (NIRS); regional cerebral oxygen saturation ($rcSO_2$); peripheral oxygen saturation (SpO_2); prolonged relative desaturation (PRD); extreme gradient boosting (XGBoost)

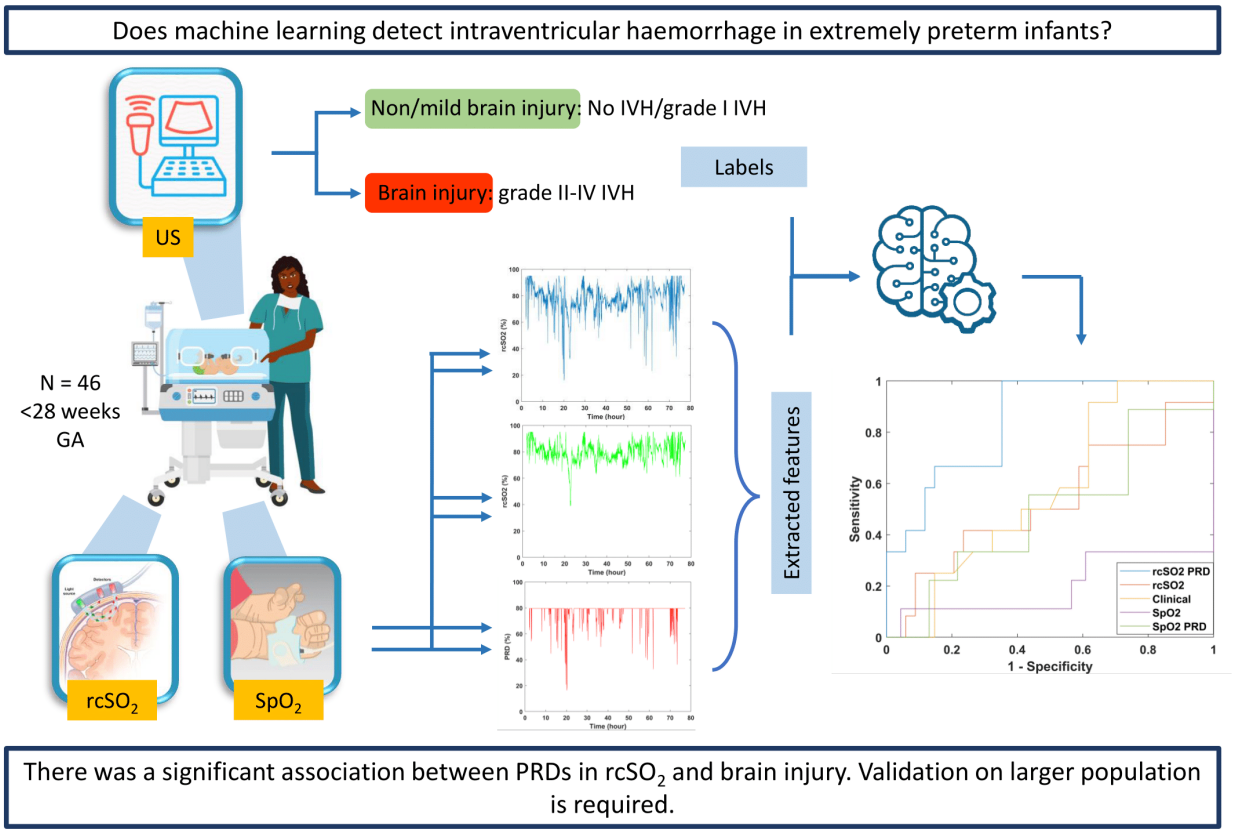

Figure 3. 1. Graphical abstract of HIP study. Created with Biorender.com

3.2. Introduction

Survival in the preterm population is improving, especially for extremely preterm infants. However, long-term adverse neurodevelopmental outcomes remain an ongoing concern, with morbidity increasing with decreasing gestational age (Cheong et al., 2017; Bulbul et al., 2020; Juul et al., 2022). A recent systematic review suggested that between 5–52% of preterm infants will develop some degree of intraventricular haemorrhage (IVH); the disparity attests to the variability in clinical practice and potential diversity within this particular patient population (Siffel et al., 2021). Many studies have associated IVH in extremely preterm infants with poor neurodevelopment in the early years of life (Allan et al., 1997; Adams-Chapman et al., 2008). A recent study examined children who were born extremely preterm but were assessed during school years (age 8) and reported that all grades of IVH were associated with a higher risk of cerebral palsy and that higher grades of IVH were associated with a higher risk of impaired academic scores (Hollebrandse et al., 2021). The duration and severity of the physiological insults or intrinsic vulnerability corresponding to the different grades of IVH are unknown (du Plessis & Volpe, 2002). Matsushita et al. (2022) performed a retrospective study examining potential similarities using 62 clinical features from 215 individual infants born <1000 g. Their cluster analysis of the data revealed six distinct phenotypic clusters, some of which were associated with IVH. The authors' unsupervised machine learning approach may contribute to a better understanding of the IVH population in the future (Matsushita et al., 2022).

Hypoxia is believed to be a contributory factor in the development of IVH. A recent study found that infants with IVH spent a greater percentage of time with a heavier burden of cerebral hypoxia, compared to those who did not have IVH (Ng et al., 2020). This is congruent with changes in systematic and cerebral haemodynamics that reveal a pattern consistent with a hypoperfusion–reperfusion cycle (Noori et al., 2014). Impaired cerebral autoregulation may result in cerebral blood flow disturbance and potential rupture of the fragile vasculature of the germinal matrix, resulting in IVH (O'Leary et al., 2009; Alderliesten et al., 2013; Martini et al., 2022).

Near-infrared spectroscopy (NIRS) is a non-invasive optical technology that is used for continuous bedside monitoring of regional cerebral oxygen saturation ($rcSO_2$) and provides information on neonatal cerebral haemodynamics (Pavlek et al., 2021). Measurement of cerebral oxygenation may be an important tool to guide treatment and prevent cerebral hypoxia (Kalteren et al., 2021) in the most immature infants (Pavlek et al., 2021). Cerebral NIRS has become commonplace in clinical practice (Plomgaard et al., 2019; van Bel et al., 2008). However, a recent meta-analysis, including data from 2606 infants, concluded that there were insufficient data to support or reject the benefit of cerebral NIRS monitoring for improved clinical outcome measures (Hansen et al., 2022). This is not surprising as there is no general agreement concerning the absolute values of $rcSO_2$ associated with brain damage. These absolute values have ranged from $rcSO_2 < 50\%$ (Alderliesten et al., 2014; Verhagen et al., 2015) to $rcSO_2 < 65\%$ (Alderliesten et al., 2016), and in one recent randomised trial there was no association between $rcSO_2 < 55\%$ or $rcSO_2 > 85\%$ and adverse long-term outcomes (Plomgaard et al., 2019). The variability in absolute values of $rcSO_2$ between NIRS devices and sensors and between different gestational

ages makes it difficult to reach a consensus on normal values of $rcSO_2$ in preterm infants (Alderliesten et al., 2016; Dix et al., 2013). Therefore, alternative methods of describing the continuous signal should be evaluated.

We have previously employed signal processing methods to investigate the association of cerebral oxygenation in preterm infants born less than 32 weeks of GA with IVH and periventricular leukomalacia (PVL). We found that features of the signal amplitude within certain frequency bands (0.9–3.6 mHz) were useful for detecting brain injury (O'Toole et al., 2016). Subsequently, we detected the presence of desaturation waveforms in $rcSO_2$ in extremely preterm NIRS recordings and reported that removing these prolonged relative desaturations (PRDs; data driven desaturations) increased the predictability of the NIRS signals in detecting brain injury (O'Toole et al., 2018). However, this was based on a relatively small sample size (n = 10). The objective of the current study was, therefore, to isolate PRDs in $rcSO_2$ and SpO_2 signals in preterm infants less than 28 weeks, and using machine learning models, explore their putative relationship with brain injury in preterm infants. Furthermore, we sought to examine the potential value of combining clinical features with features from the NIRS signals for detecting preterm brain injury.

3.3. Methods

3.3.1. Study Design and Participants

The current study analysed data derived from a multicentre clinical trial, the Management of Hypotension in Preterm Infants (HIP, Trial registration number NCT01482559, EudraCT 2010-023988-17) (Dempsey et al., 2021). The infants were recruited between February 2015 and September 2017 at Cork University Maternity

Hospital. Infants were considered for inclusion if they met the following criteria: (i) were born with a gestational age of less than 28 weeks; (ii) had an indwelling arterial line in place to monitor blood pressure; (iii) showed no significant intraventricular haemorrhage (grade 3 or 4) on a cranial ultrasound scan; (iv) and experienced low blood pressure, defined as a mean blood pressure one mmHg or more below a mean value corresponding to their gestational age in completed weeks, persisting for at least 15 minutes within the first 72 hours after birth. Patients were excluded if attending clinicians deemed them unlikely to survive, major congenital anomalies, or evidence of severe hypovolemia. Data from 46 extremely preterm infants were analysed in this study, including both male (n = 25) and female (n = 21) infants. The mean birth weight of the infants was 767.41 g ± 155.57 g, 20 of whom were diagnosed with hypotension. All infants underwent continuous (>24 h) $rcSO_2$ measurements using NIRS over the first 72 h and cranial ultrasounds performed during the first week of life. A subset of these infants (n = 32) also had continuous SpO_2 data available

(Figure 3. 2). This study was approved by the Clinical Research Ethics Committee, Cork, ECM 5(2) 15 January 2013.

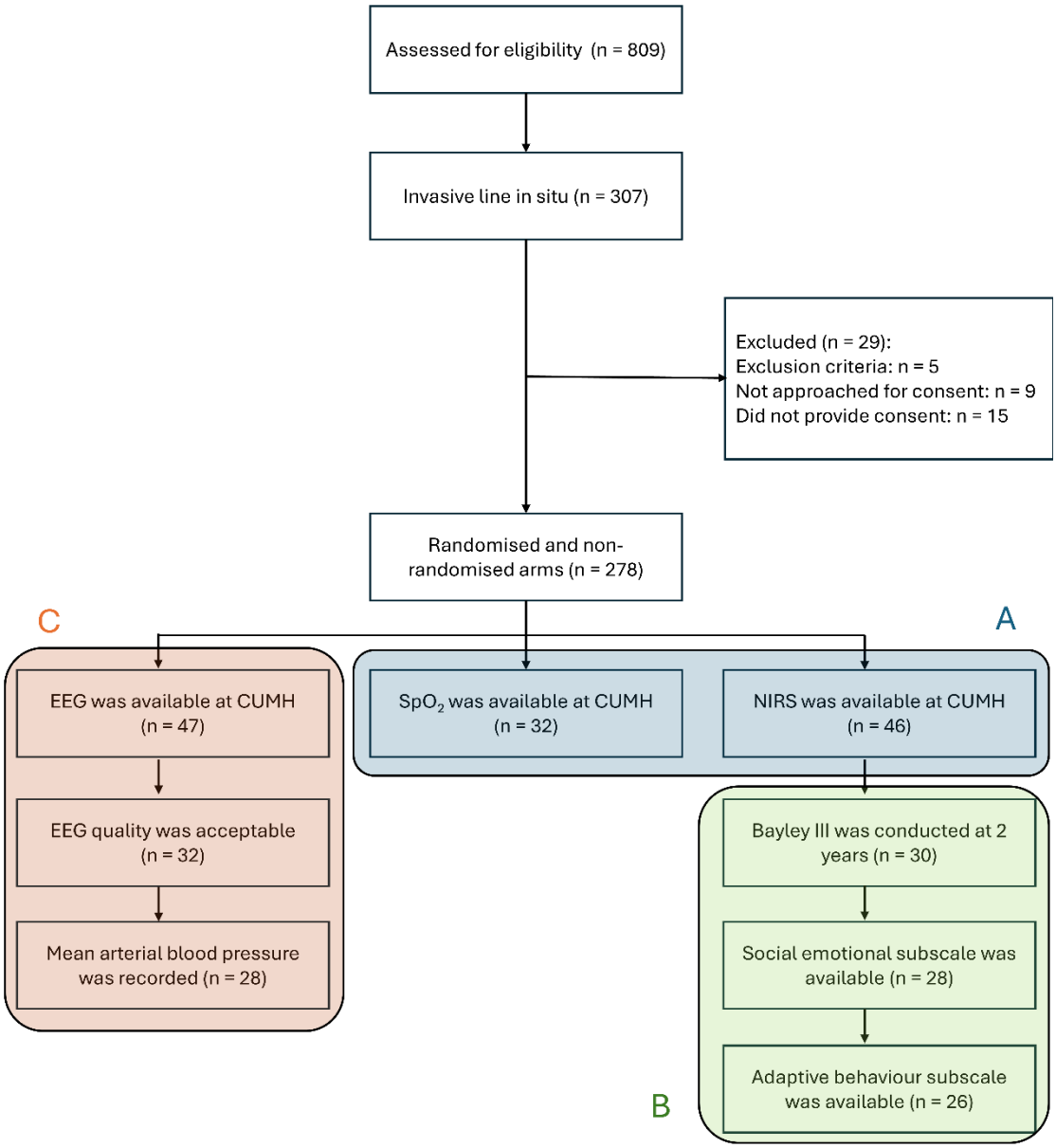

Figure 3. 2. HIP trial flow diagram. Data collected in section [A] has been used in current study. Data collected in section [B] was utilised in the study described in 3.7. and data collected in section [C] was utilised in the study described in section 3.8.

3.3.2. Data Collection

The INVOS 5100 device, (Covidien Mansfield, MI, USA) was used with the neonatal transducer, INVOS OxyAlert NIRSensor (Covidien, Mansfield, MI, USA) to make continuous measurements of $rcSO_2$. The cerebral sensor was placed on the right frontotemporal area of the forehead, measuring the ratio of oxygenated haemoglobin

to the total haemoglobin in the tissue beneath. When available, the Moberg CNS device (Moberg, PA, USA) was used to time-synchronise and store the $rcSO_2$ and peripheral oxygen saturation (SpO_2) data.

SpO_2 was recorded using a pulse oximeter (IntelliVue, MP70, Philips Healthcare, Best, The Netherlands, or equivalent). SpO_2 data were only available for infants whose $rcSO_2$ data was stored using a connected device (Moberg Neuroscan, Ambler, PA, USA) (32/46). SpO_2 data were collected with two sampling frequencies of 1 and 0.5 Hz and stored for later analysis, and all patient information was replaced by individual research codes.

Clinical ultrasound recordings were performed using a Philips HD-11XE ultrasound system and probe C8-5. Ultrasounds were reviewed and graded by experienced paediatric radiologists, who were blinded to the patients' clinical characteristics and haemodynamic findings. Volpe's criteria (Volpe, 2008) were used to classify IVH, and the highest grade of IVH identified by ultrasound in the first week of life was used in a dichotomous outcome label. For the purpose of our machine learning model, brain injury was defined as IVH grade II-IV in the first week of life, and IVH grade I or no IVH was classified as non/mild brain injury for this study (Payne et al., 2013). It is important to note that infants that were labelled as IVH grade I in our study did not progress to IVH II, and their haemorrhage often improved within the first week.

A combination of clinical data, used by clinicians for the early identification of infants at risk of IVH, were analysed in this study. These clinical attributes included the following binary variables: sex, hypotension, receiving any inotrope, and the presence of chorioamnionitis in utero. Other continuous variables included birth weight (g) and

head circumference (cm), and discrete variables included Apgar score in the first 5 min of life and gestational age (GA, days).

3.3.3. Signal Processing

The INVOS device records using a nonuniform sampling frequency, typically between 1/5 and 1/6 Hz. At this sampling frequency, these devices need external memory to store data. When this device was not available, the INVOS device stored data in internal memory with a nonuniform sampling frequency typically between 1/34 and 1/35 Hz. To generate a uniform sampling rate, cubic spline interpolation was used to fill in the missing data (Ouchi et al., 2022). The $rcSO_2$ signal was then up sampled to a sampling frequency of 10 Hz, and a low-pass filter (a zero-phase finite impulse response filter, FIR) was used to prevent aliasing before down-sampling to 1/6 Hz. Missing data that were filled in using cubic spline interpolation were removed.

In some cases, the NIRS probe became loose, detached or was temporarily removed during recordings over 72 h. In these cases, $rcSO_2$ was not recorded or saturated at the minimum value of 15% (Hessel et al., 2014). Thus, in data points equivalent to 15%, a collar of 30 s was applied, and those data points were removed.

To preprocess the SpO_2 signals, first values of less than 20% or sudden changes (more than 4% in one second) with a collar of 30 s were removed, as these are indicative of movement or device artefacts (Buekers et al., 2019). Missing data were interpolated using cubic spline interpolation (Ouchi et al., 2022), and the signal was down-sampled, after applying an appropriate anti-aliasing low-pass filter, to 1/6 Hz for agreement with the $rcSO_2$ signal. Missing data prior to down-sampling were then removed.

3.3.4. Extracting Prolonged Relative Desaturations

A decomposition method, designed specifically to extract PRDs from $rcSO_2$ signals in preterm infants (Ashoori et al., 2021), was used to extract PRDs from both the $rcSO_2$ and SpO_2 signals. This method applies a discrete cosine transform to the signals before using singular spectrum analysis to extract the transient-like components (O'Toole et al., 2016). This PRD decomposition method is a data-driven operation that we have shown to be effective in isolating the PRDs from synthesised NIRS-like signals (Ashoori et al., 2021). The duration of these PRDs typically lies in the 2-to-15-min range, and these desaturations have been defined and excluded using data-driven methods rather than using an absolute value as a threshold.

Three different modalities of the $rcSO_2$ were analysed: the $rcSO_2$ unprocessed, the $rcSO_2$ signal without the PRD component, and the $rcSO_2$ PRD component alone. For the first two modalities (i.e., $rcSO_2$ and $rcSO_2$ without the PRDs), the following methods were employed. First, the signals were filtered using a filter bank according to a dyadic frequency response. Five zero-phase finite-impulse response filters—with a frequency bandwidth of a/(2b), where a = fs /2 and b = 0,1,2,3,4—were used for band-pass filtering. Next, quantitative features were extracted for each filtered signal over a 4 h epoch with a 50% overlap. The number of epochs varied between 14 and 37, depending on the duration of recorded NIRS.

3.3.5. Feature Extraction

Amplitude-modulation features included the mean, standard deviation (SD), the 5^{th} and 95^{th} percentiles of the envelope, skewness, and kurtosis of the signal. Instantaneous frequency (IF) was estimated using a central-finite difference of the

phase of the signal; mean, SD, skewness, kurtosis, and the 5^{th} and 95^{th} percentiles of the IF were again used as features. Fractal dimension (FD) was estimated using the Higuchi method (Higuchi, 1988). The postnatal age of the infants in each epoch was added to the feature set, resulting in a total feature set of 66 features.

A distinct set of features was measured directly from the extracted PRDs: frequency of the PRDs per hour, total power, envelope summarised in mean and SD, Hjorth parameters (activity, mobility, and complexity), interspike interval summarised in mean and standard deviation, time spent below 63% $rcSO_2$ (85% for SpO_2 transients), the average of the nadir amplitude of PRDs, the average of the downward slope (the slope of the line between the PRD's baseline and nadir), the average of the upward slope (the slope of the line between the PRD's nadir and baseline), and averaged duration of the PRDs. The total feature set for PRDs contained 14 features. Some of these features are illustrated in Figure 3. 3. The entire process, from signal decomposition to feature extraction, was also applied to the SpO_2 signal.

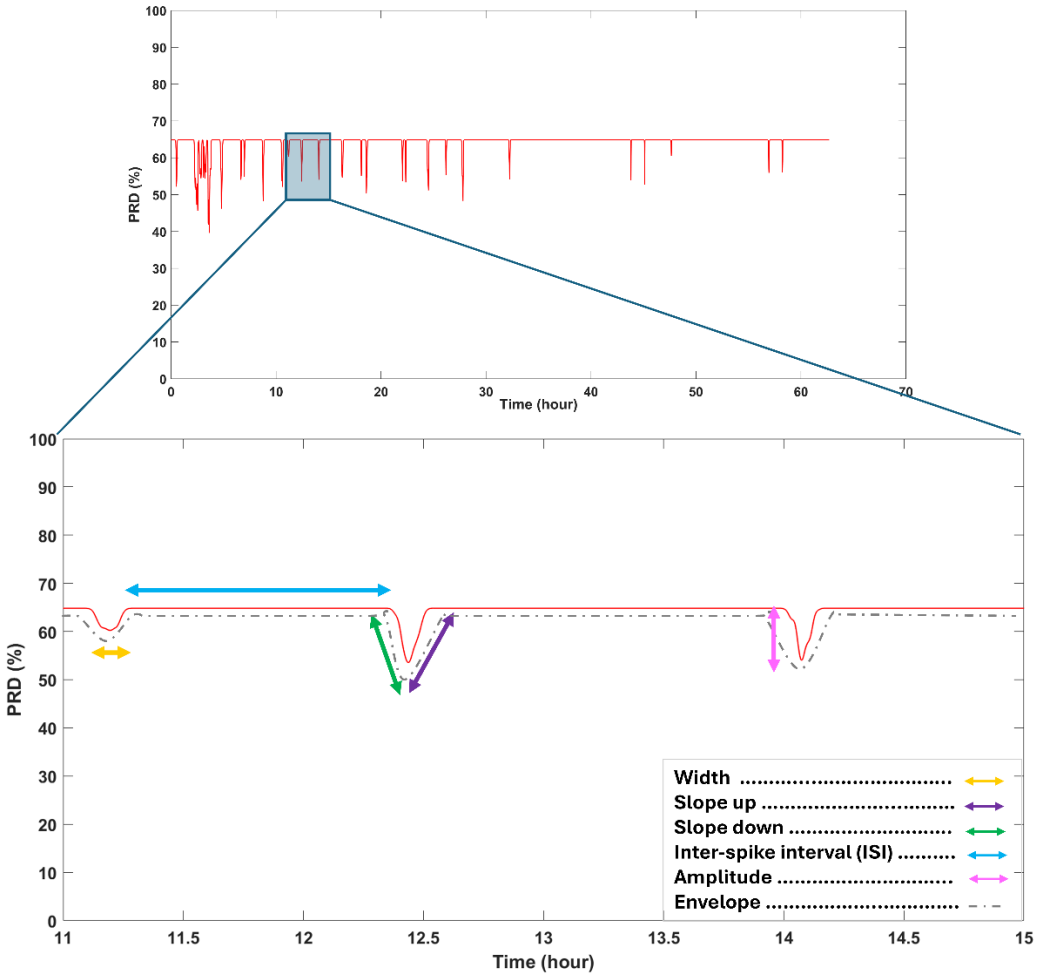

Figure 3. 3. Illustration of some of the quantitative features extracted from PRDs.

3.3.6. Machine Learning Models

A predictive model of brain injury was developed using a sequential ensemble of decision trees, known as an extreme gradient boosting machine (XGBoost). To reduce variance in the model, a common problem with small noisy data sets, regularisation was increased from default values by setting the maximum tree depth to 3. The total number of trees was 50, and the learning rate was 0.1. The feature set of 66 features per each 4 h epoch was used to train and test the model, using a leave-one-baby-out cross-validation procedure. In this method, the features derived from one infant were

left out, and the remaining data were used to make the model, and then the model was tested on the excluded infant. This process was repeated for all the infants in the study, a total of 46 times, to overcome overfitting.

This approach was used to develop separate models for the $rcSO_2$ and SpO_2 signals, and then again for extracted PRD components. Feature importance was estimated for significant models, to examine how each feature contributed to the model's prediction.

Due to its superior performance on nosier data sets, a bagging ensemble known as a random forest was used to develop a predictive model using recorded clinical attributes. The random forest combines multiple decision trees developed independently on different subsets of data. The default parameters of the random forest were used with 500 trees. Similarly, a leave-one-baby-out cross-validation procedure was used to train and test the model.

3.3.7. Combining Models

To test if clinical information could enhance the predictability of detecting brain injury, the $rcSO_2$ model and clinical model were combined using a late-stage fusion approach. Specifically, the probabilities generated from the $rcSO_2$ model were combined with the probability of the clinical-feature model using the geometric mean. The same approach was applied to combining the SpO_2 and clinical models. All the steps taken to process the signal, extract the PRDs and features, and utilise the machine learning model are presented in *Figure 3. 4*.

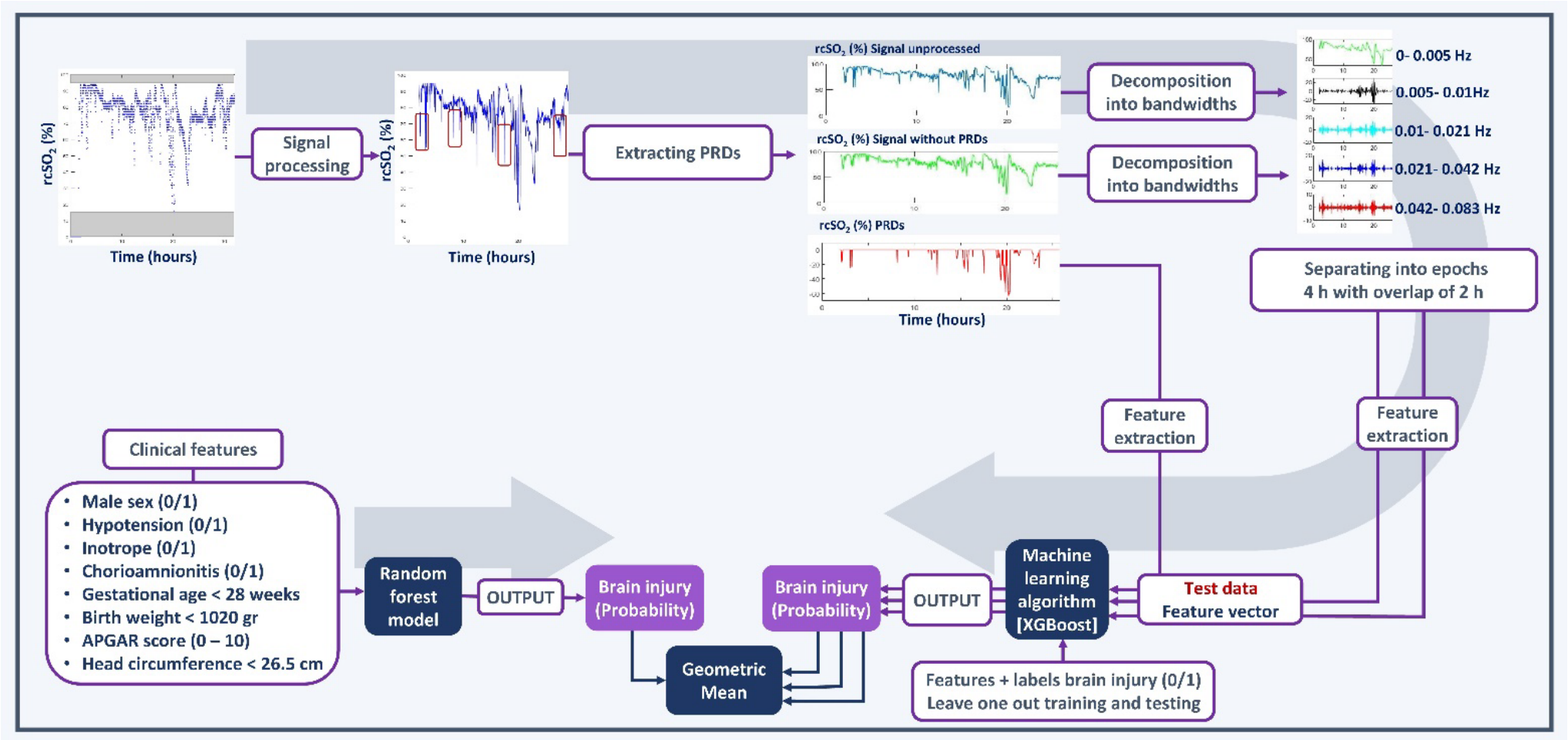

Figure 3. 4. Summary of the steps taken to process the signal, extract the relative prolonged desaturations (PRDs) and features, and utilise the machine learning model

3.3.8. Statistical Analysis

Fisher's exact test was used to compare the proportion of infants with brain injury between the two $rcSO_2$ sampling frequencies (~1/6 and ~1/35 Hz). To evaluate the ability of each model to detect brain injury, the area under the receiver operating characteristic curve (AUC) and its corresponding 95% confidence interval (CI) were analysed. AUC was considered significant if the value of AUC and the lower CI were greater than 0.5. An AUC value of 0.5 indicates that the model performs no better than a chance in distinguishing between true and false positives, so any value greater than 0.5 is an improvement over random guessing (Fan et al., 2006). CIs were calculated using a bootstrapping procedure with resampling (with replacement) on a per-infant basis. In SpO_2 XGBoost models, a hyperparameter, scale-pos-weight, was added and set to the ratio of the number of negative to positive samples to account for class imbalance in the dataset. The threshold used on the model probability for calculating sensitivity, specificity, and accuracy was 0.4; thus, any predicted probability scores greater than or equal to 0.4 were considered positive predictions. Matthew's correlation coefficient (MCC) was also used as a performance metric of the classification models. Additional analysis was performed to calculate the AUC of the separate variables of PRDs, to test how each variable performed in distinguishing between outcome labels. Furthermore, the use of time spent below threshold values ($<63\%$ $rcSO_2$, $<85\%$ SpO_2) in the predictability of brain injury was examined. This analysis was conducted to compare the efficacy of our machine learning models, which utilises numerous quantitative features, with that of current threshold-based methodologies. The grand average of all extracted PRDs from IVH and non/mild IVH

groups was calculated and reported in Figure 3. 5 to illustrate the conformation of the PRDs in each group.

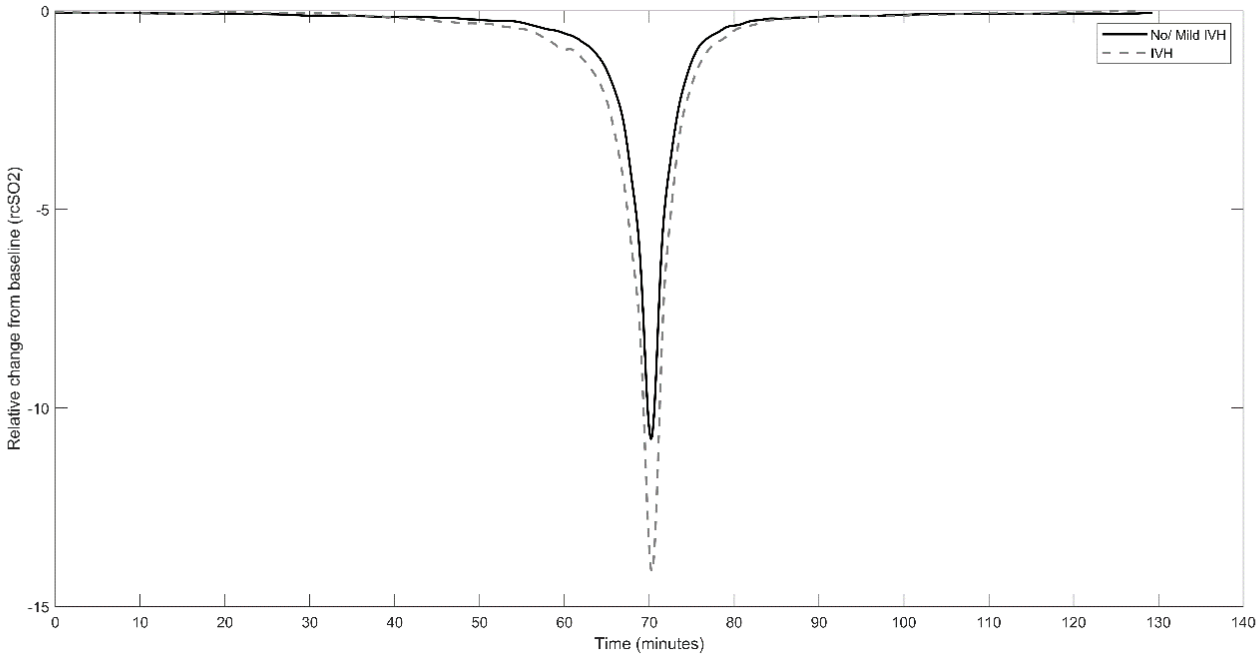

Figure 3. 5. Averaged curve of all $rcSO_2$ PRDs in the intraventricular haemorrhage group (dashed line) vs. no/mild intraventricular haemorrhage group (solid line); X-axis indicates the time in minutes when the grand average of $rcSO_2$ PRDs starts to deviate from baseline, reaches the nadir, and increases to baseline again.

3.4. Results

This study utilised data gathered from 46 infants born less than 28 weeks of GA with $rcSO_2$ recorded for >24 h. The clinical characteristics of infants included in this study are detailed in Table 3. 1. We found no significant association between sampling frequency and outcome indicating that sampling frequency was not a confounding factor (p = 0.505, Fisher's exact test). The average duration of the $rcSO_2$ recordings and deleted data due to artefact removal were 60.98 h and 0.004 h, respectively. Averaged duration of recorded SpO_2 and deleted data due to artefact removal were 63.79 h and 1.49 h, respectively.

Neither a single clinical attribute nor the combination of all attributes in our model was predictive of the short-term clinical outcome: the random forest model had a median (95% CI) testing AUC of 0.57 (0.39–0.76) (Table 3. 2). Thus, we did not find evidence that clinical data, individually or combined, can detect IVH in the first week after birth.

The $rcSO_2$ models before or after PRD removal were not significantly associated with IVH injury (AUC 0.53, CI = 0.31–0.74 and AUC = 0.54, CI = 0.33–0.74, respectively). Combining these $rcSO_2$ models with the clinical model did not improve the performance of the models (Table 3. 2). However, the model using the isolated $rcSO_2$ PRDs was significantly associated with brain injury, with an AUC of 0.85 (0.72–0.95). The sensitivity and specificity of this model were 0.85 and 0.58, respectively. Matthew's correlation coefficient (MCC) was 0.57. Adding the clinical model to the $rcSO_2$ PRD model showed no practical improvement in performance (AUC = 0.86 (0.74–0.96), sensitivity = 0.94, specificity = 0.25, MCC = 0.61) (Table 3. 2). For

comparison with the current literature, we also tested if the threshold value of 63%, i.e., the time $rcSO_2$ spent below 63%, was a useful predictor, but this marker was not predictive of brain injury in our cohort (AUC 0.59, CI = 0.40–0.78) (Table 3. 2).

Following analysis of the individual features extracted from $rcSO_2$ PRDs, we report that only mean amplitude was significantly associated with IVH with an AUC of 0.73 (95% CI: 0.53–0.92) (Table 3. 3), which was less robust than the XGBoost $rcSO_2$ PRDs model. The grand average of the extracted PRDs among all infants in the IVH group vs. non/mild IVH group is presented in Figure 3. 5. A higher amplitude of deflection from the baseline in the IVH group compared with the non/mild IVH group is evident. SpO_2 was recorded for 32 infants. None of the three SpO_2 models were significantly associated with brain injury (Table 3. 2). Combination with the clinical model did not improve the detection of brain injury. For comparison with the current literature, we also tested if the threshold value of 85%, i.e., the time SpO_2 spent below 85%, was a useful predictor, but this marker was not predictive of brain injury in our cohort (AUC 0.52, CI = 0.28–0.76) (Table 3. 2).

Table 3. 1. Clinical data of the subset of infants from the HIP trial included in the current study.

Clinical features	Brain injury (n = 12)	No/mild injury (n = 34)
Sex (male) (% of total number of infants in group)	8 (67%)	17 (50%)
Hypotension (% of total number of infants in group)	7 (58%)	13 (38%)
Inotrope (% of total number of infants in group)	3 (25%)	6 (18%)
Chorioamnionitis (% of total number of infants in group)	0 (0%)	5 (15%)
Gestational age (days) Mean (SD)	178.5 (7.5)	181.3 (8.8)
Birth weight (g) Mean (SD)	769.2 (173.7)	766.8 (151.5)
APGAR score (5 min) Mean (SD)	7.0 (2.0)	6.9 (1.9)
Head circumference (cm) Mean (SD)	23.3 (1.5)	23.3 (1.5)

Table 3. 2. Area under the curve (AUC) values for the signals used to predict brain injury in the first week of life.

Model	AUC	95% confidence interval
Clinical data	0.575	0.390 - 0.759
$rcSO_2$	0.569	0.362 - 0.779
$rcSO_2$ without PRDs	0.576	0.365 - 0.780
$rcSO_2$ PRDs	0.846*	0.736 - 0.964
$rcSO_2$ and clinical data	0.581	0.400 - 0.767
$rcSO_2$ without PRDs and clinical data	0.608	0.412 - 0.793
$rcSO_2$ PRDs and clinical data	0.860 *	0.758 - 0.974
SpO_2	0.198	0.000 - 0.459
SpO_2 without PRDs	0.261	0.061 - 0.545
SpO_2 PRDs	0.493	0.264 - 0.741
SpO_2 and clinical data	0.324	0.133 - 0.546
SpO_2 without PRDs and clinical data	0.348	0.151 - 0.579
SpO_2 PRDs and clinical data	0.454	0.235 - 0.697
$rcSO_2$ time spent below 63%	0.593	0.399 - 0.775
SpO_2 time spent below 85%	0.522	0.277 - 0.759

*indicates significant AUC

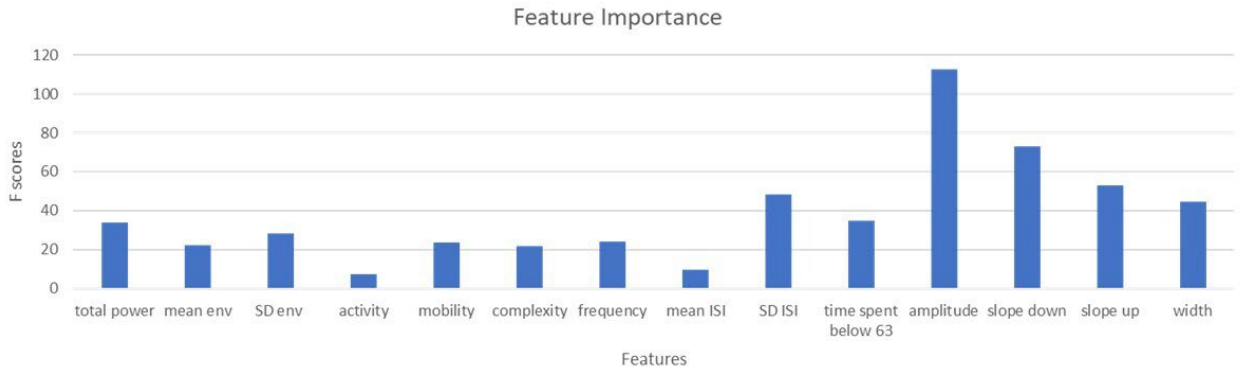

Figure 3.6. Illustration of feature importance of the XGBoost model using rcSO2 prolonged relative desaturations (PRDs) in predicting intraventricular haemorrhage.

Table 3. 3. Area under the curve (AUC) values for the individual features of rcSO2 PRDs used to predict brain injury in the first week of life.

Feature	AUC	95% confidence interval
Frequency of the transients per hour	0.409	0.201 - 0.619
Total power	0.368	0.191 - 0.560
Envelope (mean)	0.397	0.214 - 0.592
Envelope (standard deviation)	0.539	0.352 - 0.738
Hjorth parameters (activity)	0.603	0.399 - 0.802
Hjorth parameters (mobility)	0.409	0.214 - 0.602
Hjorth parameters (complexity)	0.569	0.353 - 0.775
inter-spike interval (mean)	0.532	0.306 - 0.748
inter-spike interval (standard deviation)	0.5049	0.282 - 0.714
Time spent below 63%	0.691	0.494 - 0.861
Nadir amplitude of PRDs (mean)	0.733*	0.530 - 0.919
Slope down (mean)	0.689	0.474 - 0.883
Slope up (mean)	0.669	0.477 - 0.838
Duration of the PRDs (mean)	0.603	0.422 - 0.770

* indicates significant AUC

3.5. Discussion

This study set out to examine the potential utility of machine learning models of $rcSO_2$ signals recorded in the first 72 h after birth in extremely preterm infants, and their usefulness in detecting IVH in the first week after birth. Our results demonstrate that a data-driven combination of extracted features from isolated PRDs of $rcSO_2$ signal was associated with IVH in this cohort of extremely preterm infants.

Previous studies have employed different methods for interpreting NIRS data as an early predictor of IVH. The absolute value of the NIRS signal is used as a criterion for intervention in some NICUs; however, NIRS values vary with gestational age and are dependent upon different algorithms incorporated into the devices (Verhagen et al., 2015). The absolute value of NIRS, being predictive of adverse outcome, ranged from <50% (Alderliesten et al., 2014; Verhagen et al., 2015) to <65% (Alderliesten et al., 2016) with varying sensors. SafeBoosC-III, the randomised clinical trial, used cerebral oximetry during the first 72 h after birth to guide intervention in extremely preterm infants. The authors report that the use of NIRS did not alter the incidence of death or severe brain injury at 36 weeks' postmenstrual age after birth compared with infants assigned to receive usual care (Hansen et al., 2023). In this trial, if infants randomised to the NIRS group had cerebral oxygenation below the threshold for hypoxia, treatment was considered (Hansen et al., 2019). Of note, the time $rcSO_2$ spent below 63% was not predictive of brain injury in the current preterm cohort (AUC 0.593 CI 0.399–0.775). The potential uncertainty relating to absolute NIRS values necessitates the development of alternative methods, including the use of other features of the signal for their potential to predict outcomes.

The results of the current study indicate that the features we extracted from the $rcSO_2$ signal, before and after excluding PRDs, were not predictive of IVH. These findings are in contrast with previous signal processing methods that proposed an improvement in performance when the PRDs were removed (O'Toole et al., 2016). However, this earlier study covered a wider GA (<32 weeks), used shorter epochs (2 h), had a different sampling frequency (1/35 Hz) compared with what we used (1/6 Hz), and was limited by a small sample size (n = 10). Interestingly, however, in this current study, features arising from the $rcSO_2$ PRDs were associated with IVH. If validated, AI recognition of this novel feature of NIRS signal during bedside monitoring could facilitate the timely implementation of neuroprotective strategies for the infant.

The PRDs were extracted from the NIRS signal using a previously described method; this procedure is a data-driven tool that identifies transient-like waveforms of the order of one to tens of minutes within a signal. Therefore, the PRDs are not predefined events determined by absolute amplitude, duration, or frequency. Post-extraction analysis of the PRDs, as illustrated in Figure 3. 5, indicates that they are events lasting minutes with a relative change in signal of approximately 11–14%. Features of these estimated PRDs are then combined using a machine learning model, a process that can detect variances not discernible visually and also a process that due to its complexity can be difficult to relate back to signal characteristics.

This study contributes to the recent debate about the role of $rcSO_2$ in predicting early adverse outcomes. We must strive to overcome current limitations in the interpretation of NIRS with the use of innovative analysis. The quantification of $rcSO_2$ is considered to arise from venous/arterial blood (70%/30%) and is influenced by

many potential variables, including perfusion, cerebral autoregulation, cerebral activity, and oxygen extraction, which make it more challenging to interpret (Suppan et al., 2022). Previous studies have reported a strong correlation between cerebral oxygen desaturation and low cardiac output in preterm infants (Bresesti et al., 2021; Janaillac et al., 2018). The continuous and simultaneous measurement of mean arterial blood pressure, cardiac output, and EEG brain activity could provide additional insight if incorporated into the analysis of $rcSO_2$.

SpO_2 has been used to guide respiratory care. In 2007, the American Academy of Pediatrics recommended a range of 85–95% in preterm infants, and in 2010 the recommended target range was set to 85–93% by the European Association of Perinatal Medicine (Sweet et al., 2008; The American Academy of Pediatrics and the American College of Obstetricians and Gynecologists, 2007). More recently, large clinical studies, such as NeOProM (Neonatal Oxygenation Prospective Meta-analysis) have narrowed the recommended range of SpO_2 (Askie et al., 2018). Pooled data from the NeOProM clinical trial reported that extremely preterm infants with SpO_2 values of 85–89% were at higher risk of mortality and necrotizing enterocolitis compared with ones with SpO_2 values of 91–95%. However, the risk of retinopathy of prematurity was higher in preterm infants with higher levels of SpO_2 (Askie et al., 2018). Sullivan et al. (2018) suggested that the combined features of SpO_2 (mean, SD, kurtosis, and skewness) with clinical data in the first 12 h and the first 7 days of life were associated with severe IVH (grade III and IV) and NEC. In terms of absolute values, Vesoulis et al. (2019) studied 645 infants born <32 weeks of GA and proposed that the duration of time spent with $SpO_2 \leq 70\%$ was correlated with severe grade III and IV IVH. Moreover, a lower level of SpO_2 was associated with IVH grades III and IV

in very low birth weight infants (Zanelli et al., 2023). However, in the current study, we did not find an association between features extracted from the SpO_2 signal, including and excluding PRDs or with time spent below $SpO_2 \leq 85\%$, with IVH outcome. If the isolated PRDs in the $rcSO_2$ were caused by systemic hypoxemia, we reasoned that PRDs isolated from the SpO_2 signal would also be predictive of IVH outcome. This would be significantly advantageous as the use of pulse oximetry is more widespread than cerebral oxygen monitoring. However, we did not find features of isolated PRDs from the SpO_2 signal that were associated with IVH injury.

SpO_2 is dependent on detecting a variance in transmitted light. Thus, when perfusion decreases, pulse amplitude gets smaller and pulse oximetry readings are adversely affected. As a result, hypotension and hypothermia that cause poor peripheral perfusion can render pulse oximetry prone to error (DeMeulenaere, 2007). Furthermore, pulse oximetry is influenced by the presence of foetal haemoglobin (FHb) (Pritišanac et al., 2021). FHb is the main oxygen carrier during pregnancy and starts to be replaced by adult haemoglobin from the 20th week of gestation (Sankaran et al., 2013). FHb has a higher affinity for oxygen compared with adult haemoglobin and does not provide enough oxygen diffusion and delivery in neonates. Thus, the probability of higher concentration of FHb and increased affinity for oxygen and the fact that 20 out of 46 infants were hypotensive might contribute to the poor association between SpO_2 and IVH outcome in our cohort.

PRDs were evident in all infants and were extracted from both $rcSO_2$ and SpO_2. Further investigation in a subset of infants revealed that there were both asynchronous and synchronous PRDs in both signals. These events in SpO_2 may

represent systemic hypoxemia brought about by poor gas exchange or decreased perfusion. Independent decreases in $rcSO_2$ may reflect selective overt impairment of regional cerebral perfusion or instances of increased oxygen utilisation in the face of enhanced functional demand with inadequate neurovascular coupling.

A limitation of this study is that the outcome was defined based on the highest grade of IVH diagnosed using ultrasound in the first week of life, and the exact time of the IVH occurrence was unknown. Furthermore, SpO_2 was recorded for only 32 out of 46 infants, and SpO_2 and $rcSO_2$ were time-synchronised for only 26 infants. Moreover, the signal decomposition method used to extract the PRDs performed well in isolating the desaturations that were long (average of 8 min), but many shorter (approximately <1 min) desaturation events were not captured using this method. Algorithms could be developed to isolate these briefer transients and test their predictability of IVH in future studies.

This study proposes that the features extracted from the $rcSO_2$ signal contain information that may be useful in the early detection of brain injury, which may not be the case for the SpO_2 signal. Decreases in cerebral oxygen saturation may reflect hypoxia, vasoconstriction, low blood flow, and/or impaired autoregulation. It is not possible to determine the individual or combined elements of each of these possibilities. However, what is clear is that a combination of quantitative features of these relative cerebral desaturations (PRDs) is associated with brain injury in extremely preterm infants. The incorporation of machine learning methods needs to be validated in future large cohorts of extremely preterm infants.

3.6. References

Adams-Chapman, I., Hansen, N. I., Stoll, B. J., Higgins, R., & NICHD Research Network. (2008). Neurodevelopmental outcome of extremely low birth weight infants with posthemorrhagic hydrocephalus requiring shunt insertion. *Pediatrics*, *121*(5), e1167-e1177.

Alderliesten, T., Dix, L., Baerts, W., Caicedo, A., Van Huffel, S., Naulaers, G., Groenendaal, F., Van Bel, F., & Lemmers, P. (2016). Reference values of regional cerebral oxygen saturation during the first 3 days of life in preterm neonates. *Pediatric Research*, *79*(1), 55-64.

Alderliesten, T., Lemmers, P.M., Smarius, J.J., van de Vosse, R.E., Baerts, W., & van Bel, F. (2013). Cerebral oxygenation, extraction, and autoregulation in very preterm infants who develop peri-intraventricular hemorrhage. *The Journal of Pediatrics*, *162*(4), 698-704.

Alderliesten, T., Lemmers, P. M., van Haastert, I. C., de Vries, L. S., Bonestroo, H. J., Baerts, W., & van Bel, F. (2014). Hypotension in preterm neonates: low blood pressure alone does not affect neurodevelopmental outcome. *The Journal of Pediatrics*, *164*(5), 986-991.

Allan, W. C., Vohr, B., Makuch, R. W., Katz, K. H., & Ment, L. R. (1997). Antecedents of cerebral palsy in a multicenter trial of indomethacin for intraventricular hemorrhage. *Archives of Pediatrics & Adolescent Medicine*, *151*(6), 580-585.

Ashoori, M., Dempsey, E. M., McDonald, F. B., & O'Toole, J. M. (2021, November). Sparse-Denoising Methods for Extracting Desaturation Transients in Cerebral

Oxygenation Signals of Preterm Infants. In *2021 43rd Annual International Conference of the IEEE Engineering in Medicine & Biology Society (EMBC)* 1010-1013. IEEE.

Askie, L.M., Darlow, B.A., Finer, N., Schmidt, B., Stenson, B., Tarnow-Mordi, W., Davis, P.G., Carlo, W.A., Brocklehurst, P., Davies, L.C., & Das, A. (2018). Association between oxygen saturation targeting and death or disability in extremely preterm infants in the neonatal oxygenation prospective meta-analysis collaboration. *The Journal of the American Medical Association*, *319*(21), 2190-2201.

Bresesti, I., Avian, A., Bruckner, M., Binder-Heschl, C., Schwaberger, B., Baik-Schneditz, N., Schmölzer, G., Pichler, G., & Urlesberger, B. (2021). Impact of bradycardia and hypoxemia on oxygenation in preterm infants requiring respiratory support at birth. *Resuscitation*, *164*, 62-69.

Buekers, J., Theunis, J., De Boever, P., Vaes, A.W., Koopman, M., Janssen, E.V., Wouters, E.F., Spruit, M.A., & Aerts, J.M. (2019). Wearable finger pulse oximetry for continuous oxygen saturation measurements during daily home routines of patients with chronic obstructive pulmonary disease (COPD) over one week: observational study. *JMIR mHealth and uHealth*, *7*(6), p.e12866.

Bulbul, L., Elitok, G.K., Ayyıldız, E., Kabakcı, D., Uslu, S., Köse, G., Tiryaki Demir, S., & Bulbul, A. (2020). Neuromotor Development Evaluation of Preterm Babies Less than 34 Weeks of Gestation with Bayley III at 18-24 Months. *BioMed Research International*, *2020*(1), p.5480450.

Cheong, J.L., Doyle, L.W., Burnett, A.C., Lee, K.J., Walsh, J.M., Potter, C.R., Treyvaud, K., Thompson, D.K., Olsen, J.E., Anderson, P.J., & Spittle, A.J. (2017). Association

between moderate and late preterm birth and neurodevelopment and social-emotional development at age 2 years. *JAMA Pediatrics*, *171*(4), e164805-e164805.

DeMeulenaere, S. (2007). Pulse oximetry: uses and limitations. *The Journal for Nurse Practitioners*, *3*(5), 312-317.

Dempsey, E.M., Barrington, K.J., Marlow, N., O'Donnell, C.P.F., Miletin, J., Naulaers, G., Cheung, P.Y., Corcoran, J.D., El-Khuffash, A.F., Boylan, G.B., & Livingstone, V. (2021). Hypotension in Preterm Infants (HIP) randomised trial. *Archives of Disease in Childhood-Fetal and Neonatal Edition*, *106*(4), 398-403.

Dix, L. M., van Bel, F., Baerts, W., & Lemmers, P. (2013). Comparing near-infrared spectroscopy devices and their sensors for monitoring regional cerebral oxygen saturation in the neonate. *Pediatric Research*, *74*(5), 557-563.

du Plessis, A. J., & Volpe, J. J. (2002). Perinatal brain injury in the preterm and term newborn. *Current Opinion in Neurology*, *15*(2), 151-157.Fan, J., Upadhye, S., & Worster, A. (2006). Understanding receiver operating characteristic (ROC) curves. *Canadian Journal of Emergency Medicine*, *8*(1), 19-20.

Hansen, M.L., Hyttel-Sørensen, S., Jakobsen, J.C., Gluud, C., Kooi, E.M., Mintzer, J., de Boode, W.P., Fumagalli, M., Alarcon, A., Alderliesten, T., & Greisen, G. (2024). Cerebral near-infrared spectroscopy monitoring (NIRS) in children and adults: a systematic review with meta-analysis. *Pediatric Research*, *96*(4), 856-867.

Hansen, M.L., Pellicer, A., Gluud, C., Dempsey, E., Mintzer, J., Hyttel-Sørensen, S., Heuchan, A.M., Hagmann, C., Ergenekon, E., Dimitriou, G., & Pichler, G. (2019). Cerebral near-infrared spectroscopy monitoring versus treatment as usual for

extremely preterm infants: a protocol for the SafeBoosC randomised clinical phase III trial. *Trials*, *20*, 1-11.

Hansen, M.L., Pellicer, A., Hyttel-Sørensen, S., Ergenekon, E., Szczapa, T., Hagmann, C., Naulaers, G., Mintzer, J., Fumagalli, M., Dimitriou, G., & Dempsey, E. (2023). Cerebral oximetry monitoring in extremely preterm infants. *New England Journal of Medicine*, *388*(16), 1501-1511.

Hessel, T. W., Hyttel-Sorensen, S., & Greisen, G. (2014). Cerebral oxygenation after birth–a comparison of INVOS® and FORE-SIGHT™ near-infrared spectroscopy oximeters. *Acta Paediatrica*, *103*(5), 488-493.

Higuchi, T. (1988). Approach to an irregular time series on the basis of the fractal theory. *Physica D: Nonlinear Phenomena*, *31*(2), 277-283.

Hollebrandse, N. L., Spittle, A. J., Burnett, A. C., Anderson, P. J., Roberts, G., Doyle, L. W., & Cheong, J. L. Y. (2021). School-age outcomes following intraventricular haemorrhage in infants born extremely preterm. *Archives of Disease in Childhood-Fetal and Neonatal Edition*, *106*(1), 4-8.

Janaillac, M., Beausoleil, T. P., Barrington, K. J., Raboisson, M. J., Karam, O., Dehaes, M., & Lapointe, A. (2018). Correlations between near-infrared spectroscopy, perfusion index, and cardiac outputs in extremely preterm infants in the first 72 h of life. *European Journal of Pediatrics*, *177*, 541-550.

Juul, S.E., Wood, T.R., Comstock, B.A., Perez, K., Gogcu, S., Puia-Dumitrescu, M., Berkelhamer, S., Heagerty, P.J., Ahmad, K.A., Baserga, M., & Bendel-Stenzel, E. (2022). Deaths in a modern cohort of extremely preterm infants from the preterm

erythropoietin neuroprotection trial. *JAMA Network Open*, *5*(2), e2146404-e2146404.

Kalteren, W. S., Verhagen, E. A., Mintzer, J. P., Bos, A. F., & Kooi, E. M. (2021). Anemia and red blood cell transfusions, cerebral oxygenation, brain injury and development, and neurodevelopmental outcome in preterm infants: a systematic review. *Frontiers in Pediatrics*, *9*, 644462.

Martini, S., Czosnyka, M., Smielewski, P., Iommi, M., Galletti, S., Vitali, F., Paoletti, V., Camela, F., Austin, T., & Corvaglia, L. (2022). Clinical determinants of cerebrovascular reactivity in very preterm infants during the transitional period. *Pediatric Research*, *92*(1), 135-141.

Matsushita, F. Y., Krebs, V. L. J., & de Carvalho, W. B. (2022). Identifying clinical phenotypes in extremely low birth weight infants—an unsupervised machine learning approach. *European Journal of Pediatrics*, 1-13.

Ng, I. H. X., Da Costa, C. S., Zeiler, F. A., Wong, F. Y., Smielewski, P., Czosnyka, M., & Austin, T. (2020). Burden of hypoxia and intraventricular haemorrhage in extremely preterm infants. *Archives of Disease in Childhood-Fetal and Neonatal Edition*, *105*(3), 242-247.

Noori, S., McCoy, M., Anderson, M. P., Ramji, F., & Seri, I. (2014). Changes in cardiac function and cerebral blood flow in relation to peri/intraventricular hemorrhage in extremely preterm infants. *The Journal of Pediatrics*, *164*(2), 264-270.

O'Leary, H., Gregas, M.C., Limperopoulos, C., Zaretskaya, I., Bassan, H., Soul, J.S., Di Salvo, D.N., & du Plessis, A.J. (2009). Elevated cerebral pressure passivity is associated with prematurity-related intracranial hemorrhage. *Pediatrics*, *124*(1), 302-309.

O'Toole, J. M., Dempsey, E. M., & Boylan, G. B. (2018, July). Extracting transients from cerebral oxygenation signals of preterm infants: a new singular-spectrum analysis method. In *2018 40th Annual International Conference of the IEEE Engineering in Medicine and Biology Society (EMBC)* 5882-5885. IEEE.

O'Toole, J. M., Kenosi, M., Finn, D., Boylan, G. B., & Dempsey, E. M. (2016, August). Features of cerebral oxygenation detects brain injury in premature infants. In *2016 38th Annual International Conference of the IEEE Engineering in Medicine and Biology Society (EMBC)* 3614-3617. IEEE.

Ouchi, E., Usuniwa, H., Nemoto, K., & Inagaki, T. (2022). Simultaneous measurement under resting-state of autonomic nervous activity and brain activity by near-infrared spectroscopy alone. *Infrared Physics & Technology*, *122*, 104065.

Pavlek, L. R., Mueller, C., Jebbia, M. R., Kielt, M. J., & Fathi, O. (2021). Near-infrared spectroscopy in extremely preterm infants. *Frontiers in Pediatrics*, *8*, 624113.

Payne, A.H., Hintz, S.R., Hibbs, A.M., Walsh, M.C., Vohr, B.R., Bann, C.M., Wilson-Costello, D.E., & Eunice Kennedy Shriver National Institute of Child Health and Human Development Neonatal Research Network (2013). Neurodevelopmental outcomes of extremely low-gestational-age neonates with low-grade periventricular-intraventricular hemorrhage. *JAMA Pediatrics*, *167*(5), 451-459.

Plomgaard, A.M., Alderliesten, T., van Bel, F., Benders, M., Claris, O., Cordeiro, M., Dempsey, E., Fumagalli, M., Gluud, C., Hyttel-Sorensen, S., & Lemmers, P. (2019). No neurodevelopmental benefit of cerebral oximetry in the first randomised trial (SafeBoosC II) in preterm infants during the first days of life. *Acta Paediatrica*, *108*(2), 275-281.

Pritišanac, E., Urlesberger, B., Schwaberger, B., & Pichler, G. (2021). Accuracy of pulse oximetry in the presence of fetal hemoglobin—a systematic review. *Children*, *8*(5), 361.

Sankaran, V. G., & Orkin, S. H. (2013). The switch from fetal to adult hemoglobin. *Cold Spring Harbor Perspectives in Medicine*, *3*(1), a011643.

Siffel, C., Kistler, K. D., & Sarda, S. P. (2021). Global incidence of intraventricular hemorrhage among extremely preterm infants: a systematic literature review. *Journal of Perinatal Medicine*, *49*(9), 1017-1026.

Sullivan, B. A., Wallman-Stokes, A., Isler, J., Sahni, R., Moorman, J. R., Fairchild, K. D., & Lake, D. E. (2018). Early pulse oximetry data improves prediction of death and adverse outcomes in a two-center cohort of very low birth weight infants. *American Journal of Perinatology*, *35*(13), 1331-1338.

Suppan, E., Pichler, G., Binder-Heschl, C., Schwaberger, B., & Urlesberger, B. (2022). Three physiological components that influence regional cerebral tissue oxygen saturation. *Frontiers in Pediatrics*, *10*, 913223.

Sweet, D., Bevilacqua, G., Carnielli, V., Greisen, G., Plavka, R., Didrik, S.O., Simeoni, U., Speer, C.P., Soler, A., Valls, I., & Halliday, H. (2008). European consensus guidelines on

the management of neonatal respiratory distress syndrome. *Zhonghua er ke za zhi= Chinese journal of pediatrics*, *46*(1), 30-34.

The American Academy of Pediatrics and the American College of Obstetricians and Gynecologists (2007). Guidelines for Perinatal Care. *American Academy of Pediatrics: Elk Grove Village, IL, USA*.

Van Bel, F., Lemmers, P., & Naulaers, G. (2008). Monitoring neonatal regional cerebral oxygen saturation in clinical practice: value and pitfalls. *Neonatology*, *94*(4), 237-244.

Verhagen, E. A., Van Braeckel, K. N., van der Veere, C. N., Groen, H., Dijk, P. H., Hulzebos, C. V., & Bos, A. F. (2015). Cerebral oxygenation is associated with neurodevelopmental outcome of preterm children at age 2 to 3 years. *Developmental Medicine & Child Neurology*, *57*(5), 449-455.

Vesoulis, Z.A., Bank, R.L., Lake, D., Wallman-Stokes, A., Sahni, R., Moorman, J.R., Isler, J.R., Fairchild, K.D., & Mathur, A.M. (2019). Early hypoxemia burden is strongly associated with severe intracranial hemorrhage in preterm infants. *Journal of Perinatology*, *39*(1), 48-53.

Volpe, J.J. (2008). Neurology of the Newborn, 5th ed.; Saunders Elsevier: Philadelphia, PA, USA.

Zanelli, S. A., Abubakar, M., Andris, R., Patwardhan, K., Fairchild, K. D., & Vesoulis, Z. A. (2023). Early vital sign differences in very low birth weight infants with severe intraventricular hemorrhage. *American journal of perinatology*, *40*(11), 1193-1201.

3.7. Machine Learning Models Using NIRS and Clinical Data Predicts Two-year Neurodevelopmental Outcomes in Infants Born Extremely Preterm

3.7.1. Abstract:

Adverse short- and long-term neurodevelopmental outcomes are the primary concerns in extremely preterm infants. While short-term outcomes provide clinically useful information, radiological assessments at early time points have limitations. Due to the rapid growth, development, and repair that occur during infancy, long-term follow-up outcomes are far more impactful. In a follow-up study, we aimed to explore if $rcSO_2$ signal features could predict adverse neurodevelopmental outcomes at two years of age. Of the 46 infants initially studied in the HIP trial, 30 were followed up at two years, and neurodevelopmental outcome was assessed using the Bayley Scales of Infant and Toddler Development—Third Edition (Bayley-III). In this study, machine learning models were developed using features extracted from NIRS signals during the first 72 hours of life to predict two-year neurodevelopmental outcomes. Our findings indicate that models based on $rcSO_2$ features and clinical data could predict adverse language, motor and adaptive behaviour outcomes in this population (AUC = 0.818, 95% CI = 0.556-1.000; AUC = 0.787, 95% CI = 0.625-0.929; AUC = 0.781, CI = 0.545 - 0.973, respectively). These findings suggest that certain features in NIRS signals can predict adverse neurodevelopmental outcomes at two years of age. However, further studies with larger populations and greater statistical power are necessary to validate these results.

3.7.2. Introduction

Survival rates in the preterm population, particularly among extremely preterm infants, are improving, yet long-term neurodevelopmental challenges remain a major concern (Cheong et al., 2017; Bulbul et al., 2020).

Hypotension is a common issue in extremely preterm infants, and inotrope therapy is the typical approach for treatment. However, there are concerns that inotrope therapy may be associated with a higher prevalence of intraventricular haemorrhage (IVH) and poor long-term outcomes (Batton et al., 2009; Faust et al., 2015; Batton et al., 2016). IVH is associated with the apoptosis of precursor oligodendrocyte cells (Ballabh & de Vries, 2021). Oligodendrocytes are responsible for myelination in the developing brain, the lack of which leads to neuronal deficits disrupting neural communication. This leads to both motor and cognitive deficits in the long-term (Kuo & Huang, 2021; Ballabh & de Vries, 2021). Additionally, periventricular leukomalacia (PVL), characterised by white matter loss around the ventricles, is frequently observed in preterm infants with IVH, and which is also associated with poor long-term outcomes (Shooman et al., 2009; Robinson, 2012; Ballabh & de Vries, 2021).

The combination of the loss of oligodendrocytes, impaired myelination, and white matter injury sets the stage for long-term neurodevelopmental impairments. Infants that have experienced significant IVH are at a high risk of developing cerebral palsy, which is characterised by motor deficits such as spasticity, weakness, and impaired coordination (Inder et al., 2023). Additionally, the disruption of normal brain development affects cognitive functions, leading to difficulties with learning,

memory, attention, and executive functions as the child grows (Doyle & Anderson, 2010).

The Bayley-III is a standardised assessment tool used to evaluate the neurodevelopmental outcomes of infants and young children, typically between 1 month and 42 months of age (Bayley, 2006). The test is designed to measure various aspects of development, including cognitive, language, motor, social-emotional, and adaptive behaviour skills.

In section 3.5. we reported that by utilising $rcSO_2$ signal features we could predict adverse short-term outcome defined as death or IVH level III-IV confirmed by cranial ultrasound. Yet, if features of cerebral oxygenation during the first days of life can be utilised to predict two-year neurodevelopmental outcomes, this would potentially extend the utility of advanced $rcSO_2$ signal analysis and machine learning approaches. Therefore, the aim of this study was to explore if $rcSO_2$ signal features could predict adverse neurodevelopmental outcomes at two-years of age.

3.7.3. Methods

Study Design and Participants

Out of the 46 infants initially examined in HIP trial, as detailed in section 3.3.1, 30 infants were followed up at two years of age by a registered paediatric physiotherapist at University College Cork. The neurodevelopmental outcomes were evaluated using the Bayley-III (Figure 3. 2).

Long-term Neurodevelopmental Outcomes

The Bayley Scales of Infant and Toddler Development—Third Edition3 (Bayley-III) was utilised as an assessment tool for long-term outcomes of infants enrolled in the HIP trial (Dempsey et al., 2021). The primary outcome was neurodevelopmental status, categorised as a binary variable; if any of the subscales were classified as abnormal, the overall outcome was considered abnormal. Additionally, the subscales of the neurodevelopmental outcomes were analysed individually, each serving as the outcome in separate models.

NIRS

We utilised the same signal features from the HIP trial, including $rcSO_2$, filtered $rcSO_2$, and PRDs extracted from $rcSO_2$, described in section 3.3.5 for this study.

Clinical Features at Birth

A combination of clinical data (explained in detail in 3.3.2) including sex, hypotension, use of inotropes, the presence of chorioamnionitis in utero, birth weight (g), head circumference (cm), Apgar scores at 5 minutes of life and gestational age (GA, days) was analysed to assess their ability to predict long-term adverse outcomes both independently and in combination with $rcSO_2$ components.

Machine Learning

As explained in detail in 3.3.6, XGBoost models were developed using features extracted from $rcSO_2$ components. The hyperparameters for these models were consistent with those used in the machine learning model from the HIP study. Both overall outcomes and subcategory labels were utilised for training and testing the models.

3.7.4. Results

The HIP trial was designed to assess the impact of different management strategies for hypotension in extremely low gestational age newborns, including the use of dopamine versus a restrictive approach, and collected neurodevelopmental outcomes to determine the effect on survival without neurodevelopmental disability at 2 years of age (Dempsey et al., 2014; Demsey et al., 2021).

Of the 46 infants enrolled in the HIP trial, only 30 were followed up for recording of neurodevelopmental outcomes. Of these 30 assessments, data for the social-emotional subscale were available for 28 infants, and data for adaptive behaviour were available for 26 infants.

We report that machine learning (XGBoost) models based on $rcSO_2$ features, with and without PRDs, in combination with clinical data, were predictive of the language and motor subscales (AUC = 0.818, 95% CI = 0.556 - 1.000, and AUC = 0.787, 95% CI = 0.625 -0 929). Additionally, the model that combined $rcSO_2$ PRDs with clinical data was predictive of adaptive behaviour (AUC = 0.781, 95% CI = 0.545 - 0.973). Neither the clinical data nor the features extracted from $rcSO_2$ signals alone were able to predict adverse neurodevelopmental outcomes (Table 3. 4).

Table 3. 4. Area under the curve (AUC) values for the models based on $rcSO_2$ signal features used to predict long-term neurodevelopmental outcome at two years of age.

	Overall outcome (n = 26)	**Cognition (n = 30)**	**Language (n = 30)**	**Motor (n = 30)**	**Social emotional scale (n = 28)**	**Adaptive behaviour (n = 26)**
Clinical feature	AUC = 0.580 (0.349 - 0.788)	AUC = 0.37 (0.169 - 0.591)	AUC = 0.588 (0.329 - 0.815)	AUC = 0.697 (0.489 - 0.899)	AUC = 0.257 (0.082 - 0.468)	AUC = 0.375 (0.178 - 0.615)
$rcSO_2$	AUC = 0.625 (0.407 - 0.829)	AUC = 0.625 (0.382 - 0.867)	AUC = 0.435 (0.174 - 0.718)	AUC = 0.547 (0.313 - 0.787)	AUC = 0.438 (0.226 - 0.667)	AUC = 0.394 (0.179 - 0.643)
$rcSO_2$ + Clinical features	AUC = 0.607 (0.384 - 0.832)	AUC = 0.685 (0.448 - 0.902)	***AUC = 0.818 * (0.571 - 1.000)***	***AUC = 0.760 * (0.548 - 0.935)***	AUC = 0.438 (0.214 - 0.672)	AUC = 0.294 (0.082 - 0.534)
Filtered $rcSO_2$	AUC = 0.567 (0.316 - 0.790)	AUC = 0.645 (0.404 - 0.864)	AUC = 0.469 (0.223 - 0.716)	AUC = 0.502 (0.276 -0.730)	AUC = 0.444 (0.239 - 0.659)	AUC = 0.387 (0.168 - 0.650)
Filtered $rcSO_2$ + Clinical features	AUC = 0.6295 (0.415 - 0.849)	AUC = 0.705 (0.490 - 0.911)	***AUC = 0.818 * (0.556 - 1.000)***	***AUC = 0.787 * (0.625 -0 929)***	AUC = 0.454 (0.245 - 0.684)	AUC = 0.344 (0.131 - 0.596)
$rcSO_2$ PRD	AUC = 0.495 (0.268 - 0.716)	AUC = 0.665 (0.433 - 0.888)	AUC = 0.550 (0.285 - 0.799)	AUC = 0.615 (0.380 - 0.839)	AUC = 0.454 (0.224 - 0.683)	AUC = 0.656 (0.407 - 0.870)
$rcSO_2$ PRD + Clinical features	AUC = 0.509 (0.293 - 0.741)	AUC = 0.615 (0.346 - 0.869)	AUC = 0.450 (0.199 - 0.707)	AUC = 0.597 (0.361 - 0.826)	AUC = 0.658 (0.421 - 0.893)	***AUC = 0.781 * (0.545 - 0.973)***

3.7.5. Discussion

Hypotension resulting from prematurity, along with IVH, PVH, and associated white matter injury and hypoxia, can significantly elevate the risk of long-term adverse outcomes in preterm infants (Shooman et al., 2009; Robinson, 2012; Ballabh & de Vries, 2021). Early prediction of these potential long-term injuries within the first days of life can assist clinicians and families in tailoring interventions and treatments more effectively, ensuring that they are as targeted and beneficial as possible.

This study highlighted the significant role of clinical data in enhancing the predictive power of models for long-term adverse outcomes, particularly when combined with features extracted from NIRS data. While clinical data were not sufficient to predict long-term outcomes, their integration with NIRS-derived features provided a more comprehensive understanding of brain health. This study reveals that oxygen dysregulation in early life is associated with poor developmental outcomes even at two-years. This underscores the importance of early monitoring of physiological signals, and cerebral oxygenation in particular, in the first days of life, offering valuable insights into brain function.

Machine learning models, developed from features extracted from NIRS signals within the first 72 hours of life, showed potential for predicting adverse outcomes in language, motor skills, and adaptive behaviour, offering valuable opportunities for early intervention strategies. However, social-emotional outcome was not predicted by features extracted from NIRS signals. One reason might be that the social-emotional factor is likely influenced by a multitude of factors that are not captured through $rcSO_2$ signals alone. Social-emotional outcomes depend on environmental,

psychological, and socio-interactive factors (Malik & Marwaha, 2018). These elements might not be directly related to physiological data, and therefore the predictive power of $rcSO_2$ signals on such outcomes is likely to be limited.

It is important to note that neurodevelopmental outcomes were available for only 30 infants, with only 28 having data for the social-emotional scale and 26 for adaptive behaviour. These sample sizes are quite limited for machine learning models, and the results should be interpreted with caution. Future studies should focus on larger sample sizes and incorporate more comprehensive brain imaging techniques, such as MRI.

3.7.6. References

Ballabh, P., & de Vries, L.S. (2021). White matter injury in infants with intraventricular haemorrhage: mechanisms and therapies. *Nature Reviews Neurology*, *17*(4), 199-214.

Batton, B., Li, L., Newman, N.S., Das, A., Watterberg, K.L., Yoder, B.A., Faix, R.G., Laughon, M.M., Stoll, B.J., Higgins, R.D., & Walsh, M.C. (2016). Early blood pressure, antihypotensive therapy and outcomes at 18–22 months' corrected age in extremely preterm infants. *Archives of Disease in Childhood-Fetal and Neonatal Edition*, *101*(3), F201-F206.

Batton, B., Zhu, X., Fanaroff, J., Kirchner, H. L., Berlin, S., Wilson-Costello, D., & Walsh, M. (2009). Blood pressure, anti-hypotensive therapy, and neurodevelopment in extremely preterm infants. *The Journal of Pediatrics*, *154*(3), 351-357.

Bayley, N. (2006). Bayley scales of infant and toddler development. PsychCorp. *San Antonio TX*.

Bolisetty, S., Dhawan, A., Abdel-Latif, M., Bajuk, B., Stack, J., Oei, J.L., Lui, K., & New South Wales and Australian Capital Territory Neonatal Intensive Care Units' Data Collection (2014). Intraventricular hemorrhage and neurodevelopmental outcomes in extreme preterm infants. *Pediatrics*, *133*(1), 55-62.

Bulbul, L., Elitok, G.K., Ayyıldız, E., Kabakcı, D., Uslu, S., Köse, G., Tiryaki Demir, S., & Bulbul, A. (2020). Neuromotor Development Evaluation of Preterm Babies Less than 34 Weeks of Gestation with Bayley III at 18-24 Months. *BioMed Research International*, *2020*(1), p.5480450.

Cheong, J.L., Doyle, L.W., Burnett, A.C., Lee, K.J., Walsh, J.M., Potter, C.R., Treyvaud, K., Thompson, D.K., Olsen, J.E., Anderson, P.J., & Spittle, A.J. (2017). Association between moderate and late preterm birth and neurodevelopment and social-emotional development at age 2 years. *JAMA Pediatrics*, *171*(4), e164805-e164805.

Dempsey, E.M., Barrington, K.J., Marlow, N., O'Donnell, C.P.F., Miletin, J., Naulaers, G., Cheung, P.Y., Corcoran, J.D., El-Khuffash, A.F., Boylan, G.B., & Livingstone, V. (2021). Hypotension in Preterm Infants (HIP) randomised trial. *Archives of Disease in Childhood-Fetal and Neonatal Edition*, *106*(4), 398-403.

Dempsey, E.M., Barrington, K.J., Marlow, N., O'donnell, C.P., Miletin, J., Naulaers, G., Cheung, P.Y., Corcoran, D., Pons, G., Stranak, Z., & Van Laere, D. (2014). Management of hypotension in preterm infants (The HIP Trial): a randomised controlled trial of hypotension management in extremely low gestational age newborns. *Neonatology*, *105*(4), 275-281.

Doyle, L. W., & Anderson, P. J. (2010). Adult outcome of extremely preterm infants. *Pediatrics*, *126*(2), 342-351.

Faust, K., Härtel, C., Preuß, M., Rabe, H., Roll, C., Emeis, M., Wieg, C., Szabo, M., Herting, E., & Göpel, W. (2015). Short-term outcome of very-low-birthweight infants with arterial hypotension in the first 24 h of life. *Archives of Disease in Childhood-Fetal and Neonatal Edition*, *100*(5), F388-F392.

Inder, T. E., Volpe, J. J., & Anderson, P. J. (2023). Defining the neurologic consequences of preterm birth. *New England Journal of Medicine*, *389*(5), 441-453.

Kuo, L.T., &Huang, A.P.H. (2021). The pathogenesis of hydrocephalus following aneurysmal subarachnoid hemorrhage. *International Journal of Molecular Sciences*, *22*(9), p.5050.

Malik, F., & Marwaha, R. (2018). Developmental stages of social emotional development in children. *In StatPearls*.

Robinson, S. (2012). Neonatal posthaemorrhagic hydrocephalus from prematurity: pathophysiology and current treatment concepts: a review. *Journal of Neurosurgery: Pediatrics*, *9*(3), 242-258.

Shooman, D., Portess, H., & Sparrow, O. (2009). A review of the current treatment methods for posthaemorrhagic hydrocephalus of infants. *Cerebrospinal Fluid Research*, *6*(1), 1-15.

3.8. Blood Pressure and EEG

3.8.1. Abstract

Hypotension is an ongoing clinical concern in preterm infants, as it has been associated with adverse short- and long-term consequences. We sought to examine the trend of blood pressure in the first days of life and investigate the relationship between quantitative electroencephalography (EEG) characteristics and mean arterial blood pressure (MABP) in extremely preterm infants. We analysed a subset of infants enrolled in the Management of Hypotension in Preterm infants (HIP) trial (n = 28), of which all were <28 weeks of gestational age (GA). For each infant we examined one hour of EEG records at 6-hour intervals and documented MABP for the first 60 hours of life. The EEG signals were pre-processed, first automatically using a MATLAB code, and then screened manually by a neonatal EEG expert for artefacts. Quantitative features were extracted from the EEG signals using previously published methods. Changes in MABP over time were analysed by repeated measures analysis of variance (rANOVA) examining two factors: GA (<26 or >26 weeks), and if they were hypotensive or normotensive. Putative correlations between EEG features and MABP were assessed using partial correlation adjusting for GA. MABP increased in the first hours of life (p= 0.02). We demonstrated weak but significant correlations between MABP and EEG quantitative features after adjusting for GA. Amplitude kurtosis in all bandwidths, inter-burst interval (IBI) length and IBI number were negatively correlated with MABP, while range EEG in all bandwidths and IBI burst percentage were positively correlated with MABP.

In conclusion, we identified a correlation between MABP and a number of quantitative EEG features in extremely preterm infants, independent of gestational age, suggesting MABP may be an important biomarker of brain activity.

3.8.2. Introduction

Hypotension is frequently identified and treated in extremely preterm infants. However, there is significant variation in clinical practices of how this is achieved (Dempsey & Barrington, 2006; Laughon et al., 2007). Although statistical associations have been found between hypotension and negative short- and long-term outcomes, a systematic review of the literature was unable to establish clear criteria for defining hypotension (Dempsey & Barrington, 2007).

One of the major concerns regarding low blood pressure in infants born preterm is the risk of clinically significant hypoperfusion (Goldsmith & Keels, 2022). Despite reduced systemic vascular resistance arising from immature sympathetic control, these infants can have regular systemic blood flow, and sufficient oxygen delivery to their tissues (Groves et al., 2008; Victor et al., 2006). Careful monitoring of these infants without pharmacological intervention (known as 'permissive hypotension') may be a suitable approach rather than resorting to using medication (Dempsey et al., 2009). Treatment of hypotension in preterm infants may not only be of no benefit but could also potentially be harmful and have negative effects including fluctuations in blood pressure that could contribute to the rupturing of fragile blood vessels. A study by the Canadian Neonatal Network revealed that interventions for hypotension were linked to a rise in severe brain injury (Synnes et al., 2001). The typical course of treatment involves administering one or more fluid boluses followed by dopamine (Subhedar, 2003). Observational data has indicated a connection between the administration of fluid boluses and intracranial bleeding (Goldberg et al., 1980). Additionally, dopamine increases blood pressure in infants mainly by inducing

vasoconstriction, which could lead to a decrease in overall systemic perfusion (Zhang et al., 1999; Osborn et al., 2002).

At present, there is no universally validated clinical scoring method for diagnosing shock or insufficient systemic perfusion in premature infants. The evaluation of the sufficiency of blood flow to vital organs is primarily based on subjective assessment. Clinical examinations involve evaluating capillary refill time, skin tone, body temperature, and urine output. Capillary refill time values have been determined for full-term newborns (Raju et al., 1999), but data for preterm infants are scarce (Wodey et al., 1998; Osborn et al., 2004). While the accuracy of each separate measure in predicting poor perfusion is not high, combining multiple signs seems to enhance the ability to identify patients with a greater risk of adverse outcomes (Dempsey et al., 2009). Echocardiography is one of the primary non-invasive, yet non-continuous measures of cardiac output in the preterm infant. Alternative methods such as transcranial doppler are not commonly used due to limitations of the method (Murphy et al., 2023).

Physiological function of neuronal networks requires a continuous supply of energy and oxygen and relies upon adequate delivery of these resources via blood flow to meet local demands (Watts et al., 2018). The electrical activity of the brain can be measured using EEG and in neonatal intensive care units it is used to monitor critically ill infants. EEG is a non-invasive and portable technology that allows for the continuous assessment of cortical function at the cot side, with minimal interruption to standard clinical care (Pavlidis et al., 2017). However, the correlation between mean arterial blood pressure and EEG activity in preterm infants has not yet been

investigated, and new insights could potentially aid the decision making around treating preterm infants with low blood pressure. The objective of this study was therefore to examine if specific quantitative EEG features were associated with mean arterial blood pressure.

3.8.3. Methods

Study Design and Participants

This research analysed data from a multicentre clinical trial, The Management of Hypotension in Preterm Infants (HIP, Trial registration number NCT01482559, EudraCT 2010-023988-17) (Dempsey et al., 2021). This study was approved by the Clinical Research Ethics Committee, Cork, ECM 5(2) 15 January 2013. Written informed consent was obtained from the parents of all participating infants, in accordance with the ethical standards set by the Clinical Research Ethics Committee, UCC and the principles of the Declaration of Helsinki (World Medical Association, 2013). The HIP trial compared the standard management using dopamine and a more conservative treatment strategy. In this approach, known as permissive hypotension, hypotensive infants are not given intervention if they display signs of adequate clinical perfusion. They are carefully monitored, and intervention is only initiated if clinical assessment indicates reduced perfusion. The two interventions being compared were saline bolus followed by dopamine versus saline bolus followed by placebo (Dempsey et al., 2021). The study recruited extremely preterm infants between February 2015 and September 2017 at Cork University Maternity Hospital (Figure 3. 2).

EEG

A subset of infants (n = 49) participating in the HIP trial had coincident continuous multi-channel EEG to determine the effects of mean BP on cerebral electrical activity and to assess end-organ perfusion (Dempsey et al., 2014). EEG was recorded for the first 72 hours of life. Disposable electrodes were positioned on the central (C3 and

C4) and frontal (F3 and F4) areas as well as reference electrodes (Fz) and a ground electrode placed behind the left ear in accordance with international 10:20 system of electrode configuration. 1-hour epochs at 6-hour intervals were extracted using the Nicolet EEG viewer software. Two subgroups were assessed: ≤25 weeks + 6days of GA or ≥26 weeks. The threshold was based on previously published data (O'Toole et al., 2016). The <26 weeks EEG is markedly different from an EEG in an infant >26 weeks, primarily due to the rapid maturation of the brain and the development of neural circuits and so the quantitative features differ greatly (O'Toole et al., 2016). These differences include the emergence of more consistent background activity, the appearance of more synchronised waveforms, and the development of sleep-state differentiation (O'Toole et al., 2016).

Signal Processing

The unprocessed EEG data underwent pre-processing including artefact removal using NEURAL package (Neonatal Eeg featURe set in mAtLab; https://github.com/otoolej/qEEG_feature_set) followed by bandpass filtering and down-sampling (O'Toole & Boylan, 2017). The process of artefact removal specifically targeted significant artefacts like improper electrode placement, electrode coupling, electrode impedance, sudden jumps in amplitudes or large-amplitude segments caused by movement. After removing artefacts, a bandpass filter ranging from 0.5 to 30 Hz was utilised to eliminate both low- and high-frequency artefacts, followed by down-sampling to 64 Hz (O'Toole & Boylan, 2017). EEG signals were screened manually by neonatal neuro physiologist Prof. Geraldine Boylan, and the epochs with unacceptable quality were removed. The high-quality EEG signals were separated into four distinct bandwidth frequencies: [0.5 – 3; 3 – 8; 8 – 15; 15 – 30] Hz.

Feature Extraction

Quantitative characteristics from the EEG signals were extracted using the NEURAL package (O'Toole & Boylan, 2017). Utilising the bipolar arrangement of the EEG (F3 – C3 & F4 – C4) amplitude, frequency, and connectivity features were evaluated within brief time intervals using a shifting window of 64 seconds with 50% overlap. Subsequently, the median value was utilised to summarise these attributes across all intervals. Inter-burst intervals were evaluated individually for each channel before summarisation using the median value across all channels. For each 1-hour EEG epoch, 50 features were obtained (Table 3. 5).

Table 3. 5. The features extracted from EEG signals

Feature category	Feature
Amplitude	Amplitude kurtosis
	Amplitude skewness
	rEEG median
	rEEG lower margin (5th percentile)
	rEEG upper margin (95th percentile)
	rEEG asymmetry (measure of skew about median)
Frequency	Spectral power
	Spectral relative power (normalised to total spectral power)
	Spectral flatness
	Spectral difference: difference between consecutive spectral estimates
	Spectral edge frequency: 95% of spectral power contained between 0.5 and cut-off frequency *
	Fractal dimension *
Connectivity	Coherence mean value
Inter-burst interval	95% inter-burst interval *
	Median inter-burst interval *
	Burst percentage *
	Number of bursts *

Features were estimated for each epoch before being decomposed into frequency bandwidths*

Mean Arterial Blood Pressure (MABP)

Mean arterial blood pressure (MABP) was monitored continuously using an umbilical arterial catheter in infants with hypotension that were randomised to one of two therapeutic strategies. Hypotension was defined as a mean blood pressure 1 mm Hg or more below a mean blood pressure value equivalent to the GA in completed weeks, which persisted over a 15-min period (Dempsey et al., 2014). MABP measurements were recorded and saved only once every hour. For consistency with EEG recording, we used MABP measurements taken every 6 hours. Normotensive

patients recruited into the study but not randomised to any treatment arm were monitored either invasively or non-invasively. The MABP corresponding to the EEG epochs with 6-hour intervals were isolated for analysis.

Statistics

Changes in MABP over time were analysed by repeated measures one-way mixed model (rANOVA). Difference in MABP between factors GA (<26 or >26 weeks), and hypotension diagnosis (hypotensive or normotensive) was analysed by repeated measures two-way mixed model (rANOVA). Putative correlations between EEG features and MABP were assessed using partial correlation adjusting for GA. The statistical significance level (α) was set at 0.05 for all analyses. Strength of correlation was defined based on R value, which measures the strength and direction of a linear relationship between two variables, ranging from -1 to 1. A weak correlation typically has an R-value close to 0, indicating little to no linear relationship between the variables. This means that changes in one variable do not reliably predict changes in the other (Asuero et al., 2016).

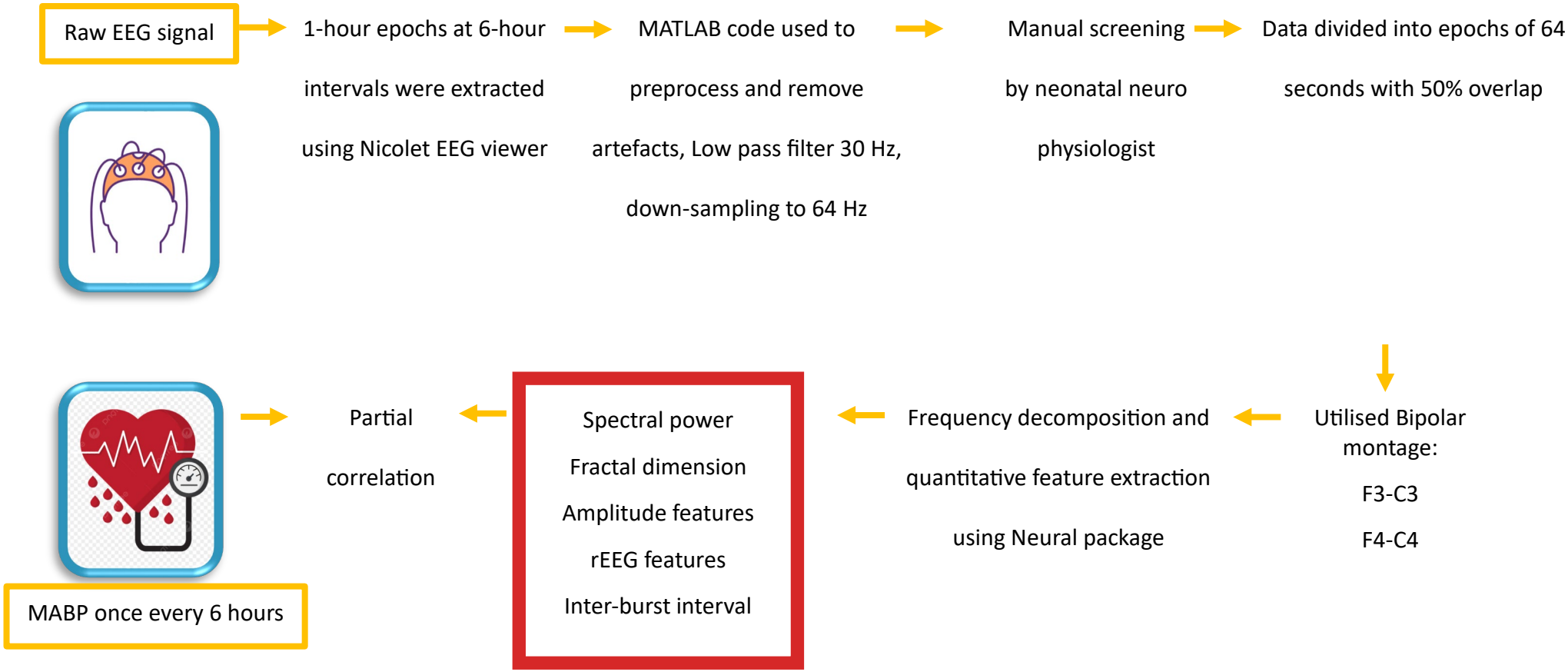

Figure 3.7. Summary of the workflow for EEG signal processing.

3.8.4. Results

Data Available

MABP and EEG were processed during the initial 60 hours of life in 28 infants who had EEG signals of acceptable quality and corresponding MABP recordings for analyses. These infants were categorised based on GA (≤25 weeks + 6days of GA or ≥26 weeks), and blood pressure status (hypotensive or normotensive), as outlined in *Table 3. 6*. The average duration of recorded EEG was 57.06 hours.

Table 3. 6. Number of infants in each group

	<26 weeks	≥26 weeks
Normotensive	n = 6	n = 12
Hypotensive	n = 8	n = 2

Mean Arterial Blood Pressure

The repeated measure ANOVA model of MABP over time revealed a significant increase in MABP during the first hours of life (p-value = 0.02) (Figure 3. 5).

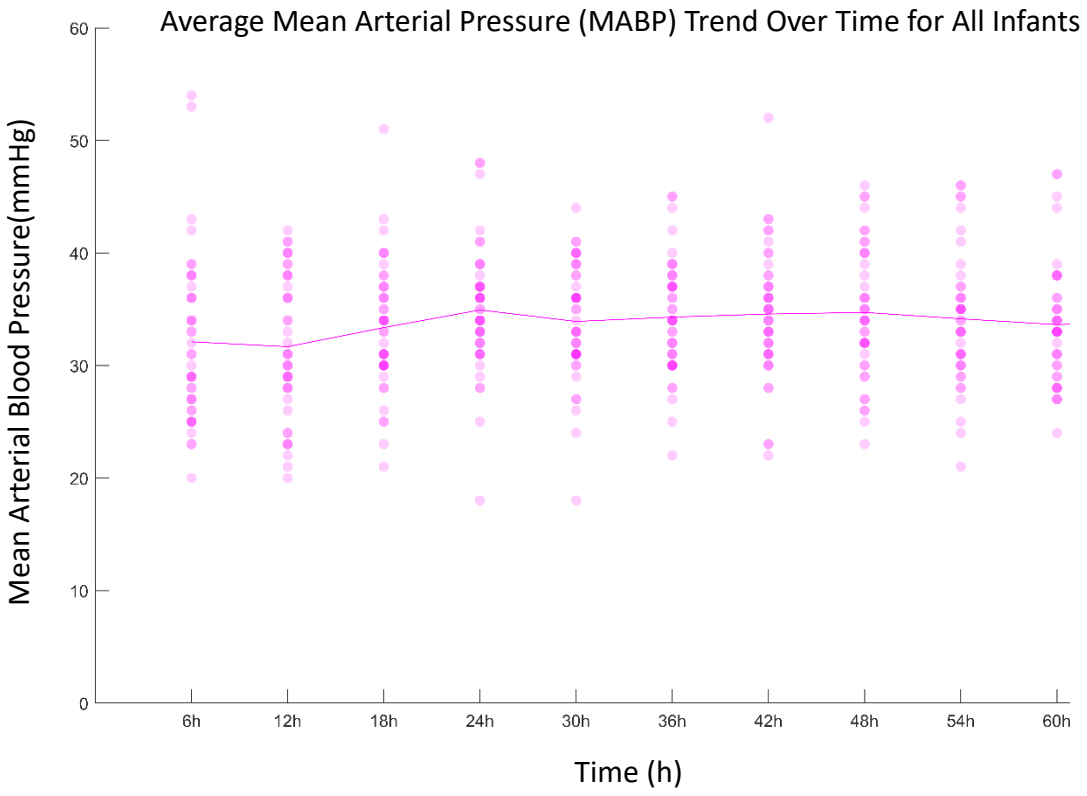

Figure 3. 8. Average of Mean arterial Blood Pressure (MABP) trend over time for all infants (n = 28)

There was no significant difference in MABP between hypotensive infants (treated/untreated) and normotensive infants, born <26 weeks' GA or ≥ 26 weeks of GA over their first 60 hours post-partum (GA p = 0.84, Hypotension p = 0.55, GA x Hypotension p = 0.70).

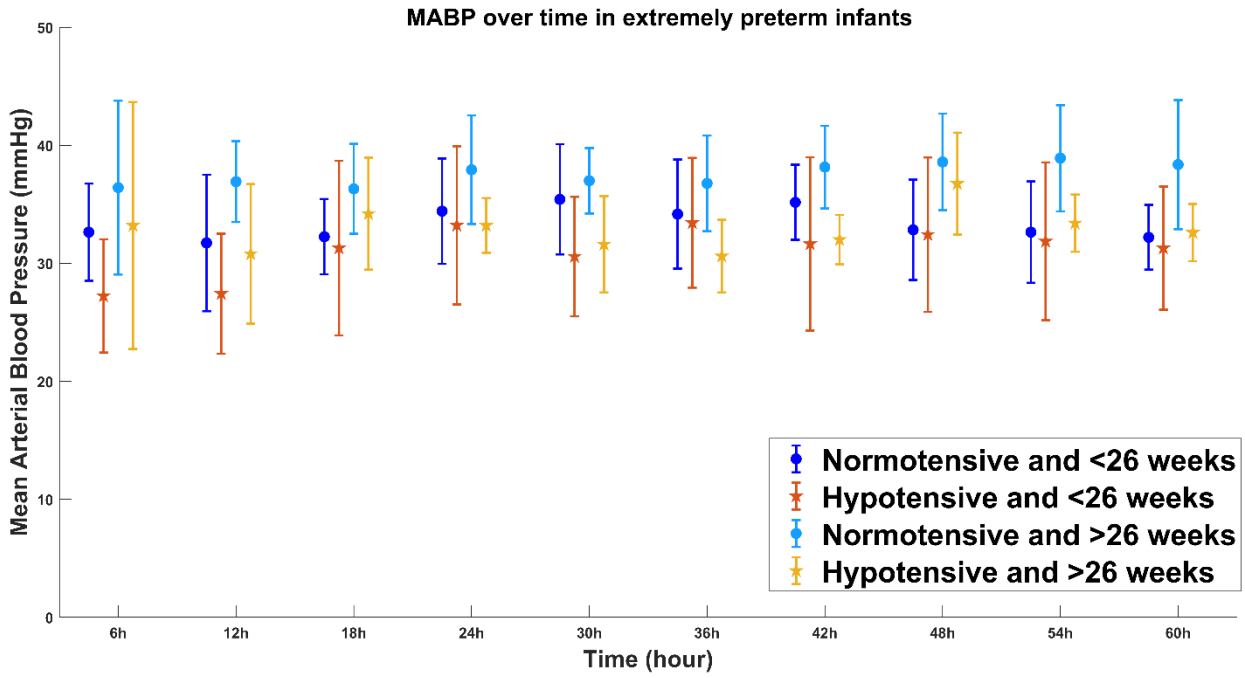

Figure 3. 9. Mean ± SD MABP over time for four distinct groups: Normotensive <26weeks' GA, Normotensive <26 weeks' GA, for Hypotensive ≥26weeks' GA, Hypotensive ≥26 weeks' GA.

Correlation Between MABP and EEG Features

There were weak but significant correlations between MABP and EEG quantitative features, after adjusting for GA. Amplitude kurtosis in all bandwidths, inter-burst interval (IBI) length and IBI number were negatively correlated with MABP, while range EEG in all bandwidths and IBI burst percentage were positively correlated with

MABP (Table 3. 7). The correlation between MABP and other EEG features not mentioned here was not significant.

Table 3. 7. Partial correlation between MABP and EEG quantitative features and corresponding p values

EEG features	Bandwidth frequency	R	p value
Amplitude kurtosis	0.5 – 4	-0.22	$p < 0.001$
	4 – 7	-0.20	$p < 0.001$
	7 – 13	-0.21	$p < 0.001$
	13 – 30	-0.17	0.004
rEEG median	0.5 – 4	0.19	0.001
	4 – 7	0.14	0.02
	7 – 13	0.13	0.02
	13 – 30	0.12	0.046
IBI length median	----	-0.15	0.01
IBI burst percentage	----	0.16	0.007
IBI burst number	----	-0.16	0.006

3.8.5. Discussion

This study aimed to explore the changes of MABP over time in extremely preterm infants and explore the potential correlation between EEG signals recorded within the first 60 hours after birth and MABP.

We observed that the average MABP among infants increased over time. This is consistent with previous studies, that found a significant elevation in blood pressure in the first 48 hours of life in preterm infants with birth weight ≤ 1500 g (Bada et al., 1990). Furthermore, Kent et al. (2007) proposed that MABP increased between day 1 and day 2 of life in healthy term neonates. They also suggested that premature infants achieved blood pressure stabilisation after two weeks of life, and at that point, their blood pressure was similar to that of full-term infants (Kent et al., 2009). These findings may highlight the importance of permissive hypotension, as blood pressure increases in the first days of life when left untreated. However, some infants in the current cohort received dopamine treatment, and it is still unclear whether the increase in their blood pressure was caused by intervention or occurred naturally.

The cohort of preterm infants diagnosed with hypotension did not have significantly different MABP compared to those classified as normotensive regardless of GA. This may reflect adequate clinical treatment of hypotension or suggest that those healthy patients with low blood pressure can quickly improve blood pressure status over the first days of life.

We identified a weak correlation between MABP and several quantitative EEG features in extremely preterm infants, independent of gestational age, suggesting MABP could be a biomarker of brain activity. Some of these correlations were

negative whilst others were positive but were sensitive to blood pressure/ cerebral perfusion pressure.

Out of the initial sample of n = 49 participants with EEG recordings, only n = 28 EEG recordings met the criteria for acceptable quality and were therefore included in further analyses. A clear limitation of this study was the sample size; a significant proportion of participants were excluded due to a high percentage of artefacts or data recorded with quality issues in some channels, though not uniformly across all channels. Future studies would benefit from considering the implications of the study design when framing the secondary objectives of the study. EEG changes with gestational age and subgroup analysis is required when examining features. Also, particular attention is required when there is prolonged EEG monitoring and collection to ensure higher quality recordings from infants. The current study is subject to several limitations. Firstly, the relatively low number of participants reduced the statistical power, particularly as participants were further divided into subgroups based on gestational age and diagnosis of hypotension, leading to smaller sample sizes within each group. This was primarily due to low recruitment within the trial attributed to the strict inclusion criteria (Dempsey et al., 2014). Additionally, the randomisation of the hypotension group and subsequent treatment with either dopamine or placebo introduced variability that made it challenging to account for the potential impact of treatment method on changes in MABP. Moreover, the data collected for MABP, and 1-hour epoch EEGs were analysed at 6-hour intervals, which may not fully capture dynamic changes over shorter time frames. Continuous monitoring of these biomarkers could offer clinicians valuable insights into defining MABP patterns and customising individualised treatment strategies.

3.8.6. References

Asuero, A.G., Sayago, A., & González, A.G. (2006). The correlation coefficient: An overview. *Critical Reviews in Analytical Chemistry*, *36*(1), 41-59.

Bada, H.S., Korones, S.B., Perry, E.H., Arheart, K.L., Ray, J.D., Pourcyrous, M., Magill, H.L., Runyan III, W., Somes, G.W., Clark, F.C., & Tullis, K.V. (1990). Mean arterial blood pressure changes in premature infants and those at risk for intraventricular hemorrhage. *The Journal of Pediatrics*, *117*(4), 607-614.

Dempsey, E. M., & Barrington, K. J. (2006). Diagnostic criteria and therapeutic interventions for the hypotensive very low birth weight infant. *Journal of Perinatology*, *26*(11), 677-681.

Dempsey, E. M., & Barrington, K. J. (2007). Treating hypotension in the preterm infant: when and with what: a critical and systematic review. *Journal of Perinatology*, *27*(8), 469-478.

Dempsey, E.M., Barrington, K.J., Marlow, N., O'donnell, C.P., Miletin, J., Naulaers, G., Cheung, P.Y., Corcoran, D., Pons, G., Stranak, Z., & Van Laere, D. (2014). Management of hypotension in preterm infants (The HIP Trial): a randomised controlled trial of hypotension management in extremely low gestational age newborns. *Neonatology*, *105*(4), 275-281.

Dempsey, E.M., Barrington, K.J., Marlow, N., O'Donnell, C.P.F., Miletin, J., Naulaers, G., Cheung, P.Y., Corcoran, J.D., El-Khuffash, A.F., Boylan, G.B., & Livingstone, V. (2021). Hypotension in Preterm Infants (HIP) randomised trial. *Archives of Disease in Childhood-Fetal and Neonatal Edition*, *106*(4), 398-403.

Dempsey, E. M., Al Hazzani, F., & Barrington, K. J. (2009). Permissive hypotension in the extremely low birthweight infant with signs of good perfusion. *Archives of Disease in Childhood-Fetal and Neonatal Edition*, *94*(4), F241-F244.

Goldberg, R. N., Chung, D., Goldman, S. L., & Bancalari, E. (1980). The association of rapid volume expansion and intraventricular haemorrhage in the preterm infant. *The Journal of paediatrics*, *96*(6), 1060-1063.

Goldsmith, J. P., & Keels, E. (2022). Recognition and management of cardiovascular insufficiency in the very low birth weight newborn. *Pediatrics*, *149*(3), e2021056051.

Groves, A. M., Kuschel, C. A., Knight, D. B., & Skinner, J. R. (2008). Relationship between blood pressure and blood flow in newborn preterm infants. *Archives of Disease in Childhood-Fetal and Neonatal Edition*, *93*(1), F29-F32.

Kent, A. L., Kecskes, Z., Shadbolt, B., & Falk, M. C. (2007). Normative blood pressure data in the early neonatal period. *Paediatric Nephrology*, *22*, 1335-1341.

Kent, A. L., Meskell, S., Falk, M. C., & Shadbolt, B. (2009). Normative blood pressure data in non-ventilated premature neonates from 28–36 weeks gestation. *Paediatric Nephrology*, *24*, 141-146.

Laughon, M., Bose, C., Allred, E., O'Shea, T.M., Marter, L.J.V., Bednarek, F., Leviton, A., & ELGAN Study Investigators (2007). Factors associated with treatment for hypotension in extremely low gestational age newborns during the first postnatal week. *Pediatrics*, *119*(2), 273-280.

Murphy, E., Healy, D. B., Chioma, R., & Dempsey, E. M. (2023). Evaluation of the hypotensive preterm infant: evidence-based practice at the bedside?. *Children*, *10*(3), 519.

Osborn, D., Evans, N., & Kluckow, M. (2002). Randomised trial of dobutamine versus dopamine in preterm infants with low systemic blood flow. *The Journal of Pediatrics*, *140*(2), 183-191.

Osborn, D. A., Evans, N., & Kluckow, M. (2004). Clinical detection of low upper body blood flow in very premature infants using blood pressure, capillary refill time, and central-peripheral temperature difference. *Archives of Disease in Childhood-Fetal and Neonatal Edition*, *89*(2), F168-F173.

O'Toole, J. M., & Boylan, G. B. (2017). NEURAL: quantitative features for newborn EEG using Matlab. *arXiv preprint arXiv:1704.05694*.

O'Toole, J. M., Boylan, G. B., Vanhatalo, S., & Stevenson, N. J. (2016). Estimating functional brain maturity in very and extremely preterm neonates using automated analysis of the electroencephalogram. *Clinical Neurophysiology*, *127*(8), 2910-2918.

Pavlidis, E., Lloyd, R. O., & Boylan, G. B. (2017). EEG-a valuable biomarker of brain injury in preterm infants. *Developmental Neuroscience*, *39*(1-4), 23-35.

Raju, N. V., Maisels, M. J., Kring, E., & Schwarz-Warner, L. (1999). Capillary refill time in the hands and feet of normal newborn infants. *Clinical Pediatrics*, *38*(3), 139-144.

Subhedar, N. V. (2003, December). Treatment of hypotension in newborns. In *Seminars in neonatology* (Vol. 8, No. 6, pp. 413-423). WB Saunders.

Synnes, A. R., Chien, L. Y., Peliowski, A., Baboolal, R., & Lee, S. K. (2001). Variations in intraventricular haemorrhage incidence rates among Canadian neonatal intensive care units. *The Journal of Pediatrics*, *138*(4), 525-531.

Victor, S., Appleton, R. E., Beirne, M., Marson, A. G., & Weindling, A. M. (2006). The relationship between cardiac output, cerebral electrical activity, cerebral fractional oxygen extraction and peripheral blood flow in premature newborn infants. *Pediatric Research*, *60*(4), 456-460.

Watts, M. E., Pocock, R., & Claudianos, C. (2018). Brain energy and oxygen metabolism: emerging role in normal function and disease. *Frontiers in Molecular Neuroscience*, *11*, 216.

Wodey, E., Pladys, P., Betremieux, P., Kerebel, C., & Ecoffey, C. (1998). Capillary refilling time and hemodynamics in neonates: a Doppler echocardiographic evaluation. *Critical Care Medicine*, *26*(8), 1437-1440.

World Medical Association (2013). World Medical Association Declaration of Helsinki: ethical principles for medical research involving human subjects. *The Journal of the American Medical Association*, *310*(20), 2191-2194.

Zhang, J., Penny, D. J., Kim, N. S., Yu, V. Y. H., & Smolich, J. J. (1999). Mechanisms of blood pressure increase induced by dopamine in hypotensive preterm neonates. *Archives of Disease in Childhood-Fetal and Neonatal Edition*, *81*(2), F99-F104.

University College Cork, Ireland
Coláiste na hOllscoile Corcaigh

CORA
Cork Open Research Archive
Cartlann Taighde Oscailte Chorcaí

Ashoori, M. 2024. AI-based analysis of cerebral oxygenation in preterm and term infants. PhD Thesis, University College Cork.

Please note that Chapter 4 (pp. 219-258) is unavailable due to a request by the author.

CORA Cork Open Research Archive http://cora.ucc.ie

Chapter 5. Multi-model Assessment of Newborns at Risk of Neonatal Hypoxic Ischaemic Encephalopathy – The MONItOr Study

Title: Machine Learning Models of Cerebral Oxygenation ($rcSO_2$) for Brain Injury Detection in Neonates with Hypoxic-Ischaemic Encephalopathy

Minoo Ashoori MSc [1,2], John M. O'Toole PhD [1,3], Aisling A. Garvey PhD [1,3,4], Ken D. O'Halloran PhD [1,2], Brian Walsh PhD [1,3,4], Michael Moore MD [5], Andreea M. Pavel MD [1,3,4], Geraldine B. Boylan PhD [1,3], Deirdre M. Murray PhD [1,3], Eugene M. Dempsey MD [1,3,4], and Fiona B. McDonald PhD *[1,2]

1. INFANT Research Centre, University College Cork, Cork, Ireland

2. Department of Physiology, School of Medicine, College of Medicine and Health, University College Cork, Cork, Ireland

3. Department of Paediatrics and Child Health, University College Cork, Cork, Ireland

4. Department of Neonatology, Cork University Maternity Hospital, Cork, Ireland

5. Department of Radiology, Cork University Hospital, Cork, Ireland

Corresponding author: Fiona McDonald, Department of Physiology, School of Medicine, College of Medicine and Health, University College Cork, Western Gateway Building, Western Rd. Ireland. Email: Fiona.mcdonald@ucc.ie, Phone: 021-4205432

5.1. Abstract:

The present study was designed to test the potential utility of regional cerebral oxygen saturation ($rcSO_2$) in detecting term infants with brain injury. The study also examined whether quantitative $rcSO_2$ features are associated with grade of hypoxic ischaemic encephalopathy (HIE). We analysed 58 term infants with HIE (>36 weeks of gestational age) enrolled in a prospective observational study. All newborn infants had a period of continuous $rcSO_2$ monitoring and magnetic resonance imaging (MRI) assessment during the first week of life. $rcSO_2$ Signals were pre-processed and quantitative features were extracted. Machine-learning and deep-learning models were developed to detect adverse outcome (brain injury on MRI or death in the first week) using the leave-one-out cross-validation approach and to assess the association between $rcSO_2$ and HIE grade (modified Sarnat – at 1 h). The machine-learning model ($rcSO_2$ excluding prolonged relative desaturations) significantly detected infant MRI outcome or death in the first week of life [area under the curve (AUC) = 0.73, confidence interval (CI) = 0.59−0.86, Matthew's correlation coefficient = 0.35]. In agreement, deep learning models detected adverse outcome with an AUC = 0.64, CI = 0.50−0.79. We also report a significant association between $rcSO_2$ features and HIE grade using a machine learning approach (AUC = 0.81, CI = 0.73−0.90). We conclude that automated analysis of $rcSO_2$ using machine learning methods in term infants with HIE was able to determine, with modest accuracy, infants with adverse outcome. De novo approaches to signal analysis of NIRS holds promise to aid clinical decision making in the future.

Keywords: regional cerebral oxygen saturation ($rcSO_2$), extreme gradient boosting (XGBoost), Convolutional neural network (CNN), Magnetic resonance imaging (MRI), term, neonatal brain injury, hypoxia-ischaemia, inflammation, oxygen delivery, deep learning.

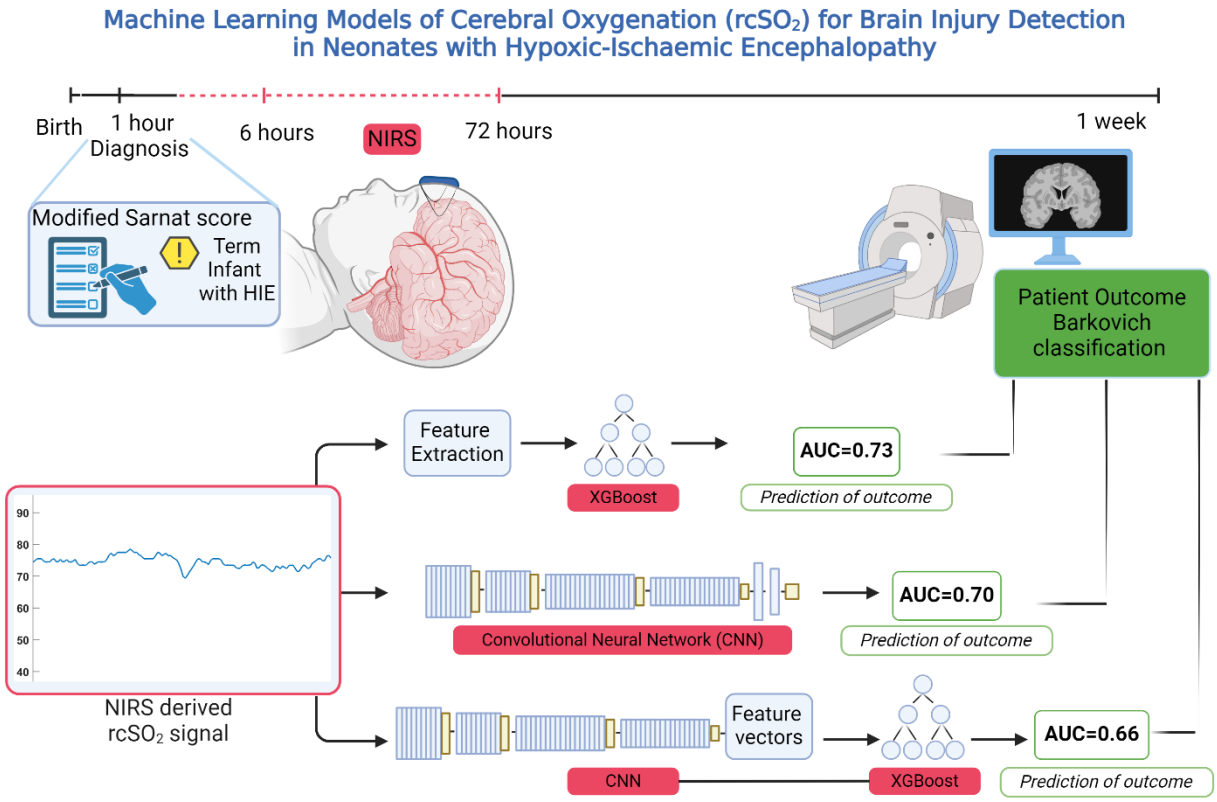

Figure 5. 1. Graphical abstract of MONItOr study. NIRS data was collected from term infants diagnosed with HIE using modified Sarnat score at 1 hour. NIRS data were processed, and several machine learning algorithms were trained and utilised to test if features of $rcSO_2$ could predict short-term brain injury, an outcome assessed by MRI/ death. The performance of the models was assessed using receiver operating curves (ROC) and area under the curve (AUC) values were reported. Created with Biorender.com

5.2. Introduction:

Hypoxic-ischaemic encephalopathy (HIE) is the most common cause of brain injury in full-term neonates. Infants with HIE are at risk of significant long-term neurodevelopmental impairments (Belet et al., 2004; Van Handel et al., 2007; Van Schie et al., 2015). Therapeutic hypothermia (TH), the current gold standard treatment for HIE, is indicated in term infants with moderate and severe HIE (Papile et al., 2014). To be effective, it is crucial to initiate TH within a timeframe of six hours after ischaemic injury, which in clinical practice corresponds to the first six hours after birth (Kattwinkel et al., 2010).

Near infrared spectroscopy (NIRS) exhibits promise as a non-invasive bedside device for the measurement of regional cerebral oxygen saturation ($rcSO_2$) in infants with HIE (Mitra et al., 2020; Garvey et al., 2022). $rcSO_2$ is a relevant regional measurement in the organ arguably of greatest risk during HIE. The $rcSO_2$ measure reflects the saturation of haemoglobin: deoxyhaemoglobin within small vessels located in the measurement compartment. The arterial to venous ratio in neonates in this compartment is reported to be 15:85 (Watzman et al., 2000). Suppan and colleagues (2022) discussed in depth the contribution of oxygen content, circulation, and oxygen extraction to the $rcSO_2$ and highlighted the challenges in interpreting absolute values and trends of rcSO2, which halts its routine use at the bedside.

Many studies to date have focused on comparing changes in mean absolute $rcSO_2$ values over time between HIE infants to determine if there are any detectable common patterns that are associated with poor clinical outcomes. Newborns who experience severe hypoxia and later develop brain injury have been reported to

exhibit higher $rcSO_2$ compared to newborns who do not develop brain injury (Toet et al., 2006; Lemmers et al., 2013; Dehaes et al., 2014; Peng et al., 2015; Tekes et al., 2015; Jain et al., 2017), but others have found no association (Shellhaas et al., 2013).

The utility of using mean absolute $rcSO_2$ values as predictors of adverse outcomes has been explored previously and may be clinically beneficial (Goeral et al., 2017; Niezen et al., 2018). Considering the moment-to-moment fluctuations that occur in metabolism and the cardiorespiratory system, quantitative characteristics of the NIRS signal may be a more appropriate approach than using mean values.

Physiology is dynamic in nature and the fluctuations and waveforms around the mean may contain relevant information that can be utilised. There are many ways to summarise a fluctuating biological signal to examine its trend beyond the mean. In this study we quantify complex details of the $rcSO_2$ biological signal, measuring changes in both its amplitude and frequency by manual feature engineering. Additionally, with the advent of convolutional neural networks (CNN) we can now exclude manual feature engineering processes and use end-to-end optimisation to objectively identify features in a signal that best predict outcome.

The novelty and strength of both machine learning approaches are that the algorithm can combine a selection of features together to predict outcome rather than one quantitative method (such as mean) to summarise the signal. To assess the potential utility of $rcSO_2$ signal analysis in providing a simple and immediate evaluation of early-life brain health, we sought to implement automated detection models of NIRS using computer-based algorithms. We tested the potential utility of $rcSO_2$ in detecting term infants with brain injury. To evaluate the utility of $rcSO_2$ over other readily available

clinical variables associated with brain injury, we also created separate machine learning models using clinical variables for performance comparison. In addition, we examined if quantitative $rcSO_2$ features are associated with the grade of HIE classified by modified Sarnat score at 1 hour.

5.2. Methods:

5.2.1. Ethical Approval

This was a secondary data analysis of a prospective observational study carried out at Cork University Maternity Hospital, Ireland (Multi-model Assessment of Newborns at Risk of Neonatal Hypoxic Ischaemic Encephalopathy – The MONItOr Study; Garvey et al., 2022). Ethical approval for the study was obtained from the Clinical Research Ethics Committee of the Cork Teaching Hospitals (ECM 5(5)04/07/17). The study conformed to the standards set by the Declaration of Helsinki, except for registration in a database (World Medical Association, 2013). It included infants born at >36 weeks' gestational age admitted to the neonatal unit and meeting study criteria including an Apgar score <5 at 5 minutes, postnatal resuscitation lasting > 10 minutes, pH < 7.1 or base deficit > 16 mmol/l, or lactate levels > 9 mmol. Infants with evolving encephalopathy, assessed using the modified Sarnat Score within 1 hour after birth, were categorised into mild, moderate, or severe HIE. This system measures various factors including consciousness, muscle tone, tendon reflexes, complex reflexes, and autonomic function (Chalak et al., 2018). Based on this categorisation, cases of moderate to severe encephalopathy received TH (Shankaran et al., 2005). Data from all the infants recruited to the MONItOr study were included in this analysis.

5.2.2. Data Collection

Cerebral oxygenation was measured using NIRS, a continuous non-invasive device (INVOS 5100 with neonatal transducer, INVOS OxyAlert NIRSensor, Covidien, Mansfield, MI, USA). The NIRS sensor was placed on the right frontotemporal

forehead area. Monitoring of cerebral oxygenation in the recruited infants commenced on the first day following birth and continued for up to 5 days.

5.2.3. MRI

MRI scans were recorded in the first week postpartum and graded by a paediatric radiologist and a neonatologist using the Barkovich classification system (Garvey et al., 2022). In the Barkovich MRI scoring system, two distinctive patterns of brain injury are taken into consideration: watershed-distribution of injury and deep grey matter injury (Barkovich et al., 1998). Any grade of abnormalities in either of these sub regions as determined by MRI or mortality within the first week were defined an adverse outcome.

5.2.4. HIE Classification and Adverse Outcome

Severity of HIE grade was classified (mild [1], moderate [2], severe [3]) according to the modified Sarnat score at 1hr. HIE infants were also grouped for analysis based on TH treatment (mild [0], moderate & severe [1]). The utility of HIE grade or HIE-TH grouping to detect adverse outcome (MRI/death) was assessed using the area under the receiver operating characteristic curve (AUC).

5.3.5. Signal Processing

The INVOS device records signals using a nonuniform sampling frequency, typically ranging from 1/6 to 1/5 Hz. The signals were resampled to a uniform sampling and the artefacts were removed using a previously described method (Ashoori et al., 2023). Prolonged relative desaturations (PRDs), defined as $rcSO_2$ desaturations relative to their respective baseline, were extracted using a discrete cosine transform and singular spectrum analysis as described previously (Ashoori et al., 2021; Ashoori

et al., 2023) (Figure 5. 2). The $rcSO_2$ data were analysed using three different versions of the signal: $rcSO_2$, $rcSO_2$ without the PRD signal component, and the PRD component alone. Initially, $rcSO_2$ and $rcSO_2$ without the PRDs underwent spectral decomposition into 5 specific bandwidths (Ashoori et al., 2023), and quantitative features were extracted over 4-hour epochs with 50% overlap, resulting in 4 to 54 epochs per NIRS record (Figure 5. 2). Signal amplitude features were selected based on previous work performed by our group (O'Toole et al., 2016). MATLAB (version 2020b, The MathWorks Inc.) was employed for the preprocessing of NIRS signals, extracting PRDs and computing their various features. Figure 5. *3* illustrates features extracted from one epoch of $rcSO_2$. Distinct methods were applied to the PRD component of the $rcSO_2$, with a different set of quantitative features extracted directly from the individual PRDs as described previously (Ashoori et al., 2023).

We also extracted fifteen one-hour epochs of $rcSO_2$ data from each infant at intervals of 6-hours across 6 – 84 hours after birth and computed the mean of the absolute values of $rcSO_2$ for each epoch.

5.3.6. Machine Learning

Quantitative $rcSO_2$ features were combined using a gradient-boosting machine known as extreme Gradient Boosting (XGBoost), with hyperparameter tuning for optimal performance. The model's effectiveness was assessed using Leave-One-Out Cross-Validation (LOOCV). LOOCV is a robust validation method where each data set (infant) is used as the validation set once, while the rest of the data serves as the training set. This approach uses all available data for both training and validation, maximising the use of a limited data set while helping to prevent overfitting. It also

ensures a comprehensive unbiased assessment of the model's performance. The models included a binary classifier for detecting adverse outcomes and a multi-class classifier for grading HIE severity (both defined previously). Three separate XGBoost models were developed for each signal type: $rcSO_2$, $rcSO_2$ without PRDs, and PRDs. Feature importance was estimated for significant models, to examine how each feature contributed to the model's performance. When there was a significant association between the machine learning and adverse outcome, follow-up analysis was performed using the infants with MRI injury. An ordinal scale from 0 to 3 was created: 0 for normal in both watershed-distribution of injury and deep grey matter injury subregions, 1 for isolated watershed injury, 2 for isolated deep grey matter injury, and 3 for abnormalities in both or death in the first week. An XGBoost regression model was applied and evaluated through LOOCV, by root mean squared error (RMSE). Correlation between predicted and assigned ordinal grades was assessed as a performance measure. Python (version 3.10) was used to develop the XGBoost models, using CPU resources for training and model evaluation.

A combination of clinical data, commonly used for the early identification of infants at risk of HIE (Wiberg at al., 2010), were analysed for predictive value. These clinical attributes included Apgar scores at 1 and 5 minutes of life, postnatal pH, base deficit, and lactate values. Clinical attributes were combined using a random forest model of adverse outcome (MRI outcome or death).

5.3.7. Deep Learning

In addition to using XGBoost, we also explored deep learning, specifically a 1D convolutional neural network (CNN) using the $rcSO_2$ as the 1D input signal to predict

outcome. We used 30-minute epochs of $rcSO_2$ with a 50% overlap. In total, the dataset consisted of 12,394 epochs from 58 infants. To design the CNN models, we systematically explored different architecture configurations, guided by the testing performance from a 5-fold cross validation. 5-fold cross-validation is a technique used to assess the performance of a model by dividing the dataset into five equal subsets, training the model on four of the subsets, and testing it on the remaining subset, repeating this process five times with each subset used once as the testing dataset. This training-testing method was selected for the multiple design experiments as it is more computationally efficient than LOOCV. Once suitable architecture was identified, we fine-tuned hyperparameters, again guided by a 5-fold cross validation process. PyTorch (version 1.13.1) in Python was utilised for developing and training the CNN models, with computations accelerated using a NVIDIA GPU on a desktop computer.

5.3.8. CNN- XGBoost

We adopted a combined CNN- XGBoost approach to utilise the strengths of CNN for feature extraction and XGBoost for classification. This approach has demonstrated significant efficacy on smaller data sets, such as ours (Thongsuwan et al., 2021). In this method, CNN was optimised and trained using the same architecture explained above, stopping at the last fully connected layer. The data (features) at this array of 256 numbers was used as the input of XGBoost model. The XGBoost model was trained using the LOOCV method to classify the $rcSO_2$signals according to outcomes.

5.3.9. Statistical Analysis

To evaluate the performance of models and the absolute mean $rcSO_2$ values to detect brain injury, AUC and its corresponding 95% confidence interval (CI) were used. We evaluated the performance of the multi-class classification models using the micro-average AUC generated from the multiROC package in R (version 4.2.3). (Wei at al., 2018). Matthew's correlation coefficient (MCC) was included as an additional performance metric for the classification models. In all models the significance level was set at $p < 0.05$.

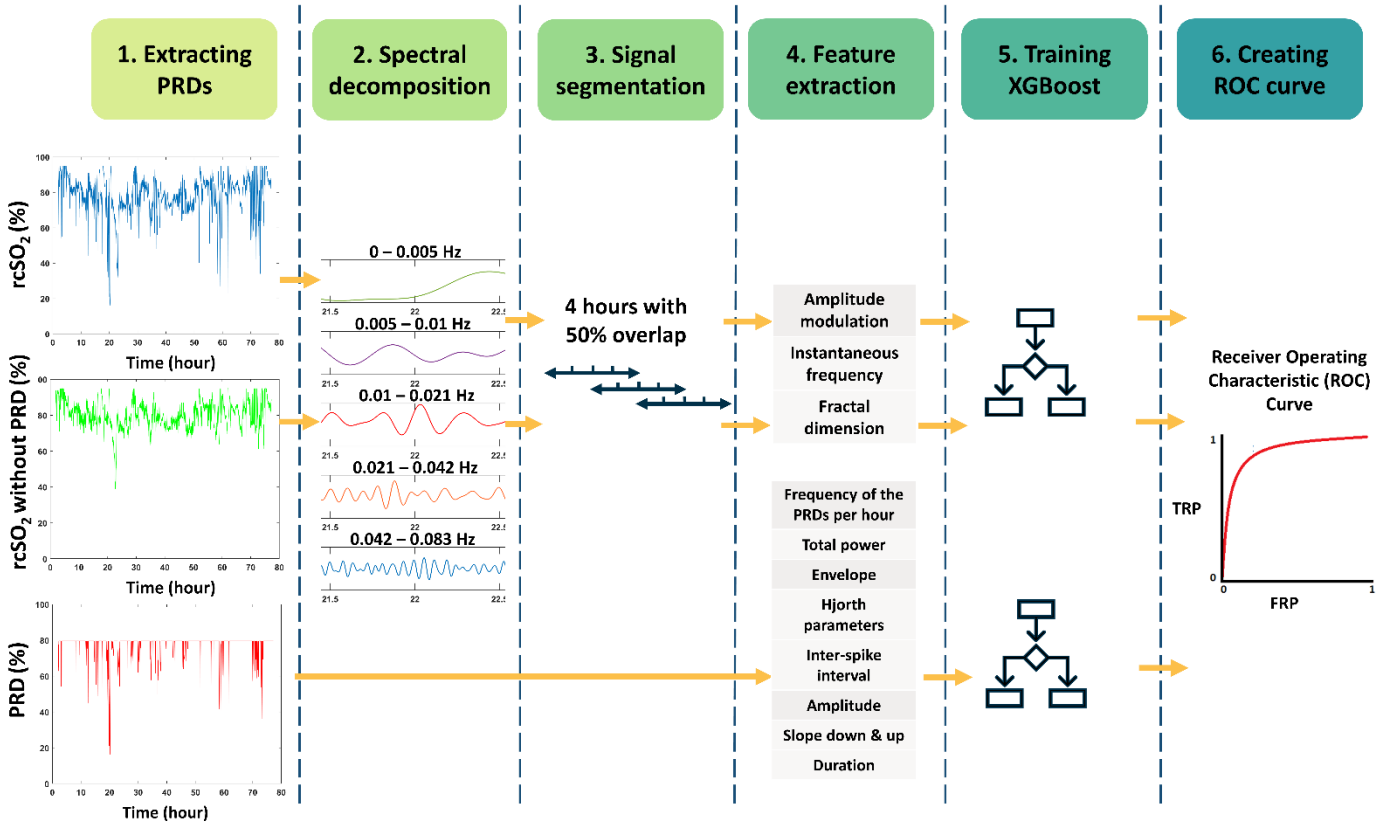

Figure 5. 2. Illustration of NIRS signal processing: extraction of prolonged relative desaturations (PRDs) using discrete cosine transform and singular-spectrum analysis (Ashoori et al., 2021) and decomposition of $rcSO_2$ signal (blue) into $rcSO_2$ without PRDs (green) and PRDs (red) (1), decomposition of $rcSO_2$ and $rcSO_2$ without PRDs signals into 5 frequency bandwidths: [0 – 0.005 Hz], [0.005 – 0.01 Hz], [0.01 – 0.021 Hz], [0.021 – 0.042 Hz] and [0.042 – 0.083 Hz] (2), division of each bandwidth into 4-hour epochs with 2 hours of signal overlap (3). The signal features were then extracted (4) and machine learning models (XGBoost) were trained using extracted features (5). The model compared the predicted values with actual labels and AUC of the models were plotted (6).

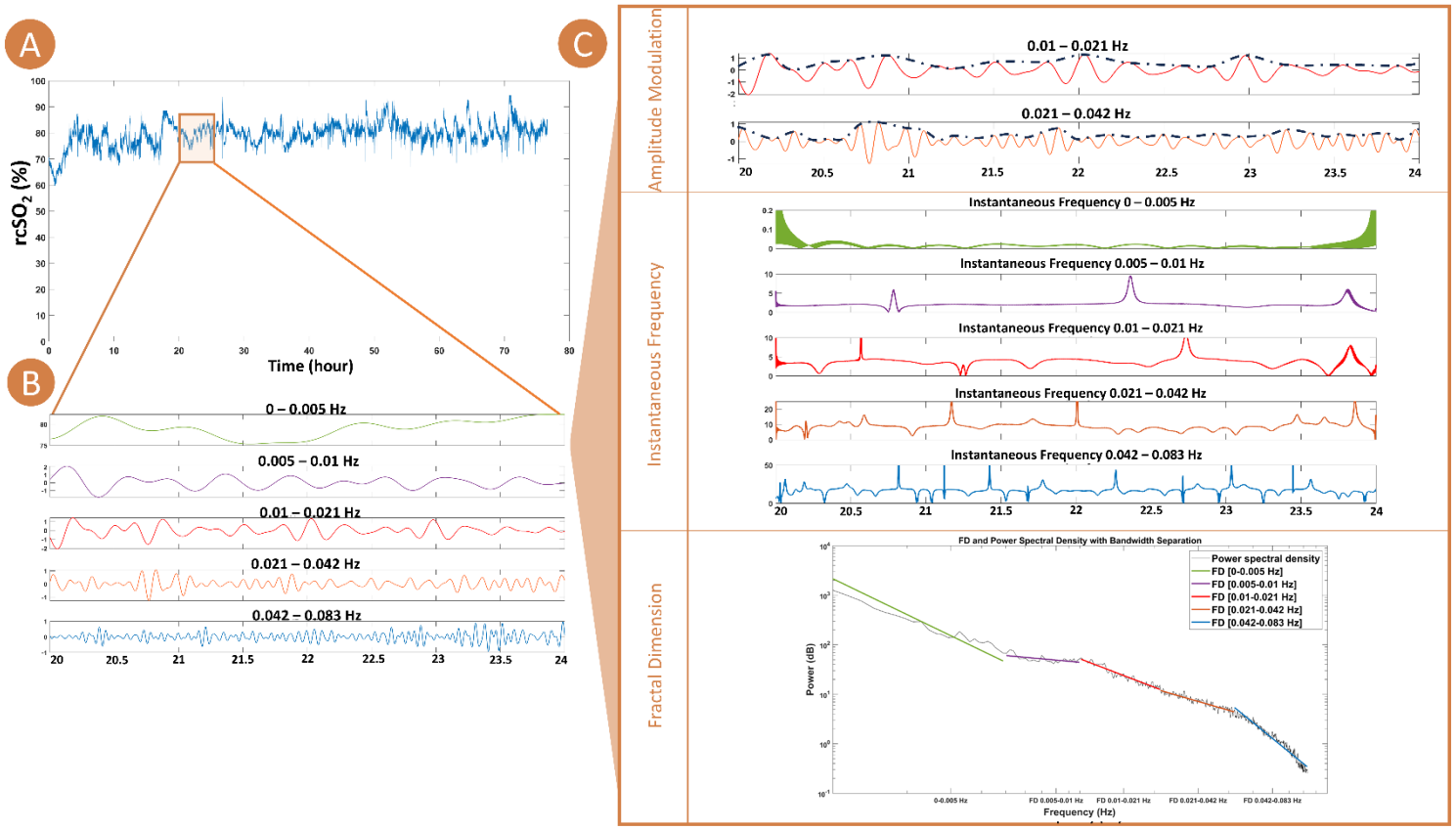

Figure 5. 3. Illustration of features extracted from $rcSO_2$ signals: A. raw trace of regional cerebral oxygen saturation signal ($rcSO_2$). B. Illustration of the signal decomposition into 5 bandwidths during a 4-hour epoch in $rcSO_2$. C. Illustration of quantitative features extracted from different bandwidths. The features extracted included amplitude-modulation features, instantaneous frequency (IF) and fractal dimension (FD)

5.4. Results:

This study was performed using data collected from infants enrolled in the MONItOr study. We analysed infants' cerebral NIRS signal recordings that were captured within the first days of life. In addition, we utilised their documented outcomes including 1hr modified Sarnat score, and MRI/death recorded within the first week of life (n=58 infants). Demographics of the cohort according to grade of HIE are displayed in Table 5. 1. All the infants received a diagnosis of HIE within 1 hour after birth: 28 infants with mild HIE, 24 with moderate HIE, and 6 with severe HIE. A total of 30 infants with moderate and severe HIE underwent TH. The median duration of $rcSO_2$ monitoring was 49.58 hours per patient (range: 10-111 hours). All recordings began in the first 24 hours of life (within 6 hours after birth for 33 infants, between 6 and 12 hours for 22 infants, and between 12 and 24 hours for 3 infants). Sixteen infants had an adverse MRI finding, 2 infants died, and 40 infants had a normal MRI. Apgar scores (1 and 5 min), postnatal pH, base deficit, and lactate values, combined using a random forest algorithm were not predictive of outcome (AUC = 0.52, CI = 0.34 - 0.69). Assessing the potential predictive capabilities of HIE grade based on modified Sarnat in 1hr (mild [1], moderate [2], severe [3]) for MRI outcome or death, we found that it significantly predicted adverse outcome (AUC = 0.66; CI = 0.51 - 0.81), while normothermia or TH-treated infants(mild [0], moderate & severe [1]) did not (AUC = 0.61; CI = 0.47 - 0.75). Our analysis of the mean absolute values of $rcSO_2$ within discrete epochs revealed that this measurement was not useful, for this cohort, in predicting adverse outcome at one week (Figure 5. 4).

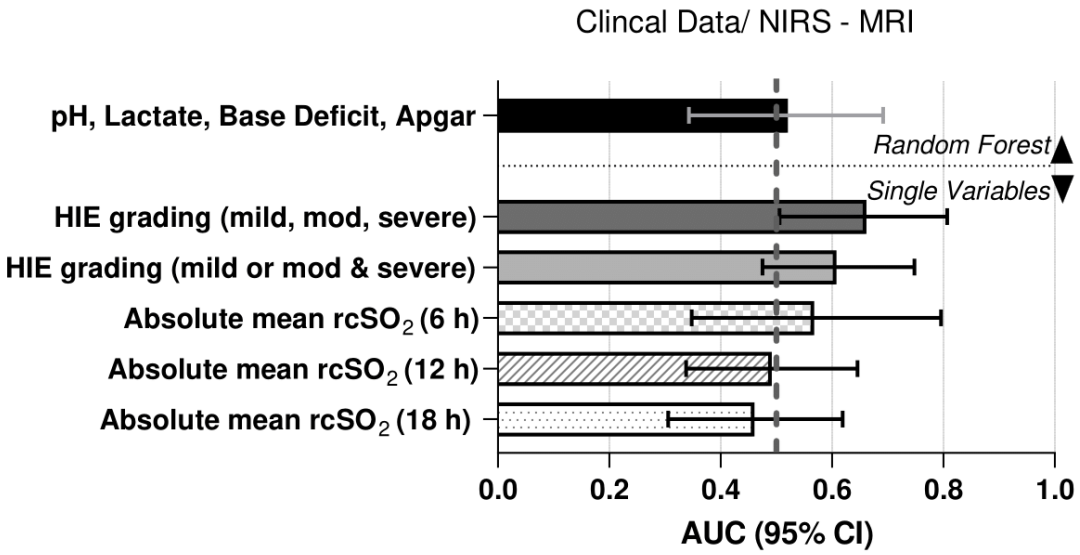

Figure 5. 4. The AUC of the ROC along with the bootstrapping 95% confidence intervals are illustrated for HIE grading, categorised in two ways: based on modified Sarnat in 1hr - mild [1], moderate [2], severe [3]; based on receiving TH - mild [0], moderate & severe [1], the mean absolute rcSO₂ at 6-, 12-, and 18-hours postnatal age. Random forest model was made using clinical data (Apgar scores at 1 and 5 minutes of life, postnatal pH, base deficit, and lactate values). The default parameters of the random forest were used with 500 trees.

5.4.1. Machine Learning

The XGBoost model was developed to determine if $rcSO_2$ signal features could determine outcome either as assessed by MRI or death in the first week, or HIE grade (modified Sarnat – 1hr). The median number of epochs used in the XGBoost models per infant was 21 epochs (range: 4 – 54). The $rcSO_2$ models could determine MRI outcomes or death in the first week both before and after the removal of PRDs (AUC = 0.70, CI = 0.55 - 0.83; MCC = 0.42, threshold = 0.33 and AUC = 0.73, CI = 0.59 - 0.86, MCC = 0.35, threshold = 0.12, respectively)(Figure 5. 5). However, the model utilising extracted PRD features did not detect adverse outcomes effectively (AUC = 0.45, CI = 0.27 - 0.62) (Figure 5. 5). Estimating feature importance in the $rcSO_2$ before and

after removal of PRDs showed that a range of features contributed to the XGBoost model, the top three were: the mean and 95th percentiles of the envelope in the first frequency band (0 - 0.005 Hz), and 5th percentiles of the envelope in the fifth frequency band (0.042 - 0.083 Hz). After finding that our model using $rcSO_2$ features could detect normal/adverse MRI outcomes or death, we conducted a follow-up analysis on MRI data subsets (deep grey matter and watershed injuries) and found a modest correlation between the predicted values and the actual ordinal grades (R^2 = 0.21).

To explore potential associations between NIRS features and HIE grade (modified Sarnat – 1hr), we developed multiclass XGBoost models with the grade of HIE as the outcome (where 0, 1 and 2 represent mild, moderate, and severe HIE, respectively). Employing this method, we report that the machine learning model could determine HIE grade: $rcSO_2$ AUC = 0.76, CI = 0.65 – 0.92; $rcSO_2$ without PRDs AUC = 0.81, CI = 0.73 – 0.90; PRDs AUC = 0.72, CI = 0.59 – 0.85 (Figure 5. 6).

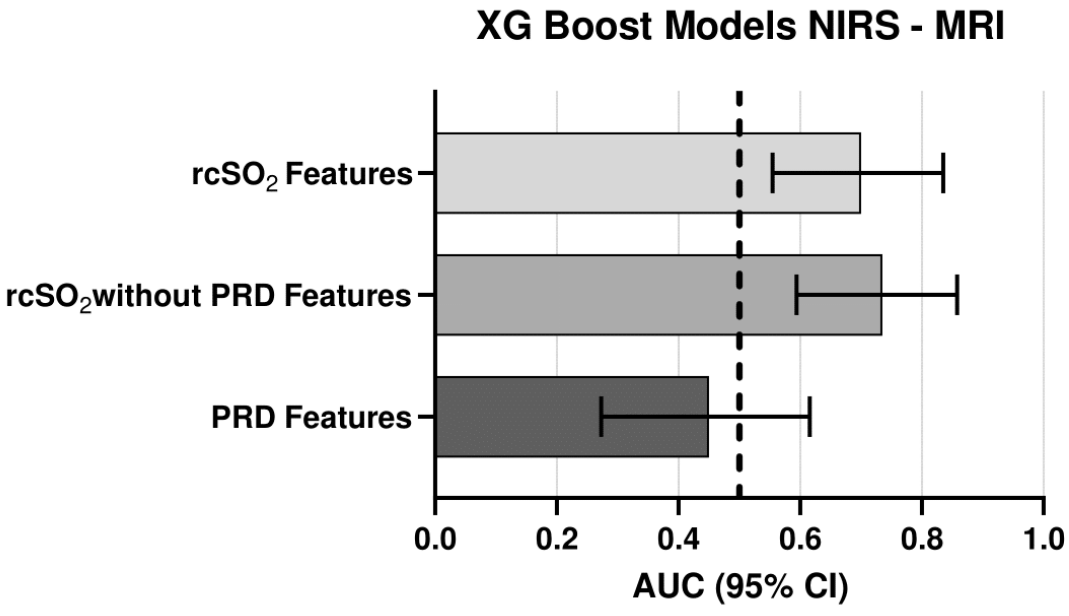

Figure 5. 5. The AUC of the ROC along with the bootstrapping 95% confidence intervals are illustrated for the binary XGBoost models based on features of $rcSO_2$, $rcSO_2$ without features, and PRDs.

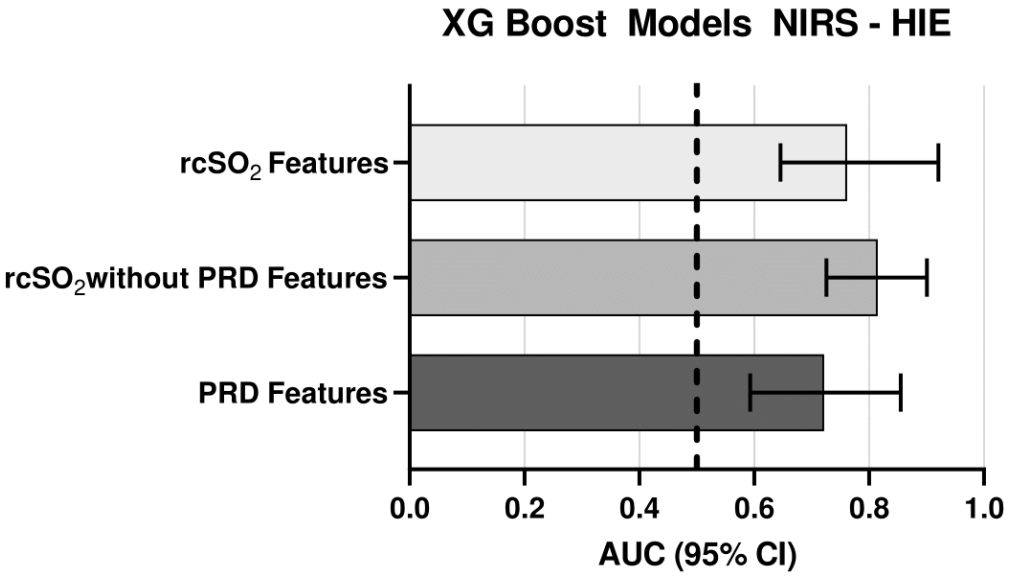

Figure 5. 6. The AUC of the ROC along with the bootstrapping 95% confidence intervals are illustrated for the multi-class XGBoost models based on features of $rcSO_2$, $rcSO_2$ without features, and PRDs.

5.4.2. Deep Learning

The details of the effective architecture when analysing 30-min signals can be found in Table 5. 2. The model was trained with 265k parameters. The median number of epochs used in the CNN models per infant was 175 (range: 37 – 440). The model was evaluated to explore the potential capabilities of NIRS signals for detecting adverse outcomes.

The results of deep learning models were promising, although they did not outperform the machine-learning models. 1D CNN model on epochs of 30 minutes, detected adverse outcomes with AUC (AUC = 0.64, CI = 0.5 – 0.79) (Figure 5. 7).

5.4.3. CNN-XGBoost

Furthermore, CNN-XGBoost, was trained and tested on 30-min epoch signals. We found a significant AUC using this method, AUC = 0.66, CI = 0.50 - 0.81 (Figure 5. 7).

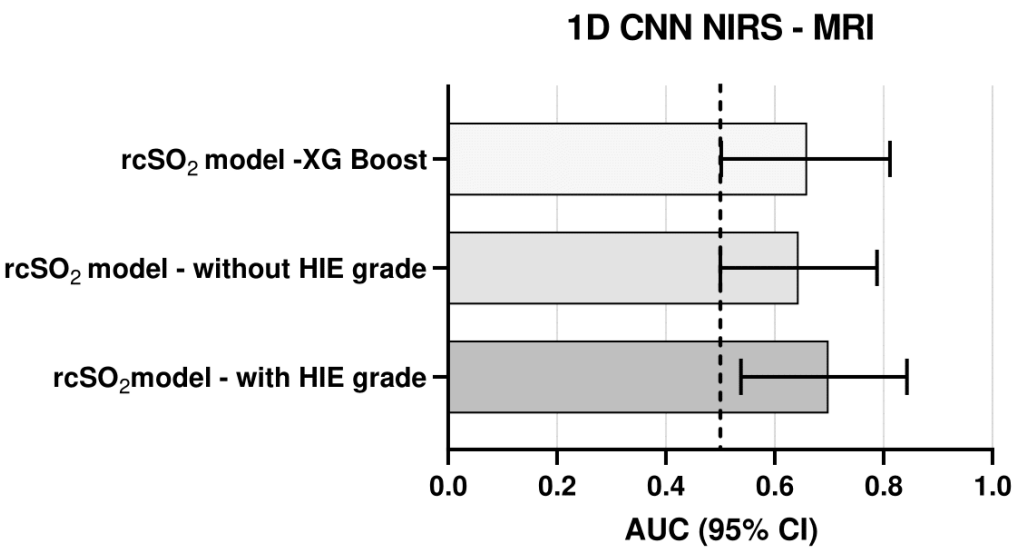

Figure 5. 7. The AUC of the ROC along with the bootstrapping 95% confidence intervals are illustrated for the binary 1D-CNN model based on $rcSO_2$, and CNN-XGBoost model.

Table 5. 1. Demographics of infants included in study.

	Mild n = 28	Moderate n = 24	Severe n = 6
Abnormal outcome (%)	6 (21%)	7 (29%)	5 (83%)
TH (Yes/No)	No	Yes	Yes
Sex (%)	18 male (64%)	12 male (50%)	4 male (67%)
Gestational age weeks; mean (± SD)	39.07 (1.63)	38.58 (1.69)	39.5 (0.84)
Birthweight kg; mean (± SD)	3.36 (0.53)	3.27 (0.53)	3.58 (0.23)
Apgar score 1 min; mean (± SD)	4.75 (2.77)	1.92 (1.21)	0.67 (0.52)
Apgar score 5 min; mean (± SD)	7.50 (2.27)	4.46 (1.74)	1.67 (1.37)
Postnatal pH; mean (± SD)	7.16 (0.16)	7.12 (0.18)	7.12 (0.19)
Base deficit; mean (± SD)	-7.50 (7.55)	-13.15 (5.20)	-15.70 (7.41)
Lactate values; mean (± SD)	9.48 (4.70)	10.56 (4.83)	11.05 (5.76)
NIRS recordings started at the first 6 hours after birth	15	15	3
NIRS recordings started 6-12 hours after birth	10	9	3
NIRS recordings started 12-24 hours after birth	3	0	0

*Table 5. 2. Architecture Details of the Convolutional Neural Network Model. The model consists of 5 convolutional layers (Conv 1D) followed by two fully connected (FC) layers. Each convolutional layer, except layer 5, had batch normalisation, followed by leaky ReLU activation and maxpool layer (Maxpool 1D). Before convolutional layer #5, the HIE grade is imported to the model as the vector of values, ranging from 1 to 3, and layer 5 had convolution 1*1, which was used to reduce the dimension of the input. Then dropout (p=0.2) and fully connected layers followed, and the activation of the last layer, was sigmoid function. The output was a number between 0 and 1, estimating the probability of MRI outcome or death. Furthermore, this model was run without adding the HIE grade in the layer 5, to investigate if the NIRS signals detect outcomes without knowledge of the HIE grade.*

Layer	Input	Number of filters	Filter size	Stride	Dropout	Output shape
Conv 1D	(1*300)	8	7	1	-	(8*294)
Maxpool 1D	(8*294)	-	2	2	-	(8*147)
Conv 1D	(8*147)	8	5	1	-	(8*143)
Maxpool 1D	(8*143)	-	2	2	-	(8*71)
Conv 1D	(8*71)	16	3	1	-	(16*69)
Maxpool 1D	(16*69)	-	2	2	-	(16*34)
Conv 1D	(16*34)	16	3	1	-	(16*32)
Maxpool 1D	(16*32)	-	2	2	-	(16*16)
Flatten	(16*16)	1	-	-	-	(1*256)
Add HIE grade	(1*256)	1	-	-	-	(2*256)
Conv 1D	(2*256)	1	1	1	-	(1*256)
Dropout	(1*256)	-	-	-	0.2	(1*256)
FC	(1*256)	-	-	-	-	(1*1024)
FC	(1*1024)	-	-	-	-	(1*1)

5.5. Discussion:

This study reports that quantitative $rcSO_2$ features combined using machine learning models were predictive of adverse outcome/brain injury. The machine learning approach utilising NIRS $rcSO_2$ signal features has potential as a biomarker of brain injury in term infants with HIE.

The features extracted from NIRS signals in our study are summarised into three categories. The amplitude modulation refers to changes in the magnitude or intensity of the signal over time. Increases in amplitude may indicate periods of higher cerebral blood flow (CBF), or lower oxygen consumption leading to higher oxygen content in the brain (NIRS is a venous weighted measurement). Instantaneous frequency features refer to the rate at which the phase of the signal changes over time. In other words, it quantifies the changing NIRS signal as it oscillates or cycles within a specific time window. It can be indicative of dynamic alterations in CBF, changes in arterial oxygen saturation or oxygen utilisation of the brain over time. Fractal dimension indicates the complexity of the signal, offering insights into the detailed pattern of cerebral oxygenation. Changes in fractal dimension may reflect alterations in the underlying regulatory mechanisms governing cerebral blood flow dynamics, such as neurovascular coupling and autoregulation. However, it should be noted that the machine-learning models learn complex nonlinear combinations of these features, therefore making interpretation difficult by obscuring the connection to the outcome groups.

Feature importance identified specific components in the low-frequency bandwidth as playing a significant role in contributing to the model's performance. Although

these low-frequency features are related to the trend of $rcSO_2$ signal, our analysis of mean absolute values $rcSO_2$ were not significantly associated with outcome. Our previous study, Chapter 3, found significant correlations between $rcSO_2$ PRDs in extremely preterm infants and intraventricular haemorrhage (IVH) confirmed by ultrasound in extremely preterm infants (Ashoori et al., 2023). In the present study a cohort of term infants with HIE, PRD features were not significant predictors of adverse MRI or death in the first week of life. While PRDs are evident in both term and preterm populations with adverse outcome, the frequency of the desaturations appears to be less in the term cohort. Wintermark et al. (2014) found that therapeutic hypothermia significantly decreased the number and duration of cerebral oxygen desaturations in infants with HIE compared to normothermic infants. Infants with HIE exhibit mitochondrial dysfunction during the secondary deterioration associated with HIE, with an associated loss in oxidative metabolism. Brain cells may also use less oxygen and contribute to higher cerebral venous oxygenation, as measured by NIRS, arising from a decrease in brain function and/or viability which would lower oxygen demand (Zhang et al., 2021; Dhillon et al., 2022). The follow-up analysis on the MRI data taking into account the sub-regions of injury showed a significant correlation between the machine learning model and the degree of MRI injury, thus demonstrating the potential of machine learning models of $rcSO_2$ to detect the severity of brain injury when evaluated by MRI outcomes.

Previous studies identified a weak association between mean absolute values of $rcSO_2$ within 6-hour intervals during the first 60 hours of life and adverse short-term outcomes (AUC = 0.56; Goeral et al., 2017). Also, similar to our previous findings, no correlation was found between mean $rcSO_2$ and adverse outcomes. This observation

also aligns with research conducted by Garvey et al., (2022) performed on the same data set, that did not find an association between any $rcSO_2$ and adverse MRI outcomes or fractional tissue oxygen extraction (FTOE) and outcome at 6 and 12h. Yet we revealed that by utilising quantitative $rcSO_2$ features and a machine learning model we were able to predict adverse MRI outcomes or death in the first week. The computational power of the algorithms and the extensive quantitative analysis of NIRS to extract useful features, contributed to stronger detection capabilities of the $rcSO_2$ measurement compared to previous studies using only mean absolute $rcSO_2$ values (Goeral et al., 2017). Our analysis involved extracting and combining features from continuous NIRS signals, even during hypothermia, and still exhibited the potential to detect outcomes. Time of NIRS assessment in relation to the initial hypoxic-ischaemic injury likely influences the associations observed. Niezen et al., (2018) reported an absence of association between mean $rcSO_2$ values and severely adverse outcomes within the initial 48 hours after birth. However, at 72 hours after birth and subsequent rewarming, $rcSO_2$ mean-values demonstrated significant predictive capabilities.

The severity, duration and timing of the initial hypoxic ischaemic injury is variable across patients with HIE, and the postnatal evolution of HIE may also be variable. It is possible that infants with HIE progress to more severe grades of HIE. Power et al., (2019) highlighted that the modified Sarnat score was an essential component for the assessment and evaluation of infants with neonatal encephalopathy. They emphasised the use of this clinical grading scale and the benefits of its use as a standardised approach to performing systematic neurological examination and documentation of pertinent neurological findings. We also agree with Power et al.,

(2019) that the value of the Sarnat Score when evaluating infants with suspected HIE within the first few hours, has increased with the advent of therapeutic hypothermia (TH) and the need to evaluate the neurological response to treatment in those who undergo the TH. The early diagnosis of HIE using the modified Sarnat score is important to direct clinical care. We found that HIE grading based on assessment using Sarnat score at 1 hour of life was weakly predictive of adverse outcomes. This is consistent with previous studies that have shown that HIE grading is a useful metric for assessing the risk of brain injury in infants (Rutherford et al., 2010). It is important to acknowledge that the Sarnat score incorporates some subjective measurements based on clinical signs that are assessed at only one point in time (in the first hour of life in this cohort) and does not take into account evolving injury or therapeutic interventions. In addition, the Sarnat score is reportedly challenging to perform by inexperienced staff and in practice is often poorly documented (Power et al., 2019). Nonetheless we found that a machine learning model of NIRS features could determine HIE grade (modified Sarnat – 1hr), indicating that cerebral NIRS measures some aspects of brain oxygenation that are discriminatory in the context of encephalopathy.

We developed CNN and CNN-XGBoost models to extract features from the NIRS signals. To the best of our knowledge, our research represents the first instance of applying deep learning methods to the analysis of NIRS signals recorded from neonates with HIE. The primary advantage of deep learning, specifically CNNs, lies in its ability to automatically extract high level and abstract features directly from raw data, thus eliminating the need for manual feature engineering. Moreover, CNNs are often the preferred choice for classification due to their capacity to model

hierarchical and complex patterns, which often generalise better on unseen datasets. However, it is important to note that CNN models exhibit superior performance when a substantial dataset is available, rather than a limited one (Bailly et al., 2022). Although our findings demonstrate that by employing CNNs for the analysis of NIRS signals, we can significantly detect adverse outcomes in term infants with HIE, the XGBoost model with the engineered features performs better. As the variability in NIRS signals between neonates is the primary interest in this study rather than across time segments within the same NIRS signal, our dataset of 58 babies is small in the context of deep learning, and this small dataset necessitates a smaller network. With access to NIRS signal from more patients, the CNN model may be preferable to the XGBoost and features approach, enabling end-to-end optimisation of the training task with a greater potential to generalise outside of the training and testing data. A more extensive dataset would allow the model to encounter a multitude of patterns and further refine its predictive abilities through learning. Development of a web-based version of the CNN model will be explored in the future as a potential way to refine and expand upon the CNN models generated which could improve with the addition of more data.

Our study has some limitations. First, as alluded to above, our sample size was relatively small; this sample size may not have been optimal for CNN models, which may affect the generalisability and robustness of our findings related to deep learning. Moreover, the XGBoost and CNN models have numerous hyperparameters that required optimisation. While we made every effort to fine-tune these parameters extensively without overfitting, it is worth noting that covering all

possible hyperparameter combinations is not feasible, which could potentially introduce bias or underfitting.

Another notable limitation of our study was the lack of precise information regarding the initiation of TH during the recording period and limited data collection after rewarming. Therapeutic hypothermia can change the trends and patterns of NIRS signals, potentially affecting the quantitative features of these signals (Peng et al., 2015). Future research should explore the utility of quantitative $rcSO_2$ features extracted from NIRS data at defined epochs such as delivery room, prior to initiation of TH, during TH and after rewarming, using machine learning models. Nonetheless, our results indicate that NIRS derived $rcSO_2$, coupled with machine learning methods, has the potential to predict brain injury, even in the context of ongoing TH. Regarding the NIRS recording itself, the INVOS device has a maximum reading of 95% $rcSO_2$ (Hessel et al., 2014), which results in a saturated output signal devoid of signal characteristics and therefore information when the $rcSO_2$ exceeds 95%. As a result, the features extracted from the signal, as well as the PRDs, will not capture changes occurring in this range. Furthermore, it is important to note that in this study, the adverse outcomes were observed in the short term (the first week of the life); but these findings should not be generalised to long-term patient outcomes without further testing. Barkovich MRI classification or early death as an outcome measure has without doubt its limitations, relying on a single investigative modality that is not always reflective of long-term physiology in terms of adverse behavioural, motor and neurocognitive developmental outcomes. Even so, it represents an important short-term outcome measure prior to discharge. Studies by Charon et al., (2016), Bhroin et al., (2022), Kang et al., (2023) and Andorka et al., (2024) report good agreement

between Barkovich scoring and long-term outcome, although other more novel methods such as Weeke Score perform better (Bhroin et al., 2022; Kang et al., 2023; Andorka et al., 2024). The results of the recent SafeBoosC-III trial (Hansen et al., 2023), albeit on preterm infant cohort, highlighted that NIRS monitoring alone does not significantly improve patient outcome and suggests a need to try alternative analysis methods but also the potential revision of corrective therapeutic approaches for abnormal patterns of cerebral oxygenation. This study illustrates one potential avenue for alternative $rcSO_2$ signal analysis.

Recent advancements in machine learning have led to the development of algorithms capable of monitoring neonatal EEGs to detect seizures in both term and preterm infants (Pavel et al., 2020; O'Shea et al., 2021). Such advances hold great promise for offering real-time decision-making support in neonatal intensive care units. However, there remains a paucity of studies examining EEG and NIRS concurrently, particularly their roles in detecting adverse outcomes during the first week of life. Goeral et al., (2017) achieved improved predictability by combining mean absolute NIRS data with blood pressure and aEEG using a logistic regression method. Enhancing the accuracy of machine learning models through the integration of NIRS with other clinical measurements, such as EEG and blood pressure, using multimodal models could offer significant improvements.

In conclusion, our study demonstrated that machine learning models of NIRS signals have the potential to provide objective, continuous and automated detection of adverse short-term outcomes in term infants with HIE. We found a significant correlation between a machine learning model of NIRS features, HIE grade and MRI

severity or death. Our study suggests that NIRS will be a valuable tool for monitoring and protecting the brain health of term infants with HIE if advanced signal analysis methods are utilised and paired with improved therapeutic approaches. Further studies in larger more diverse cohorts are needed to validate our results.

5.6. References

Andorka, C., Barta, H., Sesztak, T., Nyilas, N., Kovacs, K., Dunai, L., Rudas, G., Jermendy, A., Szabo, M., & Szakmar, E. (2024). The predictive value of MRI scores for neurodevelopmental outcome in infants with neonatal encephalopathy. *Pediatric Research,* 1-8.

Ashoori, M., Dempsey, E.M., McDonald, F.B., & O'Toole, J.M. (2021). Sparse-denoising methods for extracting desaturation transients in cerebral oxygenation signals of preterm infants. In: Proceedings of the 2021 43rd Annual International Conference of the IEEE Engineering in Medicine & Biology Society (EMBC); 2021 Nov 1-5; Guadalajara, Mexico. 1010-1013.

Ashoori, M., O'Toole, J.M., O'Halloran, K.D., McCarthy, E., Livingstone, V., & Dempsey, E.M. (2023). Machine learning detects intraventricular haemorrhage in extremely preterm infants. *Children*, 10(6), 917.

Bailly, A., Blanc, C., Francis, É., Guillotin, T., Jamal, F., Wakim, B., & Roy, P. (2022). Effects of dataset size and interactions on the prediction performance of logistic regression and deep learning models. *Computer Methods and Programs in Biomedicine*, *213*, 106504.

Barkovich, A.J., Hajnal, B.L., Vigneron, D., Sola, A., Partridge, J.C., Allen, F., Ferriero, D.M., & Edwards, M.S.B. (1998). Prediction of neuromotor outcome in perinatal asphyxia: evaluation of MR scoring systems. *American Journal of Neuroradiology*, 19(1), 143-149.

Belet, N., Belet, U., İncesu, L.Ü., Ertem, Ü., & Koç, Z. (2004). Hypoxic-ischaemic encephalopathy: correlation of serial MRI and outcome. *Pediatric Neurology*, 31(4), 267-274.

Bhroin, M.N., Kelly, L., Sweetman, D., Aslam, S., O'Dea, M.I., Hurley, T., Slevin, M., Murphy, J., Byrne, A.T., Colleran, G., & Molloy, E.J. (2022). Relationship between MRI scoring systems and neurodevelopmental outcome at two years in infants with neonatal encephalopathy. *Pediatric Neurology*, *126*, 35-42.

Chalak, L.F., Nguyen, K.A., Prempunpong, C., Heyne, R.J., Thayyil, S., & Azzopardi, D.V. (2018). Prospective research in infants with mild encephalopathy identified in the first six hours of life: neurodevelopmental outcomes at 18–22 months. *Pediatric Research*, 84(6), 861-868.

Charon, V., Proisy, M., Bretaudeau, G., Bruneau, B., Pladys, P., Beuchee, A., Burnouf-Rose, G., Ferré, J.C., & Rozel, C. (2016). Early MRI in neonatal hypoxic-ischaemic encephalopathy treated with hypothermia: prognostic role at 2-year follow-up. *European Journal of Radiology*, *85*(8), 1366-1374.

Dehaes, M., Aggarwal, A., Lin, P.Y., Fenoglio, A., Roche-Labarbe, N., Deen, M.J., & Grant, P.E. (2014). Cerebral oxygen metabolism in neonatal hypoxic ischaemic encephalopathy during and after therapeutic hypothermia. *Journal of Cerebral Blood Flow & Metabolism*, 34(1), 87-94.

Dhillon, S.K., Gunn, E.R., Lear, B.A., King, V.J., Lear, C.A., Wassink, G., Bennet, L., Williams, C.E., & Gunn, A.J. (2022). Cerebral oxygenation and metabolism after hypoxia-ischaemia. *Frontiers in Pediatrics*, 10, 925951.

Garvey, A.A., O'Toole, J.M., Livingstone, V., Boylan, G.B., & Dempsey, E.M. (2022). Evolution of early cerebral NIRS in hypoxic ischaemic encephalopathy. *Acta Paediatrica*, 111(10), 1870-1877.

Garvey, A.A., Pavel, A.M., Murray, D.M., Boylan, G.B., & Dempsey, E.M. (2022). Does early cerebral near-infrared spectroscopy monitoring predict outcome in neonates

with hypoxic ischaemic encephalopathy? A systematic review of diagnostic test accuracy. *Neonatology*, 119(1), 1-9.

Goeral, K., Urlesberger, B., Giordano, V., Czaba, C., & Schmolzer, G.M. (2017). Prediction of outcome in neonates with hypoxic-ischaemic encephalopathy II: role of amplitude-integrated electroencephalography and cerebral oxygen saturation measured by near-infrared spectroscopy. *Neonatology*, 112(3), 193-202.

Hansen, M.L., Pellicer, A., Hyttel-Sørensen, S., Ergenekon, E., Szczapa, T., Hagmann, C., Naulaers, G., Mintzer, J., Fumagalli, M., Dimitriou, G., & Dempsey, E. (2023). Cerebral oximetry monitoring in extremely preterm infants. *New England Journal of Medicine, 388*(16), 1501-1511.

Hessel, T.W., Hyttel-Sorensen, S., & Greisen, G. (2014). Cerebral oxygenation after birth—a comparison of INVOS® and FORE-SIGHT™ near-infrared spectroscopy oximeters. *Acta Paediatrica*, 103(5), 488-493.

Jain, S.V., Pagano, L., Gillam-Krakauer, M., Slaughter, J.C., Pruthi, S., & Engelhardt, B. (2017). Cerebral regional oxygen saturation trends in infants with hypoxic-ischaemic encephalopathy. *Early Human Development*, 113, 55-61.

Kang, O.H., Jahn, P., Eichhorn, J.G., Dresbach, T., Müller, A., & Sabir, H. (2023). Correlation of different mri scoring systems with long-term cognitive outcome in cooled asphyxiated newborns. *Children*, *10*(8), p.1295.

Kattwinkel, J., Perlman, J.M., Aziz, K., Colby, C., Fairchild, K., Gallagher, J., Haskell, S., Hazinski, M.F., Halamek, L.P., & the Neonatal Resuscitation Writing Group. (2010). Part 15: neonatal resuscitation: 2010 American Heart Association guidelines for cardiopulmonary resuscitation and emergency cardiovascular care. *Circulation*, 122(18_suppl_3), S909-S919.

Lemmers, P., Zwanenburg, R.J., Benders, M.J., de Vries, L.S., Groenendaal, F., & van Bel, F. (2013). Cerebral oxygenation and brain activity after perinatal asphyxia: does hypothermia change their prognostic value? *Pediatric Research*, 74(2), 180-185.

Mitra, S., Bale, G., Meek, J., Tachtsidis, I., & Robertson, N.J. (2020). Cerebral near infrared spectroscopy monitoring in term infants with hypoxic ischaemic encephalopathy—a systematic review. *Frontiers in Neurology,* 11, 393.

Niezen, C.K., Bos, A.F., Sival, D.A., Meiners, L.C., & Ter Horst, H.J. (2018). Amplitude-integrated EEG and cerebral near-infrared spectroscopy in cooled, asphyxiated infants. *American Journal of Perinatology,* 35(9), 904-910.

O'Shea, A., Ahmed, R., Lightbody, G., Pavlidis, E., Lloyd, R., Pisani, F., Palmu, K., Stevenson, N.J., & Temko, A. (2021). Deep learning for EEG seizure detection in preterm infants. *International journal of neural systems,* 31(08), 2150008.

O'Toole, J.M., Kenosi, M., Finn, D., Boylan, G.B., & Dempsey, E.M. (2016). Features of cerebral oxygenation detects brain injury in premature infants. In: Proceedings of the 2016 38th Annual International Conference of the IEEE Engineering in Medicine and Biology Society (EMBC); 2016 Aug 16-20; Orlando, FL, USA. pp. 3614-3617.

Papile, L.A., Baley, J.E., Benitz, W., Eichenwald, E., Carlo, W.A., & Committee on Fetus and Newborn. (2014). Hypothermia and neonatal encephalopathy. *Pediatrics*, 133(6), 1146-1150.

Pavel, A.M., Rennie, J.M., de Vries, L.S., Blennow, M., Foran, A., & Boylan, G.B. (2020). A machine-learning algorithm for neonatal seizure recognition: a multicentre, randomised, controlled trial. *The Lancet Child & Adolescent Health*, 4(10), 740-749.

Peng, S., Boudes, E., Tan, X., Saint-Martin, C., Shevell, M., & Wintermark, P. (2015). Does near-infrared spectroscopy identify asphyxiated newborns at risk of developing

brain injury during hypothermia treatment? *American journal of perinatology,* 32(6), 555-564.

Power, B., McGinley, J., & Murphy, J.F. (2019). The modified sarnat score in the assessment of neonatal encephalopathy: a quality improvement initiative. *Archives of Disease in Childhood*, 104(Suppl 3), A71.

Rutherford, M., Ramenghi, L.A., Edwards, A.D., Brocklehurst, P., Halliday, H., & Azzopardi, D. (2010). Assessment of brain tissue injury after moderate hypothermia in neonates with hypoxic–ischaemic encephalopathy: a nested substudy of a randomised controlled trial. *The Lancet Neurology*, 9(1), 39-45.

Shankaran, S., Laptook, A.R., Ehrenkranz, R.A., Tyson, J.E., McDonald, S.A., Donovan, E.F., Fanaroff, A.A., Poole, W.K., & Stevenson, D.K. (2005). Whole-body hypothermia for neonates with hypoxic–ischaemic encephalopathy. *New England Journal of Medicine*, 353(15), 1574-1584.

Shellhaas, R.A., Thelen, B.J., Bapuraj, J.R., Zempel, J.M., Ewen, J.B., & Ahmad, K.A. (2013). Limited short-term prognostic utility of cerebral NIRS during neonatal therapeutic hypothermia. *Neurology*, 81(3), 249-255.

Suppan, E., Pichler, G., Binder-Heschl, C., Schwaberger, B., & Urlesberger, B. (2022). Three physiological components that influence regional cerebral tissue oxygen saturation. *Frontiers in Pediatrics*, *10*, p.913223.

Tekes, A., Poretti, A., Scheurkogel, M.M., Huisman, T.A.G.M., & Northington, F.J. (2015). Apparent diffusion coefficient scalars correlate with near-infrared spectroscopy markers of cerebrovascular autoregulation in neonates cooled for perinatal hypoxic-ischaemic injury. *American Journal of Neuroradiology*, 36(1), 188-193.

Thongsuwan, S., Jaiyen, S., Padcharoen, A., & Agarwal, P. (2021). ConvXGB: A new deep learning model for classification problems based on CNN and XGBoost. *Nuclear Engineering and Technology*, *53*(2), 522-531.

Toet, M.C., Lemmers, P.M., van Schelven, L.J., & van Bel, F. (2006). Cerebral oxygenation and electrical activity after birth asphyxia: their relation to outcome. *Pediatrics*, 117(2), 333-339.

Van Handel, M., Swaab, H., De Vries, L.S., & Jongmans, M.J. (2007). Long-term cognitive and behavioral consequences of neonatal encephalopathy following perinatal asphyxia: a review. *European Journal of Pediatrics*, 166, 645-654.

Van Schie, P.E.M., Schijns, J., Becher, J.G., Barkhof, F., van Weissenbruch, M.M., & Vermeulen, R.J. (2015). Long-term motor and behavioral outcome after perinatal hypoxic-ischaemic encephalopathy. *European Journal of Paediatric Neurology*, 19(3), 354-359.

Watzman, H.M., Kurth, C.D., Montenegro, L.M., Rome, J., Steven, J.M., & Nicolson, S.C. (2000). Arterial and venous contributions to near-infrared cerebral oximetry. *The Journal of the American Society of Anesthesiologists*, *93*(4), 947-953.

Wei, R., Wang, J., Jia, W., & Wei, M.R. (2018). Package 'multiROC'. Technical report. CRAN. Available from: https://cran.r-project.org/web/packages/multiROC/m

Wiberg, N., Källén, K., Herbst, A., & Olofsson, P. (2010). Relation between umbilical cord blood pH, base deficit, lactate, 5-minute Apgar score and development of hypoxic ischaemic encephalopathy. *Acta Obstetricia et Gynecologica Scandinavica,*, 89(10), 1263-1269.

Wintermark, P., Hansen, A., Warfield, S.K., Dukhovny, D., & Soul, J.S. (2014). Near-infrared spectroscopy versus magnetic resonance imaging to study brain perfusion in

newborns with hypoxic–ischaemic encephalopathy treated with hypothermia. *Neuroimage*, 85, 287-293.

World Medical Association (2013). World Medical Association Declaration of Helsinki: ethical principles for medical research involving human subjects. *The Journal of the American Medical Association*, *310*(20), 2191-2194.

Zhang, L., Dai, L., & Li, D. (2021). Mitophagy in neurological disorders. *Journal of Neuroinflammation*, 18(1), 297.

Additional Information

Data Availability

Computational models are stored on GITHUB (https://github.com/Minimnim/Monitor.git), the patient dataset used in the publication cannot be shared.

Authorship

ED, FMD, MA, KOH, DM, GB, JOT, AG were responsible for conception and design of the work. DM, GB, AG, BW, MM, AP, ED were responsible for data collection. MA, JOT and FMD performed the formal analysis. MA, JOT, KOH, ED and FMD were responsible for interpretation of the data. MA and JOT performed validation. KOH, JOT, ED and FMD provided resources and supervision for the study. MA, JOT and FMD designed and performed the visualisation of methods and results. MA and FMD wrote the original draft. All authors reviewed and edited the manuscript critically for important intellectual content.

All authors have approved the final version of the manuscript; agree to be accountable for all aspects of the work in ensuring that questions related to the accuracy or integrity of any part of the work are appropriately investigated and resolved; and all persons designated as authors qualify for authorship, and all those who qualify for authorship are listed.

Acknowledgements

We would like to acknowledge the contribution of Lavinia Panaite, Jackie O'Leary and Mary Anne Ryan in the MONItOr Study.

Competing interests

Authors have no conflicts of interest to declare.

The results of this study have been presented as posters at The Physiological Society's main meeting Physiology 2023, Harrogate, UK; Paediatric Academic Societies 2023, Washington, D.C. USA, and International Neonatology Association Conference 2023, Dublin, Ireland.

Funding

This project was funded by Science Foundation Ireland (SFI 18/SIRG/5483 to FMD, 15/SIRG/3580 to JOT), National Children's Research Centre (D/18/6 to AG). MA was funded by Department of Physiology, School of Medicine, College of Medicine and Health, University College Cork, Cork, Ireland.

Chapter 6. AI Competition

6.1. Introduction

Impaired oxygen delivery or blood flow to the brain during birth can result in brain damage, leading to a condition known as hypoxic-ischaemic encephalopathy (HIE), which is the primary cause of mortality and disability among full-term newborns (van Schie et al., 2015). HIE can lead to neonatal death or significant neurological and neurodevelopmental issues such as cerebral palsy, epilepsy, or learning impairments (Perez et al., 2013). HIE consists of an initial injury followed by a latent period lasting about six hours before entering a secondary phase characterised by programmed cell death (Bennet et al. 2006; Wassink et al. 2014). Therapeutic hypothermia (TH) is presently the sole available treatment for infants with moderate to severe HIE and must be initiated prior to the onset of the secondary injury phase to be effective (Committee on Fetus and Newborn, 2014; Kattwinkel et al., 2010).

The electroencephalogram (EEG) enables continuous bedside monitoring of cerebral function. The typical EEG background pattern can change because of an HIE insult and provide valuable information about cerebral dysfunction (Walsh et al., 2011). Moreover, these deviations are linked to unfavourable neurodevelopmental outcomes (Murray et al., 2009). Monitoring the severity of ongoing encephalopathy through EEG can be highly beneficial, especially when initiated during the early phase of injury to identify infants who may benefit from TH (Tagin et al., 2012).

However, the review of EEG often requires specialised expertise that may not always be available in neonatal care units. This study was conducted as part of an EEG machine learning competition. The competition task was to use computer-based

methods to automate the grading of background EEG activity in order to provide an objective measure that can efficiently monitor many neonates.

6.2. Methods

6.2.1. Study Design and Participants

Data were obtained from a clinical trial involving medical devices to evaluate the performance of a machine-learning algorithm in detecting seizures (Pavel et al., 2020; Pavel et al., 2022). Neonates meeting specific criteria were admitted to the neonatal intensive care unit and underwent EEG monitoring because they were deemed at risk for seizures. The current dataset comprised 53 full-term newborns admitted to the neonatal intensive care unit (NICU) at Cork University Maternity Hospital in Ireland. All infants had been diagnosed with hypoxic-ischaemic encephalopathy (HIE). The study to capture the EEG data was authorised by the Cork Research Ethics Committee of the Cork Teaching Hospitals. Written and informed consent from a guardian or parent was obtained before enrolling neonates in the study, in accordance with the ethical standards set by the Clinical Research Ethics Committee and the principles of the Declaration of Helsinki (World Medical Association, 2013). Publication of the fully anonymised dataset, including data cleaning, was approved by the Cork Research Ethics Committee, ensuring that researchers have access to high-quality, ready-to-use data (O'Toole et al., 2023).

6.2.2. EEG

EEG recordings were conducted shortly after birth and continued for an extended period of up to 100 hours. Two different EEG machines, the NicoletOne ICU Monitor (Natus, Middletion, WI, USA) and the Neurofax EEG-1200 (Nihon Khoden, Tokyo,

Japan) were used for recording. The sampling frequencies were at 256 Hz and 200 Hz. Disposable electrodes were placed over the central (C3 and C4), frontal (F3 and F4), occipital (O1 and O2), and temporal (T3 and T4) regions and at the midline (Cz), based on a modified version of the 10:20 international system (Pavel et al., 2022). A maximum of 5 one-hour epochs with minimal artefacts were selected per neonate within the first 48 hours after birth, totalling in 169 high-quality epochs included in the dataset.

Two clinical physiologists specialising in neonatal EEG, individually assessed each epoch using an established EEG classification system. In cases where the individual assessments differed, the experts collaboratively reviewed the epoch and reached a consensus grade. The grading criteria encompass various measures of amplitude and frequency, continuity, normal and abnormal patterns, symmetry, and synchrony of activity between hemispheres, as well as the presence or absence of sleep-wake cycling. 4 grades were used: normal or mildly abnormal (grade 1), moderately abnormal (grade 2), severely abnormal (grade 3), and inactive (grade 4) (Murray et al., 2009). Out of the total 169 epochs, n = 105 were accompanied by labels, while n = 64 lacked any label.

6.2.3. Signal Processing

The EEGs were captured in a busy intensive-care setting, and some contained artefacts. These artefacts can stem from biological sources like sweat, muscle, and respiration, as well as non-biological sources such as interference from nearby devices like the 50 Hz electrical power supplies. Furthermore, periodic inspections of electrode impedance lead to pauses in EEG recording, leading to periods of flat or

near-zero EEG activity. A bandpass filter of 0.5 – 30 Hz was employed to remove the low- and high- frequency artefacts, followed by down-sampling to 64 Hz. NEURAL package was used to extract the quantitative features from the EEG signals, using the bipolar montage of the EEG. The EEG signals were decomposed into four different bandwidth frequencies: [0.5–4; 4–7; 7–13; 13-30] Hz (O'Toole & Boylan, 2017).

6.2.4. Feature Extraction

The extracted features include four main categories: Amplitude, frequency, connectivity and inter-burst interval features - https://github.com/otoolej/qEEG_feature_set (Table 6. 1) (O'Toole & Boylan, 2017). Amplitude, frequency, and connectivity features were assessed over short epochs, so these features were computed within a short time window (64 seconds) that was shifted over time with 50% overlapping. Then, the median value was employed to summarise these characteristics across all epochs. In the case of inter-burst intervals, assessments were conducted individually for each channel before summarising using the median value across all channels. Furthermore, some features were extracted from each frequency band, and some were estimated for the signal before being decomposed (indicated by * in Table 6. 1). In total, 102 features were extracted from each epoch.

6.2.5. Machine Learning

A sequential ensemble of decision trees known as extreme gradient boosting machine (XGBoost) was utilised to develop a predictive model for grade of EEG. The features extracted from the epochs with labels were utilised to train the model, while the unlabelled epochs served as the testing dataset. The regularisation parameters

were optimised to improve the model's settings and enhance its performance. This process involved systematically exploring various combinations of hyperparameters and selecting the most effective configuration for our specific task. The hyperparameters that were explored included learning rate (0.001, 0.005, 0.01, 0.05, 0.1, 0.2, 0.3), maximum tree depth (2, 3, 4, 5, 6, 7), column sample by tree (0.5, 0.6, 0.7, 0.8, 0.9, 1), gamma values (0, 1, 2), minimum child weight (1, 2, 3), and total number of trees (10, 50, 100, 200, 300, 400, 500). Nested Leave-One-Out Cross-Validation (LOOCV) technique was utilised for parameter optimisation which is a reliable validation method ensuring comprehensive assessment of the model's performance while overcoming overfitting issues. Inner LOOCV was used to select the best hyperparameters package and an outer LOOCV was employed to evaluate the overall model performance. To assign a grade to each signal, a multiclass classification model with 4 grades was implemented.

6.2.6. Model Evaluation

After the model was constructed, it was utilised to predict grades leveraging features extracted from the testing dataset. Subsequently, these results were uploaded to the EEG machine learning competition website (https://www.infantcentre.ie/2022/07/06/machine-learning-competition), which contained the ground truth for comparison with our predictions. The performance of the model was evaluated using various metrics such as accuracy, precision, recall, MCC and F1 score.

Table 6. 1. Features extracted from EEG signals

Feature category	Feature
Amplitude	Amplitude total power
	Amplitude SD
	Amplitude kurtosis
	Amplitude skewness
	Envelope mean
	Envelope SD
	rEEG mean
	rEEG median
	rEEG lower margin (5^{th} percentile)
	rEEG upper margin (95^{th} percentile)
	rEEG width (upper margin – lower margin)
	rEEG SD
	rEEG coefficient of variation
	rEEG asymmetry (measure of skew about median)
Frequency	Spectral power
	Spectral relative power (normalised to total spectral power)
	Spectral flatness
	Spectral entropy
	Spectral difference: difference between consecutive spectral estimates
	Spectral edge frequency: 95% of spectral power contained between 0.5 and cut-off frequency *
	Fractal dimension *
Connectivity	Brain symmetry index
	Correlation between envelopes of hemisphere-paired channels
	Coherence mean value
	Coherence maximum value
	Coherence frequency of maximum value
Inter-burst interval	95% inter-burst interval *
	Median inter-burst interval *
	Burst percentage *
	Number of bursts *

6.3. Results:

The distribution of all 4 grades for the 169 epochs is summarised in Table 6. 2. The number of epochs was not the same for all the neonates, and Table 6. 3 demonstrates the number of epochs per neonate. The hyperparameter optimisation to enhance the model's performance on this task suggested setting the learning rate to 0.01, maximum tree depth at 7, column sample by tree at 0.9, gamma values to 0, minimum child weight to 1, and a total number of trees at 500. Using these parameters to apply LOOCV on the training dataset resulted in accuracy = 0.86, precision = 0.78, recall = 0.77, MCC = 0.72 and F1 score = 0.77. Applying the developed model on the testing dataset, resulted in accuracy = 0.89, precision = 0.87, recall = 0.82, MCC = 0.80 and F1 score = 0.84. The details of the precision, recall, MCC and F1 score among grades for training and testing datasets are presented in Table 6. 4.

Table 6. 2. Distribution of 4 grades of EEG

Grade	n (%)
1	104 (61.54%)
2	31 (18.34%)
3	22 (13.02%)
4	12 (7.10%)

Table 6. 3. Distribution of number of EEG epochs available per neonate

Number of epochs per neonate	n (%)
1	5 (9.43%)
2	11 (20.75%)
3	14 (26.41%)
4	15 (28.31%)
5	8 (15.10%)

Table 6. 4. Model performance metrics for training and testing (unseen) dataset

Dataset	Metric	Grade 1	Grade 2	Grade 3	Grade 4	Mean
Training dataset	Precision	0.92	0.89	0.67	0.64	0.78
	Recall	0.95	0.76	0.67	0.7	0.77
	MCC	0.84	0.78	0.62	0.63	0.72
	F1 score	0.94	0.82	0.67	0.67	0.77
Testing dataset	Precision	0.93	0.7	0.86	1	0.87
	Recall	1	0.7	0.6	1	0.82
	MCC	0.90	0.64	0.68	1	0.80
	F1 score	0.96	0.7	0.71	1	0.84

6.4. Discussion:

This study explored the potential utility of machine learning models in analysing EEG signals in grading the severity of background abnormalities in term patients enrolled less than 6 hours after birth.

Several algorithms have been developed to assess the EEG for Hypoxic-Ischaemic Encephalopathy. Stevenson et al., (2013) introduced a technique for extracting non-stationary characteristics from the time-frequency distribution (TFD). The procedure involved the extraction of features related to amplitude modulation and instantaneous frequency. Additionally, these extracted attributes were integrated alongside traditional quantitative EEG metrics by employing a multi-class linear discriminant classifier. They reported an accuracy of 0.83. Amplitude modulation refers to fluctuations in the signal's amplitude over time, reflecting the strength or intensity of synchronised neural activity. In infants with HIE, changes in amplitude modulation may indicate disrupted or altered neural synchronisation caused by brain injury resulting from a lack of oxygen and blood flow. Furthermore, instantaneous frequency features could provide valuable insights into the dynamic and transient changes in neural oscillations and frequency content. In infants with HIE, the frequency of neural activity within the EEG can change due to brain damage. For instance, there may be an increase in slower delta frequencies, reflecting impaired cortical activity and neural dysfunction (Shibata & Otsubo, 2020).

Furthermore, Matić et al., (2014) introduced a methodology that employed tensors to analyse continuous EEG data. Initially, the EEG signals were segmented adaptively, following which, three distinct features were extracted from each segment to

construct a tensor; these features were peak-to-peak amplitude, global spatial amplitude, duration of the consecutive segments having the same amplitude class. Subsequently, this tensor was subjected to reduction via multi-dimensional decomposition techniques prior to integration through a least-squares support vector machine (SVM) algorithm. They achieved an accuracy of 0.89 to grade background EEG abnormalities. The peak-to-peak amplitude measures the difference between the highest and lowest points within an EEG segment and can indicate suppressed brain activity resulting from HIE (Awal et al., 2016). Global spatial amplitude represents the global amplitude across multiple EEG channels at a specific time point and provides an overview of how amplitude of the neural activity is distributed spatially across the brain, offering an insight into the global severity of brain dysfunction. For instance, a predominance of low amplitude segments across channels suggests widespread suppression of brain activity, a hallmark of severe HIE (Awal et al., 2016). Another feature used by Matić et al., (2014) was the duration of the consecutive segments having the same amplitude class, which can show the duration of EEG suppression as an indicator of HIE grade.

Matić et al. (2015) also presented a methodology that integrated a dynamic inter-burst intervals detection mechanism with a multi-class SVM classifier to improve accuracy. In infants with HIE, the ability of the brain to generate continuous, synchronised activity is impaired and EEG signals contain periods of suppression and bursts of high-amplitude electrical activity, which reflect brief episodes of neuronal firing (Raurale et al., 2019). Thus, inter-burst intervals, can give an overview of EEG signal suppression between neural firing episodes.

Moreover, Ahmed et al. (2016) utilised an expanded set of 55 features encompassing elements from time and frequency to build a Gaussian mixture model (GMM) supervector, combined using an SVM. They reported an accuracy of 0.87.

Raurale et al. (2021) integrated a quadratic time-frequency distribution with a convolutional neural network to create a model capable of classifying EEG grades in HIE. They achieved an accuracy of 0.89 on the development dataset and 0.69 on the unseen testing dataset. While this approach eliminates the need for manual feature design and selection by automatically extracting them, our model still surpasses its performance.

The proposed XGBoost model demonstrated exceptional performance, ranking as the second-best model in the EEG machine learning competition hosted by the INFANT centre, outperforming many state-of-the-art methods. This achievement underscores my innovative approach to automating analysis on early predictive EEG recordings recorded in the first 6 hours of life. This report suggests that automated analysis of EEG in the first hours of life is feasible and has a strong capacity to provide essential information for parents and healthcare professionals. This helps in making more informed choices concerning newborn care and treatment plans.

6.5. References

Ahmed, R., Temko, A., Marnane, W., Lightbody, G., & Boylan, G. (2016). Grading hypoxic–ischaemic encephalopathy severity in neonatal EEG using GMM supervectors and the support vector machine. *Clinical Neurophysiology*, *127*(1), 297-309.

Awal, M.A., Lai, M.M., Azemi, G., Boashash, B., & Colditz, P.B. (2016). EEG background features that predict outcome in term neonates with hypoxic ischaemic encephalopathy: A structured review. *Clinical Neurophysiology*, *127*(1), 285-296.

Bennet, L., Roelfsema, V., Pathipati, P., Quaedackers, J. S., & Gunn, A. J. (2006). Relationship between evolving epileptiform activity and delayed loss of mitochondrial activity after asphyxia measured by near-infrared spectroscopy in preterm fetal sheep. *The Journal of Physiology*, *572*(1), 141-154.

Committee on Fetus and Newborn, Papile, L. A., Baley, J. E., Benitz, W., Cummings, J., Carlo, W. A., Eichenwald, E., Kumar, P., Polin, R. A., Tan, R. C., & Wang, K. S. (2014). Hypothermia and neonatal encephalopathy. *Pediatrics*, *133*(6), 1146–1150.

Kattwinkel, J., Perlman, J.M., Aziz, K., Colby, C., Fairchild, K., Gallagher, J., Hazinski, M.F., Halamek, L.P., Kumar, P., Little, G., & McGowan, J.E. (2010). Part 15: neonatal resuscitation: 2010 American Heart Association guidelines for cardiopulmonary resuscitation and emergency cardiovascular care. *Circulation*, *122*(18_suppl_3), S909-S919.

Matić, V., Cherian, P.J., Jansen, K., Koolen, N., Naulaers, G., Swarte, R.M., Govaert, P., Van Huffel, S., & De Vos, M. (2015). Improving reliability of monitoring background

EEG dynamics in asphyxiated infants. *IEEE Transactions on Biomedical Engineering*, *63*(5), 973-983.

Matic, V., Cherian, P.J., Koolen, N., Naulaers, G., Swarte, R.M., Govaert, P., Van Huffel, S., & De Vos, M. (2014). Holistic approach for automated background EEG assessment in asphyxiated full-term infants. *Journal of Neural Engineering*, *11*(6), p.066007.

Murray, D. M., Boylan, G. B., Ryan, C. A., & Connolly, S. (2009). Early EEG findings in hypoxic-ischaemic encephalopathy predict outcomes at 2 years. *Pediatrics*, *124*(3), e459-e467.

O'Toole, J. M., & Boylan, G. B. (2017). NEURAL: quantitative features for newborn EEG using Matlab. *arXiv preprint arXiv:1704.05694*.

O'toole, J. M., Mathieson, S. R., Raurale, S. A., Magarelli, F., Marnane, W. P., Lightbody, G., & Boylan, G. B. (2023). Neonatal EEG graded for severity of background abnormalities in hypoxic-ischaemic encephalopathy. *Scientific Data*, *10*(1), 129.

Pavel, A.M., Rennie, J.M., de Vries, L.S., Blennow, M., Foran, A., Shah, D.K., Pressler, R.M., Kapellou, O., Dempsey, E.M., Mathieson, S.R., & Pavlidis, E. (2020). A machine-learning algorithm for neonatal seizure recognition: a multicentre, randomised, controlled trial. *The Lancet Child & Adolescent Health*, *4*(10), 740-749.

Pavel, A.M., Rennie, J.M., de Vries, L.S., Blennow, M., Foran, A., Shah, D.K., Pressler, R.M., Kapellou, O., Dempsey, E.M., Mathieson, S.R., & Pavlidis, E. (2022). Neonatal seizure management: is the timing of treatment critical?. *The Journal of Pediatrics*, *243*, 61-68.

Perez, A., Ritter, S., Brotschi, B., Werner, H., Caflisch, J., Martin, E., & Latal, B. (2013). Long-term neurodevelopmental outcome with hypoxic-ischaemic encephalopathy. *The Journal of Pediatrics*, *163*(2), 454-459.

Raurale, S. A., Boylan, G. B., Mathieson, S. R., Marnane, W. P., Lightbody, G., & O'Toole, J. M. (2021). Grading hypoxic-ischaemic encephalopathy in neonatal EEG with convolutional neural networks and quadratic time–frequency distributions. *Journal of Neural Engineering*, *18*(4), 046007.

Raurale, S.A., Nalband, S., Boylan, G.B., Lightbody, G., & O'Toole, J.M. (2019, July). Suitability of an inter-burst detection method for grading hypoxic-ischemic encephalopathy in newborn EEG. In *2019 41st Annual International Conference of the IEEE Engineering in Medicine and Biology Society (EMBC)* 4125-4128. IEEE.

Shibata, T., & Otsubo, H. (2020). Phase-amplitude coupling of delta brush unveiling neuronal modulation development in the neonatal brain. *Neuroscience Letters*, *735*, p.135211.

Stevenson, N. J., Korotchikova, I., Temko, A., Lightbody, G., Marnane, W. P., & Boylan, G. B. (2013). An automated system for grading EEG abnormality in term neonates with hypoxic-ischaemic encephalopathy. *Annals of Biomedical Engineering*, *41*, 775-785.

Tagin, M. A., Woolcott, C. G., Vincer, M. J., Whyte, R. K., & Stinson, D. A. (2012). Hypothermia for neonatal hypoxic ischaemic encephalopathy: an updated systematic review and meta-analysis. *Archives of Pediatrics & Adolescent Medicine*, *166*(6), 558-566.

van Schie, P. E., Schijns, J., Becher, J. G., Barkhof, F., van Weissenbruch, M. M., & Vermeulen, R. J. (2015). Long-term motor and behavioral outcome after perinatal hypoxic-ischemic encephalopathy. *European Journal of Paediatric Neurology*, *19*(3), 354-359.

Walsh, B. H., Murray, D. M., & Boylan, G. B. (2011). The use of conventional EEG for the assessment of hypoxic ischaemic encephalopathy in the newborn: a review. *Clinical Neurophysiology*, *122*(7), 1284-1294.

Wassink, G., Gunn, E. R., Drury, P. P., Bennet, L., & Gunn, A. J. (2014). The mechanisms and treatment of asphyxial encephalopathy. *Frontiers in Neuroscience*, *8*, 40.

World Medical Association, 2013. World Medical Association Declaration of Helsinki: ethical principles for medical research involving human subjects. *The Journal of the American Medical Association*, *310*(20), 2191-2194.

Chapter 7. Thesis Discussion and Conclusion

7.1. Overview of Main Findings

Preventing and mitigating brain injury in newborns, particularly in preterm infants, represents a significant unmet clinical need due to its potential to cause lifelong impairments, including developmental delays, cognitive deficits, and motor dysfunction. As such, early detection and intervention are key for improving outcomes. Artificial intelligence tools have the potential to analyse complex data patterns from continuous measurements of vital signs in real time, thereby offering clinicians insights into early signs of brain injury that would otherwise be missed. This integration of neonatal monitoring with AI could transform care, enabling earlier diagnosis, more personalised treatments, and ultimately better long-term outcomes for affected infants.

At the start of my PhD research, I explored the extraction of advanced engineered features from a pattern within NIRS derived- $rcSO_2$ signals, which we termed Prolonged Relative Desaturations (PRDs). These PRDs are data-driven desaturation events, lying in the 2-to-15-minute range, characterised by haemoglobin oxygen desaturation lasting several minutes, with a relative change in the oxygen saturation ranging approximately between 11% and 14%. By isolating these PRDs and deriving various features directly from them, and then implementing machine learning techniques, we developed predictive models. In our studies, we demonstrated that combining the features extracted from $rcSO_2$ PRDs using XGBoost significantly detected the occurrence of moderate and severe Intraventricular Haemorrhage (IVH) in extremely preterm infants. This observation was validated through replication in a

larger cohort of patients, drawn from a multicentre study, thereby reinforcing the robustness of our findings.

Having evidence of the utility of advance NIRS-signal analysis in extremely preterm infants to predict IVH outcome, I was interested in exploring its utility in other cohorts. Utilising the MONItOr data set I explored the utility of NIRS features collected from term infants diagnosed with HIE at 1 hour of life. Using this approach, we found that specific features within the NIRS signals, after the PRDs were extracted, had a strong correlation with adverse outcomes as detected by MRI. To push the boundaries of our analysis further, we also incorporated deep learning techniques. By leveraging these advanced computational models, we enabled the automatic extraction of features and patterns within the NIRS signals. The deep learning models were particularly effective in identifying subtle and complex patterns that were predictive of adverse outcomes, further enhancing our ability to detect and predict these events in early life.

Furthermore, by extracting key characteristics from EEG signals, I developed AI models capable of detecting the severity of EEG background abnormalities in term infants with HIE. In preterm infants, my analysis revealed associations between some specific EEG features and mean arterial blood pressure, highlighting the potential of EEG-based AI models to provide valuable insights into both neurological function and hemodynamic stability in vulnerable neonatal populations.

Our findings suggest that the information embedded in the NIRS and EEG signals, especially when combined with sophisticated signal processing techniques, offers a

novel means of analysing clinical data that may be superior to traditional analytical methods, which typically focus only on absolute values of NIRS signals. By leveraging the detailed characterisation of significant cardiovascular/respiratory events that are captured in the form of PRDs, we can enhance the accuracy and effectiveness of early detection strategies, which should ultimately improve clinical outcomes for vulnerable infants in the NICU.

7.2. Contribution to the Field

In summary, our research highlights the significant potential of AI for detecting and predicting adverse outcomes in the first days of life. The application of AI enables clinicians to maximise the utility of data recorded from newborns, moving beyond the reliance on single variables for intervention. Instead, AI facilitates more comprehensive monitoring and predictive analytics that take into account interindividual differences among infants. By employing automated algorithms that are capable of understanding and learning complex, nonlinear relationships between various variables, AI enhances the ability to identify early warning signs and trends that may not be immediately apparent using traditional methods. This not only improves the precision of clinical assessments but also supports clinicians in making more informed and timely decisions, reducing the likelihood of errors due to fatigue or human limitations.

The implications of this work are substantial, offering the potential for earlier detection of complications, more accurate prognoses, and better long-term outcomes for both preterm and term infants.

7.3. Strength and Limitations

This thesis is strengthened by the utilisation of state-of-the-art AI methods for detecting adverse outcomes in neonates. The study benefits from access to data from multicentre projects, which enhances the generalisability of the models we developed. Studies specifically targeting preterm infants often have smaller sample sizes due to the rarity of certain conditions and the complexity of data collection in neonatal intensive care units. For instance, some studies that focus on specific conditions, such as apnoea of prematurity, have sample sizes as small as 20 participants. The strength of multicentre projects lies in their ability to pool data from several institutions, thereby increasing sample sizes.

However, there are notable limitations to this work. Since none of the datasets were originally collected for the purposes of this thesis, certain data were unavailable. For instance, the lack of precise information regarding maternal clinical history and the exact timing of injury is a significant limitation. If the data had been specifically collected for this research, additional brain scans could have been performed to more accurately determine the timing of the injury. However, the risk benefit ratio to the patient, including the potential harm from additional exposure to imaging, and the feasibility of performing repeated scans must also be carefully considered.

Limited sample sizes posed a challenge in this study. AI models are known for their data-intensive nature, requiring large datasets for effective training. While the clinical study included relatively large cohorts for a niche population, in the context of data science and AI, the sample size was still relatively small, which may have impacted the robustness and generalisability of the AI models developed.

7.4. Recommendations for Future Research

Future research in this area should prioritise the integration of data from multiple centres to significantly increase sample sizes, thereby enhancing the statistical power and generalizability of AI models. Collaborative platforms or websites that facilitate the collection and sharing of data across different centres would be invaluable in this regard. Such platforms could enable scientists to access larger, more diverse datasets, thereby improving the robustness of predictive models. However, ensuring the privacy and confidentiality of patient data is paramount. This will require the development of secure, standardised protocols for data sharing that comply with ethical guidelines and legal regulations. In Ireland, the storage of biological signals is not done routinely, largely due to General Data Protection Regulation (GDPR) constraints and the high cost of retaining these records. Furthermore, these platforms are labour-intensive to maintain and require rigorous monitoring of data quality and careful documentation of the devices used to monitor patients, as poor-quality data can lead to unreliable outcomes. Therefore, ensuring high standards of data accuracy and consistency is essential for the success of such systems.

In addition to expanding the dataset, future research should explore the use of multimodal datasets to improve the accuracy of brain injury detection and prognosis. While this thesis primarily focused on NIRS data, the integration of other modalities, such as EEG and ECG, could provide a more comprehensive understanding of neonatal brain function. Multimodal approaches allow for the capture of different physiological signals, offering a more holistic view of the brain's condition and potentially leading to more accurate and timely interventions. Synchronisation of

devices would add further value by enabling a unified software system to capture and store live data, ensuring that all signals are accurately aligned for better analysis and clinical decision-making.

Moreover, conducting multimodal studies on animal models could provide valuable insights into the mechanisms of brain injury and the effectiveness of various interventions. These studies could serve as a foundation for developing and refining multimodal AI models, which could then be applied to clinical settings. Collecting and analysing data from such studies would not only enhance our understanding of brain injury but also contribute to the development of more effective, individualised treatment strategies for infants.

Overall, the future of research in this field lies in the collaboration between multiple centres, the integration of multimodal data, and the ethical handling of sensitive information. Additionally, better collaboration between gynaecologists, neonatologists, and paediatricians is essential for long-term follow-up and more cohesive data collection. Continued collaboration between data scientists, basic researchers, and neonatologists will also play a crucial role in advancing our understanding. By addressing these areas, we can move closer to achieving more precise and personalised care for infants at risk of brain injury.